LEABHARLANN CHOLÁISTE NA TRÍONÓIDE, BAILE ÁTHA CLIATH | TRINITY COLLEGE LIBRARY DUBLIN
Ollscoil Átha Cliath | The University of Dublin

Terms and Conditions of Use of Digitised Theses from Trinity College Library Dublin

Copyright statement

All material supplied by Trinity College Library is protected by copyright (under the Copyright and Related Rights Act, 2000 as amended) and other relevant Intellectual Property Rights. By accessing and using a Digitised Thesis from Trinity College Library you acknowledge that all Intellectual Property Rights in any Works supplied are the sole and exclusive property of the copyright and/or other IPR holder. Specific copyright holders may not be explicitly identified. Use of materials from other sources within a thesis should not be construed as a claim over them.

A non-exclusive, non-transferable licence is hereby granted to those using or reproducing, in whole or in part, the material for valid purposes, providing the copyright owners are acknowledged using the normal conventions. Where specific permission to use material is required, this is identified and such permission must be sought from the copyright holder or agency cited.

Liability statement

By using a Digitised Thesis, I accept that Trinity College Dublin bears no legal responsibility for the accuracy, legality or comprehensiveness of materials contained within the thesis, and that Trinity College Dublin accepts no liability for indirect, consequential, or incidental, damages or losses arising from use of the thesis for whatever reason. Information located in a thesis may be subject to specific use constraints, details of which may not be explicitly described. It is the responsibility of potential and actual users to be aware of such constraints and to abide by them. By making use of material from a digitised thesis, you accept these copyright and disclaimer provisions. Where it is brought to the attention of Trinity College Library that there may be a breach of copyright or other restraint, it is the policy to withdraw or take down access to a thesis while the issue is being resolved.

Access Agreement

By using a Digitised Thesis from Trinity College Library you are bound by the following Terms & Conditions. Please read them carefully.

I have read and I understand the following statement: All material supplied via a Digitised Thesis from Trinity College Library is protected by copyright and other intellectual property rights, and duplication or sale of all or part of any of a thesis is not permitted, except that material may be duplicated by you for your research use or for educational purposes in electronic or print form providing the copyright owners are acknowledged using the normal conventions. You must obtain permission for any other use. Electronic or print copies may not be offered, whether for sale or otherwise to anyone. This copy has been supplied on the understanding that it is copyright material and that no quotation from the thesis may be published without proper acknowledgement.

Detection, Expression and Elucidation of the Mechanism of Action of Mitochondrial Uncoupling Protein 1.

A dissertation submitted to Trinity College, Dublin for the degree of Doctor of Philosophy

By

Eamon Patrick Breen

Department of Biochemistry

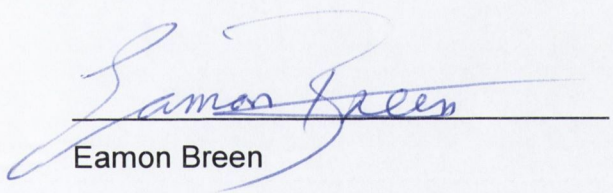
Trinity College, Dublin

November 2005

TRINITY COLLEGE
12 MAY 2006
LIBRARY DUBLIN
THESIS
7893

Declaration

I, the undersigned, declare that this thesis is entirely my own work, except where otherwise accredited and that it has not been submitted for a degree in any other university or institution. This thesis may be borrowed or copied upon request with the permission of the Librarian, University of Dublin, Trinity College.



Eamon Breen

Abstract

A system for overexpression of recombinant proteins in *E. coli* is defined. Using subcloning techniques the cDNAs for human uncoupling proteins (hUCP) 1, 2 and 3 were introduced to the pET expression system for *E. coli*. Inducible expression is conferred upon the bacteria. Expression of hUCP2 and hUCP3 was possible in the commonly used strain of expression bacterium *E. coli* BL21 pLysS. However, hUCP1 was not expressed in these bacteria. A codon bias for human mRNA codons was investigated using the BL21 Codon-Plus strain which has only three under-represented codons, but expression failed. However, using the BL21 derivative strain Rosetta pLysS, which possess all under-represented human codons on the pRARE plasmid, expression of hUCP1 was possible. Codon bias was obviously a problem for expression of hUCP1 in BL21 pLysS and BL21 Codon-Plus *E. coli*. All UCPs expressed were accumulated in inclusion bodies as aggregated proteins.

Detection of UCP protein and distinguishing between UCP1, UCP2 and UCP3 were also investigated. Specific and antigenic peptides for UCP1 and UCP3 were identified using Kyte-Doolittle plots for each protein. These peptides were coupled to adjunct and used to raise polyclonal antibodies in rabbits. The antibodies produced were tested for immunoreactivity with all hUCPs expressed. An anti-peptide antibody for UCP1 was shown to be specific for UCP1 and discriminatory over UCP2 and UCP3. Also, an anti-peptide antibody for UCP3 was shown to be specific for UCP3 and discriminatory over UCP1 and UCP2.

One of the priorities was to reinvestigate the buffering mechanism of action of UCP. Native uncoupling protein 1 (UCP1) was purified from rat mitochondria by hydroxyapatite chromatography and identified by peptide mass mapping and tandem mass spectrometry. Native rUCP 1 was reconstituted into liposomes and proton flux through UCP1 was shown to be fatty-acid dependent and GDP-sensitive. In order to investigate the mechanism of action of UCP1, whether or not hydrophilic modification of the ω-carbon of palmitate affected its transport function was determined. It is shown that H^+ flux was greater through native rUCP1-containing proteoliposomes when facilitated by less hydrophilically modified palmitate (palmitate>ω-methoxypalmitate≥ω-hydroxypalmitate, with little or no proton flux due to glucose-*O*-ω-palmitate or undecanesulfonate). We show that non-H^+ dependent charge transfer was greater when facilitated by less hydrophilically modified palmitate (palmitate/undecanesulfonate>ω-methoxypalmitate>ω-hydroxypalmitate, with no non-H^+-dependent charge transfer flux due to glucose-*O*-ω-palmitate). It is also shown that the GDP-inhibitable oxygen consumption rate in brown adipose tissue (BAT) mitochondria was reversed by palmitate (as expected), but not by glucose-*O*-ω-palmitate. The data are consistent with the model that UCP 1 flips long-chain-fatty-acid anions and contradict the buffering model of UCP 1 function.

The lauric acid analogue undecanesulfonate has a low pK_a of 2 and is a permanent anion at physiological pH values. In its anionic form. it has been used as a probe for measuring the anionic activity of UCPs. As the protonophore model of UCP function predicts that UCP flips the anion fatty acids,

undecanesulfonate has been used to show this activity. It has been shown that UCP1 can be inserted into liposomes in two orientations with respect to the nucleotide-binding site. A 50:50 orientation of UCP1 with the nucleotide-binding site facing into the lumen of proteoliposomes or facing out of the proteoliposomes was found with the reconstitution technique used. When measuring undecanesulfonate transport by UCP1, the orientation of the protein was found to be inconsequential. Undecanesulfonate is transported with similar K_m values regardless of orientation. This indicates that access of the fatty acid anion to its binding site is equidistant from either side.

Having successfully expressed hUCP1, an investigation of the competence of the reconstituted protein was undertaken. *E.-coli*-expressed hUCP1 has been purified and reconstituted into proteoliposomes. hUCP1 was found to be activated by fatty acids (laurate and palmitate) but inhibition by nucleotides was found to be absent. Laurate was transported with a V_{max} value of 2.7 μmoles H^+/min/mg and a K_m value of 82 μM. Palmitate was transported with a V_{max} value of 2.9 μmoles H^+/min/mg and a K_m value of 27.6 μM. Coenzyme Q, once thought to be a cofactor for UCP function, was not found to affect transport via hUCP1.

Acknowledgements

First and foremost I have to thank my supervisor Dr. R.K. Porter for giving me this opportunity. Richie, with so much passion for your work, you are a true scientist! The most important thing that you have taught me is that just because a result isn't what you want doesn't make it bad! Your help in the final hours will be appreciated always. I have to thank Dr. Orla Cunningham for starting me off, the first person to take me under her wing and she led by great example. You are long gone but not forgotten. Then, of course, there's Dr. Tony McElligott, who was also one of my early mentors. You gave me a great start in the lab and continued support: words cannot express my gratitude.

Dr. Audrey Carroll, Dr. Clare Brennan and Dr. Oliver Joyce (alphabetical order – no preferences!) – as you all left me one by one, what was I to do but to finish! You led by great example. Audrey, you were literally and figuratively there behind me, I have gained a fantastic friend and meet a great researcher. Clare, we went through a lot and still are and have a great friendship as a result and a future marriage? – who knows what life will throw at us but I do know that we can beat it. Oliver, you were there surrounded by us UCP-people and always held your own. You also led the way to getting this doctorate thing! Thank you, you have been gone too long.

Joe Healy and Orla Hart, we all wrote up together and I must say that the support, mutual moaning, coffee and dragging to the pub were always appreciated. Aoife Cullen, how did you put up with us? You're a saint! However, you were never far behind when the pub (or more) beckoned. Dr. Jeff O'Sullivan, you seemed to be there in the pub also, surprise, surprise. I must also mention Lab 1, past and present for all the help and for adopting me into their fold, and making me feel so welcome, especially Martha Motherway. Dr. Sinead Boyce, thank you for all your word of encouragement and for listening to me moan!

Dr. Beth Brint (Missprint!!!) you waited a long time for me, thank you. Thank you for the chats, drinks, fags and, most importantly the support. Lab 4, especially Gavin, Ed, Seamus and Bertie, for always being so helpful and generous. All on the Ground floor (Biotech) for always being so helpful. I must especially mention Dr. Caroline Jefferies for being so understanding and for taking the risk and employing me!!!

The Prep. Room, Ronnie, Roisin, Bernie, Clarice and Brian for always helping me out, leaving doors open, loans and internal organs! Kyran, for being so understanding, Mary-Pat for, well, being Mary-Pat, you are a gem! Bioresources – esp. Ann, Brian, Breda, so helpful, understanding and great for a chat! Thank you to all my friends in Biochem, for everything.

I must mention Prof. Martin Klingenberg, one of the great pioneers of the UCP world, who was an inspiration and Dr. Karim Echtay, who was the first person to teach me reconstitution. Thanks also have to go to Dr. Keith Garlid, another great pioneer in the field, for inviting me to Oregon and to Dr. Martin Jabůrek for teaching the reconstitution in this thesis.

The Colraine gang. Such a cracking bunch of people and you welcomed me in with open arms. I feel privileged to be considered one of you. Especially Dr. Mags McDonagh, what can I say? Thank you. I can't describe what a good friend you have become. Dr. Frank O Farrell and Ms Trish Fitzsimmons, thank you for being such truly dear friends, for nights out and in, always a pleasure.

To 69 Ansell Rd, all therein and associated, the parties, what parties!

To 64 Malahide Rd for putting up with crazy Eamon and not questioning. Thanks to Andrea Pappin for this laptop and a unique friendship and you know what you did, it is appreciated, Patrick Forsyth, for that hug.

To Gallaghers, Bernie, Rita, Michael and David for just being there and giving me that peace of mind.

Gillian Forrest, you moved far away and I got stuck in this thesis but you still remembered, thank you. Roisin Kelly for asking and also knowing when not to.

Justin Murphy, my oldest friend, what can I say? I can't. Thank you. Olivia Leslie, the support, the friendship, the belief, I truly treasure your friendship. Tara Butler, you know, you know, it has always been you. I thank the three of you again, for what? It has no words, I hope you understand.

To Dr. Tony McElligott: you get a second mention because you are special and that is it.

Thanks also to Conor Breen and Catherine Breen for the belief and support, only a sibling could give.

My parents, the best people ever. I owe you everything and you ask for nothing, what the hell? How good can two people be? For understanding and for not understanding but still always believing in me and making me the person that I am today. I hope I can make you nearly as proud of me as I am of you. Thank you.

Table of Contents

Declaration i

Abstract ii

Acknowledgements v

Table of contents vii

Abbreviations and Acronyms xi

1. Introduction

1.1 Mitochondria 1

1.2 Oxidative Phosphorylation 1

1.2.2 *What is coupling/uncoupling?* 2

1.2.2.1 Artificial uncoupling agents 3

1.2.2.2 Natural uncoupling agents 4

1.2.2.3 Protein aspect of uncoupling 4

1.3 Brown Adipose Tissue 5

1.4 Uncoupling protein 1 (UCP1) 7

1.4.1 Sequence and Structure of UCP1 8

1.4.2 Activation of UCP1 9

1.4.3 Function and Mode of Action of UCP1 9

1.4.3.1 The fatty acid protonophore model of UCP1-mediated H^+ flux 11

1.4.3.2 The fatty acid buffering mechanism of UCP1-mediated H^+ flux 12

1.5 UCP Homologs 13

1.5.1 Uncoupling protein 2 13

1.5.2 Uncoupling protein 3 14

1.5.3 Uncoupling protein 4 16

1.5.4 Uncoupling protein 5 16

1.5.5 Plant uncoupling proteins 17

1.6 *E. coli* expression of membrane proteins 18

1.6.1 *E. coli* expression of UCPs 19
1.7 Reconstitution 20
1.7.1 Reconstitution of UCPs 21
1.7.2.1 Reconstitution of expressed UCPs 22
1.8 UCPs and reactive oxygen species 23
1.9 Aims of this study 26

2. Materials and Methods
2.1 Materials 27
2.1.1 General chemicals and conditions 27
2.1.2 List of suppliers 28
2.2 Methods 30
2.2.1 Bacterial strains, culture media and plasmid vectors 30
2.2.2 Purification of plasmid DNA 31
2.2.2.2 Midi-scale preparation from *E. coli* 32
2.2.3 Restriction digests of plasmid DNA 33
2.2.4 Purification of DNA fragments from agarose gels 34
2.2.5 Ligation 34
2.2.6 Preparation and transformation of competent cells 34
2.2.6.1 Preparation of fresh competent cells 34
2.2.6.2 Transformation of competent cells 35
2.2.7 Expressoin of protein and isolation of inclusion bodies from *E. coli* 35
2.2.7.1 Expression of protein 35
2.2.7.2 Isolation of inclusion bodies 36
2.2.8 Estimation of protein concentratin: Method of Markwell *et al.*, (1978) 36
2.2.9 Sodium dodecyl sulphate – polyacrylamide gel electorphoresis (SDS-PAGE) and staining. 37
2.2.9.1 Gel preparation and electrophoresis 37
2.2.9.2 Coomassie Blue R staining of polyacrylamide gels 37

2.2.9.3 Colloidal B staining for polyacrylamide gels 38
2.2.10 Detection of UCPs by immunoblotting 38
2.2.11 Cold-adaptation of Syrian golden hamsters and wistar rats 39
2.2.12 Preparation of mitochondria from BAT 39
2.2.13 Preparation of mitochondria from skeletal muscle 40
2.2.14 Preparation of mitochondria from liver and thymus 41
2.2.15 Purification of native UCP1 from BAT mitochondria 42
2.2.15.1 Preparation of lipids and hydroxylapatite 42
2.2.15.2 Protein solubilization 42
2.2.16 Extraction and purification of hUCP1 from inclusion bodies 43
2.2.17 Reconstitution of UCP1 into liposomes 44
2.2.17.1 Preparation of lipids and columns 44
2.2.17.2 Preparation of proteoliposomes 44
2.2.18 Fluorescent measurements of potassium ion (K^+) flux 45
2.2.19 Estimation of protein concentration in the presence of high concentration of lipids using Amido Black 10B: Kaplan *et al.*, (1985) 46
2.2.20 Oxygen consumption by non-phosphorylating BAT mitochondria 47
2.2.21 Statistical analysis 47

3. Overexpression of hUCP1, hUCP2 and hUCP3 and characterisation of anti-UCP1 and anti-UCP3 antibodies

3.1 Introduction 48
3.2 Results 50
3.3 Discussion 53

4. Investigation into the fatty-acid buffering model for rUCP1 using fatty-acid analogues.

4.1 Introduction 57
4.2 Results 60

4.3 Discussion 64

5. Investigation into the molecular mechanism of haUCP1 function using undecanesulfonate

5.1 Introduction 70

5.2 Results 72

5.3 Discussion 74

6. Functional reconstitution of bacterially expressed hUCP1

6.1 Introduction 78

6.2 Results 81

6.3 Discussion 84

7. General discussion

7.1 General discussion 88

8. Bibliography

8.1 Bibliography

Abbreviations and Acronyms

ANC	adenine nucleotide carrier
ADP	adenosine diphosphate
AMP	adenosine monophosphate
ATP	adenosine triphosphate
BAT	brown adipose tissue
BSA	bovine serum albumin
BMCP1	brain mitochondrial carrier protein 1
cAPK	cAMP-dependent protein kinase
CCCP	carbonyl cyanide *m*-chlorophenylhydrazone
cDNA	complementary DNA
DTT	dithiothreitol
CMC	critical micellar concentration
CoA	co-enzyme A
CoQ	co-enzyme Q
Da	dalton
DNP	2,4-dinitrophenol
E. coli	*Escherichia coli*
EDTA	ethylenediamine tetraacetic acid
EGTA	ethylene glycol-bis(β-aminoethylether)-N,N,N',N'–tetraacetic acid
ELISA	enzyme-linked immunosorbent assay
EtBr	ethidium bromide
FCCP	carbonylcyanide-*p*-trifluoromethoxy-phenylhydrazone
(x) *g*	(times) acceleration due to gravity
GDP	guanosine diphosphate
Glucose-*O*-ω-palmitate	ω-glucopyranoside palmitic acid
h	human
ha	hamster

IPTG	isopropyl-β-thiogalactosidase
Δp	proton electrochemical gradient
ΔpH	pH difference
ΔΨ	electrical difference
m	mouse
MIM	mitochondrial inner membrane
MOM	mitochondrial outer membrane
MQAE	N-(ethoxycarbonylmethyl)-6-methoxyquinolinium bromide
nc	*neurospora crassa*
OD	optical density
PBFI	potassium-binding benzofurane isophthalate
PMSF	phenylmethylsulfonylfluoride
PVDF	polyvinylidene difluoride
rt	room temperature
SDW	sterile distilled water
SDS-PAGE	sodium dodecyl sulfate-polyacrylamide gel electrophoresis
SPQ	6-methoxy-*N*-(3-sulfopropyl)quinolinium
SUV	small unilamellar vesicle
TAE	Tris–acetate–EDTA buffer
TCA	trichloroacetic acid
TE	Tris–EDTA buffer
TEA	tetraethylammonium
TES	*N*-tris(hydroxymethyl)methyl-2-aminoethanesulfonic acid
Tris	tris(hydroxymethyl)aminomethane
TX-100	triton-X 100
UCP	uncoupling protein

"Many miles, many roads I have travelled
Fallen down on the way
Many hearts, many years have unravelled
Leading up to today……

I have no regrets
There's nothing to forget
All the pain was worth it

Not running from the past
I tried to do what's best
I know that I deserve it"

From "I deserve it" by M. Ciccone and M. Ahmadzai

Mam and Dad, I owe you everything.

I did it for myself.

I dedicate it to Tony.

Chapter One

Introduction

1.1 Mitochondria

The symbiosis that resulted in the organelle, the mitochondrion, can arguably be called one of the most important examples of symbiosis in evolution. Mitochondria are present in virtually all eukaryotic cells, both plant and animal; they are about the size of an *E. coli* bacterium, having typically an ellipsoid shape, and they are approximately 0.5 μm in diameter and 1 μm in length. Structurally they consist of a smooth mitochondrial outer membrane (MOM) and a mitochondrial inner membrane (MIM), which, together, form two compartments, the intermembrane space and the matrix (Figure 1.1). The matrix is highly concentrated with the enzymes of oxidative metabolism, as well as substrates, nucleotide cofactors and inorganic ions. The matrix also contains mitochondrial genetic machinery, namely DNA, RNA and ribosomes. While the MOM is freely permeable to most small molecules, the MIM is not so permeable. The surface area of the MIM is vastly increased as it is organized in extensively folded cristae this allows for the many reactions that take place in the membrane, in particular, generation of adenosine triphosphate (ATP). The mitochondrion creates an abundance of the high-energy compound ATP, which is then used for most energy-requiring reactions in the cell/body. The electron transport chain and the ATP-synthase molecule are responsible for the production of ATP. The chemiosmotic theory best describes how this ATP is made (Mitchell, 1961).

1.2 Oxidative Phosphorylation

The energy from the downhill movement of electrons, from the oxidation of substrates, is transferred to the high-energy bond of ATP by phosphorylation of ADP (Nicholls, 1992). Hence, this process has been termed "oxidative phosphorylation". The reducing equivalents NADH and $FADH_2$ are derived from the oxidation of carbohydrates and fatty acids. Electrons are donated by NADH and $FADH_2$ to the electron transport chain. The electron transport chain is located in the mitochondrial inner membrane.

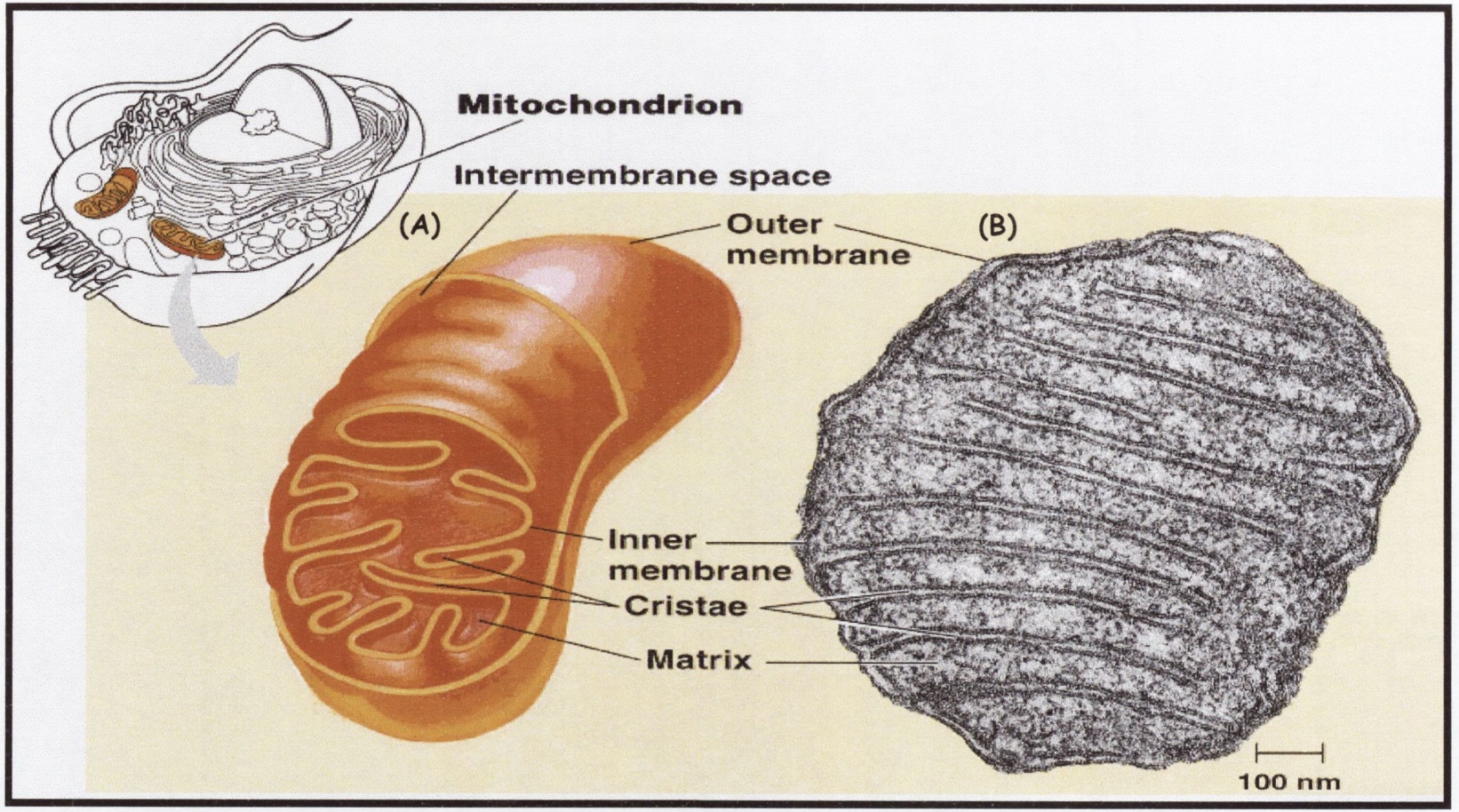


Figure 1.1 Anatomy of the Mitochondrion. (A) Schematic representation of a mitochondrion. Each mitochondrion will hold thousands of copies of the electron transport chain and ATP-synthase complexes which are found on the mitochondrial inner membrane. **(B)** An electron micrograph of a mitochondrion illustrating the extensive folding of the cristae some of which span the width of a single mitochondrion.

(www.uwinnipeg.Ca/~simmons/cm1503/mitochondria.htm)

The movement of the electrons down the electron transport chain coincides with the translocation of protons (H^+) from the matrix, across the inner membrane, to the inter-membrane space. Translocation of H^+ occurs at specific protein complexes. The ultimate acceptor of the electrons is O_2, which is then converted into H_2O. This translocation creates a delocalized trans-membrane proton electrochemical gradient (Δp). The majority of Δp is made up of the electrical difference ($\Delta\Psi$) resulting from the translocations. Due to the H^+ being buffered, the difference in pH (ΔpH) across the inner membrane is low, being around 0.5 units. The mitochondrial inner membrane has a high electrical resistance. The electrical potential is usually around 200 mV, which is equivalent to 300,000 $V.cm^{-1}$ across the hydrophobic core (Nicholls and Ferguson, 1992).

Δp is potential energy that can be used to do work. Work, such as the transport of metabolites across the inner membrane e.g. ADP-ATP exchange, phosphate/proton symport. However, Δp is also used for ATP synthesis from matrix ADP and phosphate. The protons are driven into the matrix, from the inter membrane space through the ATP-synthase protein complex, and the phosphorylation of ADP to form ATP is catalysed. The ATP-synthase complex is located on the inner membrane and extends into the matrix (Abrahams *et al.,* 1994).

1.2.2 *What is coupling/uncoupling?*

Substrate-level phosphorylation was the first demonstration of coupling. This occurs in glycolysis using 1,3-bisphosphoglycerate as a "high-energy" compound. One of the bonds between oxygen and a phosphate moiety in this compound has a low hydrolysis energy, so, when this bond is broken the energy released is used to form the "high-energy" bond between ADP and the phosphate. In this way, the breaking of one bond is coupled to the formation of another. In a similar way, oxidation is coupled to phosphorylation; as already mentioned, the protons translocated across the mitochondrial inner membrane due to oxidation of substrates sets up a

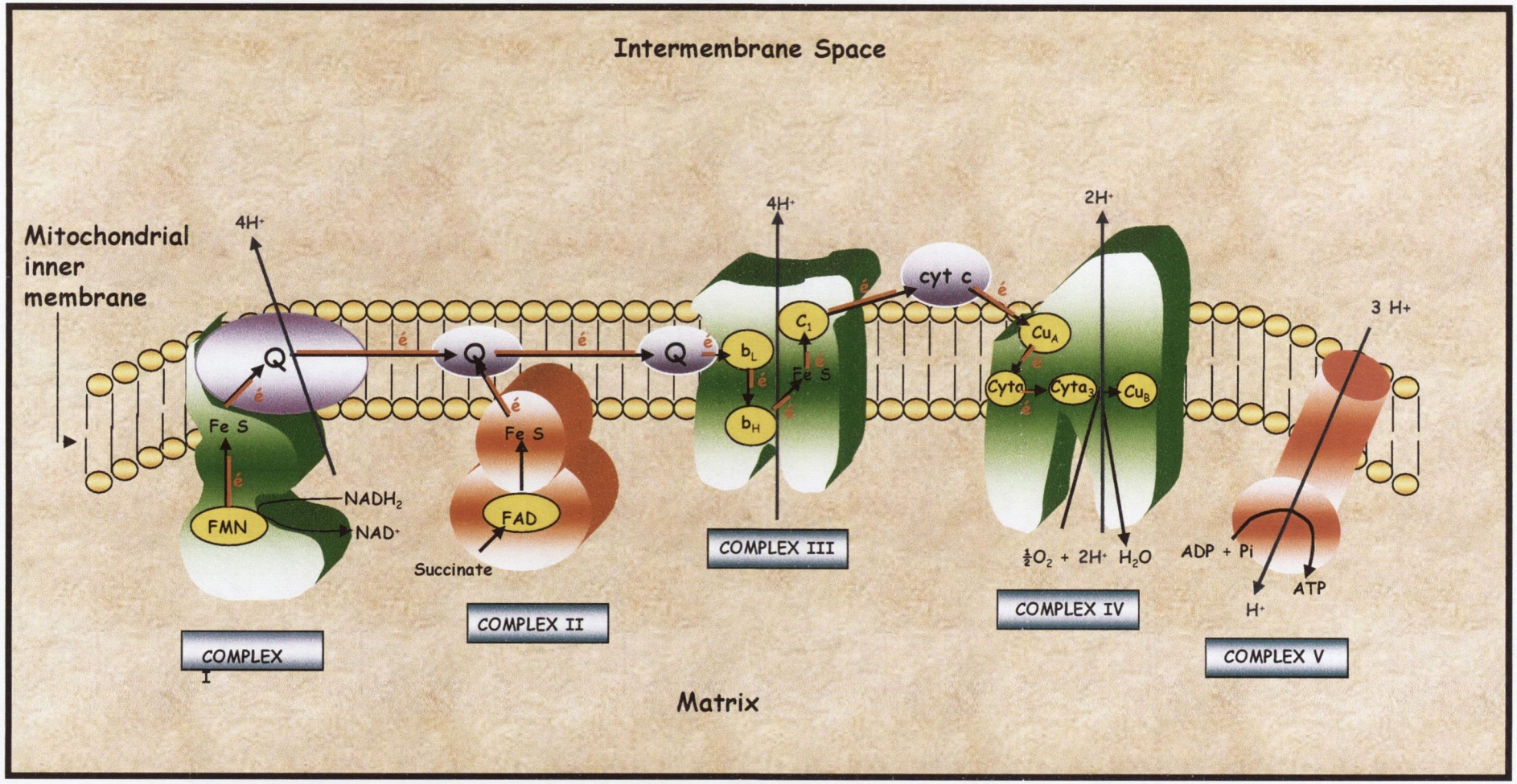


Figure 1.2: An overview of the redox carriers in the mitochondrial respiratory chain.

A diagram of the mitochondrial electron-transport chain indicating the pathway of electron transfer (black) and proton pumping (red). Electrons are transferred between Complexes I and III by the membrane-soluble CoQ and between Complexes III and IV by the peripheral membrane protein, cytochrome C. Complex II transfers electrons from succinate to CoQ. Diagram reproduced with kind permission of Dr. Audrey Carroll.

proton electrochemical gradient (Δp) across the membrane. Δp is used to make ATP by allowing the H^+ to move back across the membrane and converting the potential energy into kinetic energy (movement of the ATP synthase) and trapping the potential energy, or Δp, in the "high-energy" bond of ATP. In short, ATP synthesis is coupled to oxygen consumption by Δp.

Uncoupling arises when the Δp created by oxidation of substrates (i.e. H^+ pumping into the intermembrane space) is not used for phosphorylation, i.e., there is a short circuit in the system. It is correct to say that all mitochondria are uncoupled to some degree. This is exemplified by the fact that; mitochondria in state – 4 respiration or under non-phosphorylating conditions (i.e. in the absence of ADP or in the presence of the ATP-synthase inhibitor oligomycin) still consume oxygen and maintain a membrane potential. Oxygen consumption under these conditions is due to a leakage of H^+ across the inner membrane of the mitochondrion. This H^+ leak is thought to be a non-enzymic diffusion process across the inner membrane of all mitochondria and displays a non-linear dependence on its driving force, Δp, such that the leak is maximal when the mitochondria are not making ATP and minimal when they are (Brown and Brand, 1986). Proton leak is not an artefact of mitochondrial isolation, as it has been found in mitochondria in situ in a variety of tissues and cells such as liver, thymus, lymphocytes, thymocytes, skeletal muscle, heart and brown adipose tissue (Nicholls and Rial, 1974; Brand *et al.,* 1994; Rolfe and Brand, 1997). Proton leak accounts for 20% of resting oxygen consumption of cells and up to 30% of the resting oxygen consumption of rat hindquarter skeletal muscle. These percentages are very high, so they must in turn, be important in the energy budget (Rolfe and Brand, 1996).

1.2.2.1 Artificial uncoupling agents

The first uncoupler described was arsenate in 1939 (Skulachev, 1998). Arsenate binds to ADP to form ADP-arsenate and prevents the formation of ATP. It basically effects the final step of the process,

phosphorylation, and then decomposes to give ADP and arsenate again. Perhaps the most infamous of all artificial uncouplers would be 2,4-dinitrophenol (DNP). DNP is a hydrophobic weak acid that when in its ionic form has a delocalized negative charge so it can cross the membrane in the ionized or unionized form. Bielawski *et al.* (1966) showed that DNP worked by increasing the H^+ conductance of the membrane. DNP has been used to reduce body fat in humans (Parascandola, 1974). DNP was introduced as an anti-obesity drug in the 1930s and was used with considerable success, though reports of side effects and some deaths from overdose led to it being removed from the market by the US Food and Drug Administration (FDA) in 1938. Another artificial uncoupler that is used for in vitro studies on mitochondria is carbonylcyanide-*p*-trifluoromethoxy-phenylhydrazone (FCCP), which also works as a hydrophobic weak acid.

1.2.2.2 Natural uncoupling agents

It has long been know that fatty acids have an uncoupling effect on mitochondria (Lardy and Pressman, 1956). Fatty acids are able to traverse the membrane in their protonated form (Andreyev *et al.,* 1989). Subsequent loss of H^+ would allow for uncoupling. The resultant anion then tends to occupy a position in the lipid-water interface, with the carboxylate group facing the water and the hydrocarbon 'tail' penetrating into the membrane core (Skulachev, 1991). The efficiency of fatty acids as uncouplers is quite low due to the fact that the anionic form is poorly permeable in the membrane (Kamp and Hamilton, 1992). Unlike the artificial uncouplers DNP and FCCP, fatty-acid anions have a strongly localized negative charge.

1.2.2.3 Protein aspect of uncoupling

It would appear that, with all forms of uncoupling of mitochondria there is some involvement of proteins. In the case of DNP; addition of the specific inhibitor of the adenine nucleotide carrier (ANC), carboxyatractyloside, can partially recouple the DNP-uncoupled mitochondria (Andreyev *et al.,* 1989). It is unknown how proteins can be

involved in this process but they may be involved in transmembrane diffusion of anionic uncoupler. In the case of fatty acids, Skulachev (1988) has proposed that the protein component is involved in translocation of the fatty-acid anion across the membrane. The proteins in question are the ANC and the uncoupling protein (UCP).

1.3 Brown Adipose Tissue

The earliest known reference for brown adipose tissue (BAT) is probably that of Conrad Gessner (1551). He recognized it as a distinct tissue from white adipose tissue when examining the interscapular tissue of the marmot. The true role of BAT was not described until the 1960s when its function as a thermogenic effector was established (reviewed by Smith and Horwitz, 1969). BAT occurs unequivocally in mammals (Afzelius, 1970) particularly in newborn mammals that lack fur, including humans, as well as hibernating mammals. The phylogeny of BAT is still unknown, but it seems to be a tissue that has emerged late in the course of evolution, in parallel with the development of homeothermy and, more specifically, with the capacity for thermoregulation by non-shivering thermogenesis (Néchad, 1986).

We have known for a long time that the levels of ATP-synthase complex in BAT mitochondria are markedly lower than those in other tissues: the molar ratio of ATP-synthase molecules to respiratory chains in BAT is only 10% of the ratio that is seen in other tissues such as the heart (Cannon and Vogel, 1977). Oxidative processes predominate in BAT mitochondria. As not much ATP is made or work done, such as concentration of ions, this oxidation releases heat like combustion of any fuel. It is the burning of fuels such as fatty acids in BAT mitochondria that is the source of heat production in this tissue. While BAT accounts for only 1% of the body mass of a rat, it nevertheless accounts for approximately 50% of heat production in non-shivering thermogenesis in the cold-acclimated rat (Foster and Frydman, 1979; Foster, 1986).

The major reason for the brown colour of BAT is its extensive blood supply, although the high levels of mitochondrial cytochromes and flavin compounds also contribute to a lesser extent (Smith and Horwitz, 1969). BAT is served by blood vessels from major arteries and veins; in fact, the branching in the tissue is so extensive that each adipocyte is in contact with two or more capillaries (Néchad, 1986). This blood supply allows for a rich supply of oxygen and substrates to the mitochondria and for the efficient deployment of heat produced, otherwise the tissue would overheat!

BAT possesses a very rich sympathetic innervation, which is responsible for the rapid on-off control of its thermogenic function. The addition of noradrenalin to isolated brown adipocytes causes an increase in the respiratory rate of these cells. The β_3-adrenoreceptor is expressed mainly in white and brown adipocytes and this receptor is responsible for this increased respiratory rate. Noradrenalin binding causes an increase in cyclic AMP (cAMP), which, in turn, activates cAMP-dependent protein kinase (cAPK). cAPK phosphorylates triacylglycerol lipase, thereby causing an increase in free-fatty acids in the brown adipocyte (reviewed by Nicholls and Locke, 1984; see Figure 1.4).

The inherent uncoupledness of BAT mitochondria was noticed when they were first studied. Lepovsky *et al* (1959) studied P:O ratios in BAT mitochondria and compared them to the results obtained from liver mitochondria; they found the P:O ratio for BAT was almost zero and that of liver was 1.8 eventhough 'oxygen uptake was similar to that of the liver particles'. This uncoupling or lack of respiratory control would allow BAT mitochondria to respire at a much faster rate than liver mitochondria and therefore allow for the thermogenesis characteristic of BAT. If BAT mitochondria were under respiratory control, they would only be able to respire at a rate that justified regeneration of ATP used. Rafael *et al.* (1969) found that addition of purine nucleotides along with albumin restored respiratory control. The requirement for removal of fatty acids, for recoupling BAT mitochondria, was supported by the findings of Hittelman *et al.* (1969)

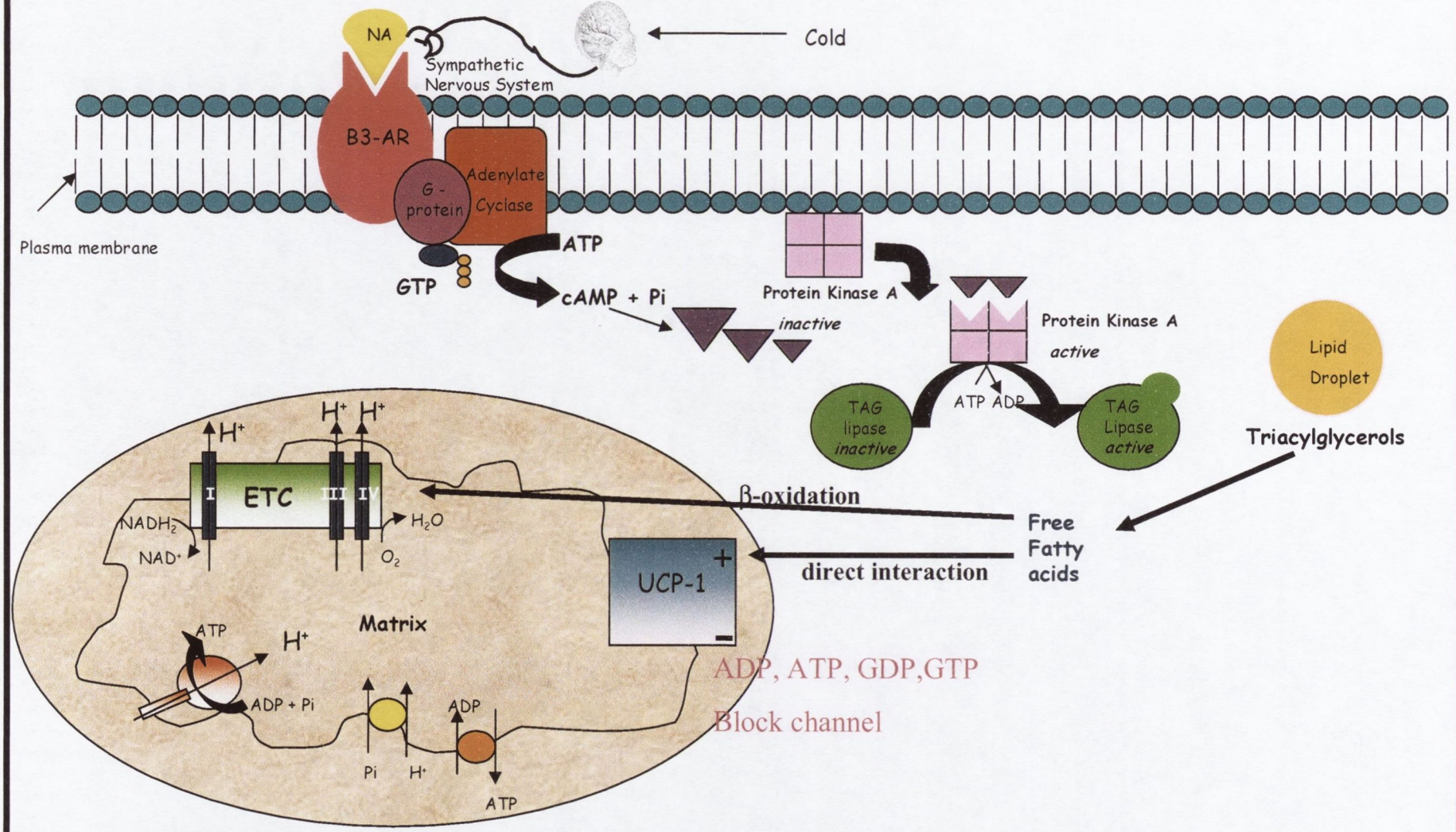


Figure 1.3: The mechanism of hormonally induced uncoupling of oxidative phosphorylation in brown fat mitochondria. Diagram reprinted with kind permission of Dr. Audrey Carroll.

when they used a combination of coenzyme A (CoA), ATP and carnitine to activate and promote the oxidation of the fatty acids.

In 1973, some classic swelling experiments on BAT mitochondria by Nicholls and Lindberg gave some very interesting results and more clues as to how these mitochondria supported their high respiration rate and thermogenesis. BAT mitochondria are permeable to Cl^- at neutral pH values. The swelling of mitochondria in KCl medium, following the addition of valinomycin, allows for the transport of K^+. So swelling could be driven by the entry of Cl^-. Liver or heart mitochondria do not show this Cl^- permeability. The swelling in KCl medium containing valinomycin could be inhibited by GDP but not by albumin. BAT mitochondria display a much higher permeability to H^+ than other mitochondria, such as those from liver. This increased H^+ permeability was shown by swelling mitochondria in KCl or NH_4Cl medium containing nigericin and, on inhibiting the swelling with albumin, swelling could be resumed on addition of an uncoupler. These discoveries were vital for understanding how BAT mitochondria worked.[1] This H^+ permeability was causing uncoupling of oxidative phosphorylation, which permitted the increased oxidation of fatty acids.

1.4 Uncoupling Protein 1 (UCP1)

The knowledge accumulated about BAT and its mitochondria drove researchers to seek the molecular basis of increased proton and chloride permeability. Nicholls (1976) described an atractylate-insensitive high-affinity, saturable, GDP binding site. At the same time, a prominent 32-kDa protein band was noted in sodiumdodecylsulfate polyacrylamide gel electrophoresis (SDS-PAGE) of BAT mitochondria that varied depending on the cold-adapted status of the animal (Ricquier and Kader, 1976). With this knowledge, UCP1 was identified using a photo-affinity analogue of ATP to

[1] It took them two years to realise the implications. As stated by Nicholls himself in 2001 "In the context of 1972, Peter Mitchell's chemiosmotic hypothesis was understood by very few mitochondriologists". This uncoupling caused by H^+ leak added more weight to Mitchell's argument proposed 12 years earlier (with no experimental proof!)

label the protein, and SDS-PAGE (Heaton *et al.,* 1978). Lin and Klingenberg (1980) purified the 32-kDa protein to 90% purity and it retained its GDP binding activity. Their method was based on their procedure for the isolation of the ANC using hydroxyapatite (HTP). The use of HTP chromatography is not fully understood but is known to be based on adsorption. It is assumed that HTP functions as a mixed-bed ion exchanger and, because of this, some carrier proteins do not bind at all as the large detergent shell associated with these proteins shields the charged amino acids (Kramer and Palmieri, 1989). Taking advantage of UCP1's stability at room temperature allowed for it to be separated from the ANC, which is partially denatured and adsorbed to HTP under conditions used by Lin and Klingenberg (1980). GDP binding studies on this purified protein indicated that the functional form is a homodimer. An ELISA demonstrated that UCP1 (or thermogenin as it was initially called) occurred exclusively in BAT mitochondria (Cannon *et al.,* 1982) and accounted for between 5 and 10% of total mitochondrial protein. More recently, in our laboratory, we have generated novel, well-substantiated results illustrating the presence of UCP1 mRNA and protein in thymus mitochondria and UCP1 protein in thymus cell (thymocyte) mitochondria (Carroll *et al.*, 2005). UCP1 expression was established using a commercially available (Calbiochem), polyclonal anti-UCP1 antibody. Sequence analysis studies on a purified sample of thymus mitochondria unequivocally revealed the occurrence of UCP1 (Carroll *et al.*, 2005).

1.4.1 Sequence and Structure of UCP1

UCP1 was sequenced in 1985 and was found to have 306 amino acids, with a calculated molecular mass (Mr) of 33,215 Da. UCP1 contains 42% polar residues with an excess of nine positive charges. The sequence is distantly homologous to many mitochondrial inner-membrane proteins, such as the ANC. More importantly, however, is the tripartite structure of these proteins, which comprises three similar sequences of ~100 residues each. A similarity can be seen between these three sequences, with

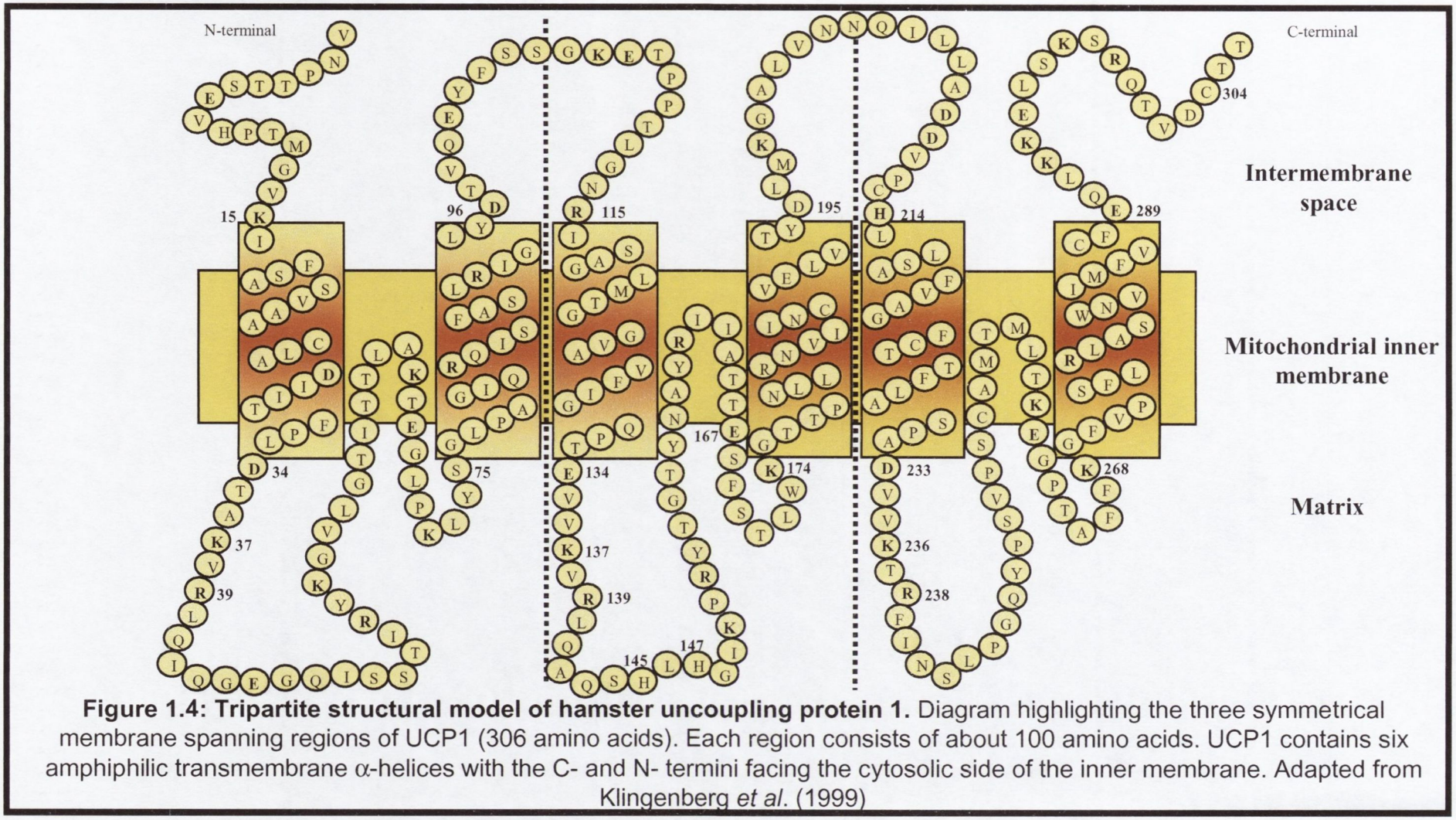


Figure 1.4: Tripartite structural model of hamster uncoupling protein 1. Diagram highlighting the three symmetrical membrane spanning regions of UCP1 (306 amino acids). Each region consists of about 100 amino acids. UCP1 contains six amphiphilic transmembrane α-helices with the C- and N- termini facing the cytosolic side of the inner membrane. Adapted from Klingenberg *et al.* (1999)

sequences 1 and 2 being particularly similar (Aquila, *et al.,* 1985). Examination of the sequence, and the use of chemical and immunological probes, has led to the proposed structure of six transmembrane helices with both the C- and N-termini protruding to the cytosolic side and three intermembrane loops between each pair of helices (Figure 1.4; Klingenberg *et al.,* 1999). There is a high degree of sequence homology between UCP1s from different species. For example, human and rat UCP1 are 79% identical (Klaus *et al.*, 1991).

1.4.2 Activation of UCP1

Noradrenalin, released from sympathetic terminals, activates BAT UCP1 in response to chronic overeating, cold exposure and β-adrenergic agonists (Ricquier *et al.*, 1986). The main role of BAT is to promote thermogenesis (*i.e.* UCP1 activation), cell division and UCP1 synthesis (Cannon *et al.*, 1996). It does this by creating a cascade of events culminating in UCP1 activation. Activation of surface β-adrenoceptors coupled via G-proteins to adenylyl cyclase leads to an increase in cAMP. cAMP typically activates protein kinase A (PKA), which acts to phosphorylate hormone-sensitive lipase, the enzyme that hydrolyses triacylglycerol (TAG) stores releasing free fatty acids (FFA), which activate UCP1 resulting in subsequent thermogenesis. FFA also activate cAMP-response-element-binding-protein (CREB), which stimulates transcription from the UCP1 gene (Palou *et al.*, 1998). UCP1 proton transport activity is inhibited by binding of purine nucleotides (GDP, GTP, ADP, ATP) to a specific site located on the outer leaflet of UCP1 itself. This action is also summarized in Figure 1.3.1.

1.4.3 Function and Mode of Action of UCP1

Work on BAT in the 1970s was instrumental in predicting UCP1's function in the mitochondrion. BAT UCP1 uncoupling of oxidative

phosphorylation is inhibited by purine nucleotides and activated by nanomolar amounts of FFAs and by long chain fatty-acyl CoA esters in isolated mitochondria (Nicholls and Rial, 1974). Direct evidence of the H^+ and Cl^- transport was available by reconstituting UCP1 into phospholipid vesicles. Klingenberg and Winkler (1985) described the H^+ activity while Strieleman *et al.* (1985) reported slow $^{36}Cl^-$ uptake. As Klingenberg and Winkler (1985) were unable to detect any Cl^- activity they interpreted the results of Strieleman *et al.'s* (1985) as being due to impurities. Ježek *et al.* (1990) finally confirmed the Cl^- transport and Ježek and Garlid (1990) went on to describe many competitive inhibitors of Cl^- transport. It seemed that the number of anions transported was much larger than suspected, but strong structural requirements of the anion were shown; monovalency, polar groups that were not attached to alkyl or aryl chains and transport that increased with hydrophobicity. One interesting fact is that no physiologically important anions have been shown to be transported by UCP1 (Ježek and Garlid, 1990).

The physiological relevance of transporting Cl^- is not apparent but the relevance of H^+ activity is and it became the focus of attention. Since Klingenberg and Winkler's (1985) reconstitution experiments, reconstitution became the best tool for deducing the molecular mechanism by which UCP worked. Fatty acids are indispensable when it comes to H^+ transport in UCP1 and this is agreed by most groups (Strieleman *et al.,* 1985b; Winkler and Klingenberg, 1994; Ježek *et al.,* 1994). A free carboxy group at the α-end of the fatty acid is also indispensable as this is where the H^+ will ultimately come from. When using the reconstituted system, high concentrations of fatty acids are required, up to 300 μM (Winkler and Klingenberg, 1994), so affinity for fatty acids seems to be low. Parallel with this low affinity is the lack of structural requirement. It would appear that the minimum requirement is hydrophobicity with a minimum chain length of C_{10}. Phenyl substitutions are tolerated as are hydrophilic substitutions as the ω-end (Winkler and Klingenberg, 1994). These facts of fatty-acid structure are agreed, as is the fact that UCP1 can uncouple by causing a net movement

of H^+ across the membrane. Exactly how UCP1 achieves this is where the dichotomy lies and there are two proposed mechanisms of action.

1.4.3.1 The fatty-acid protonophore mechanism of UCP-mediated H^+ flux.

This model of UCP uncoupling was first introduced by Vladimir Skulachev in 1991 and has been supported by Keith Garlid (Ježek *et al.,* 1994). In this model, UCP does not transport H^+ but translocates (or flip-flops) fatty-acid anions from the inner to the outer leaflet of the inner membrane. The transport is driven by the high, inside-negative, membrane potential. The fatty acid is now protonated and can rapidly flip-flop back to the inner leaflet unassisted, and deprotonation completes the cycle and therefore uncoupling. Thus, fatty acids act as cycling protonophores. The fatty acids act as the uncouplers as they bring the H^+ across the membrane. The transport of the fatty-acid anion is slow and restricts the cycle, but this is overcome by the protein flipping the anion. This mechanism implies that UCP can be considered a member of the anion transport family. This mechanism of action is summarized in Figure 1.4.2

Evidence favouring the fatty-acid protonophore model derives in large part from the discovery that alkylsulfonates ranging in alkyl chain length from C_1 to C_{16} are transported by UCP1 (Ježek *et al.,* 1990; Garlid *et al.,* 1996; Jabůrek *et al.,* 2001). Both the V_{max} and the apparent affinity ($1/K_m$) for transport increase with increasing chain length. Alkylsulfonates are competitive inhibitors of UCP-mediated Cl^- transport. UCP1 has been shown to transport undecanesulfonate (an inhibitor of Cl^- transport) with a similar K_m value to that which is shown with laurate (Garlid *et al.,* 1996). Undecanesulfonate is a strong acid analogue of laurate, with a pK_a of 2, so, at physiological pH values, it is always ionized. Undecanesulfonate does not support H^+ transport through UCP as it cannot pick up H^+, so, the uncoupling that we see with a fatty acid such as laurate doesn't happen with undecanesulfonate. A criticism that undecanesulfonate was forming a ternary complex in proteoliposomes with valinomycin and potassium ions

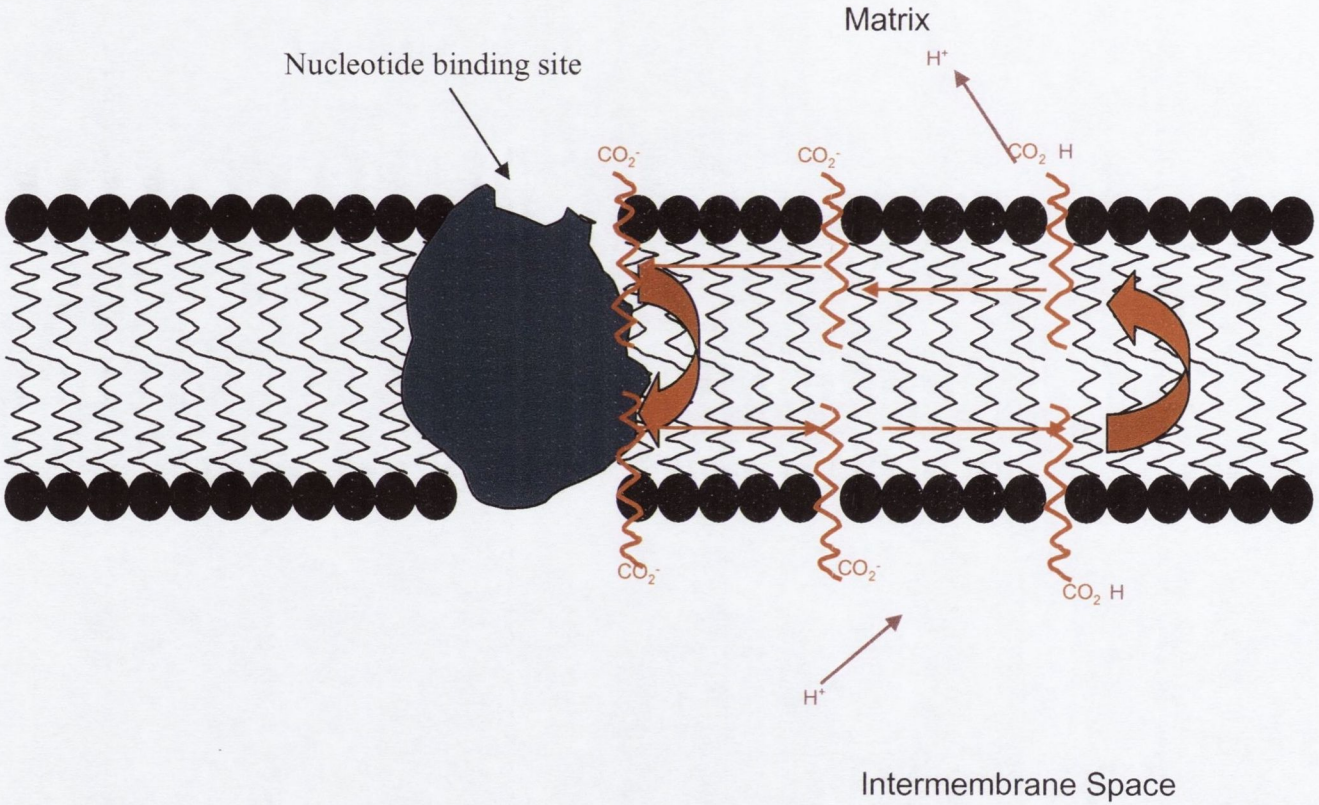


Figure 1.5 Schematic representation of the fatty acid protonophore model of UCP action
In this system fatty acids act as cycling protonophores. The protonated fatty acid flip-flops across the membrane to deliver a H^+ to the matrix. UCP1 then delivers the anion of the fatty acid back to the intermembrane space.

was answered by using a H^+ gradient and carbonyl cyanide *m*-chlorophenylhydrazone (CCCP, a protonophore; Jabůrek *et al.,* 2001). Undecanesulfonate can be converted into a pseudo fatty acid. Using the amphiphilic amine, propranolol, undecanesulfonate takes place in ion-pair transport with an H^+ across the proteoliposomes. Due to the ion-pair, undecanesulfonate can support H^+ movement across the liposome (Jabůrek *et al.,* 2001). Flip-flop-incapable fatty acids have been identified such as dodecanedioic acid (Ježek *et al.,* 1997a). In turn, Ježek *et al.* (1997b) have shown dodecanedioic acid incapable of supporting UCP1 H^+ activity. The fact that flip-flop incapable fatty acids do not support H^+ activity argues that the ability to flip-flop is a requirement for UCP1 function.

1.4.3.2 The fatty-acid buffering mechanism of UCP-mediated H^+ flux.

The fatty-acid buffering model predicts the direct H^+ transport by UCP (Winkler and Klingenberg, 1994). In this model, fatty acids donate H^+, by way of their carboxy group, to H^+-conducting amino acids of the protein itself, which then pass the H^+ to the matrix, a process that is driven by the membrane potential. When protonated, the fatty acid, can enter the protein and deliver the H^+ and the protein gives the fatty-acid anion a route so that it can return to the surface to pick up another H^+, due to its high pK_a. Thus, the energy for stripping a H^+ of its large hydration shell is overcome by the H^+ affinity of the membrane-bound fatty acid. This mechanism of action is summarized in Figure 1.4.3

There is also evidence that the buffering mechanism can be neutralised. Site-directed mutagenesis of histidines 145 and 147 or of aspartate 27 or 210 drastically reduces the H^+ transport of UCP1 (to about 10%) without affecting Cl^- transport (Bienengraeber *et al.,* 1998). All of these amino acids contain H^+-dissociating groups that facilitate the movement of H^+ down the protein. Aspartate 210 is localised on the cytosolic side, has a low pK_a value that allows it to accept and deliver the H^+ into the UCP channel. The carboxy group of the fatty acid can then accept the H^+ and donate it to further acceptors, such as histidine 145. These experiment

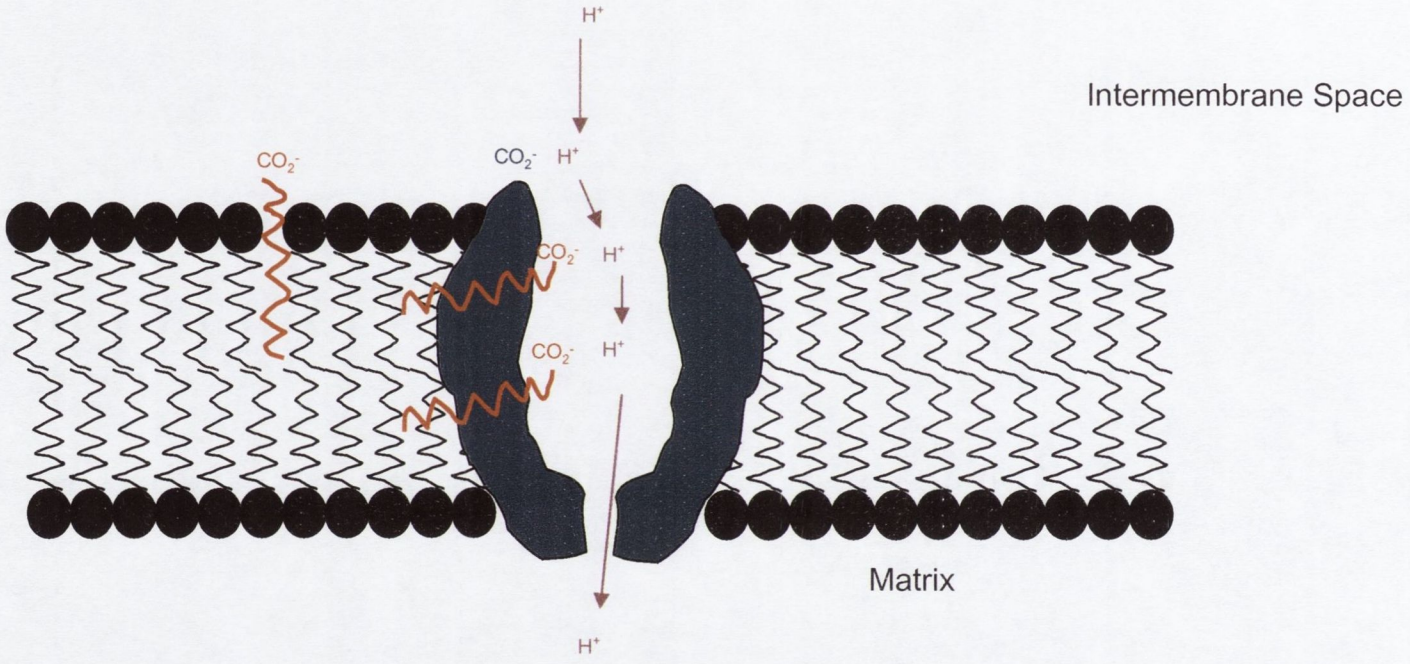


Figure 1.6 Schematic representation of the fatty-acid buffering model of UCP action
The fatty acid penetrates from the lipid phase with its carboxy group into the H^+ translocation path. Here it acts as a H^+ donor–acceptor between resident carboxy groups of the UCP. The H^+ is passed down the path and the $\Delta\Psi$ drives the H^+ into the matrix.

dissociate the uncoupling activity from anion transport whereas the protonophore method claims that anion transport is essential for uncoupling. Other experiments dissociated anion transport from uncoupling were that when *E. coli* expressed UCPs were first reconstituted they were incapable of H^+ activity but were still capable of transporting Cl^- (Echtay *et al.*, 1999). The mutation E167Q diminished Cl^- transport in *S. cerevisiae* but H^+ activity was still intact. The claim that flip-flop of the anion by the protein is essential was disputed by the fact that ω-glucopyranoside palmitic acid (glucose-*O*-ω-palmitate) can support uncoupling through UCP1 proteoliposomes (Huang and Klingenberg, 1999). This fatty acid derivative should not be able to flip with the ω-glucopyranoside terminal through the membrane since it remains anchored at the membrane surface. However, no original data were ever presented to substantiate this report nor has the synthesis, purity or stability of the resulting glycolipid ever been reported. Skulachev's initial proposal of the fatty acid protonophore model originates from some evidence that the ANC in mitochondria facilitates a small fatty-acid-dependent uncoupling that was related to the anion transport capability of the ANC. This model appears to be widely accepted in the literature, eventhough there is no evidence that the ANC transports fatty acid anions (Klingenberg and Echtay, 2001).

1.5 UCP Homologues

1.5.1 Uncoupling Protein 2

Using primers to UCP1, a novel homolog, UCP2 was discovered (Fleury *et al.,* 1997). Further analysis indicated that this novel UCP shared 59% sequence homology with UCP1 (in rats) and had an approximate molecular mass of 30 kDa (Fleury *et al.*, 1997). Northern blot analysis of mouse, rat and human tissues showed widespread expression of UCP2 mRNA in a number of tissues, including white adipose tissue (WAT), BAT, skeletal muscle, heart, placenta, brain, stomach, kidney, lung, female reproductive tract, myocytes, lymphocytes, macrophages and the Kupffer

cells of liver (Fleury *et al.*, 1997; Gimeno *et al.*, 1997; Larrouy *et al.*, 1997; Nègre-Salvayre *et al.*, 1997; Gong *et al.*, 1997; Boss *et al.*, 1998a; Hodný *et al.*, 1998; Ricquier & Bouillaud, 2000; Pecqueur *et al.*, 2001; Pedraza *et al.*, 2001; Krauss *et al.*, 2002; Horvath *et al.*, 2003; Rousset *et al.*, 2003). Conversely, UCP2 protein is only found in mouse and rat spleen, lung, stomach, kidney, thymus, WAT, pancreatic islets, macrophages and thymocytes (Ricquier & Bouillaud, 2000; Echtay and Brand, 2001; Pecqueur *et al.*, 2001; Zhang *et al.*, 2001; Krauss *et al.*, 2002; Medvedev *et al.*, 2002). The highest protein levels of UCP2 have been detected in spleen mitochondria. However, these levels are still 160-fold less than levels of UCP1 found in BAT mitochondria (Pequeur *et al.,* 2001).

Several physiological states have been shown to increase UCP2 mRNA levels in rodents. These include cold exposure (Boss *et al.*, 1997b), 48-h starvation (Boss *et al.*, 1997b) and leptin administration (Zhou *et al.*, 1997). The administration of lipopolysaccharide (LPS) and starvation have been shown to increase UCP2 protein expression in lung and stomach (Pecqueur *et al.*, 2001).

1.5.2 Uncoupling Protein 3

While searching for UCP1 homologues in skeletal muscle, a third UCP was discovered. Uncoupling Protein 3 (UCP3), a mitochondrial inner - membrane protein, was molecularly cloned initially by Boss *et al.* (1997) and shortly thereafter by Vidal-Puig *et al.* (1997) and Gong *et al.* (1997). Their studies indicated that, unlike UCP1 and UCP2, UCP3 exists as two isoforms in humans, a long form ($UCP3_L$) and a short form ($UCP3_S$). The long form consists of 312 amino acid residues, while the short form consists of 275 amino acid residues. Like other mitochondrial carriers, UCP3 has six transmembrane domains (Boss *et al.*, 1997). $UCP3_S$ lacks the sixth potential trans-membrane region and putative nucleotide binding site implicated in control of coupling efficiency of UCP1. Therefore, $UCP3_S$ exerts its biological function without control by purine nucleotides. Human UCP3

(hUCP3) has 71% sequence homology to hUCP2, and 57% sequence homology to hUCP1 (Vidal-Puig *et al.*, 1997) but is much less homologous to other members of the mitochondrial carrier super-family *e.g.* oxoglutarate carrier (~32% identical) and phosphate carrier (~25% identical).

UCP3 mRNA is expressed in skeletal muscle of humans (Vidal-Puig *et al.*, 1997). Rodents express UCP3 in skeletal muscle, BAT, spleen and thymus (Gong *et al.*, 1997; Carroll and Porter, 2004). UCP3 mRNA is most abundantly expressed in BAT. UCP3 protein has been detected in mouse and rat skeletal muscle (Ježek *et al.*, 1999; Gong *et al.*, 2000; Li *et al.*, 2000; Zhou *et al.*, 2000; Vidal-Puig *et al.*, 2000; Cadenas *et al.*, 2002; Harper *et al.*, 2002; Cunningham *et al.*, 2003; Hesselink *et al.*, 2003), BAT mitochondria (Ježek *et al.*, 1999; Gong *et al.*, 2000; Li *et al.*, 2000; Harper *et al.*, 2002; Cunningham *et al.*, 2003) and rat spleen and thymus mitochondria (Carroll and Porter, 2004). The expression of UCP3 in two such thermogenic tissues as skeletal muscle and BAT, and its relative lack of expression in other tissues such as heart (Boss *et al.*, 1997), are consistent with a possible role for UCP3 as a mediator of adaptive thermogenesis. However, it must be pointed out that despite speculation, the biological function of UCP3 is not known.

UCP3 expression is regulated by known stimuli such as thyroid hormone, β_3-adrenergic agonists, starvation, leptin administration and exercise. Thyroid hormone (T3) stimulates increased UCP3 mRNA expression in rat skeletal muscle (Lanni *et al.*, 2003; Schrauwen and Hesselink, 2003; Queiroz *et al.*, 2004; Silvestri *et al.*, 2005). In addition, UCP3 protein expression is increased in skeletal muscle from hyperthyroid rats compared to euthyroid controls (Cunningham *et al.*, 2003). Hypothyroidism in rat skeletal muscle decrease mRNA expression of UCP3. β-Adrenergic stimulation of adipose cells causes lipolysis and thermogenesis (Gong *et al.*, 1997). This is mediated largely by β_3-adrenergic receptors (Collins *et al.*, 1994). The selective β_3-adrenergic agonist CL214613 was shown to increase rat UCP3 mRNA levels in WAT but not in BAT (Gong *et al.*, 1997). In addition, β-adrenergic stimulation of

L6 myotubes (skeletal muscle cell line) with adrenalin was shown to increase UCP3 mRNA levels transiently (Nagase *et al.*, 2001). Starvation has been shown to increase UCP3 protein expression levels in mouse and rat skeletal muscle mitochondria (Boss *et al.*, 1998a; Cadenas *et al.*, 1999; Sivitz *et al.*, 1999; Moreno *et al.*, 2003). In addition, starvation was shown to increase UCP3 protein expression in thymus and spleen (lymphocyte) mitochondria (Carroll and Porter, 2004). Elevation of free fatty acids by lipid infusion, proposed as a starvation-imitating condition, also increases UCP3 gene expression in vivo (Weigle *et al.*, 1998) and in vitro (Hwang and Lane, 1999) in C_2C_{12} cells. High-fat diets increased UCP3 protein expression in skeletal muscle mitochondria by approximately 40%, compared to low fat diets (Hesselink *et al.*, 2003). Refeeding on a high-fat diet resulted in a two-fold increase in UCP3 protein expression (Crescenzo *et al.*, 2003). Leptin administration increases UCP3 mRNA in skeletal muscle and BAT of genetically obese (ob/ob) mice (lack functional leptin) (Gong *et al.*, 1997).

1.5.3 Uncoupling protein 4

More recently, a fourth UCP (UCP4) has been identified (Mao *et al.*, 1999). UCP4 is a 36 kDa protein of 323 amino acids. UCP4 is 29, 33 and 34% homologous to UCP1, UCP2 and UCP3, respectively. UCP4 transcripts are exclusively expressed in both foetal and adult brain tissues.

1.5.4 Uncoupling protein 5

A fifth, novel, brain mitochondrial carrier protein exhibiting mitochondrial uncoupling activity was cloned when expressed in yeast (Sanchis *et al.*, 1998). UCP5 is also termed brain-specific mitochondrial carrier protein or BMCP-1. UCP5 mRNA expression is widespread in the brain, with some expression in testis, heart, kidney, and uterus (Yu *et al.*, 2000). The UCP5 isoforms that have been discovered are a short form ($UCP5_S$), a short form with insert ($UCP5_{SI}$) and a long form ($UCP5_L$).

1.5.4 Plant Uncoupling Proteins

Other members of the uncoupling protein family have been found in plants including *Solanum tuberosum* uncoupling protein (StUCP) in potatoes (Laloi *et al.*, 1997). Vercesi *et al.* (1995) discovered a plant uncoupling protein (PUMP) in potato tubers. cDNAs of a UCP homologue present in *Arabidopsis thaliana* were also cloned and referred to as AtUCP or AtPUMP (Maia *et al.*, 1998). Costa *et al.* (1999) identified PUMP in tomatoes. Interestingly, using antibodies against plant UCP, Jarmuszkiewicz *et al.* (1999) detected a mitochondrial uncoupling protein in the non-photosynthetic soil amoeboid protozoan *Acanthamoeba catellanii.* Similarly, Jarmuszkiewicz *et al.* (2000) identified an uncoupling protein in mitochondria from *Candida parapsilosis* (CpUCP), a non-fermentative parasitic yeast. Recently, a new protein named avUCP, which shares 70% amino-acid identity with both UCP2 and UCP3, was identified in chicken skeletal muscle (Raimbult *et al.*, 2001).

Table 1.1: Summary of structure, function and location of the three principal uncoupling proteins

	Structure	Location	Function
UCP1			
	32 kDa protein	Brown adipose tissue	Heat production
	306 amino acids	Thymus	Unknown
UCP2	30 kDa protein	Macrophages, Spleen, Gut,	Unclear
	309 amino acids	Lung, WAT,	
		Pancreatic islets, Thymus,	
		Thymocytes, Kidney	
UCP3	34 kDa protein	Skeletal muscle	Unclear
	312 amino acids	BAT of rodents	
		Spleen	
		Thymus	

1.6 *Expression of membrane proteins in E. coli*

E. coli is often the organism of choice for expression of most soluble proteins. However, membrane protein overexpression in *E. coli* can prove difficult and eukaryotic membrane protein expression levels are generally far below those that have been achieved for globular proteins (Schertler, 1992). However, prokaryotic membrane proteins have been expressed to high levels in *E. coli,* e.g. the fucose-H^+ symporter has been overexpressed to provide levels up to 20% of membrane protein (Gunn *et al.,* 1994). The successful overexpression of this protein and others like it is likely to be due to its bacterial origin.

Functional eukaryotic membrane protein overexpression in *E. coli* has only been achieved in a few examples (reviewed by Grisshammer and Tate, 1995). Possible reasons for poor expression of membrane proteins in

general include inefficient codon usage, poor translational initiation and instability of the mRNA transcript or the target protein. Although the expression of a membrane protein in its functional state with insertion into the cell membrane is desirable, it appears that *E. coli* has a limited capacity to incorporate polytopic proteins into its cytoplasmic membrane. Expression of membrane proteins can often prove toxic to the cell, resulting in a low level of unstable recombinant protein. The deleterious effect on cell growth and viability of membrane protein expression usually arises when the recombinant protein is associated with the bacterial membranes, which results in the expressed protein being found in inclusion bodies. Deposition as inclusion bodies is generally less, or non-toxic (Fiermonte *et al.,* 1993).

High level expression of certain polytopic eukaryotic membrane proteins can be observed but usually, in the form of inactive insoluble aggregates or inclusion bodies. A protein that accumulates to high levels as inclusion bodies can be conveniently isolated. However, refolding is necessary if functional analysis is to be performed. Mitochondrial membrane proteins tend to be overexpressed in inclusion bodies. For example, the bovine mitochondrial oxoglutarate carrier has been expressed with a yield of 10 – 15 mg/l of culture and, following disaggregation of inclusion bodies with n-dodecanoylsarcosine, the carrier could be reconstituted into liposomes in an active state (Fiermonte *et al.,* 1993).

1.6.1 Expression of UCPs in *E. coli*

As mentioned before, all of the UCPs have been cloned so expression in *E. coli* was possible. Echtay *et al.* (1999) first expressed haUCP1 and hUCP3 and reported them to be expressed as inclusion bodies. Jabůrek *et al.* (1999) went on to overexpress hUCP2 and rUCP1 (Jabůrek and Garlid, 2003). To date, there has been no recorded overexpression of hUCP1.

1.7 Reconstitution

Once a membrane protein can be purified its reconstitution into artificial membranes is essential prior to identification, detailed functional characterization and structural studies. Reconstitution allows for the study of membrane proteins in isolation. Biological membranes are dynamic places and in particular, the inner membrane of mitochondria, which is made up of 75% protein and only 25% lipid. In this situation it can be difficult to measure the activity of one protein. Respiratory-chain complexes have been studied by reconstitution into phospholipid vesicles and such studies have provided insights into the transport/activity of these proteins (e.g. Ragan and Hinkle, 1975). There are many methods for reconstitution into these vesicles:

(i) Organic solvent-mediated reconstitutions is a method whereby a solution of a protein-lipid complex in apolar solvent is evapourated, rehydrated in aqueous buffer and purified by sedimentation through sucrose (e.g. Darzon *et al.,* 1980). This method gives rise to multilamellar structures that are inhomogeneous and therefore not suitable for use with more hydrophilic membrane proteins. The liposomes produced also tend to be large and osmotically fragile, so detailed studies in this system can be very difficult. Some successful reconstitutions of rhodopsin (Darszon *et al.,* 1979) and bacteriorhodopsin (Rigaud *et al.*, 1983) have been reported.

(ii) *Mechanically-mediated reconstitutions* are used when dry phospholipids are swollen in aqueous buffer to form multilamellar vesicles. These vesicles can then be used to form small unilamellar vesicles (SUVs) by mechanical manipulation; freeze-thaw cycles, French press or sonication. If protein is present, it will be incorporated into the new vesicles. No detergent is required but reproducibility is bad and proteins are easily damaged (reviewed by; Lasic, D.D., 1988). Successful reconstitution of the D-glucose carrier from red blood cells has been reported with this method (Kasahara and Hinkle, 1977)

(iii) *Direct incorporation in to preformed liposomes* involves the spontaneous incorporation of membrane proteins into preformed liposomes

in the presence of low detergent concentrations or well defined lipid composition (Racker, 1972; Eytan and Broza, 1978). This method has the advantage of uni-directional insertion but a heterogeneous distribution and impurities (like detergent) are required that affect permeability.

(iv) *Detergent-mediated reconstitution* involves solubilization of proteins with phospholipids and then removal of the detergent to form bilayer vesicles. Detergents with high critical micellar concentrations (CMCs) are used as they are removed easily by dialysis (following dilution), size-exclusion chromatography or detergent adsorbing resins (SM_2, Bio-Beads or Amberlite XAD). Most membrane proteins are isolated with the use of detergents so this method of reconstitution marries well. Non-ionic detergents are used, such as Triton X-100, ethylene ether detergents, *n*-octylglucoside or 3-[(3-cholamidopropyl)dimethylammonio]-1-propane-sulfonate. The principle is based on detergent-removal being the mirror image of solubilization – *i.e.,* gradual removal of detergent from a micellar lipid-detergent solution should lead to reassociation of lipids into a closed bilayer (Rigaud *et al.,* 1995). The advantages are rapidity and homogeneity but there can be incomplete incorporation. This has been the preferred method of UCP1 reconstitution (Bouillaud *et al.,* 1983; Strieleman *et al.,* 1985a; Winkler and Klingenberg, 1985; Jezek *et al.,* 1990).

1.7.2 Reconstitution of UCPs

Reconstitution of UCPs into phospholipid vesicles was inevitable and one of the first groups to perform UCP reconstitution was Bouillaud *et al.* (1983), who demonstrated very slow H^+ activity and little inhibition by GDP. The method for UCP1 that is widely used today was developed by Martin Klingenberg and Edith Winkler in 1985. Here, H^+ activity was very high but Cl^- activity was undetectable. Strieleman *et al.* (1985), demonstrated both H^+ and Cl^- activity and their reconstitution was the first to show the interaction between the protein and fatty acids directly.

Initially H^+ activity/movement was measured using pH electrodes (Bouillaud *et al.,* 1983) and radiolabelled chloride ($^{36}Cl^-$) was used to measure chloride efflux/accumulation (Strieleman *et al.,* 1985a). Fluorescent probes have now been found to be much better measures of transport and provide greater ease and an improved signal to noise ratio. For H^+ activity, a direct pH sensor, pyranine (Echtay *et al.,* 1997) or a TES anion sensor, 6-methoxy-*N*-(3-sulfopropyl) quinolinium (SPQ; Jezek *et al.,* 1994) are used at present. UCP1 activity regarding Cl^- can be measured directly using either SPQ or *N*-(ethoxycarbonylmethyl)-6-methoxyquinolinium bromide (MQAE) (Echtay *et al.,* 1997). Another probe, potassium-binding benzofuran isophthalate (PBFI), has also been used to show charge transfer across the membrane. It fluoresces with K^+, which can only move with co-transport of an anion or exchange with a cation (Garlid *et al.,* 1996). The systems of reconstitution of UCP1 used in this thesis are summarised in Figures 7.1.1 and 7.1.2.

Vesicles are formed by detergent-mediated reconstitution. The orientation of the protein can depend on (i) the detergent used, (ii) the speed of removal of detergent, (iii) the phospholipids present or (iv) the ionic composition of media.UCP1 can bind GDP from one side of the membrane only and, due to this it can be orientated in two ways following reconstitution. Many differences in orientation have been reported, from 90% GDP-binding site on the outside (Klingenberg and Winkler, 1985) to a 50:50 mix of orientations (Ježek *et al.,* 1990). However, orientation does not matter as transport can happen in both directions with the electric gradient modulating the protein's activity (Klingenberg and Winkler, 1985). In all systems, H^+ movement is induced by generating a membrane potential, usually by using a K^+ diffusion gradient that is dependent upon the addition of valinomycin.

1.7.2.1 Reconstitution of expressed UCPs

UCPs expressed in *E. coli* are in the aggregated form of inclusion bodies (Section 1.6.1). These proteins require solubilization and refolding

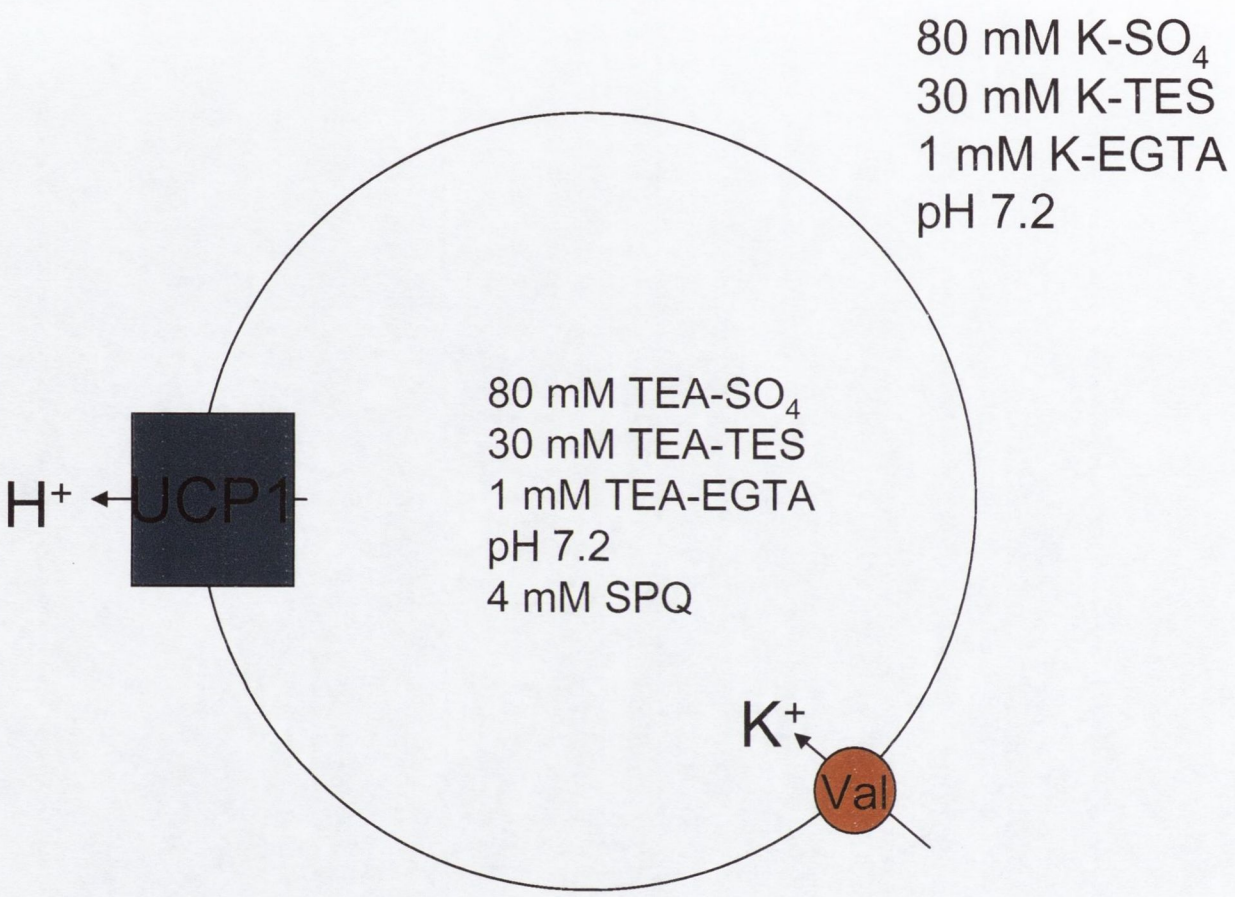


Figure 1.7 Measurement of H^+ activity of UCP1 using the fluorescent probe SPQ and a K^+ diffusion potential
The potassium ionophore valinomycin allows the inward flux of K^+ in response to the outward flux or another cation (or inward flux of anion). As TES buffer loses H^+, the concentration of TES anion increases. The TES anion quenches The fluorescence of SPQ.

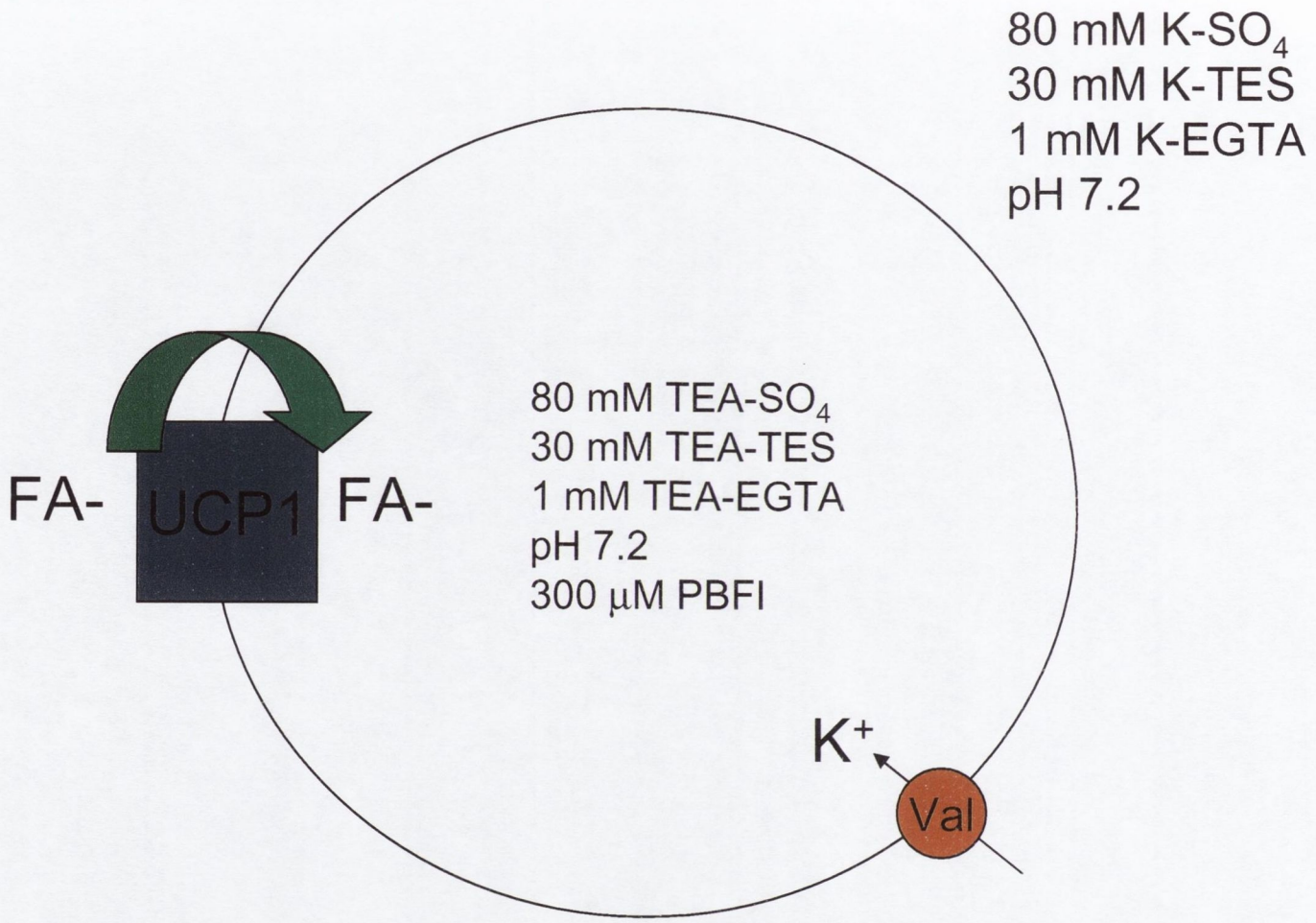


Figure 1.8 Measurement of K^+ flux in UCP-containing liposomes
The potassium ionophore valinomycin allows the inward flux of K^+ in response to the proposed inward transport of fatty acid anion. As the fluorescent probe PBFI binds K^+, the fluorescence increases.

before reconstitution. This manipulation of the protein can lead to problems regarding correct folding and, therefore, function. The first record of bacterially-expressed UCP1 and UCP3 being reconstituted showed that Cl^- activity was intact but there was no detectable H^+ activity. This sparked belief that the protein was in its correct conformation but was not working properly. Jabůrek *et al.* (1999) then showed hUCP2 and hUCP3 to be functionally active with respect to H^+ activity but inhibition by ATP was very poor. hUCP2 and hUCP3 were fully active in the presence of 100 μM ATP a concentration that would inhibit 100% of UCP1 activity! An important cofactor for H^+ transport in UCP1 was thought to be coenzyme Q (CoQ). On addition of CoQ along with fatty acid, full H^+ activity is recovered, which is highly sensitive to GDP and is only activated by oxidized CoQ (Echtay *et al.*, 2000). The need for CoQ in reconstition experiments with hUCP2 and hUCP3 was also shown (Echtay *et al.* 2001). Certain control experiments, involving the solvent for CoQ, were not performed in these studies. However, using careful refolding techniques before reconstitution, Jabůrek and Garlid (2003) demonstrated fully active rUCP1, hUCP2 and hUCP3 in the reconstituted system. In their system there was no need for the addition of CoQ, and the uncoupling activity was comparable to that of native UCP1. All proteins were inhibited by low amounts of ATP.

1.8 UCPs and reactive oxygen species

Transfer of electrons to oxygen in electron transport by cytochrome oxidase occurs one electron at a time. However, upstream of Complex IV, in Complex III and Complex I, electron transfer is rarely 100% complete, generating incompletely reduced oxygen species. These oxygen species include superoxide, hydrogen peroxide (H_2O_2) and the hydroxy radical. In addition, some enzymes, such as monoamine oxidase and amino acid oxidase, generate H_2O_2 directly. Superoxide, H_2O_2 and hydroxy radicals are more reactive than oxygen, so they are referred to collectively as reactive

oxygen species (ROS). Large-scale production of ROS has the potential to inflict considerable damage on the tissues in which they are produced.

Excluding phagocytosis, the majority of ROS are generated by the mitochondrial electron transport chain (Boss *et al.*, 2000). Using isolated mitochondria, it has been shown that production of ROS is greatly increased at times when the proton electrochemical gradient is high. Such conditions occur during state 4 respiration in isolated mitochondria when ADP is unavailable. The addition of ADP, which causes proton transport via ATP synthase and, consequently, decreases the electrochemical gradient, or an uncoupling agent, which directly decreases the electrochemical gradient, strongly suppress the formation of superoxide anion (Skulachev, 1998). It has been suggested that, under conditions that induce increased ROS production, such as cold exposure (Kaushik and Kaur, 2003; Venditti *et al.*, 2004) and endurance exercise (Du *et al.*, 1998; Bejma and Ji, 1999), UCP2 and UCP3 may function as 'mild' uncouplers of oxidative phosphorylation in order to relieve oxidative stress (Skulachev, 1996). To date, there is a limited amount of evidence supporting the possibility that UCP2 and UCP3 function to limit ROS production via 'mild' uncoupling. Firstly, UCP3 protein expression has been shown to increase following 8-weeks of cold exposure (Cunningham *et al.*, 2003). Secondly, it has previously been shown that the absence of UCP3 led to an increase in ROS production, thereby implying a role for UCP3 in preventing the formation of ROS in skeletal muscle (Vidal-Puig *et al.*, 2000). Thirdly, superoxide generated using xanthine and xanthine oxidase has been shown to increase H^+ transport through UCP1, UCP2 and UCP3 in a reaction that is inhibited by nucleotides, including GDP (Echtay *et al.*, 2002b). Fourthly, Nègre-Salvayre *et al.* (1997) showed that membrane potential and H_2O_2 production were increased in mitochondrial fractions isolated from UCP2-containing tissues (BAT, thymus and spleen) when pre-incubated with GDP leading the authors to suggest that their results may indicate that UCP2 acts as a regulator of H_2O_2 production in mitochondria. Finally, it has been shown that the GDP-sensitive H^+ conductance catalysed by UCPs increases on exposure to

superoxide (Echtay *et al.*, 2002), or to lipid peroxidation breakdown products such as 4-hydroxy-2-*trans*-nonenal (HNE) (Echtay *et al.*, 2003). These findings support the hypothesis that UCPs may function to limit ROS production.

1.9 Aims of this study

- to subclone and overexpress hUCP1, hUCP2 and hUCP3
- to characterize antibodies for UCP1, UCP2 and UCP3
- to reconstitute native UCP1
- to use modifications of the ω-end of palmitate to reinvestigate the buffering model of UCP mechanism
- to use undecanesulfonate to investigate the molecular action of UCP1
- to reconstitute hUCP1 and investigate its kinetic parameters.

Chapter Two
Materials and Methods

2.1 Materials

2.1.1 General Chemicals and Conditions

Unless otherwise stated all chemicals were supplied by Sigma and were of the highest grade available. The full names and addresses of suppliers are listed at the end of this section. All solutions were prepared using pure deionized water. Room temperature (rt) was 20 ± 5° C. All pH values are those obtained at 25°C.

Product	Supplier
Agarose	Promega
Amido Black 10B	Bio-Rad
Bacto-Agar	Becton Dickinson
BamH1	Promega
Bio-Beads SM-2	Bio-Rad
1kb DNA Ladder	Promega
ECL	Amersham
EcoR1	Promega
Hydroxylapatite	Bio-Rad
Millipore filters (0.45 μm pore size, 24 mm diam.)	Millipore
Mini-PROTEAN III Electrophoresis Cell	Bio-Rad
Mini-Trans Blot Electrophoretic Transfer Cell	Bio-Rad
Nde1	Promega
PBFI	Molecular Probes
Peptide Antibodies	Eurogentec
Prestained Protein Markers, Broad Range	New England Biolabs
Protogel (30% (w/v) Acrylamide: 0.8% (w/v) Bis-Acrylamide Stock Solution (37.5:1))	National Diagnostics
Qiagen® Plasmid Midi Kit	Qiagen
Qiagen® Hi Speed™ Plasmid Midi Kit	Qiagen
Rapid DNA Ligation Kit	Roche

Sac1	Promega
Sodium 1-undecanesulfonate	Lancaster
Sulfuric Acid	BDH
Syringe Barrels	Becton Dickinson
T4 DNA Ligase	Roche
Tryptone Peptone	Becton Dickinson
UVP white/UV Transilluminator	UVP Ltd.
Yeast Extract	Becton Dickinson

2.1.2 List of Suppliers

Amersham International plc, Amersham Place, Little Chalfont, Buckinghamshire HP7 9NA, UK

Becton Dickinson Microbiology Systems, Becton Dickinson and Co., Sparks, MD 21152, USA

Bio-Rad Laboratories Ltd., Bio-Rad House, Maylands Avenue, Hemel Hampstead, Hertfordshire HP2 7TD, UK

British Drug House (BDH) Chemicals LTD., Broom Road, Poole, Dorset, BH12 4NN, UK

Molecular Probes, INC., 4849 Pitchford Avenue, Eugene, OR 97402-9144, USA

NEW ENGLAND BioLabs UK Ltd., 73 Knowl Place, Wilbury Way, Hitchin, Hertfordshire SG4 OTY, UK

Promega Ltd., Delta House, Enterprise Road, Chilworth Research Centre, Southhampton, S01 7NS, UK

Qiagen Ltd., Boundry Court, Gatwick Road, Crawley, West Sussex RH10 2AX, UK

Roche Diagnostics Ltd., Bell Lane, Lewes, East Sussex BN7 1LG, UK

Sigma-Aldrich Company Ltd., Fancy Road, Poole, Dorset BH12 4QH, UK

UVP (Ultraviolet Products), 2066W 11th Street, Upland, CA 91786, USA.

2.2 Methods

2.2.1 Bacterial Strains, Culture Media and Plasmid Vectors

The culture media used included LB broth and LB plate medium, and these were prepared using the methods described in Sambrook *et al.*, (1989). In order to ensure that bacteria were growing optimally stocks were replated at least every 6 weeks. Long-term stocks were prepared in 35% glycerol, frozen in a -80° C freezer overnight in Styrofoam boxes and stored at -80°C.

Ampicillin (100 mg/ml), isopropyl-β-thiogalactosidase (IPTG, 1 M) and lysozyme (200 mg/ml) stocks were made up in sterile distilled water (SDW), filter-sterilized (0.2 μm pore size) and stored in aliquots at -20°C. Aliquots of phenlymethanesulfonyl fluoride (PMSF, 100 mM) were made up in isopropanol, filter-sterilized (0.2 μm pore size) and stored at 4°C, short-term or -20°C, long-term. RNase A stocks (25 mg/ml) were prepared as above, but it was necessary to boil aliquots for 15 min before storage to ensure that any residual DNase activity was removed.

All molecular-biology reagents were prepared as described in Sambrook *et al.* (1989), with autoclaving taking place at 121° C for 20 min.

The expression vector pET 21d was available commercially from Novagen. Incorporation of this vector confers resistance to 100 μg/ml ampicillin. The expression vector pET3a was a gift from Dr. Martin Klingenberg, Institute of Physiological Chemistry, University of Munich, Schillerstrasse 44, D-80336 Munich, Germany. Incorporation of this vector confers resistance to 100 μg/ml ampicillin.

E. coli strain JM109 was obtained from Sigma-Aldrich Company Ltd., Fancy Road, Poole, Dorset, BH12 4QH.

E. coli strain BL21 (DE3) pLysS was a gift from Dr. Jana Haase, Biochemistry Dept., Trinity College Dublin.

E. coli strain BL21-CodonPlus was a gift from Eleanor Dunne, Biochemistry Dept., Trinity College Dublin.

See table 2.1 for the genotypes of these bacteria.

Table 2.1 Genotypes of bacteria

Bacterium	Genotype
JM109	e14-(McrA-) recA1 endA1 gyrA96 thi-1 hsdR17(rK^- mK^+) supE44 relA1 D(lac-proAB) [F' traD36 proAB lacIqZDM15]
BL21 (DE3) pLysS	F^- ompT $hsdS_B(r_B^-m_B^-)$ gal dcm (DE3) pLysS (Cam^R)
BL21-CodonPlus(DE3)-RIL	E. coli B F^-ompT hsdS(rB-mdcm+ Tet^rgalλ(DE3)endA The [argU ileY leuW Cam^r]
Rosetta™ (DE3) pLysS	F^- ompT $hsdD_B(r_B^-m_B^-)$ gal dcm (DE3) pLysS/RARE (argU, argW, ilex, glyT,leuW, proL)

2.2.2 Purification of Plasmid DNA

2.2.2.1 Small-Scale NaOH/SDS lysis preparation from *Escherichia coli*

The selected colony was grown overnight in LB (5 ml), containing the required amount of antibiotics, at 37°C with agitation (300 rpm). Cells (1.5 ml) were pelleted at 12,000 x *g* for 1 min. Medium was aspirated off leaving the pellet as dry as possible. The pellet was then resuspended in 100 μl sterile GTE solution (25 mM Tris-HCl buffer, pH 8.0, 10 mM EDTA, 50 mM glucose) and left at room temperature for 5 min. 200 μl of freshly prepared cell lysis solution (0.2 N NaOH, 1% SDS in deionized water) was then added, gently mixed by inversion and left on ice for 5 min. 150 μl of ice-cold potassium acetate solution pH 4.8 was then added to neutralize the lysate. It was mixed by inversion and gentle vortexing for 10 s and was incubated on ice for 5 min. The lysed cells were then centrifuged at 12,000 x *g* for 5 min.

The supernatant was transferred to a fresh, sterile tube, avoiding the precipitate and 50 μg of RNase A were added and incubated at room temperature for 5 min. The supernatant was then extracted with and equal volume of phenol:chloroform:isoamyl alcohol (25:24:1, v/v/v) by vortex-mixing for 1 min and centrifuged at 12,000 x *g* for 5 min. The upper aqueous phase was transferred to another fresh, sterile tube. The aqueous phase was then extracted with an equal volume of chloroform:isoamyl alcohol (24:1, v/v), vortexed for 30 s and centrifuged at 12,000 x *g* for 2 min. The upper aqueous phase was transferred to a fresh sterile tube and 2.5 volumes of ice-cold 100% ethanol were added and then incubated at -80° C for 1 h. The precipitated DNA was pelleted by centrifugation at 12,000 x *g* for 5 min at 4°C and was washed with ice-cold 70% (v/v) ethanol. The pellet was dried at 50°C for 5 min or at room temperature for 30 min. The pellet was dissolved in 20 μl TE (10 mM Tris, 1 mM EDTA, pH 8.0) buffer or SDW was and stored at 4°C.

2.2.2.2 Midi-scale preparation from *E. coli*.

The selected colony was grown overnight in LB medium, (50 ml), containing the required amount of antibiotics, at 37°C with agitation (300 rpm). Cells were pelleted at 7,000 x *g* for 20 min at 4°C. Plasmid was purified using a QIAGEN® Plasmid Midi Kit or a QIAGEN® HiSpeed Plasmid Midi Kit. These kits were used according to the manufacturer's instructions. The kits are based on a modified alkaline lysis procedure followed by binding of plasmid DNA to QIAGEN anion-exchange resin under appropriate low-salt and pH conditions. The kits give highly pure plasmid DNA in TE buffer.

All plasmids were analysed on a 1% agarose gel containing 0.4 μg/ml ethidium bromide (EtBr) at 5 $V.cm^{-1}$ in Tris-acetate (TAE; 0.04 M Tris-acetate, 0.001 M EDTA) buffer and were visualised using a UVP white/UV Transilluminator.

2.2.3 Restriction Digests of Plasmid DNA

All plasmids were fully analysed for the presence of cDNA, encoding the required protein, using restriction endonucleases. Restriction digests were set up as outlined by the supplier of the enzyme (Promega) and are summarised in Table 2.2. In the case of double digests, two restriction enzymes were added. This mixture was then incubated at 37°C for 2–4 h. The digest was then stopped by heating the mixture to 65°C for 20 min. The restriction enzymes used to cut each cDNA sequence from the corresponding plasmid are outlined in Table 2.3.

Table 2.2: Composition of Restriction Digests

	Single Digest (μl)	Double Digest (μl)
SDW	10.5	10
Acetyl BSA (1 mg/ml)	2	2
10 x Enzyme Buffer	2	2
Restriction Enzyme 1	0.5	0.5
Restriction Enzyme 2	0	0.5
Plasmid DNA	5	5

Table 2.3: Restriction Enzyme Sites for Insertion of cDNA sequences of UCP and AAC genes

Plasmid	Restriction Enzymes
pET 21d – hUCP1	EcoR1 + Sac1
pET 21d – hUCP2	EcoR1 + Sac1
pET 21d – hUCP3	EcoR1 + Sac1
pET 3a – haUCP1	Nde1 + BamH1
pET 3a – ncAAC	Nde1 + BamH1

hUCP – human UCP

haUCP – hamster UCP

ncAAC – *Neurospora crassa* AAC

2.2.4 Purification of DNA fragments from Agarose Gels

cDNA fragments produced from restriction digests were electrophoresed on 1% agarose gels containing 4 μg/ml EtBr. The fragments were viewed over UV light and were excised using a sterile blade. The fragment was then purified using a Wizard® PCR Preps DNA purification system, according to the manufacturer's instructions.

2.2.5 Ligation

Ligation reactions were set up using a 3:1 ratio of insert to vector plasmid, which usually amounted to a total of 150–200 ng DNA. T4 DNA ligase from Promega was used which was supplied with its own 10x buffer. The ligation reaction took place in a volume of 30 μl at 4°C for 16 h with 1 unit of ligase/10 μl. However, the main ligation kit used was with the Rapid DNA Ligation Kit from Roche. The ratio of insert to vector of 3:1 was still used and the kit was followed as per the manufacturer's instructions.

2.2.6 Preparation and Transformation of Competent Cells

2.2.6.1 Preparation of fresh competent cells

A single colony of *E. coli* (JM109 or BL21 pLysS) cells was transferred to LB broth (5 ml) and incubated overnight at 37°C with agitation (300 rpm). The following day 500 μl of this culture was inoculated into fresh LB broth (50 ml) and incubated under the same conditions until the $O.D._{600}$ had reached 0.4-0.5 (in order for efficient transformation to occur, it is essential that the number of viable cells does not exceed 10^8/ml). The culture was then transferred to a sterile centrifuge tube and incubated on ice for 10 min. The cells were then centrifuged at 4,000 x *g* for 10 min at 4°C. The resulting pellet was resuspended in ice-cold calcium chloride (5 ml; 0.1 M) and was stored on ice. The cells were then harvested as before and

pellets resuspended in calcium chloride (2 ml; 0.1 M). Aliquots (200 μl) of these cells were used in transformations that were carried out on the same day.

2.2.6.2 Transformation of Competent Cells

DNA (10 ng) was added in a volume not amounting to more than 5% of the 200 μl aliquots of competent cells. The contents of the tube were mixed by gentle swirling and then stored on ice for 30 min. The cells were heat-shocked by incubation at 42°C for 2 min and were then cooled on ice for a further 2 min. LB broth (1 ml) was added to the tube and the cells were incubated at 37°C for 1 h, to allow the cells to recover. The cells were then plated onto LB plates containing 100 μg/ml ampicillin and were incubated at 37°C overnight. Colonies were then screened for the required insert.

2.2.7 Expression of protein and isolation of Inclusion Bodies from *E. coli.*

2.2.7.1 Expression of Protein.

A colony of *E. coli* cells, BL21 pLysS or Rosetta pLysS (Novagen), which has been transformed with the appropriate plasmid (pET3a or pET21d) containing cDNA for UCP or AAC was inoculated into 5 ml of LB medium containing ampicillin (100 μg/ml) and the culture was grown overnight at 37°C at 300 rpm. The following day, 1 ml of this culture was kept for isolation of plasmid and the remaining 4 ml were diluted to 500 ml and left to grow under the same conditions as before until the OD_{600} had reached between 0.4 – 0.8. The culture was then removed from the incubator and left at room temperature for 30 min. Induction of expression was carried out with 1 mM IPTG. 6 h following the addition of IPTG, the cells were harvested by centrifugation at 10,000 x *g*. The bacterial pellets were then frozen at -20°C for at least an hour but usually overnight.

2.2.7.2 Isolation of Inclusion Bodies.

Frozen bacterial pellets were thawed and completely resuspended in 20 ml solution A (50 mM Tris-HCl, 25% sucrose, pH 8.0) per gram of wet pellet. Lysozyme (200 μg/ml) was added and the cells were incubated at room temperature with gentle agitation for 30 min. After the addition of 10 mM EDTA, 1.5% Triton X-100 (TX-100), 1 mM DL-dithiothreitol (DTT) and 1 mM PMSF. Lysis was achieved using a sonicator (Braun). The suspension was sonicated at 120 Watts for a total of 5 min at 50% duty, on ice. The solution was then centrifuged at 47,200 x g for 30 min at 4° C. The pellet was then resuspended in the same volume of solution B (10 mM Tris-HCl, pH 8.0 containing 1 mM EDTA, 1 mM DTT and 1 mM PMSF) and centrifuged at 1,000 x *g* for 3 min at 4° C. The supernatant was centrifuged at 47,200 x *g* for 30 min at 4° C. The resulting inclusion bodies were washed in Solution C (100 mM Tris-HCl, pH 8.0 containing 1 M urea, 1% TX-100, 1 mM DTT) and pelleted as before. This was followed by a second wash in Solution D (100 mM Tris-HCl, pH 8.0 containing 2 M urea, 2% TX-100 and 1 mM DTT) and pelleted at 47,200 x *g* for 30 min at 4° C. The inclusion bodies were stored at -20°C.

2.2.8 Estimation of protein concentration: Method of Markwell *et al.*, (1978)

A standard protein solution (BSA) was diluted to a range of concentrations from 0 – 100 μg protein per ml, unknown samples were diluted in H_2O. A stock solution of Markwell A, containing: 2% (w/v) sodium carbonate; 0.4% (w/v) sodium hydroxide; 0.16% (w/v) potassium sodium tartrate and 1% (w/v) sodium dodecyl sulfate; and a stock solution of Markwell B containing: 4% (w/v) copper sulfate were mixed (100:1, v/v) prior to use, giving Markwell C. 1.5 ml of Markwell C was added to 0.5 ml of all the protein solutions. These were then vortexed and allowed to stand at room temperature for 10 min. An aliquot (0.15 ml) of Folin-Ciocalteau's

reagent diluted 1:1 (v/v) with distilled water was added to each tube. After 45 min, the A_{660} was measured spectrophotometrically in a Unicam 97-502 spectrophotometer. The protein concentration of an unknown sample was determined by reference to a curve of A_{660} against equivalent BSA concentrations (from 0 – 100 μg of protein/ml).

2.2.9 Sodium Dodecyl Sulfate–Polyacrylamide Gel Electrophoresis (SDS-PAGE) and staining.

2.2.9.1 Gel preparation and electrophoresis

Discontinuous SDS-PAGE was carried out according to the method of Laemmli (1970) using the Mini-PROTEAN III (Bio-Rad). A 12% (w/v) polyacrylamide (30% acrylamide/08% bis-acrylamide, (37.5:1); Protogel), 0.375 M Tris-HCl, pH 8.8 separating gel containing 0.1% (w/v) SDS was used. A 4% (w/v) polyacrylamide, 0.125 M Tris-HCl, pH 6.8, 0.1% (w/v) SDS stacking gel was layered on top and a 0.75 mm thick Teflon comb was inserted. Samples were mixed with a reducing buffer (0.0625 M Tris-HCl, pH 6.8, 10% (v/v) glycerol, 2% (w/v) SDS, 1.66% (w/v) 2-mercaptoethanol and 0.001% (w/v) bromophenol blue), boiled for 5 min and loaded onto the gel. Standard molecular mass markers were used to size calibrate all gels. Electrophoresis was carried out, as per the manufacturer's instructions, in buffer containing 25 mM Tris, 192 mM glycine and 0.1% (w/v) SDS, pH 8.3, at 200 V for 45 min.

2.2.9.2 Coomassie-Blue-R Staining of Polyacrylamide Gels

In order to visualise the proteins separated in the gel, Coomassie Blue R staining of the proteins was used. The gel was soaked in a solution containing 0.05% (w/v) Coomassie Blue R, 50% (v/v) methanol and 10% (v/v) acetic acid for 30 min. The gel was then destained over night in 50% (v/v) methanol and 10% (v/v) acetic acid.

2.2.9.3 Colloidal B Satin staining for Polyacrylamide Gels

In order to visualise the low amounts of proteins separated in the gel and to keep the sample suitable for mass-spectrometry analysis Colloidal B Satin staining of the proteins was used as described in Neuhoff *et al.*, 1998. Firstly, disposable gloves, previously soaked in ethanol were used at all times. All glassware was washed with ethanol and Ultra-high pure (UHP)-H_2O and the staining procedure was performed in a fume hood so as to reduce the possibility of contamination by keratins. SDS-PAGE gels were agitated in fixative [50% (v/v) ethanol, 3% (v/v) ortho-phosphoric acid] for 2 days at rt. Following fixation gels were washed for 3 x 30 min in UHP-H_2O. The gels were then allowed to equilibrate in Neuhoff's solution [16% (w/v) ammonium sulfate, 25% (v/v) methanol, 5% (v/v) ortho-phosphoric acid] with gentle agitation for 1 h at rt. Coomassie Brilliant Blue G-250 (1 g) was sprinkled into the Neuhoff's solution and staining was continued for 2 –3 days at rt. Once the highly stained single protein band was visible, the intact gel slice was transferred to a 20% (w/v) ammonium sulfate solution prior to sequence analysis.

2.2.10 Detection of UCPs by Immunoblotting

A 12% (w/v) polyacrylamide, 0.375 M Tris-HCl, pH 8.8, separating gel containing 0.1% (w/v) SDS with a 4% (w/v) polyacrylamide, 0.125 M Tris-HCl, pH 6.8, stacking gel containing 0.1% (w/v) SDS was employed (see Section 2.2.8). Following electrophoresis, proteins were electroblotted onto PVDF (polyvinylidene difluoride) membranes using a Bio-Rad Trans-Blot Transfer cell. The gel was incubated in transfer buffer [25 mM Tris, 192 mM glycine and 10% (v/v) methanol] for at least 15 min. PVDF membrane was wetted for 15 s in methanol and washed twice with deionised water and then soaked in transfer buffer for 5 min. The gel and PVDF were sandwiched between filter paper and scotchbrite soaked in transfer buffer, in the cassette, according to the manufacturer's instructions. Transfer was

achieved by applying a constant voltage of 100 V for 1 h with constant stirring or 30 V for 16 h with constant stirring. The membrane was blocked in PBS (8 g NaCl, 0.2 g KCl, 1.44 g Na_2HPO_4 and 0.24 g KH_2PO_4, pH 7.4) containing 0.1% (v/v) Tween-20 (PBS-Tween) and 5% (w/v) skimmed mild powder (Marvel) for 1 hours at rt. Blocking was followed by washing in PBS-Tween and incubation for 1 h at rt in a 1:5000 dilution in [PBS-Tween containing 5% (w/v) Marvel] of primary rabbit polyclonal antibodies against peptides in rUCP, rUCP2 or rUCP3 (affinity-purified by Dr. Orla Cunningham, 1999). Following PBS-Tween washing the membranes were incubated with a goat anti-rabbit horseradish peroxidase conjugated secondary antibody, at a dilution of 1:10,000 in PBS-Tween containing 5% (w/v) Marvel for 30 min to 1 h at rt. Membranes were then washed in PBS-Tween and immunoreactive proteins were detected using the ECL system and X-Ray detection film.

2.2.11 Cold-adaptation of Syrian Golden Hamsters and Wistar Rats

Syrian Golden hamsters (6 weeks old) were housed in a temperature-controlled room at 10° C for 2 days with a 12 h light/dark cycle. They were caged individually and had free access to food and water. Over the next 6 days, the temperature of the room was lowered 1° each day until the temperature was 4°C. The hamsters were kept at this temperature for the next 5 weeks. The dark cycle was increased by 30 min every day until they were in complete darkness in an attempt to force them into hibernation. Wistar rats were treated the same way except that the light cycle was kept at 12 hour light/dark cycle for the entire period of cold exposure.

2.2.12 Preparation of mitochondria from BAT.

BAT was prepared using a slightly modified version of the method of Scarpace *et al.* (1991). BAT was removed from the interscapular region of the animal between the head and shoulder blades, and from the front of the

neck and placed into a pre-weighed beaker containing 30 ml of ice-cold isolation medium 1 (5 mM TES buffer pH 7.4 containing 250 mM sucrose, 1 mM EDTA, 1 mM DTT and 10 mg/ml fatty-acid-free BSA). BAT was weighed and washed several times with isolation medium 1. The tissue was finely chopped with a scissors and poured into a Potter homogeniser with a final volume of about 20 ml. The tissue was then homogenised by hand with four to six passes using a pestle of 0.26" (loose) clearance and 8 passes using a pestle of 0.12" (tight) clearance. This homogenate was then filtered through 4 layers of muslin and the filtrate was centrifuged at 20,000 x *g* for 10 min at 4°C. The supernatant was discarded and the sides the centrifuge tubes were wiped with tissue to remove and fat deposits. The pellet was then resuspended in 40 ml of isolation medium 1 and centrifuged at 750 x *g* for 10 min at 4°C. The supernatant was centrifuged at 8,600 x *g* for 10 min at 4°C. The pellet was then resuspended in isolation medium 1 and recentrifuged at 8,600 x *g* for 10 min at 4°C. The resulting pellet was then resuspended in isolation medium 2 (5 mM TES buffer, pH 7.4, containing 250 mM sucrose, 1 mM EDTA and 0.1 mM DTT) and centrifuged at 8,600 x *g* for 10 min at 4°C. The pellet was once again resuspended in isolation medium 2 and centrifuged at 8,600 x *g* for 10 min at 4°C. The pellet was resuspended gently and thoroughly with isolation medium 2 to the desired concentration.

2.2.13 Preparation of mitochondria from skeletal muscle

Skeletal muscle mitochondria were isolated from rat hind leg muscle by the method of Bhattacharya et al., (1991). 20–30 g of hindquarter muscle (all leg and a small amount of back muscle) were removed and placed into a pre-weighed beaker containing 75 ml of ice-cold isolation medium (100 mM Tris-HCl pH 7.4 containing 100 mM Sucrose, 9 mM EDTA, 46 mM KCl, 1 mM EGTA). Skeletal muscle was weighed and washed several times in isolation medium. Muscle was finely chopped on a pre-cooled glass tile with a razor blade before being added to 200 ml of isolation medium containing

0.5% (w/v) BSA and 0.02% (w/v) nagarse and incubated on ice, with stirring, for 5 min. The tissue was further disrupted using a Waring commercial blender at half-max speed for 15 s. The homogenate was then centrifuged at 1,500 x *g* for 3 min at 4°C. The layer of BSA on top of the supernatant was removed using a spatula and the supernatant was centrifuged at 12,000 x *g* for 10 min at 4°C. The pellet was then resuspended in ~25 ml of ice-cold isolation medium containing 2% (w/v) de-fatted BSA and centrifuged at 12,000 x *g* for 10 min at 4°C. The mitochondrial pellet was then washed in isolation medium and centrifuged as before. The final pellet was then resuspended in isolation medium to the desired concentration.

2.2.14 Preparation of mitochondria from liver and thymus

Mitochondria were prepared essentially by the method of Chappell and Hansford, (1972). Tissues were removed, trimmed of connective tissue and fat and placed in a pre-weighed beaker containing ice-cold STE buffer (5 mM Tris-HCl, pH7.4 containing 250 mM Sucrose, 1 mM EGTA). Tissues were finely chopped using scissors and washed several times with ice-cold STE buffer. The tissues were then poured into a Potter homogeniser tube and homogenised by hand; using 4 passes of a pestle with 0.26 inch (loose) clearance followed by 6 passes using a pestle with 0.12 inch (tight) clearance. The homogenates were centrifuged at 800 x *g* for 3 min at 4°C. The supernatant was then centrifuged at 12,000 x *g* for 10 min at 4°C. The pellet was then washed in STE buffer containing 2% (w/v) de-fatted BSA and re-centrifuged at 12,000 x *g* for 10 min at 4°C. The pellet was finally resuspended in STE buffer and pelleted as above. The resulting pellets containing the mitochondrial fractions were resuspended in STE buffer to the desired concentration.

2.2.15 Purification of native UCP1 from BAT mitochondria

2.2.15.1 Preparation of lipids and hydroxylapatite.

To a glass tube 0.45 mg phosphatidic acid, 25.9 mg phosphatidylcholine and 1.13 mg cardiolipin were added and mixed. The tube was then placed in a water bath at 50° C and lipids were dried under a stream of nitrogen gas. The lipids were then redissolved in ether and dried to ensure that no water was present. The lipids were stored overnight in a vacuum to free the mixture of any residual solvent.

Hydroxylapatite (HTP, 0.34 g) was soaked in at least 3 ml of extraction medium (tetraethylammonium (TEA^+) salts of 25 mM SO_4^{2-}, 50 mM TES and 1.5 mM EGTA, pH 7.2) and left overnight at 4°C.

2.2.15.2 Protein Solubilization

As much as possible from here on the lipids were kept in an atmosphere of nitrogen gas to prevent oxidation. Method used was a modified version of that of Lin and Klingenberg (1980). Lipid mixture, 27 mg, which has been dried the previous night and stored under vacuum, was dissolved by heating in 54.2 μl of the detergent octylpentaoxyethylene ether (C_8E_5) and 417 μl of extraction medium, at 50°C. Sonication was used to clarify the lipids. They were cooled to rt and then kept on ice. BAT mitochondria (14 mg) were washed with 2 ml extraction medium containing 5 mg/ml defatted BSA. The mitochondria were then mixed thoroughly with the lipids from above and incubated for 10 min on ice. This mitochondria-lipid mixture was the applied to the HTP (dried by centrifugation) in a column and incubated at rt for 10 min and then at 4°C for 25 min. The column was centrifuged for 2 min at 800 x *g*. The flow-through eluate from the HTP column contained predominately UCP1.

2.2.16 Extraction and purification of hUCP1 from inclusion bodies.

The method used was that previously described by Jaburek et al. (2004). Pelleted inclusion bodies (2 mg) containing huUCP1 were washed twice in 4 ml Wash Solution [sodium salts of 0.15 M PO_4^{3-}, 25 mM EDTA, 10 mM DTT, 0.2% sodium lauroylsarcosinate (SLS), pH 7.8]. Washed inclusion bodies were pelleted at 14,000 x *g* for 15 min. Inclusion bodies were then solubilized in 4 ml Solubilization Solution (50 mM CAPS, 25 mM DTT, 2 mM PMSF, 10% glycerol, 2% SLS, pH 10 adjusted by Tris) and left at rt for 30 min with constant mixing. The extract was then centrifuged for 15 min at 14,000 x *g* to remove any unsolubilized particles. The supernatant was diluted immediately with 6 ml 10% glycerol, 1% TX-114, 1 mM ATP and 0.8 g Dowex 11A8 were added and this mixture was left at 4°C for 2 hours with constant mixing. The mixture was then passed down a 2.5 ml Dowex 11A8 column (0.5 ml/min flow-rate), supplemented with 0.1 mM ATP and 20 mg soyabean phosphatidylcholine (≥ 30%, TLC) and left at 4°C overnight with gentle agitation.

The next day the protein mixture was concentrated ~5-fold using the Amicon Ultra centrifugal filter device with a molecular weight cut off (MWCO) of 10 kDa. Aliquots of ~0.6 mg were stored at -20°C. For purification the protein sample was dialysed against Internal Medium (TEA^+ salts of 80 mM SO_4^{2-}, 30 mM TES, 1 mM EGTA, pH 7.2) twice for 3 h and once overnight at 1:100 dilution. The dialysed protein was centrifuged at 14,000 x *g* for 15 min to remove any precipitate. The protein was then mixed with 0.12 g HTP (previously soaked in internal medium and dried by centrifugation) and incubated at 4°C for 25 min. Purified protein was then collected by centrifugation at 800 x *g* for 2 min.

2.2.17 Reconstitution of UCP1 into Liposomes

2.2.17.1 Preparation of lipids and columns

For reconstitution of native UCP1 from mitochondria 0.22 mg phosphatidic acid, 12.9 mg phosphatidylcholine and 0.57 mg cardiolipin were added to a glass tube and mixed. For reconstitution of UCP1 from inclusion bodies, 28.5 mg phosphatidylcholine and 1.5 mg cardiolipin were added to a glass tube and mixed. The lipids were then dried and redissolved in ether under a stream of nitrogen gas, as before. The dried lipid mixture was stored overnight in a vacuum to free it of any residual solvent.

Biobeads SM-2 (2 ml/ml of liposomes) were suspended in internal medium and left overnight in a syringe barrel at 4°C.

Sephadex G-50-300 (3 g) was soaked in at least 50 ml of internal medium overnight at 4°C.

2.2.17.2 Preparation of proteoliposomes

UCP1 was reconstituted into liposomes using the method of Garlid et al. (1995). The lipid mixture from the previous evening was solubilized with C_8E_5 (22 μl for native-protein preparation and 55 μl for inclusion-body preparation) by heating to 50°C. Sonication was used to clarify the mixture, which was then cooled to rt and stored on ice. Flow-through eluate from HTP was measured and added to lipids. The ionic composition was adjusted to 80 mM TEA_2SO_4 and 30 mM TEA-TES to match the internal medium, the carry-over of EGTA does not require further addition. Fluorescent probe of choice was then added to the final concentration as stated in Table 2.4. If required, GDP was added at this point to ensure that an inhibitory concentration was present in the internal environment of the liposomes. This solution was vortexed gently and added to a Biobeads SM-2 column (with soaking buffer removed by centrifugation at 800 x *g* for 2 min) and incubated, with agitation, at 4°C for 2 h. The newly-formed proteoliposomes

were then collected by centrifugation at 800 x *g* for 2 min. The proteoliposomes were then added to a new Biobeads SM-2 column for 30 min at 4°C. External probe was removed by passage through Sephadex G-50-300 spin columns (5 ml/250 μl proteoliposomes), which were pre-equilibrated with internal medium. Protein-free liposomes were prepared using the same protocol.

Table 2.4 Ion-selective fluorescent probes

Probe	Ion	Excitation wavelength (nm)	Emission wavelength (nm)
SPQ	TES^-	344	443
PBFI	K^+	340	485

SPQ – 6-methoxy-*N*-(3-sulfopropyl)quinolinium

PBFI – potassium-binding benzofuran isophthalate

2.2.18 Fluorescent Measurements of potassium ion (K^+) flux.

Ion fluxes in proteoliposomes were measured using a PerkinElmer LS55 Luminescence Spectrometer. H^+ fluxes were measured by changes in intraliposomal acid concentrations, obtained by changes in the fluorescence of SPQ, which is quenched by the anion of TES. K^+ fluxes were obtained by changes in fluorescence of PBFI due to complexation with K^+. Transport was driven by a K^+ diffusion potential initiated by the addition of 50–100 nM valinomycin. External medium contained K^+ salts of 80 mM SO_4^{2-}, 30 mM TES^- and 1 mM EDTA. Proteoliposomes (1 mg phosphoplipid) were added to 1 ml external medium at 25°C.

Each preparation was individually calibrated for fluorescent probe response to appropriate ion. PBFI-containing proteoliposomes were lysed by detergent in external medium and SPQ-containing proteoliposomes were lysed in H_2O to give maximal fluorescence. The initial amount of probe was determined by standard additions of probe and intraliposomal volume was estimated from the volume of distribution of probe.

Due to probe response to ion concentration, fluorescence traces were converted to initial analyte concentrations, $[X]_{in}$. Linear regression analysis of the initial transport yielded $d[X]_{in}/dt$ in mM/s. These rates were multiplied by $V_{in}/[P]$, where V_{in} is the intraliposomal volume and [P] is protein concentration, to give flux in units of mol/(mg protein.min).

2.2.19 Estimation of Protein concentration in the presence of high concentration of lipids using Amido Black 10B: Kaplan et al., (1985)

BSA standards from 2 to 24 μg of protein were diluted to 2 ml with deionized water. The working volume of proteoliposomes was also diluted to 2 ml with deionized water. 200 μl 10% (w/v) SDS, 300 μl 1 M Tris, 1% (w/v) SDS, pH 7.5 and 600 μl 104% (w/v) TCA were added sequentially with vortexing taking place after each addition. After the TCA addition, the samples were left for at least 3 min at rt. The samples were then transferred, using a Pasteur pipette, to a Millipore filter (0.45 μm pore size, 24 mm diameter). The samples were then placed in a Millipore 12-place sampling manifold and filtered under vacuum and washed with 6% (w/v) TCA. The filters were then stirred in 200 ml staining solution [0.1% (w/v) amido black 10B in 45% (v/v) methanol and 10% (v/v) acetic acid] for 3 min, washed in deionized water and destained by 3 x 1 min washes in 200 ml destaining solution [90% (v/v) methanol and 2% (v/v) acetic acid]. The filters were then washed in deionized water and dried on blotting paper. The blue spot on each filter was cut up and placed in a 3 ml tube with 700 μl 25 mM NaOH, 0.05 mM EDTA and 50% (v/v) ethanol and incubated for at least 20 min at rt with occasional vortexing. The absorbances were then measured at 650 nm in a Unicam 97-502 spectrophotometer. The protein concentration of an unknown sample was determined by reference to a curve of A_{650} against equivalent BSA concentrations from 0 – 24 μg of protein.

2.2.20 Oxygen consumption by non-phosphorylating brown adipose tissue mitochondria

Oxygen consumption rates were measured using an Oxygraph Respirometer (Oroboros™, Innsbrück, Austria), as previously described. Mitochondria (1 mg/ml) were incubated at 37°C in medium containing 120 mM KCl, 5 mM HEPES- KOH, pH 7.4, 1 mM EGTA, 16 μM fatty-acid free BSA, 5 μM atractyloside, 5 μM rotenone and 1 μg/ml oligomycin. Non-phosphorylating (state 4) oxygen consumption rates were measured as the steady-state rates achieved on addition of 7.5 mM succinate (succinate-KOH, pH 7.4). The sensitivity of this state 4 oxygen-consumption rate to GDP (500 μM) was then determined. The sensitivity of the resulting oxygen-consumption rate to palmitate or glucose-*O*-ω-palmitate (in ethanol; 64 μM; ~40 nM free) was then determined. Finally, the mitochondrial uncoupler 2,4-dinitrophenol (DNP; 30 μM) was added to the chamber to determine the maximum oxygen consumption rate attainable due to uncoupling. The Oxygraph Respirometer was calibrated according to the procedure of Reynafarje et al. assuming that 406 nmoles of oxygen atoms were dissolved in 1 ml of ionic incubation medium at 37°C.

2.2.21 Statistical Analysis

All results are expressed as mean ± S.E.M. unless otherwise indicated. Mean values were compared using a paired student's t test. Unless otherwise stated, a p value of ≤ 0.05 was taken to indicate significance.

Chapter Three

Overexpression of hUCP1, hUCP2 and hUCP3 and characterisation of anti-UCP1 and anti-UCP3 antibodies

3.1 Introduction

UCP1 can reach levels of 20% of the protein content of BAT mitochondria (Lin and Klingenberg, 1980). Such levels provide a plentiful source of UCP1. UCP1 function can be studied in mitochondria directly (Rial *et al.,* 2004; Jabůrek *et al.,* 2001; Ježek and Garlid, 1990; Nicholls, 1976). UCP1 can also be purified (Lin and Klingenberg, 1980) and used for functional reconstitution (e.g. Bouillaud *et al.,* 1983). However, the availability of BAT is limited, requires the use of animals, and long periods of cold-adaptation are sometimes required. Another problem with BAT mitochondria is that they also contain UCP2 and UCP3, so purification of UCP1 may result in contamination. In fact, purification from any mitochondria can result in contamination from many mitochondrial transporters, such as the ATP/ADP carrier (AAC), which is the most abundant transporter in most mitochondria.

Recombinant protein provides a plentiful source of material without the expense and use of animals. Recombinant protein can also be easily purified without contamination. The homologues UCP2 and UCP3 require a recombinantly expressed protein source due to their low native expression levels. Pecqueur *et al.* (2001) showed the highest UCP2 protein levels in spleen, which are 160-fold less than those of UCP1 in BAT, with 313 ng of UCP2 protein/mg of mitochondria. UCP3 levels have yet to be quantified but preliminary work shows UCP3 mRNA to be poorly translated in muscle (Pecqueur *et al.,* 2001). Indeed, Cadenas *et al.* (2002) indicated that the level of UCP3 in the skeletal muscle of mice is ~150 ng of protein/mg of mitochondria. The initial aim of this work was to develop an overexpression system for the uncoupling proteins.

The UCP1 homologues, UCP2 and UCP3, have only been successfully expressed in *E. coli* (Jabůrek *et al.,* 1999, Echtay *et al.,* 2001). Levels in yeast have either been too low (Jabůrek *et al.,* 1999) for purification or the protein has been expressed in a "deranged" form in yeast (Heidkaemper *et al.,* 2000). The fact that any protein needs to be renatured

from inclusion bodies makes comparison with native protein or yeast-expressed protein difficult.

UCP1 has been used as a paradigm for UCP function but its study in humans has its limits due to the fact that BAT is not present in adult tissues. Recent results in our lab show that UCP1 is present in mitochondria isolated from the thymus of rats (Carroll *et al.,* 2005). So, work on UCP1 may still have relevance for human and mice models. UCP2 and UCP3 have much more relevance due to their expression in persisting tissues in humans. However, work on hUCP1 has not been recorded due to lack of availability of human BAT and an inability to express hUCP1 in *E. coli.* This work sets out to solve this latter dilemma.

By observing the pattern of expression of UCPs under a variety of physiological and pathological conditions, clues to their function can be obtained. Specific antibodies for UCPs 1, 2 and 3 are needed for such studies. Furthermore due to the sequence homology between these proteins and their tendency to be physiologically co-expressed (e.g. UCPs 1, 2 and 3 in BAT, Cunningham *et al.,* 2003; Ricquier *et al.,* 2000), it is necessary to be able to discriminate between each of these proteins. Peptide antibodies are available commercially from Calbiochem, Chemicon International and Lilly, and others have been produced in-house by a number of groups (Vidal-Puig *et al.,* 2000; Hesselink *et al.,* 2001) including our own. Kyte-Doolittle plots were applied to the protein sequences of rUCP1 and rUCP3 (Figures 3.1.1 and 3.1.2). From these plots, the peptides sequences displayed in Figure 3.2.3 were chosen to raise the antibodies. However, in most cases, the sensitivity and discriminatory nature of those antibodies to other UCPs, and mitochondrial transporters in general, have not been satisfactorily demonstrated (Hesselink *et al.,* 2001). This work sets out, using the recombinant proteins to measure the discriminatory nature of the antibodies produced.

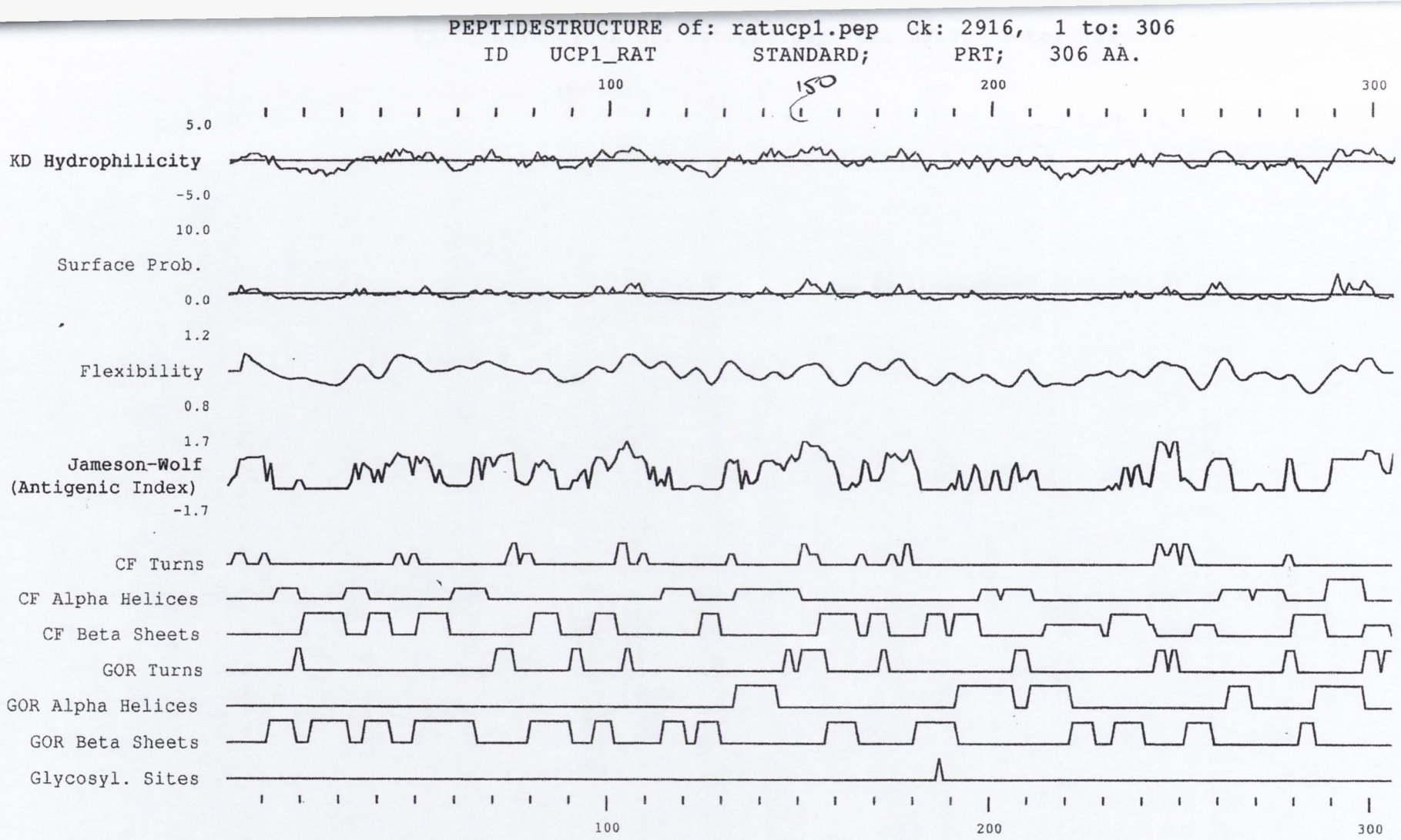


Figure 3.1.1 Kyte-Doolittle plot for rUCP1

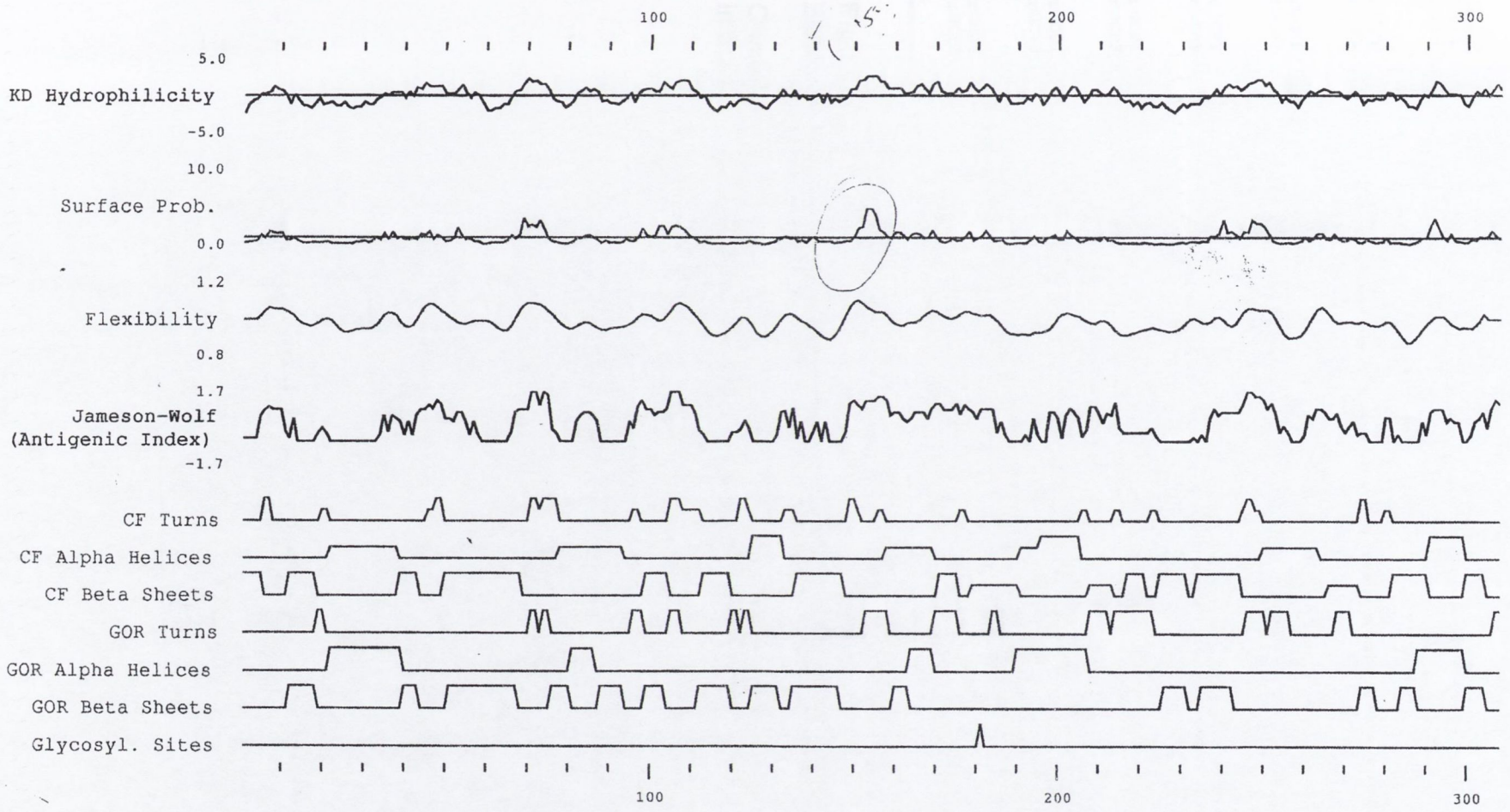


Figure 3.1.2 Kyte-Doolittle plot for rUCP3

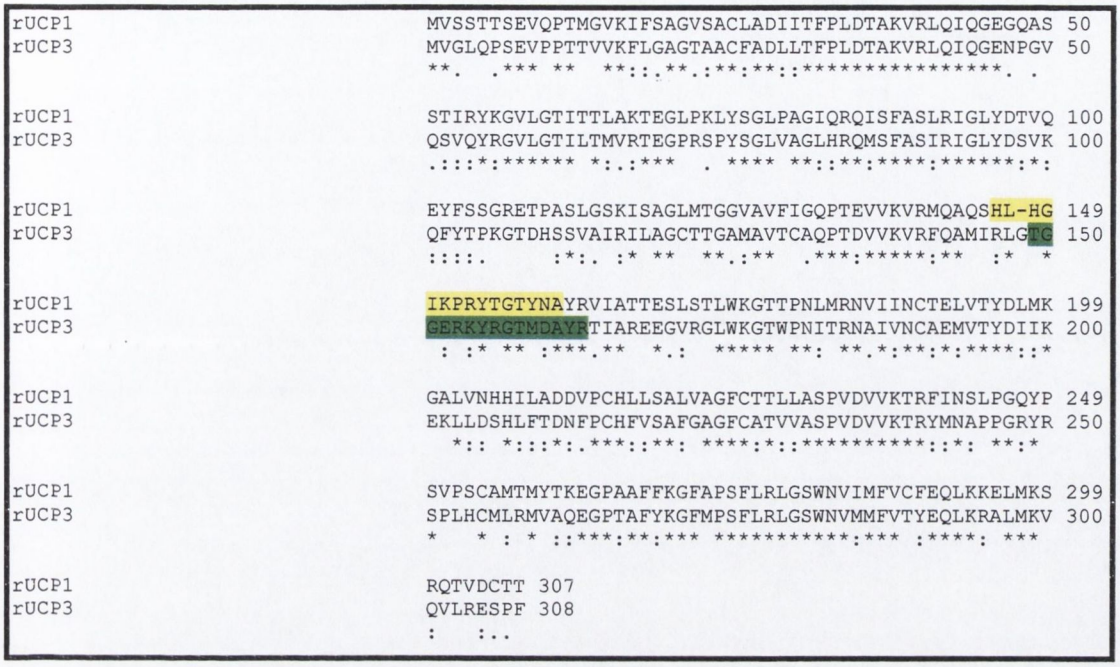


Figure 3.1.3 Multiple Sequence Alignment of rUCP1 and rUCP3 (ClustalW; www.ebi.ac.uk)

The peptide sequences of rUCP1 and rUCP3 were aligned using the ClustalW program on the www.ebi.ac.uk website. The highlighted sequences indicate to which internal peptides the antibodies were raised by Eurogentec.

3.2 Results

3.2.1 Transformation of *E. coli* with pET21d plasmid containing the relevant cDNA.

cDNAs encoding hUCP1, hUCP2 and hUCP3 were subcloned from yeast vectors into the *E. coli* expression plasmid pET21d. These plasmids and the pET3a plasmids containing cDNA for haUCP1 and ncAAC were then used to transform the BL21 pLysS, BL21 Codonplus and Rosetta pLysS strains of *E. coli*. Plasmid preparations were performed from selected colonies to confirm transformations. Restriction-enzyme analysis was performed to confirm the presence of the relevant gene. Figure 3.2.1 shows the analysed plasmids. UCP genes are confirmed by a band of 1,000 bp and the AAC by a band of 1,100 bp.

3.2.2 Purification of inclusion bodies from *E. coli.*

Protein expression was induced by the addition of 1 mM IPTG to the growing *E. coli* (2 h incubation). Inclusion bodies were then isolated according the method described in section 2.2.7.2. Coomassie staining of a typical 12.5% polyacrylamide gel (Figure 3.2.2) shows the purification of a 32-kDa protein in the inclusion-body lane. The absence of the band in pre-induced cells should also be noted.

3.2.3 Immunoblotting of *E. coli* samples.

Samples. both pre- and post-induction, as well as those taken during purification of inclusion bodies, were prepared for Immunoblotting.

Samples from BL21 pLysS containing pET21d-hUCP1 failed to show any expression of hUCP 1. Non-specific bands of the wrong size can be seen in lanes from post-induction samples but nothing can be seen in the inclusion-body fraction (Figure 3.2.3).

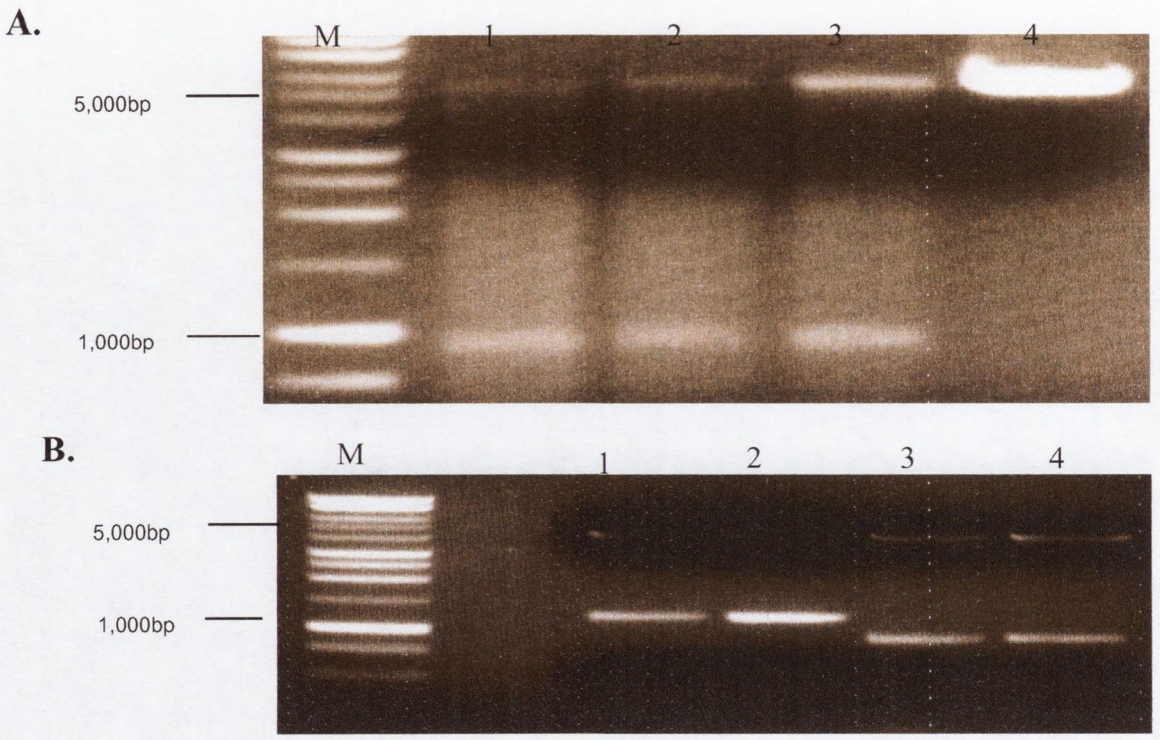


Figure 3.2.1 Restriction enzyme analysis of plasmids purified from BL21 pLysS

A. Lane 1: pET21d-hUCP1
Lane 2: pET21d-hUCP2
Lane 3: pET21d-hUCP3
Lane 4: pET21d

B. Lane 1 + 2: pET3a-ncAAC
Lane 3 + 4: pET3a-haUCP1

M: 1kb DNA Ladder, 5,000 bp and 1,000 bp fragments indicated

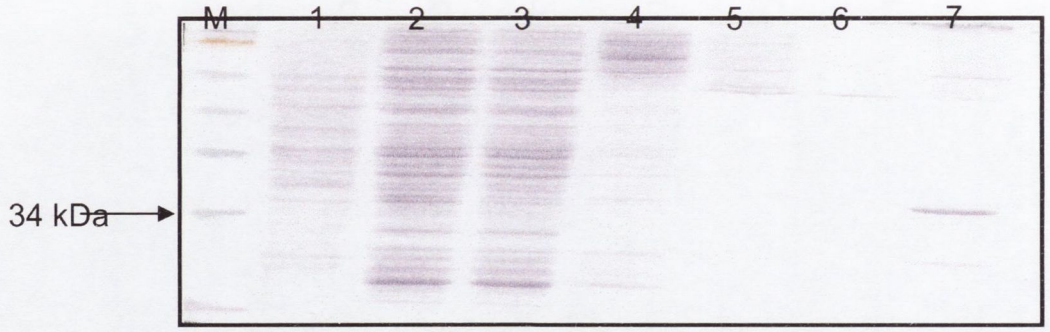


Figure 3.2.2 Purification of inclusion bodies from *E.coli*

E. coli (BL21 pLysS) transformed with the appropriate plasmid (pET21d-hUCP3 in this case) were grown to mid-log phase. A sample was taken and then protein production was induced using 1 mM IPTG for 2 h. Inclusion bodies were then purified according to method described in section 2.2.6. Samples were taken from each stage of the purification process. A 20-µg amount of protein from each sample was loaded on a 12.5% polyacrylamide gel, electrophoresed and stained with Coomassie Blue.

M: SeeBlue®Plus2 Pre-Stained Protein Markers (Invitrogen), 34 kDa indicated

1: Pre-induced whole cells

2: Post-induced whole cells

3. Supernatant 1 (Post lysis)

4: Supernatant 2 (Cell debris)

5: Supernatant 3 (First wash)

6: Supernatant 4 (Second wash)

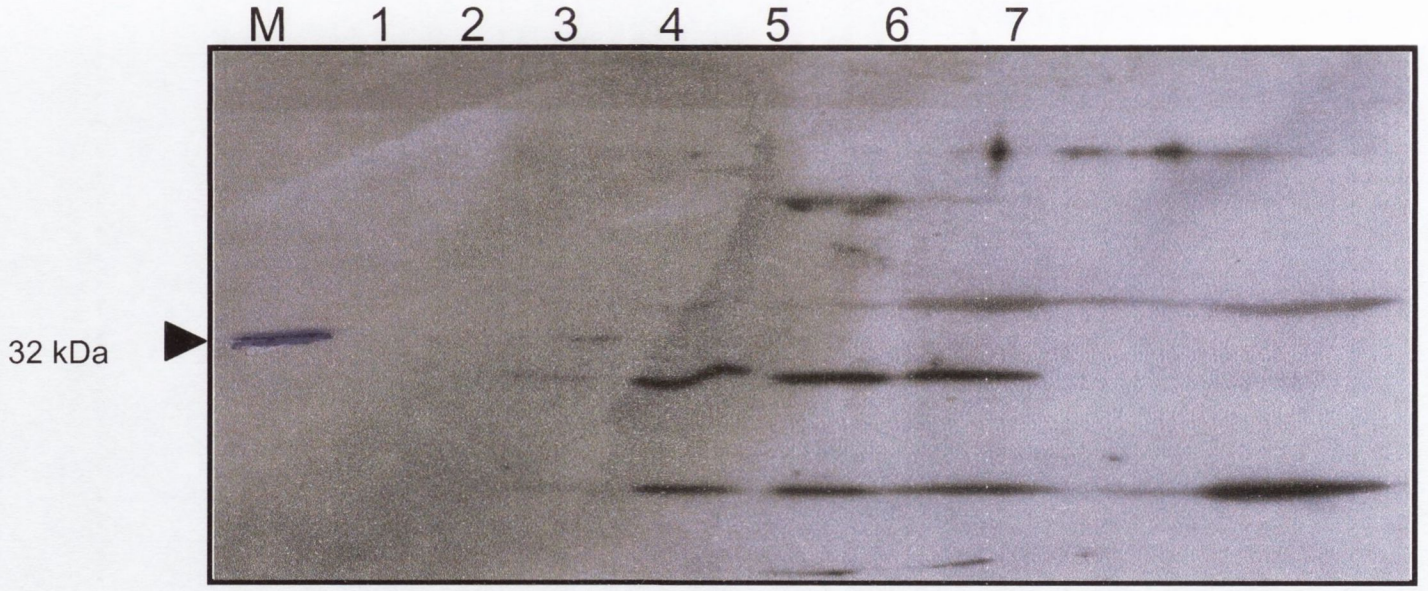


Figure 3.2.3 Immunoblot of samples from the purification steps for inclusion bodies, from *E. coli*, BL21 pLysS containing pET21d-hUCP1.

Samples (20 µg of protein) from each stage of purification for inclusion bodies were loaded and separated on a 12.5% polyacrylamide gel and transferred to PVDF membrane. Membrane was probed with an anti-UCP1 peptide antibody (Eurogentec). Positions of molecular mass standards are indicated.

M: Bio-Rad Kaleidoscope Prestained Standards
1: Post-induction whole cells
2: Supernatant 1 (post lysis)
3: Supernatant 2
4: Supernatant 3
5: Supernatant 4
6: Inclusion bodies

Samples from BL21 pLysS containing pET21d-hUCP2 show expression of UCP2 in post-induced cells. The hUCP2 protein is predominantly in the inclusion body fraction (Figure 3.2.4).

Samples of BL21 pLysS containing pET21d-hUCP3 show expression of UCP3 in post-induced cells and it is predominantly in the inclusion body fraction. Cells containing pET21d empty vector show no expression of protein (Figure 3.2.5). Cells containing empty vector did not form any significant amount of inclusion bodies (results not shown).

Samples from BL21 pLysS containing pET3a-haUCP1 show expression of UCP1 in post-induced cells. The inclusion body fraction shows a concentration of the protein expressed (Fig 3.2.6).

Samples from BL21 Codonplus containing pET21d-hUCP1 do show expression of protein with an Mr of 32 kDa. Many other lengths of protein are also seen. However this band is seen in pre-induced cells but is absent in the fraction of inclusion bodies that has very little protein (Figure 3.2.7).

The *E. coli* strain Rosetta pLysS transformed with the plasmid pET21d-hUCP1 does show specific expression of a 32-kDa protein, which is then concentrated in the inclusion body fraction. Some protein is seen in pre-induced cells. Rosetta pLysS transformed with the empty vector pET21d do not show any expression of an immunoreactive protein (Figure 3.2.8).

3.2.4 Characterisation of anti-UCP1 peptide antibody.

Inclusion bodies (10, 5 and 1 µg of protein) containing haUCP1 were prepared for immunoblotting with the anti-UCP1 peptide antibody. Samples from inclusion bodies containing hUCP2 and hUCP3 (20 µg of protein) were also included. The only signal observed was with the UCP3 inclusion bodies at a Mr of 32.4 kDa. The antibody did not show any reaction with either hUCP2 or hUCP3, as shown in Figure 3.2.9.

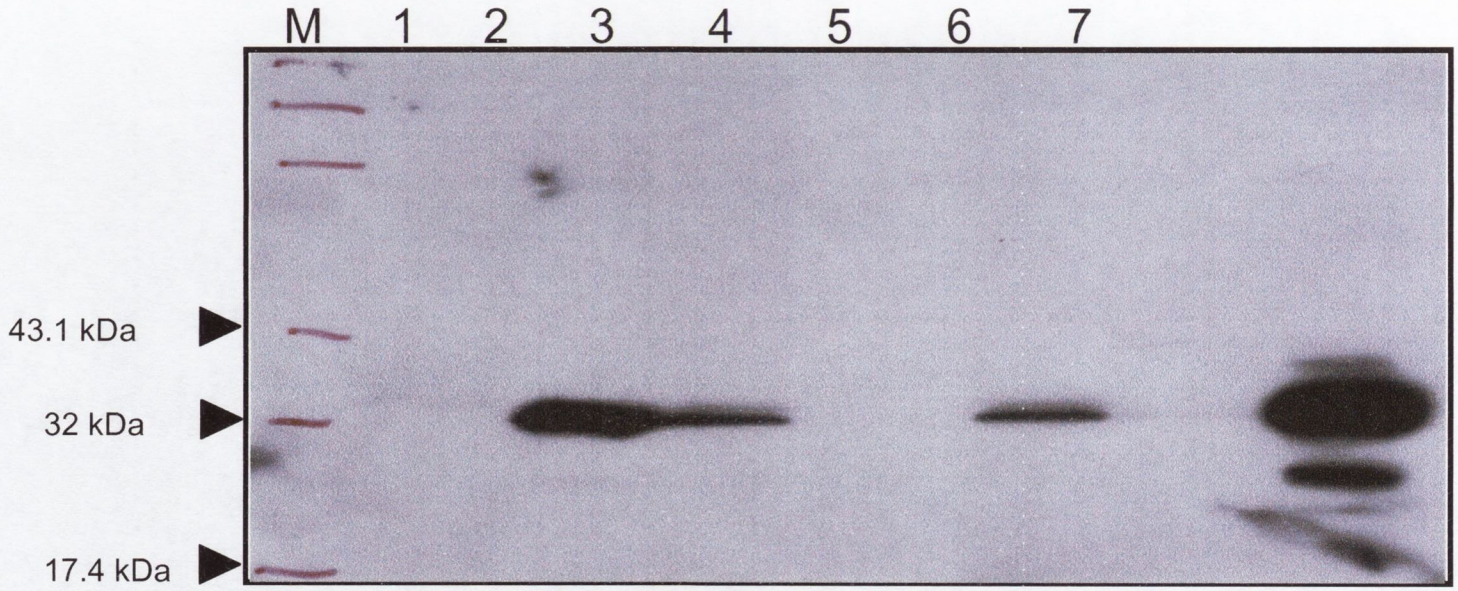


Figure 3.2.4 Immunoblot of the purification steps for inclusion bodies from *E. coli*, BL21 pLysS containing pET21d-hUCP2.

Samples (20 µg of protein) from each stage of purification for inclusion bodies were electrophoresed on a 12.5% polyacrylamide gel and transferred to PVDF membrane. Membrane was probed with an anti-UCP2 peptide antibody (Eurogentec). Positions of molecular mass standards are indicated.
M: Biorad Kaleidoscope Prestained Standards
1: Pre-induction whole cells
2: Post-induction whole cells
3: Supernatant 1 (post lysis)
4: Supernatant 2
5: Supernatant 3
6: Supernatant 4
7: Inclusion bodies

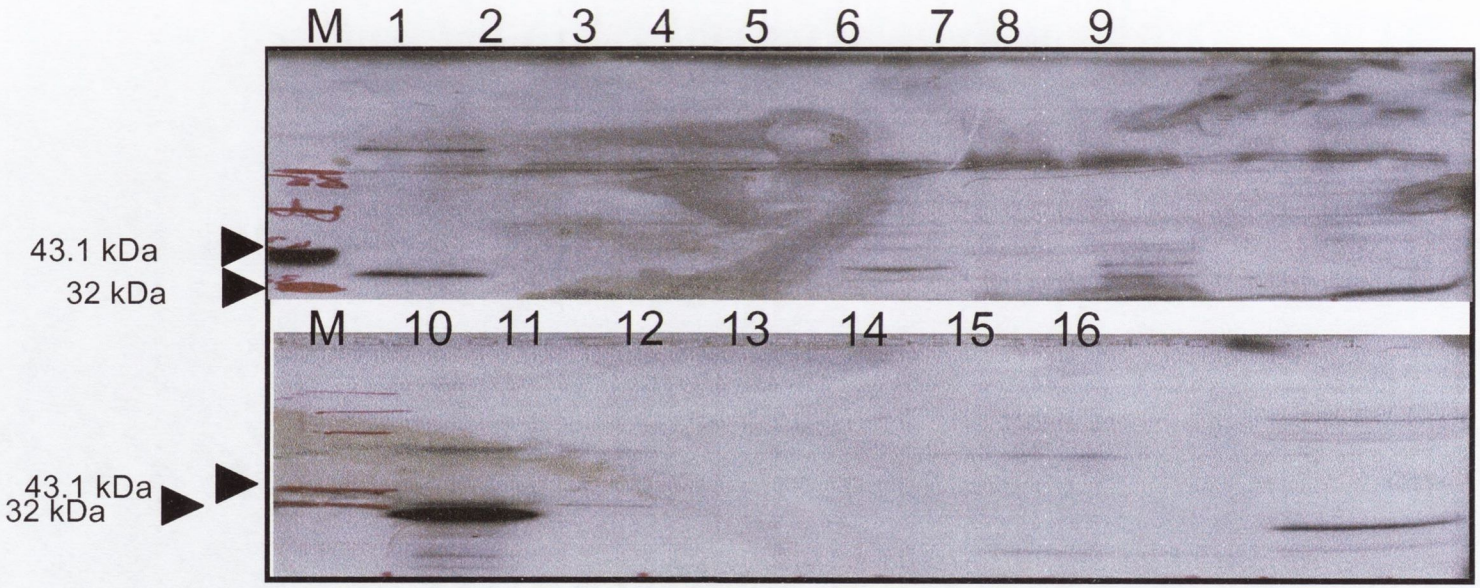


Figure 3.2.5 Immunoblot of the purification steps for inclusion bodies from *E. coli,* BL21 pLysS containing pET21d-hUCP3 or pET21d.

Samples (20 µg of protein) from each stage of purification for inclusion bodies were loaded and separated on a 12.5% polyacrylamide gel and transferred to PVDF membrane. Membrane was probed with an anti-UCP3 peptide antibody (Eurogentec). Positions of molecular mass standards are indicated.

M: Biorad Kaleidoscope Prestained Standards

1: Yeast cells expressing hUCP3
2: Pre-Induced Cells (pET21d)
3: Pre-Induced Cells(pET21d-hUCP3)
4: Post-Induced Cells (pET21d)
5: Post-Induced Cells (pET21d-hUCP3)
6: Supernatant 1 (pET21d)
7: Supernatant 1 (pET21d-hUCP3)
8: Supernatant 2 (pET21d)
9: Supernatant 2 (pET21d-hUCP3)
10: Inclusion bodies (pET21d-hUCP3)
11: Inclusion bodies (pET21d)
12: Supernatant 4 (pET21d-hUCP3)
13: Supernatant 4 (pET21d)
14: Supernatant 3 (pET21d-hUCP3)
15: Supernatant 3 (pET21d-hUCP3)
16: Yeast cells expressing hUCP3

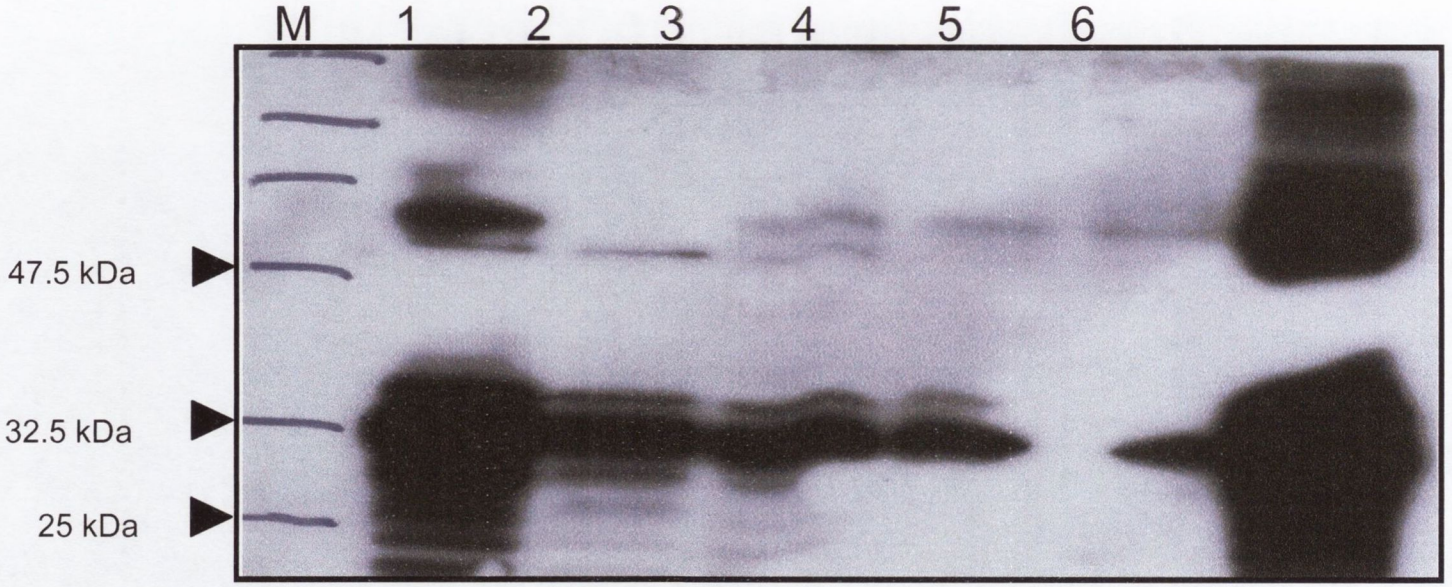


Figure 3.2.6 Immunoblot of the purification steps for inclusion bodies from *E. coli*, BL21 pLysS containing pET3a-haUCP1.

Samples (20 µg of protein) from each stage of purification for inclusion bodies were loaded and separated on a 12.5% polyacrylamide gel and transferred to PVDF membrane. Membrane was probed with an anti-UCP1 full-length antibody (Gift from Daniel Riquier, France). Positions of molecular mass standards are indicated.

M: Biorad Prestained protein markers (broad range)
1: Post-induction whole cells
2: Supernatant 1 (post lysis)
3: Supernatant 2
4: Supernatant 3
5: Supernatant 4
6: Inclusion bodies

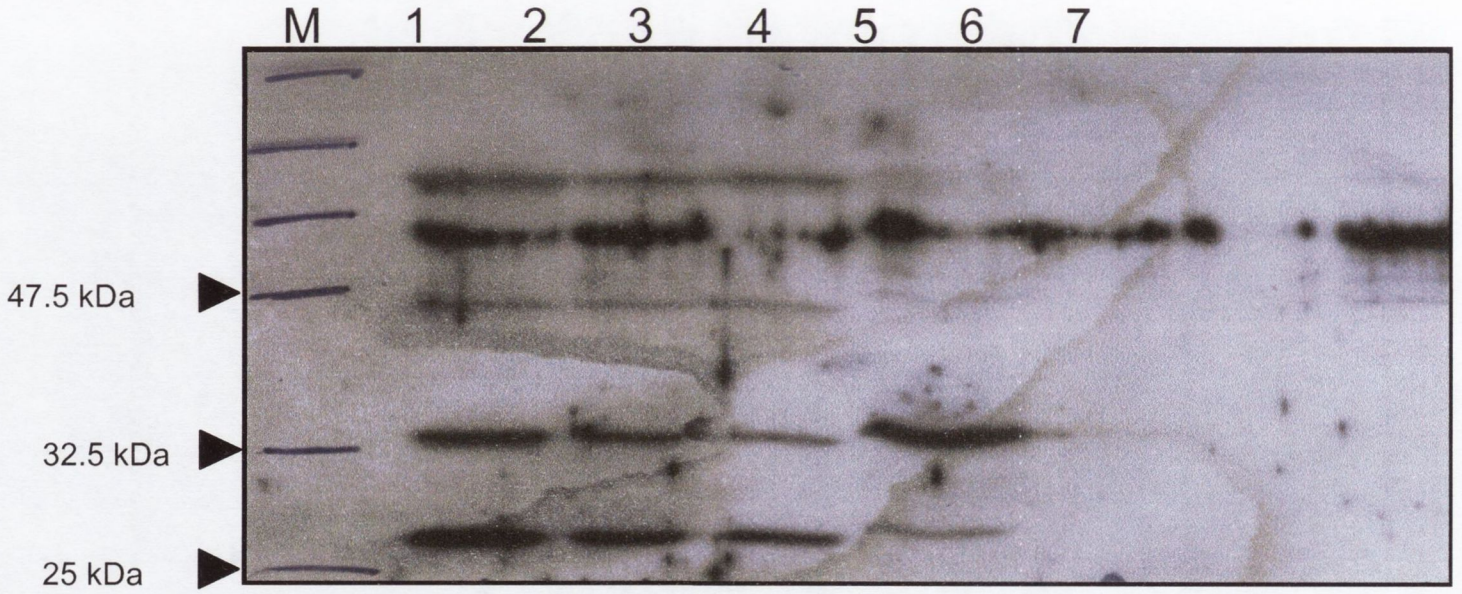


Figure 3.2.7 Immunoblot of the purification steps for inclusion bodies from *E. coli,* BL21 Codon-Plus pLysS containing pET21d-hUCP1.

Samples (20 µg of protein) from each stage of purification for inclusion bodies were loaded and separated on a 12.5% polyacrylamide gel and transferred to PVDF membrane. Membrane was probed with an anti-UCP1 peptide antibody (Eurogentec). Positions of molecular mass standards are indicated.

M: Biorad Prestained protein markers (broad range)
1: Pre-induction whole cells
2: Post-induction whole cells
3: Supernatant 1
4: Supernatant 2
5: Supernatant 3
6: Supernatant 4
7: Inclusion bodies

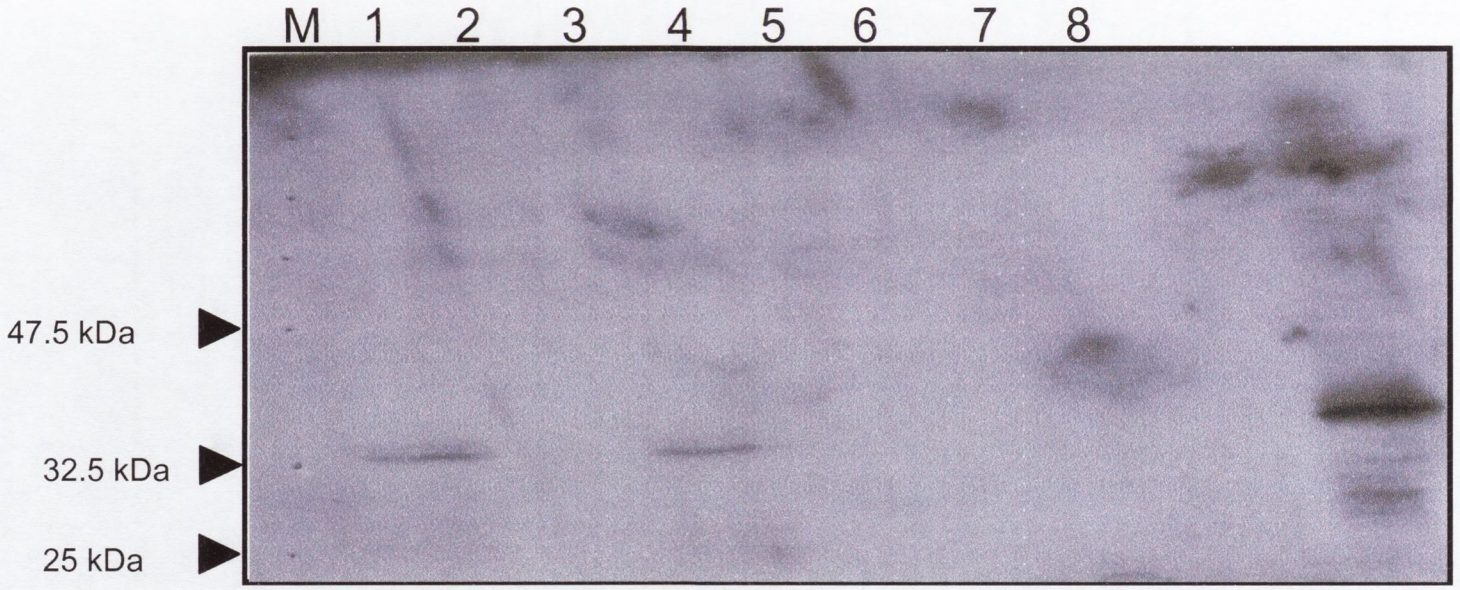


Figure 3.2.8 Immunoblot of the purification steps for inclusion bodies from *E. coli,* Rosetta pLysS containing pET21d-hUCP1.

Samples (20 µg of protein) from each stage of purification for inclusion bodies were loaded and separated on a 12.5% polyacrylamide gel and transferred to PVDF membrane. Membrane was probed with an anti-UCP1 full-length antibody (Gift from Daniel Riquier, France). Positions of molecular mass standards are indicated.

M: Biorad Prestained protein markers (broad range)
1: Pre-induction whole cells (pET21d-hUCP1)
2: Pre-induction whole cells (pET21d)
3: Post-induction whole cells (pET21d-hUCP1)
4: Post-induction whole cells (pET21d)
5: Supernatant 1 (pET21d)
6: Supernatant 2 (pET21d)
7: Inclusion bodies (pET21d)
8: Inclusion bodies (pET21d-hUCP1)

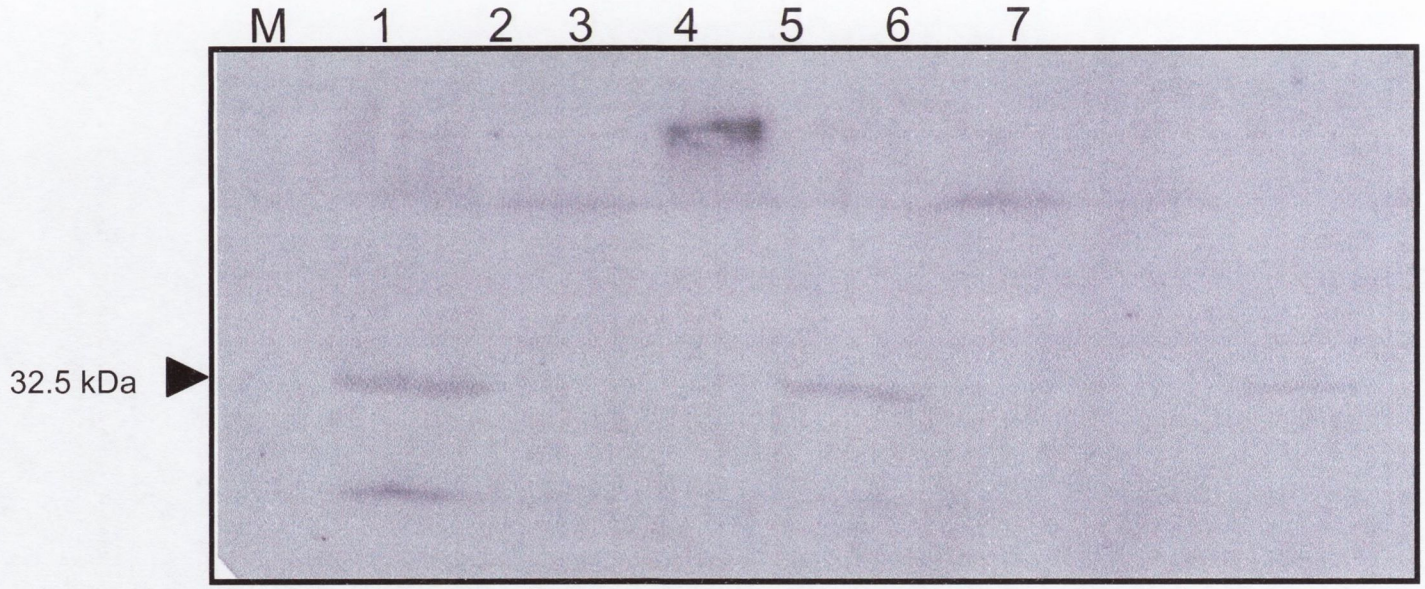


Figure 3.2.9 Characterisation of anti-UCP1 peptide antibody (Eurogentec).

Inclusion bodies (concentrations indicated below) of haUCP1, hUCP2 and hUCP3 were used. Immunoblot shows the reaction of anti-UCP1 peptide antibody (Eurogentec). Positions of molecular mass standards are indicated..

M: Biorad Prestained protein markers (broad range)
1: 10 µg haUCP1 inclusion bodies
2: 20 µg hUCP2 inclusion bodies
3: 20 µg hUCP3 inclusion bodies
4: 5 µg haUCP1 inclusion bodies
5: as lane 2
6: as lane 3
7: 1 µg haUCP1 inclusion bodies

3.2.5 Characterisation of anti-UCP3 peptide antibody.

Inclusion bodies containing haUCP1 (20 µg), hUCP2 (20 µg) and hUCP3 (20 and 10 µg) were prepared for immunoblotting with the anti-UCP3 peptide antibody. The antibody did not show any reaction with either haUCP1 or hUCP2, as shown in Figure 3.2.10.

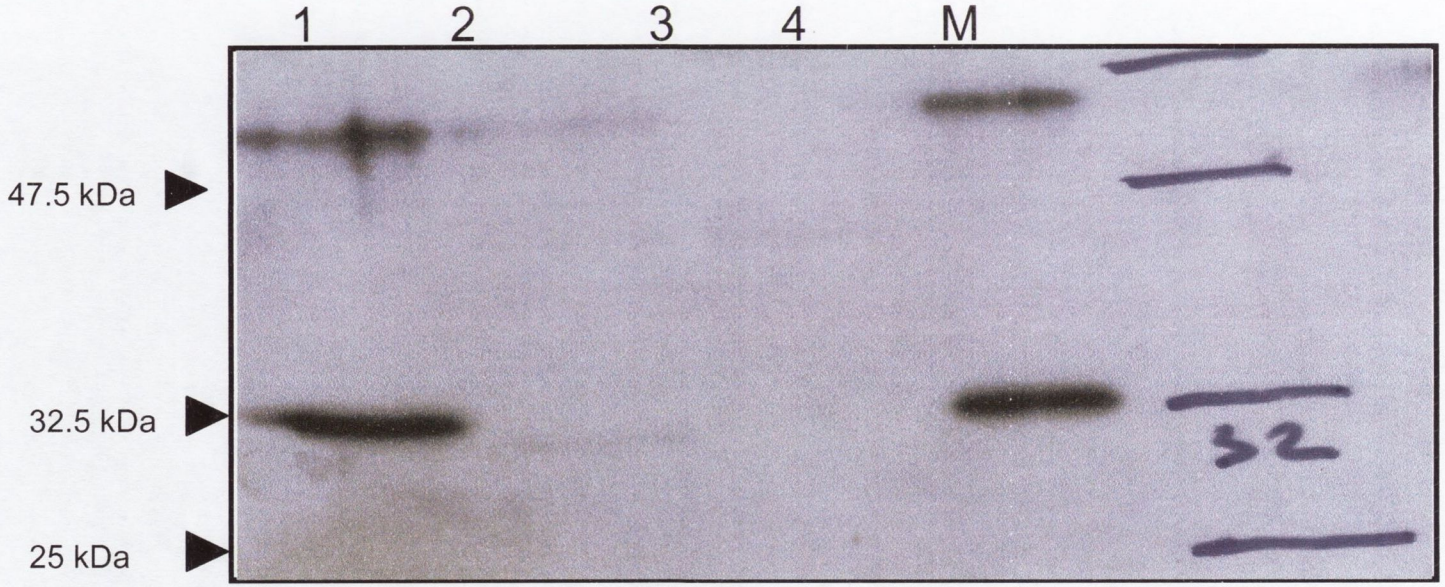


Figure 3.2.10 Characterisation of anti-UCP3 peptide antibody (Eurogentec).

Inclusion bodies (concentrations indicated below) of haUCP1, hUCP2 and hUCP3 were used. Immunoblot show the reaction of anti-UCP3 peptide antibody (Eurogentec). Positions of molecular mass standards are indicated..

M: Biorad Prestained protein markers (broad range)
1: 20 µg hUCP3 inclusion bodies
2: 20 µg hUCP2 inclusion bodies
3: 20 µg haUCP1 inclusion bodies
4: 10 µg hUCP3 inclusion bodies

3.3 Discussion

All UCP cDNAs were cloned into pET plasmids. The cDNAs were ligated in between the restriction-enzyme sites outlined in Table 2.3. Figure 3.2.1 shows the correct sized cDNA, which is excisable using the restriction sites chosen. The pET expression system is one of the most powerful systems yet developed for the cloning and expression of recombinant proteins in *E. coli*. The target genes are under the control of a strong bacteriophage T7 transcription promoter and are induced by T7 RNA polymerase. When fully induced, almost the entire cell's resources are used for target gene expression. The host strain BL21 pLysS was chosen for its compatibility with the pET system and its deficiency in lon and ompT proteases that can lead to degradation of proteins during purification. The pLysS plasmid encodes T7 lysozyme, which inhibits T7 RNA polymerase and reduces the ability to transcribe target in an uninduced state.

When membrane proteins are expressed in *E. coli* they are usually expressed as aggregates called inclusion bodies. Inclusion bodies are formed due to the bacterium's lack of ability to incorporate polytopic proteins into its cytoplasmic membrane. The protein is considered toxic by the cell and also slows down the rate of expression and growth of the cell. The insolubility of inclusion bodies confers an ease of purification upon them. There are many methods used to isolate inclusion bodies. The method used in this study was developed on the basis of work published by Echtay *et al.* (1999). This isolation of inclusion bodies makes it easier to purify them, offers a high level of purity and is cost-effective. Results of other protocols have not been shown but give similar results. Mild detergent strips inclusion bodies of any excess proteins but is unable to open up the inclusion bodies resulting in little loss of the protein expressed in the inclusion bodies. Coomassie-stained gels of purified UCP3 inclusion bodies show a strong, 32-kDa band, in the inclusion-body lane (Figure 3.2.2). The 32-kDa protein is almost an exclusive protein in this lane; pre-induced cells do not show any significant band at a Mr of 32 kDa indicating that pLysS control is working.

Expression of hUCP1 was unsuccessful in the *E. coli* strain BL21 pLysS. The BL21 pLysS host did not show any expression of a 32-kDa protein. From Figure 3.2.3, it can be seen that some lower-molecular mass bands are detected by the Eurogentec anti-UCP1 peptide antibody. No protein was detected in inclusion bodies, indicating that no full-length protein was produced. Lower molecular-mass bands may be indicative of short peptides translated from mRNA. Inability for ribosomes to read RNA can result in the ribosomes falling all the RNA, translation halting and releasing shorter peptides. Furthermore, their presence in the wash steps implies that they are soluble, thereby arguing for the problems with translation as mentioned. Although no evidence has been recorded about the inability of *E. coli* (usually the BL21 strain) to express hUCP1, personal communication with Martin Klingenberg, Mika Jacobson and Martin Jabůrek confirms this failure of expression of hUCP1 in BL21 pLysS. Most laboratories use hamster, rat or mouse cDNA in *E. coli* expression systems. Inability to express the human form suggested that the problem of expression might lie with codon bias experienced with *E. coli.* There are eight codons that are under-represented in *E. coli.* Use of BL21-CodonPLus was an attempt to overcome this bias as the *E. coli* strain contains extra arginine, isoleucine and leucine tRNA genes, which are complimentary to the human codons. An immunoreactive protein was produced by BL21-CodonPLus (Figure 3.3.7) but, as it was also present in pre-induced cells, this argues against it being hUCP1; it may be an *E. coli* protein that is native to this strain. No protein was detected in the insoluble fraction (inclusion bodies), implying, as before, that the detected protein was washed out during purification of the inclusion bodies. The fact that the protein detected was washed out implies that it is a soluble protein. A correctly expressed hUCP1, being a membrane protein, would be insoluble in the form of inclusion bodies. In addition, all preparations of *E. coli* with hUCP1 produced very little inclusion bodies (data not shown), implying that very little foreign protein was being produced. With the advent of newer strains of *E. coli* containing all of the under-represented human codons, it was decided to investigate whether or

not any of these strains could express hUCP1. One such strain was Rosetta pLysS, from Novagen. When Rosetta pLysS was transformed with pET21d-hUCP1 it did express a protein at 32 kDa, which was confirmed by Western blotting to be UCP1 (Figure 3.3.8). The protein was concentrated in the inclusion body fraction. These results are as expected for a membrane protein expressed in bacteria. All other UCPs are expressed in similar ways in bacteria (Jabůrek *et al.,* 1999). Pre-induced cells do show some expression of hUCP1, which would indicate that the pLysS control is not very good in these cells. Rosetta pLysS transformed with empty pET21d vector did not show any expression of an immunoreactive protein (Figure 3.28) so hUCP1 in pre-induced cells is indeed due to the presence of the hUCP1 gene and not to a native protein in these bacteria.

Successful expression was obtained for haUCP1, hUCP2 and hUCP3 (Figures 3.3.4, 3.3.5 and 3.3.6) in BL21 pLysS. There is obviously no codon bias for these proteins, as was found for hUCP1. No protein was detectable in any pre-induced cells when expressing these proteins. This indicates that the control that the pLysS plasmid should have conferred upon expression of protein was working correctly, i.e. no protein should be expressed in the absence of IPTG. In all cases, haUCP1, UCP2 and UCP3 were expressed predominantly in the inclusion-body fraction. From work on other mitochondrial membrane proteins, such as the oxoglutarate carrier, accumulation in inclusion bodies is to be expected (Fiermonte *et al.,* 1993). Expression of haUCP1 in BL21 pLysS may indicate that it does not suffer from codon bias as is predicted to be the case for hUCP1. In Figure 3.3.5 the results of probing BL21 pLysS transformed with empty pET21d plasmid are shown. No production of immunoreactive protein can be seen and, indeed, it appears that no inclusion bodies were formed (results not shown). Inclusion bodies are only formed in the event of production of foreign or toxic proteins, which become aggregates of improperly folded species. In the case of expression of polytopic eukaryotic membrane proteins, inclusion bodies are a good indication of protein expression. Empty plasmid should not confer any ability on the *E. coli* to express any foreign or toxic proteins.

Ability to express the UCPs now opens an avenue for analysis of their function, in isolation, when reconstituted into proteoliposomes.

On successful expression of all three uncoupling proteins, it was then possible to characterise the peptide antibodies for each UCP that had been raised in our laboratory. The ability to specifically recognise a protein is an important tool in research. The Eurogentec anti-UCP1 peptide antibody showed specificity for UCP1 over UCP2 and UCP3 (Figure 3.2.9). The peptide, CHLHGIKPRTGTYNA, was predicted on a Kyte-Doolittle plot to be hydrophilic, discriminatory, antigenic and specific for rUCP1 (Figure 3.1.1). Figure 3.2.9 shows that this antibody is incapable of detecting hUCP2 or hUCP3 but it is capable of detecting haUCP1. The levels of hUCP2 and hUCP3 used can be detected using anti-UCP2 antibodies (Figure 3.2.4) and anti-UCP3 antibodies (figure 3.2.5) respectively. The Eurogentec anti-UCP1 peptide antibody has also been shown to react with hUCP1 (results not shown).

The anti-UCP3 peptide antibody was also a successful antibody. The antibody showed specificity for UCP3 (Figure 3.2.10). The peptide, TGGERKTRGTMAYRC, was predicted on a Kyte-Doolittle plot to be hydrophilic, discriminatory, antigenic and specific for UCP3 (Figure 3.1.2). Figure 3.2.10 shows that the UCP3 antibody is unable to detect hUCP2 or haUCP1, even when similar amounts of protein detectable by anti-UCP1 (Figure 3.2.6) and anti-UCP2 (Figure 3.2.4) antibodies were loaded on the gel (Figure 3.2.10). Therefore, it can be concluded that this anti-UCP3 antibody does not react with expressed UCP1 or expressed UCP2 to any detectable level. No antibody to date has been shown to be specific for UCP3 over UCP1 and UCP2. Such a discriminatory antibody has the potential to be a valuable tool in the specific detection of UCP3.

Chapter Four

Investigation of the fatty-acid buffering model for rUCP1 using fatty-acid analogues.

4.1 Introduction

In BAT, dissipation of the proton electrochemical gradient across the mitochondrial inner membrane by UCP1 is the molecular basis of non-shivering thermogenesis in mammals, including human infants (Nicholls, 1976; Nicholls and Locke, 1984; Ricquier and Bouillaud, 1986; Cannon and Nedergaard, 2004; Nicholls, 2004). Consequently, UCP1 acts as a major regulator of metabolic flux in BAT and, as a heat regulator, in the whole animal.

UCP1 has been shown to reach levels of between 5 and 10% of total mitochondrial protein (Lin and Klingenberg, 1980; Cannon *et al.,* 1982). Its abundance compared to other mitochondrial carriers proved helpful in its isolation. Using solubilization of BAT mitochondria by the non-ionic detergent Triton X-100, followed by HTP chromatography, UCP1 was isolated to 90% homogeneity (Lin and Klingenberg, 1980). Their method was based on their procedure for the isolation of the ANC. It is this ability to isolate UCP1 to such purity that allows it to be reconstituted into proteoliposomes.

Reconstitution of native haUCP1, using detergent-mediated reconstitution protocols, has provided an assay system with which to study UCP1's mechanism of action. The method used is that of detergent-mediated reconstitution. What is clear in the reconstituted system is that there is an absolute requirement for long-chain fatty acids, to facilitate uncoupling activity and that purine nucleotides inhibit the uncoupling activity. How exactly long-chain fatty acids facilitate uncoupling is where the main dichotomy on theories of mechanism of action lies; there are two main models proposed based on the reconstituted system. The first proposes that UCP 1 acts as a H^+ conduit across the mitochondrial inner membrane and, importantly, that fatty acids act as cofactors/activators providing an additional carboxy moiety at a key intra-membrane site, thus enhancing the rate of H^+ movement (Klingenberg *et al.,* 1999; Klingenberg and Huang, 1999; Nicholls and Rial, 1999).This model has been given the name "The

fatty-acid buffering model". The second model proposes a two-step event, whereby the protonated fatty acids freely flip across the mitochondrial inner membrane, independently of UCP1; H^+ dissociate from the fatty acids into the matrix and the resulting fatty-acid anions are flipped back across the inner membrane by UCP1 (Skulachev, 1988; Garlid *et al.,* 2000). This model has been called "The fatty-acid protonophore model".

The best evidence for the fatty-acid protonophore model comes from the observation that undecanesulfonate can be flipped by UCP1. Undecanesulfonate is an analogue of laurate (a known facilitator of UCP1 activity). Undecanesulfonate - having a pK_a of 2 - is a permanent anion, at physiological pH values and cannot support H^+ activity at all. However, undecanesulfonate can act as a competitive inhibitor of UCP1's Cl^- transport and of laurate-induced H^+ activity, thereby linking anion activity with H^+ activity (Garlid *et al.,* 1996). It is this anion activity that has been proposed by Garlid's group to support the protonophore model. The transport of undecanesulfonate mimics the transport of the fatty acid anion in the two-step cycle associated with the protonophore model. Furthermore, flip-flop-incapable fatty acids have been identified, such as dodecanedioic acid (Ježek *et al.,* 1997a) and ω-glucopyranoside palmitic acid (glucose-*O*-ω-palmitate; Klingenberg *et al.,* 1999). On the one hand, Ježek *et al.* (1997b) have shown that dodecanedioic acid is incapable of supporting UCP1 H^+ activity, while, on the other hand, Klingenberg *et al.* (1999) have reported that ω-glucopyranoside palmitic acid is capable of supporting UCP1 H^+ activity. The work done by Klingenberg's group involving ω-glucopyranoside palmitic acid is the key piece of evidence to support the buffering model. However, no original data were ever presented to substantiate this report nor has the synthesis, purity or stability of the resulting glycolipid ever been reported.

The results pertaining to mechanism lead to a very confusing picture of the mechanism of UCP1 uncoupling activity. In this study, I set out to re-investigate evidence for the buffering model by using analogues of palmitic acid that were modified at the ω-end. Two of the palmitate analogues were

synthesized *de novo*, namely glucose-*O*-ω-palmitate (Gouin *et al.,* 2005) and ω-methoxypalmitate. If the buffering model is correct, modification to the ω-carbon of palmitate should not impair access of the α-carboxy group to the intra-membrane site. By contrast, the protonophore model would predict that such modifications should hinder, if not abolish, H^+ flux (and the fatty-acid anion flux) in UCP1-containing liposomes. In addition, based on the protonophore model, one would predict that ω-end modification should impair activation of GDP-inhibited UCP1 function in BAT mitochondria. The structures of the fatty-acid analogues used in this study are show in Figure 4.1. What follows are data obtained while investigating the buffering model.

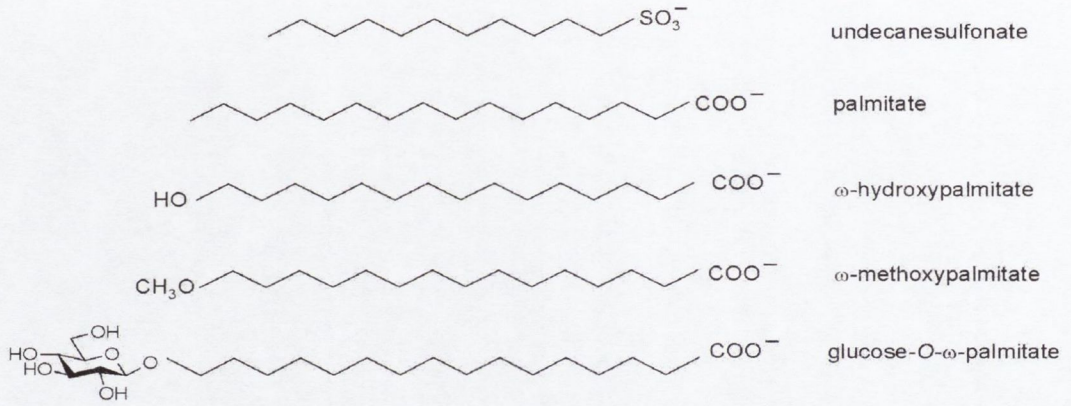


Figure 4.1.1 Structures of fatty acids and fatty-acid analogues used

4.2.1 Purification and identification of UCP1 from rat BAT mitochondria.

To establish the purity of UCP1 from rat BAT, as in all previous studies, native haUCP1 was used as the source. The mitochondria were solubilized in the non-denaturing, non-ionic detergent C_8E_5 in the presence of extra phospholipids, prior to being applied to HTP. The flow-through fraction from the HTP was subjected to 1D SDS-PAGE and stained using Colloidal Coomassie Blue G-250 to allow for analysis by mass spectrometry. Figure 4.2.1 shows that the predominant band on this gel has a Mr of approximately 30–33 kDa.

The stained band was excised using a scalpel and tryptic peptides were prepared for analysis. Seven peptides were identified using MALDI-TOF/TOF MS by peptide mass mapping by comparison with previous UCP 1 MS data (Carroll *et al.,* 2005) or by TOF/TOF analysis of the three most intense peptides in the peptide mass fingerprint spectrum. (Figure 4.2.2 B). With the latter, BLAST searching of nonredundant databases with the peptide sequences unequivocally identified mitochondrial brown fat uncoupling protein 1 (UCP1) from *Rattus norvegicus*.

4.2.2 Reconstitution of rat BAT UCP1 into liposomes.

Once UCP1 was reconstituted into liposomes, the protein content was analysed using the Amido Black protein assay (Section 2.2.20). Typically, the protein content of these vesicles was between 1 and 3 μg of protein per mg of lipid. The internal volume of the vesicles was typically 0.5 μl/mg of lipid.

Purified UCP1 was then shown to be functionally competent after reconstitution into liposomes. Figure 4.2.3 shows typical traces of changes in intraliposomal H^+ concentration as a function of time. Changes in SPQ

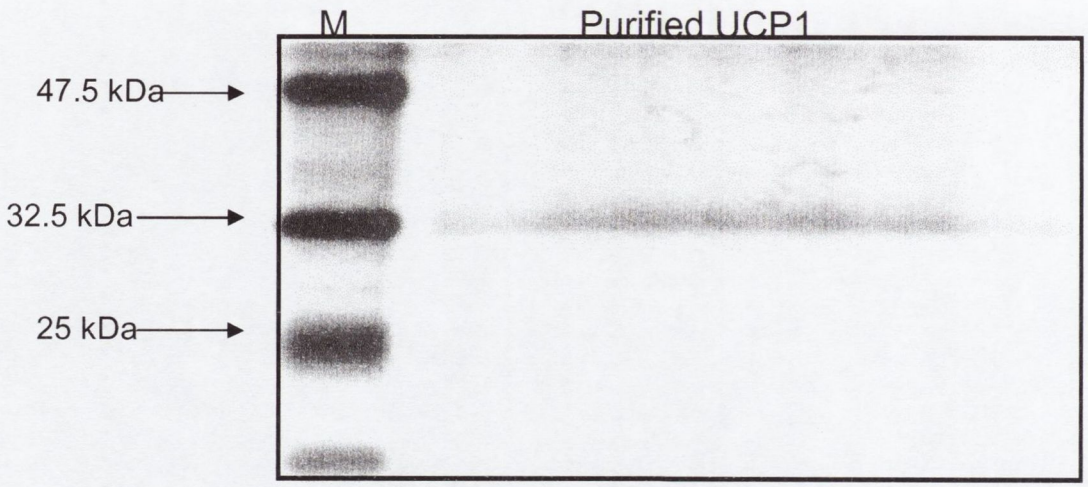


Figure 4.2.1 Colloidal Coomassie Blue G-250 stained SDS-PAGE gel of UCP1 purified from rat BAT mitochondria

UCP1 was purified from BAT mitochondria by the method of Lin and Klingenberg (1980; Section 2.2.15). The purified protein (~12 μg) was subjected to SDS-PAGE (12.5% resolving gel) in an extra-wide lane and stained with Colloidal Coomassie Blue G-250 (Section 2.2.9.3). Positions of molecular mass standards are indicated (Lane M).

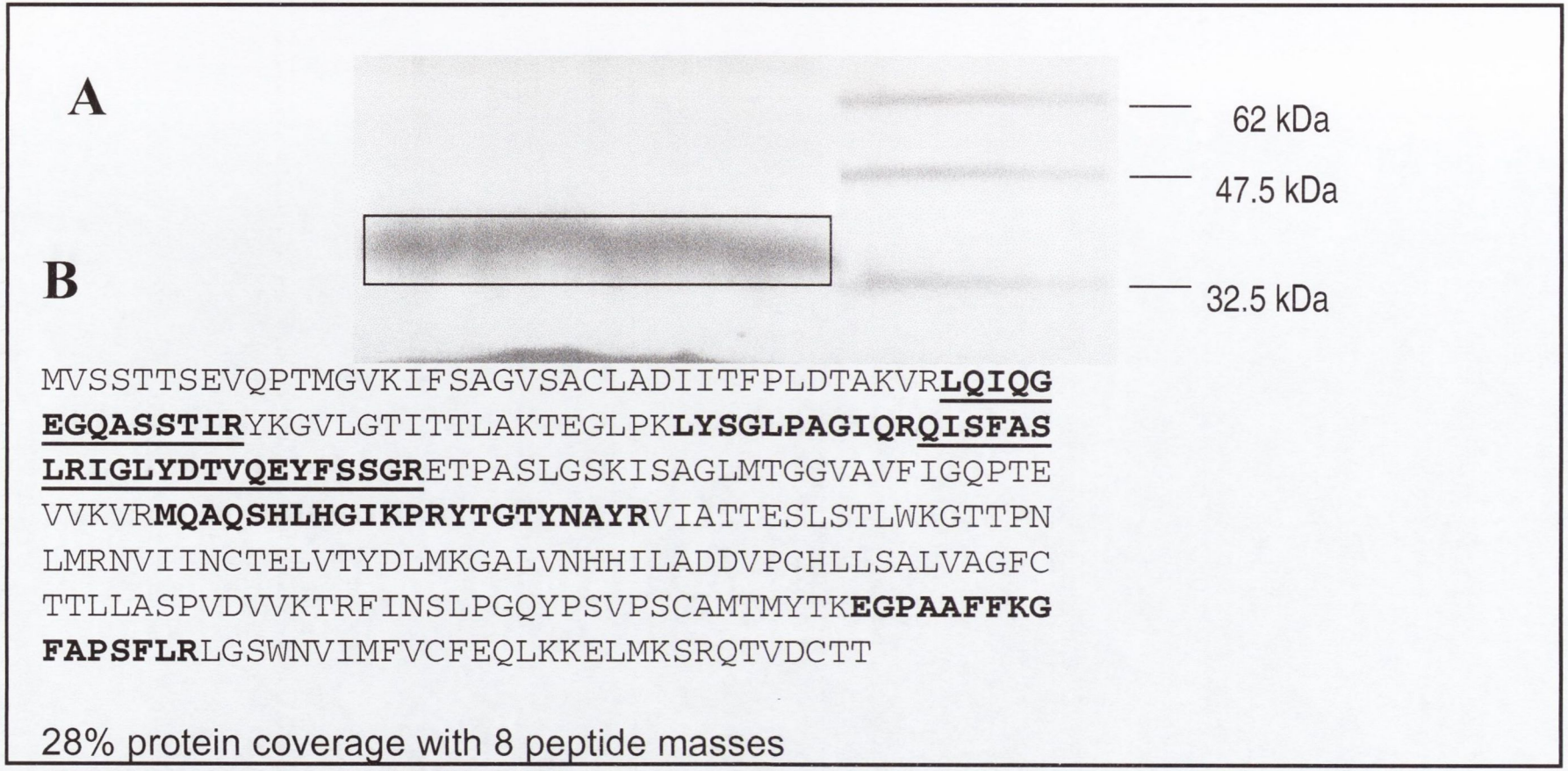


Figure 4.2.2 Identification of isolated rat brown adipose tissue UCP1 proteins by mass spectrometry.

A. One-dimensional gel electrophoresis of purified UCP1 from rat brown adipose tissue mitochondria. The gel was stained with colloidal Coomassie Blue G-250. The broad band at 30-33 kDa was excised and in-gel digestion with trypsin was performed prior to mass spectrometric analysis of tryptic cleavage products. Molecular mass markers are shown in the right-hand lane. **B.** UCP1 peptides identified by peptide mass fingerprinting. Bold: previously identified peptide sequences. Underlined: peptide sequences identified by TOF/TOF.

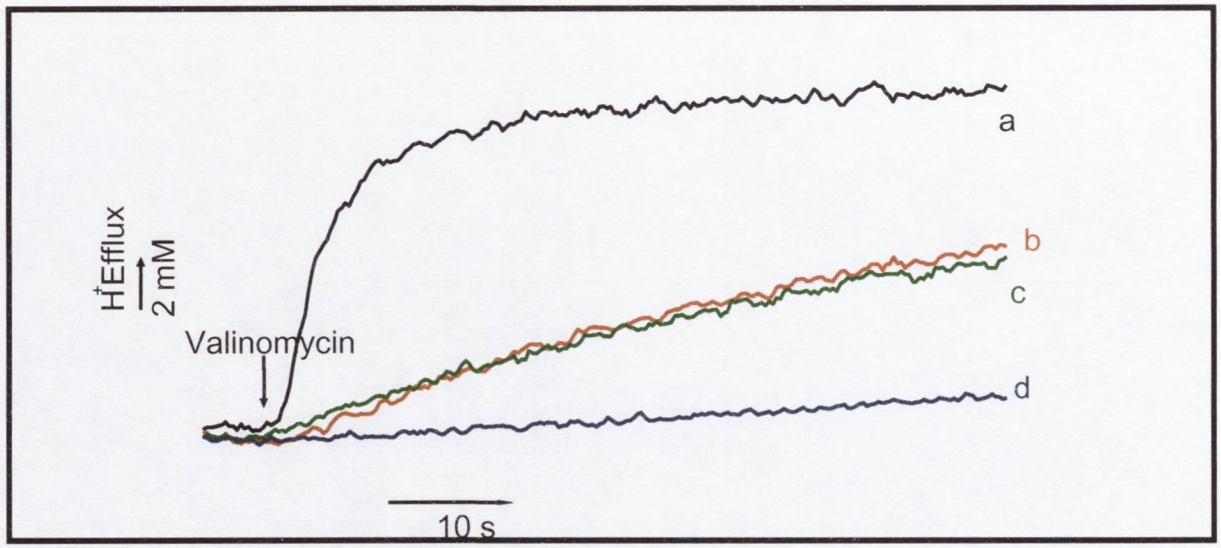


Figure 4.2.3 H^+ efflux from vesicles containing purified native rUCP1 in the presence of palmitate and GDP.

H^+ flux in proteoliposomes was determined by measuring changes in SPQ fluorescence, which is quenched by the anion of TES. Transport was initiated by the addition of 100 nM valinomycin.
Trace a: 100 µM palmitate
Trace b: 100 µM palmitate with 1 mM GDP present on both sides of the vesicle.
Trace c: 1 mM GDP present on both sides of the vesicle
Trace d: 100 µM palmitate with protein-free liposomes.
H^+ flux was measured as the initial rate of flux. The data are representative of three independent experiments performed in triplicate.

fluorescence inside the vesicle allow this to be measured as SPQ's fluorescence is quenched by the anion of TES. Fluxes were measured as the initial rate of change of $[H^+]$. Trace a shows the protein's activity in the presence of 100 μM palmitate and trace b shows the activity to be inhibited by 1 mM GDP, which is present on both sides of the vesicle membrane. Addition of valinomycin in the absence of palmitate also induces H^+ flux (trace c) but this flux is similar to H^+ flux in the presence of inhibitory amounts of GDP (trace b). Protein-free liposomes were also investigated for H^+ flux in the presence of palmitate. Trace d shows that there is little H^+ flux in protein-free liposomes on addition of valinomycin in the presence of palmitate.

4.2.3 Effects of modification of the ω-carbon of palmitate on UCP1 H^+ flux.

Once the activity of rUCP1 in the presence of palmitate had been established, the effects of modifying the ω-carbon of palmitate would be used to investigate the evidence for the buffering model. Figure 4.2.4 shows UCP1 activity in the presence of palmitate, ω-hydroxypalmitate and ω-methoxypalmitate. Substitution of palmitate with the hydrophilic moiety, OH^-, reduces palmitate's ability to activate rUCP1 (trace b). The more hydrophobic moiety of OCH_3 proves to be a better activator (trace c). The presence of 1 mM GDP on both sides of the vesicle inhibits both substituted palpitates (traces d and e). Figure 4.2.4 shows the glucose substituted glucose-*O*-ω-palmitate to be a poor activator of rUCP1 (trace b). There is little difference in the initial rate of H^+ flux in the presence of GDP (trace d). Undecanesulfonate also proves to be a poor activator of rUCP1 (trace c), as expected.

Data for initial H^+ flux in the presence of the fatty-acid analogues are summarized in Figure 4.2.6. All rates were corrected for the flux in the absence of fatty acid but the presence of GDP, i.e. non-UCP1-mediated flux. The rate for palmitate (9.9 ± 0.7 μmoles H^+/min/mg) was greater than

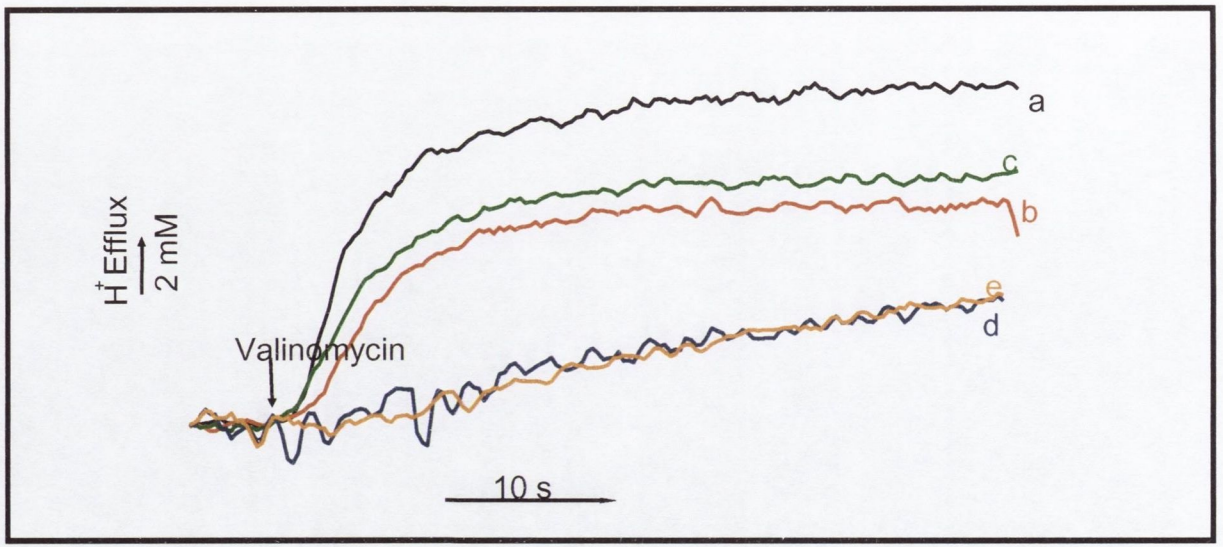


Figure 4.2.4 Palmitate and palmitate analogue-dependent H^+ efflux from vesicles containing purified native rUCP1.

H^+ flux in proteoliposomes was determined by measuring changes in SPQ fluorescence, which is quenched of by the anion of TES. Transport was initiated by the addition of 100 nM valinomycin.
Trace a: 100 µM palmitate
Trace b: 100 µM hydroxypalmitate
Trace c: 100 µM methoxypalmitate
Trace d: 100 µM hydroxypalmitate with 1 mM GDP present on both sides of the vesicle.
Trace e: 100 µM methoxypalmitate with 1 mM GDP present on both sides of the vesicle.
H^+ flux was measured as the initial rate of flux. The data are representative of three independent experiments performed in triplicate.

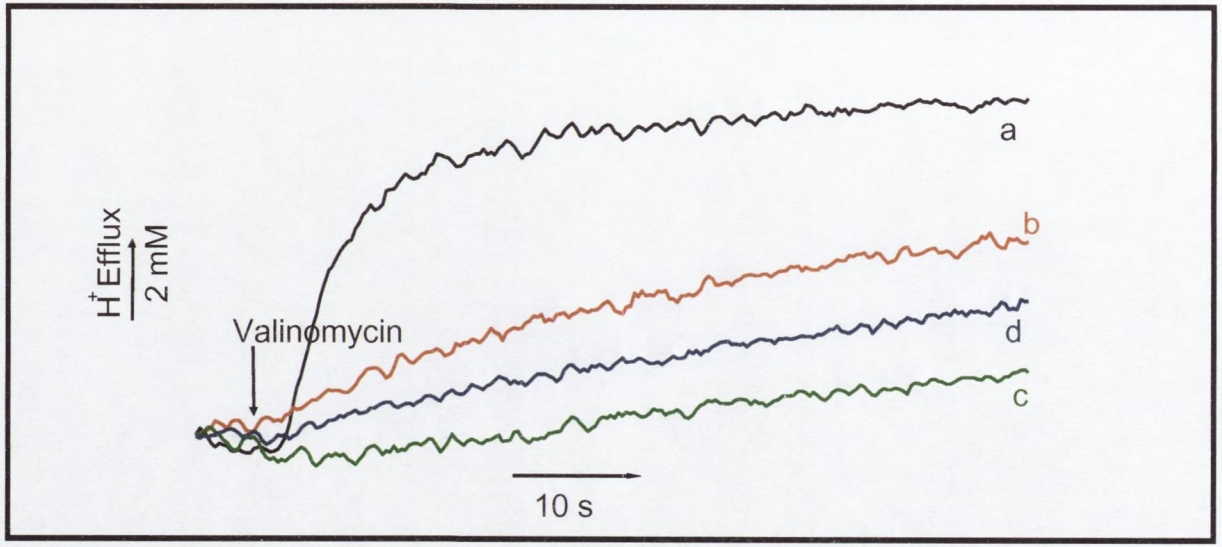


Figure 4.2.5 H^+ efflux from vesicles containing native rUCP1 in the presence of palmitate, glucose-*O*-ω-palmitate and undecanesulfonate

H^+ flux in proteoliposomes was determined by measuring changes in SPQ fluorescence, which is quenched by the anion of TES. Transport was initiated by the addition of 100 nM val.
Trace a: 100 µM palmitate
Trace b: 100 µM glucose-*O*-ω-palmitate
Trace c: 100 µM undecanesulfonate
Trace d: 100 µM glucose-O-ω-palmitate with 1 mM GDP present on both sides of the vesicle.
H^+ flux was measured as the initial rate of flux. The data are representative of three independent experiments performed in triplicate.

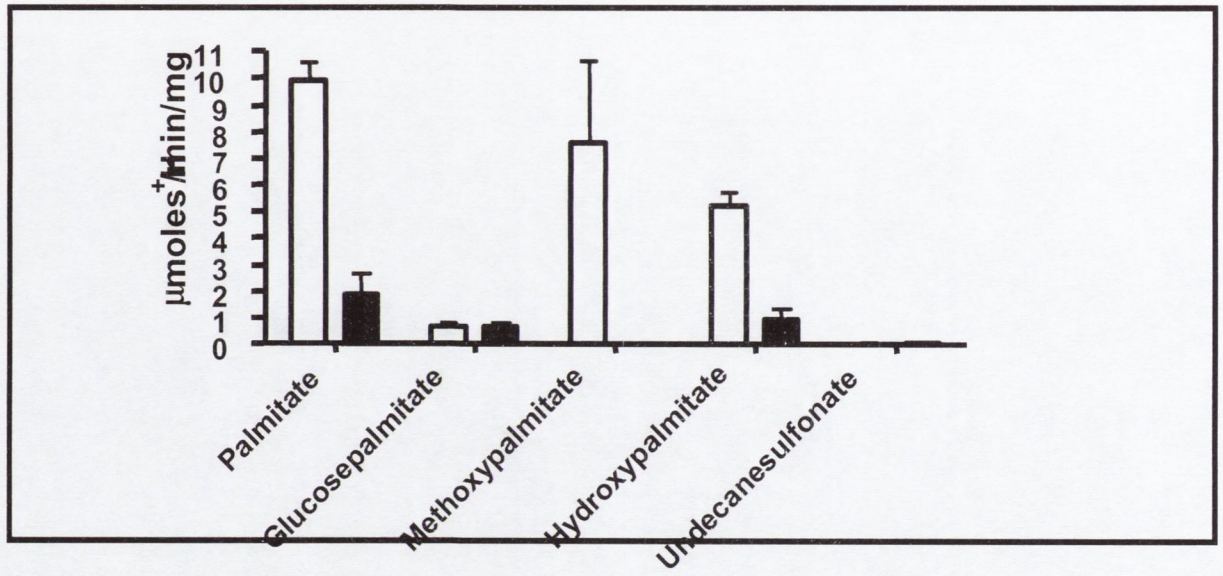


Figure 4.2.6 The effects of palmitate, palmitate analogues and undecanefulfonate on H^+ efflux from proteoliposomes containing native rUCP1.

Summary of the initial rate of H^+ effluxes in proteoliposomes containing native rUCP1 in the absence ( ) and presence ( ) of 1 mM GDP. Palmitate, palmitate analogues and undecanesulfonate were all used at 100 µM concentration. All rates are corrected for flux in the absence of added fatty acid. Data are expressed as mean ± S.E.M. of three experiments performed in triplicate.

that for ω-methoxypalmitate (7.6 ± 3.0 μmoles H^+/min/mg), which, in turn, was greater than that for ω-hydroxypalmitate (5.2 ± 0.5 μmoles H^+/min/mg). There was a statistically significant difference between the flux in the presence of palmitate when compared with the flux in the presence of glucose-*O*-ω-palmitate ($p < 0.0001$). As expected, there was a significant difference in the rate of H^+ flux when comparing palmitate in the absence and presence of GDP ($p = 0.0008$). However, there was no significant difference in H^+ flux rates when comparing glucose-*O*-ω-palmitate in the absence and presence of GDP ($p = 0.8923$).

4.2.4 Effects of fatty acid analogues on the charge-transfer assay of rUCP1.

The movement of K^+ across the vesicle membrane is an indication of the co-movement of an anion by rUCP1. Figure 4.2.7 shows a typical trace of the change in concentration of K^+ (as measured by an increase in the PBFI fluorescence inside the vesicle) as a function of time. Both palmitate and undecanesulfonate are shown to support the movement of K^+ (traces a and b) and this activity is inhibitable by GDP (traces d and e). Glucose-*O*-ω-palmitate shows poor ability to support K^+ movement in the absence (trace c) or presence of GDP (trace f).

Data for initial K^+ flux in the presence of the fatty-acid analogues are summarized in Figure 4.2.8. All rates were corrected for non-UCP1-mediated flux, *i.e.,* activity in the absence of fatty acid but the presence of GDP. Palmitate-induced activity (34.8 ± 3.9 μmoles K^+/min/mg) is greater than that of ω-methoxypalmitate- (27.1 ± 10.8 μmoles K^+/min/mg) and ω-hydroxypalmitate- (14.1 ± 1.8 μmoles K^+/min/mg) induced activity. The permanent anion of undecanesulfonate is able to support the charge-transfer activity of rUCP1 (30.7 ± 2 μmoles K^+/min/mg). There is a statistically significant difference between the fluxes for UCP1 in the presence of palmitate and glucose-*O*-ω-palmitate ($p < 0.0013$). There is a statistically significant inhibition of palmitate-induced UCP1 charge transfer

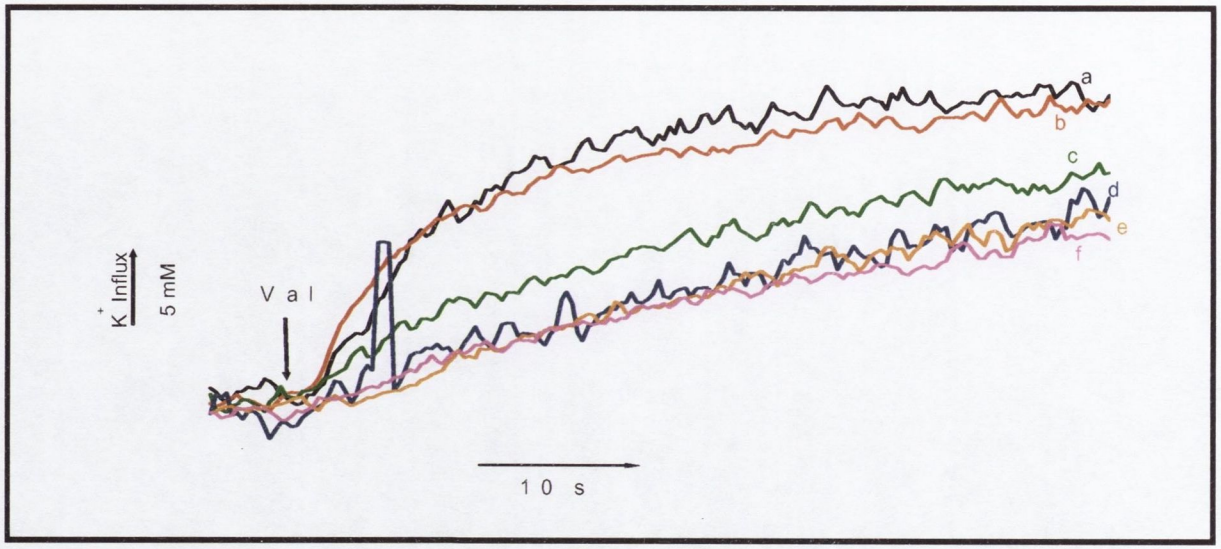


Figure 4.2.7 K^+ flux across the vesicle membrane in response to rUCP1 interaction with palmitate, glucose-*O*-ω-palmitate and undecanesulfonate.

K^+ flux in proteoliposomes is determined by measuring changes in PBFI fluorescence, which occurs on contact with K^+. This flux then corresponds to the flux of anions through rUCP1. Transport is initiated by the addition of 50 nM val.
Trace a: 100 µM palmitate
Trace b: 100 µM undecanesulfonate
Trace c: 100 µM glucose-O-ω-palmitate
Trace d: 100 µM palmitate with 1 mM GDP present on both sides of the vesicle
Trace e: 100 µM undecanesulfonate with 1 mM GDP present on both sides of the vesicle.
Trace f: 100 µM glucose-O-ω-palmitate with 1 mM GDP present on both sides of the vesicle.
K^+ flux was measured as the initial rate of flux. The data are representative of three independent experiments performed in triplicate.

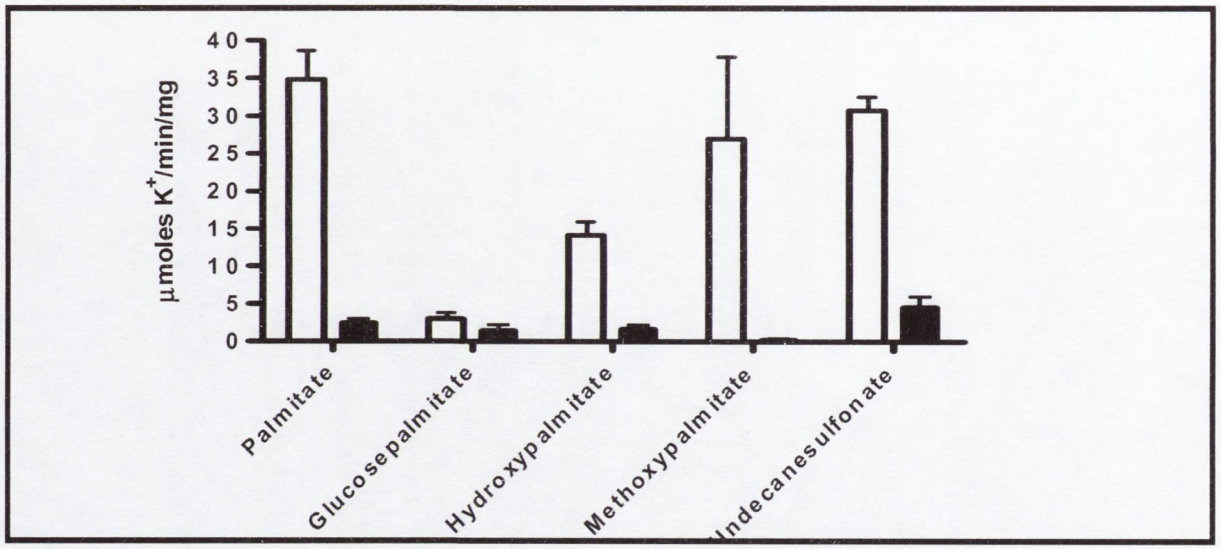


Figure 4.2.8 Transport of the anions of palmitate, palmitate analogues and undecanesulfonate via native rUCP1.

Summary of the initial rate of K^+ effluxes in proteoliposomes containing native rUCP1 in the absence ( ) and presence ( ) of 1 mM GDP. K^+ flux corresponds to the cotransport of anion by rUCP1. Palmitate, palmitate analogues and undecanesulfonate were all used at 100 µM concentration. Data are expressed as mean ± S.E.M. of three experiments performed in triplicate.

activity by GDP (p = 0.0012) whereas this is not the case for glucose-*O*-ω-palmitate (p = 0.4689).

4.2.5 Effect of palmitate and glucose-*O*-ω-palmitate on state 4 oxygen consumption in BAT mitochondria.

The function of UCP1 and its dependence on long-chain fatty acids can also be observed in BAT mitochondria. In this instance, fatty-acid-induced oxygen consumption by GDP-inhibited, non-phosphorylating mitochondria is used as an indirect measure of UCP1 activity. Figure 4.2.9 shows that the non-phosphorylating oxygen-consumption rates (state 4) of BAT mitochondria isolated from rats kept at rt in the presence of inhibitors for the ANC and ATP synthase. The state-4 oxygen-consumption rate, 1504.9 ± 40.3 pmoles O_2/s/mg protein, was significantly decreased by the addition of 0.5 mM GDP to 1127 ± 45.8 pmoles O_2/s/mg. In turn, the oxygen-consumption rate was significantly stimulated by palmitate (~ 40 nM free fatty acid) to 1658 ± 64.7 pmoles O_2/s/mg (p < 0.0001,), which is similar to the uncoupled rate (1574 ± 81.9 pmoles O_2/s/mg) induced by the addition of 30 μM DNP. Figure 4.2.10 shows that the state-4 oxygen-consumption rate, 1486.9 ± 62.9 pmoles O_2/s/mg, is inhibited by 0.5 mM GDP to 1058 ± 63 pmoles O_2/s/mg. In contrast to palmitate, this GDP-inhibited rate was not significantly stimulated by glucose-*O*-ω-palmitate (~40 nM free) but, in fact was slightly reduced (979 ± 46.9 pmoles O_2/s/mg; p = 0.032). Subsequent addition of 30 μM DNP produced an uncoupled rate of 1391.9 ± 91.6 pmoles O_2/s/mg, which is similar to the uncoupled rate of oxygen consumption for mitochondria without glucose-*O*-ω-palmitate.

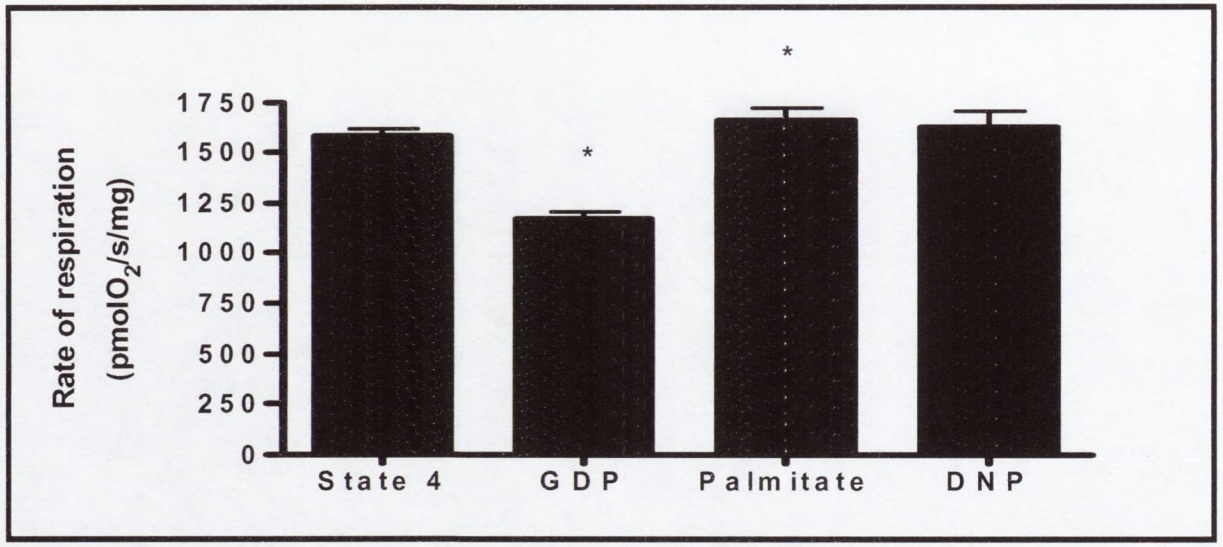


Figure 4.2.9 Effects of purine nucleotides and palmitate on state 4 oxygen consumption rates in rat BAT mitochondria.

Oxygen-consumption rates were calculated using the DatLab 2.1 program associated with the Oxygraph used. BAT mitochondria (0.1 mg/ml) were incubated in KHE medium with 16 μM BSA. GDP (0.5 mM) was used to inhibit UCP and palmitate was added at a final concentration of 64 μM (~ 40 nM free) followed by 30 μM DNP.

* Statisitical significance for the difference in rate of respiration in the presence of GDP and palmitate, as determined by the paired student's *t* test ($p < 0.0001$)

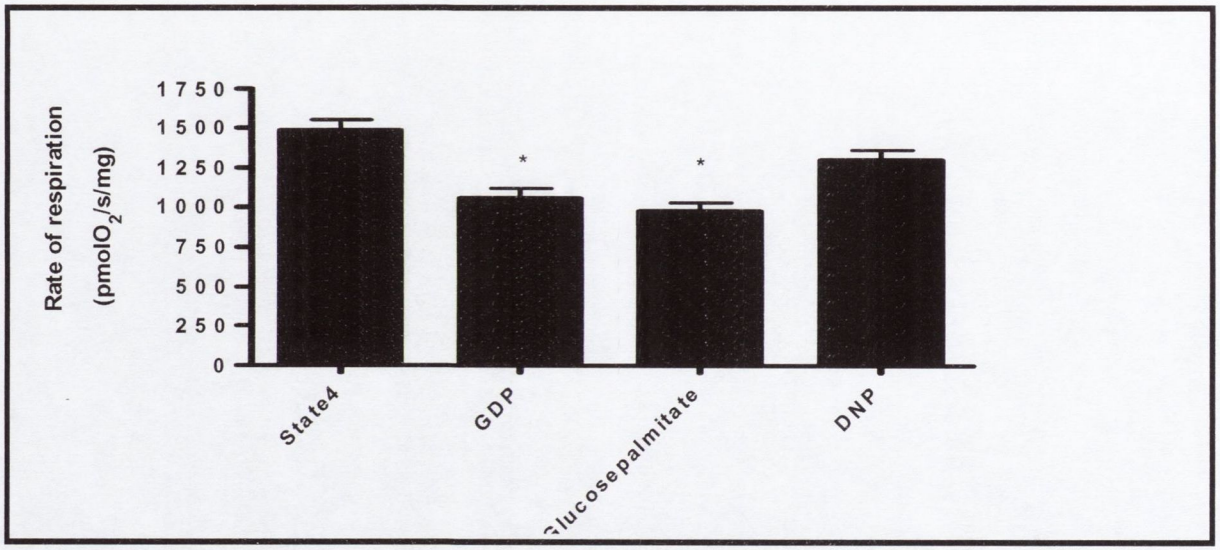


Figure 4.2.10 Effect of purine nucleotides and glucose-*O*-ω-palmitate on state-4 oxygen-consumption rates in rat BAT mitochondria.

Oxygen consumption rates were calculated using the DatLab 2.1 program associated with the Oxygraph used. BAT mitochondria (0.1 mg/ml) were incubated in KHE medium with 16 μM BSA. A steady-state respiration rate (state 4) was achieved and then 0.5 mM GDP was added followed by glucose-O-ω-palmitate at a final concentration of 64 μM (~ 40 nM free) and then 30 μM DNP.
* Statisitical significance for difference in rate of respiration in the presence of GDP and palmitate as determined by the paired student's *t* test ($p < 0.032$)

4.3 Discussion

Previously UCP1 has been purified from hamster BAT (Lin and Klingenberg, 1980) and then used for functional reconstitution experiments (Strieleman *et al.,* 1985; Klingenberg and Winkler, 1985; Ježek *et al.,* 1990).

In this study, rat BAT is used as the source of UCP1 for reconstitution. As this is the first time that rat native UCP1 has been used for reconstitution work, it was important to determine the purity of the UCP1 purified from rat BAT. Initially 1-D SDS-PAGE of HTP-purified protein yielded a single band at a Mr of 32.5 kDa (Figure 4.2.1). The predicted molecular mass for UCP1 is 33,458 Da. The protein band obtained was stained with colloidal Coomassie Brilliant Blue, excised and sent for analysis by mass spectrometry. MALDI-TOF mass spectrometry results revealed that UCP1 from rat was the predominant protein in the purified fraction. The mass spectrometry results for UCP1 from rat BAT are consistent with those presented by us for UCP1 purified from rat thymus mitochondria (Carroll *et al.,* 2005). UCP2 or UCP3 protein, both of which are known to be expressed in BAT (Carroll *et al.,* 2005; Cunningham *et al.,* 2003; Ricquier and Bouillaud, 2000; Pecqueur *et al.,* 2003) were not detected.

Once purified, rUCP1 was reconstituted into liposomes. In the absence of fatty acid, there was a low basal flux of H^+ across the membrane (Figure 4.2.3). On addition of 100 μM palmitate the H^+ flux across the membrane increased dramatically and could be inhibited back to basal levels when 1 mM GDP was present on both sides of the membrane (Figure 4.2.3). This requirement for fatty acids and inhibition by purine nucleotides concurs with findings by other groups for native haUCP1 (Strieleman *et al.,* 1985; Winkler and Klingenberg, 1994, Ježek *et al.,* 1994). The rate of transport measured here (9.9 ± 0.7 μmoles H^+/min/mg protein) is in agreement with those found for reconstituted yeast-expressed rUCP1 by Jabůrek *et al.* (1999). They found that the V_{max} value was between 10 and 30 μmoles H^+/min/mg.

Liposomes with no protein present show a negligible basal H^+ leak rate, even in the presence of fatty acid (Figure 4.2.3). However, when inactive protein is present, the H^+-leak-rate increases. The higher basal leak rate in UCP1-proteoliposomes may be due to the disruption of the membrane by insertion of the protein. Indeed, ion-leak across membranes is believed to be localized primarily to protein-lipid interfaces (Garlid *et al.,* 1989). As the leak in UCP1-proteoliposomes occurs when UCP1 is fully inhibited and no fatty acid is used, it can be considered to be UCP1-independent leak. H^+ leak due to the insertion of a protein into a membrane has been documented previously; Brand *et al.* (2005) found that by altering the ANC content of *Drosophila* mitochondria, the basal H^+-leak increased with increasing protein content and was fatty-acid independent and carboxyatractyloside-insensitive. The mechanism of this leak is, as yet, unknown and may be non-specific. It was assumed that the leak found in UCP1-inhibited liposomes is also of a non-specific nature. However, there is some evidence that UCP1 cannot take part in non-specific leak; leak in wild-type mouse BAT mitochondria with GDP is similar to UCP1-KO mouse BAT mitochondria (Monemdjou *et al.,* 1999). The sheer presence of UCP1 and its ability to affect basal H^+-leak in membranes outside of its known uncoupling activity may need to be investigated further, as it was once thought that the ANC was also once thought not to effect basal leak. (Sheldon *et al.,* 1996).

The necessity for a free carboxy group on the fatty-acid group to induce H^+-movement by UCP1 is undisputed by many groups (Winkler and Klingenberg, 1994; Garlid *et al.,* 1996; Nicholls and Locke, 1984). However, the mechanism by which the fatty acid allows UCP1 to facilitate H^+ movement is contentious. The cofactor model predicts that there is an intramembrane site within UCP1 for the α-carboxy group. In this study the mechanism of action of UCP1 was reinvestigated. Modification of the ω-carboxy group of palmitate should not impair access of the α-carboxy group to the putative intramembrane site. However, the protonophore model

proposed by Skulachev (1991) involves direct interaction of the ω-end with UCP1 so would not be expected to tolerate all modifications.

The hydroxy-substituted ω-hydroxypalmitate was found to be less active than palmitate (Figure 4.2.6). These results confirm those of Ježek *et al.* (1997a) but are in contrast to those of Winkler and Klingenberg (1994). An explanation for the contrast in results is that the now polar ω-end hinders the fatty acid's ability to partition into the hydrophobic core of the membrane. Only fatty acids that partition into the membrane can activate UCP1 (Winkler and Klingenberg, 1994). Ježek *et al.* (1997b) found that hydroxypalmitate had a reduced capacity to flip across vesicle membranes which would explain the reduced ability to activate UCP1 via the proposed protonophore model. By substituting ω-hydroxypalmitate with a methoxy group, the hydrophobic character of the ω-end increases. ω-Methoxypalmitate was found to be a better activator of UCP1 than ω-hydroxypalmitate (Figure 4.2.6). Indeed, Winkler and Klingenberg (1994) found that increasing the hydrophobicity caused an increase in the efficiency of activation so long as solubility was not compromised, as was the case here (results not shown). The results demonstrate that palmitate and ω-methoxypalmitate, which have more hydrophobic ω-ends than hydroxypalmitate, are better activators. This evidence points towards a preference for hydrophobic ω-ends on fatty acids interacting with UCP1.

A glucose substitution to the ω-end of palmitate adds a large, bulky, hydrophilic moiety to palmitate, which would anchor it to the outside of the vesicle membrane and render it incapable of flip-flop (Klingenberg and Huang, 1999). However, the free α-carboxy group would theoretically still be able to reach an intramembrane site, according to the buffering model. Glucose-*O*-ω-palmitate was found to be incapable of activating UCP1 and addition of GDP did not change the rate significantly (p=0.8923). The cofactor model of Klingenberg and Huang (1999) predicts that glucose-*O*-ω-palmitate can activate UCP1. The results obtained in the current study are in direct contrast to the unsubstantiated reports by Klingenberg and Huang (1999) that glucose-*O*-ω-palmitate was twice as effective at activating UCP1

compared to palmitate. However, it is worth reiterating that the experiments behind the results in Klingenberg and Huang (1999) with glucose-*O*-ω-palmitate have never been published nor was the stability and synthesis of their compound ever shown which raises questions as to the validity of these results (Garlid *et al.,* 2000). By contrast, the method for synthesizing glucose-*O*-ω-palmitate that was used in this study has been published (Gouin *et al.,* 2005). The product has been shown to be stable under ionic conditions and at neutral pH. Furthermore the purity of glucose-*O*-ω-palmitate has been shown to be >90% (Gouin *et al.,* 2005) by nuclear magnetic resonance (NMR).

The difference between activation by palmitate and glucose-*O*-ω-palmitate was found to be extremely significant ($p < 0.0001$). The default position resulting from the inability of glucose-*O*-ω-palmitate to activate UCP1 adds credence to the protonophore model for UCP1. This is further evidenced by studies where "flip-flop-inactive" fatty acids, such as dodecanedioic acid and phenylhexanoic acid, are incapable of supporting the H^+ activity of UCP1 (Ježek *et al.,* 1997).

The protonophore model predicts that UCP1 transports the anion of fatty acids back across the membrane to complete the uncoupling cycle (Garlid *et al.,* 1996). The reconstitution assay using the K^+ fluorescent probe, PBFI, allows for temporal separation of UCP's H^+ activity and its anion transport activity. It has long been known that UCP1 facilitates the movement of Cl^- through the mitochondrial inner membrane (Nicholls, 1974) and that fatty acids can inhibit this transport (Ježek *et al.,* 1997), factors that lead to the protonophore model. Figure 4.2.7 shows the movement of K^+ in response to movement of the fatty-acid anion. As before, we see that the charge-transfer rate was coincident with the hydrophobic nature of the modification to the ω-carbon of palmitate. That is to say, the absence of modification of the ω-carbon of palmitate gave faster rates than the methoxy-group modification, which was faster than the hydroxyl-group modification (Figure 4.2.8). As predicted and as has been shown by others, undecanesulfonate supported charge transfer by rUCP1.

Undecanesulfonate has been used as an indicator of anion transport by UCP1 due to its permanency as an anion at physiological pH values (Garlid *et al.,* 1996). By contrast, glucose-*O*-ω-palmitate did not support this charge transfer activity by rUCP1 (Figure 4.2.8). In fact, glucose-*O*-ω-palmitate gave a rate approximately one fortieth that of palmitate and there was no significant difference in the charge transfer rate due to glucose-*O*-ω-palmitate in the presence or absence of GDP (figure 4.2.8). Glucose-*O*-ω-palmitate with the hydrophilic substitution of glucose is anchored to the membrane and is excluded as a flippable substrate for UCP1 (Klingenberg and Huang, 1999). The inability of UCP1 to transport the anion of glucose-*O*-ω-palmitate counteracts the buffering model and, by default, provides further evidence in support of the protonophore model.

The effect of glucose-*O*-ω-palmitate on UCP1-dependent uncoupling in isolated BAT mitochondria was also investigated. Palmitate can relieve GDP-inhibited the state-4 uncoupled rate of respiration in isolated mitochondria (Figure 4.2.9, Desautels and Himms-Hagen, 1981; Nedergaard and Cannon, 1985). However, glucose-*O*-ω-palmitate was unable to reactivate GDP-inhibited oxygen consumption by non-phosphorylating BAT mitochondria (Figure 4.2.10). The inability of glucose-*O*-ω-palmitate to activate BAT mitochondria is consistent with the data for rUCP1 in the reconstituted system. It is important to note that glucose-*O*-ω-palmitate did not affect electron-transport-chain function as the uncoupler 2,4-DNP was still able to uncouple the mitochondria.

Taken together, modification of the ω-carbon of palmitate affects its ability to activate either UCP1's H^+ activity or charge-transfer activity. Palmitate alone or palmitate with a hydrophobic substitution, like methoxy, can still activate. The hydrophilic substitution of the hydroxy group at the ω-end of palmitate does not abolish, but does reduce, its activity, whereas the glucose substitution does abolish activity. The buffering model predicts that glucose substitution should have no effect on UCP1's uncoupling activity (Klingenberg and Huang, 1999) but the work presented here is inconsistent with this prediction. Hydrophobicity of the activating fatty acid is obviously

necessary to reach the core of the protein for fatty-acid-anion transport activity. Work shown elsewhere in this thesis demonstrates that this site is accessible from either side of the protein. Undecanesulfonate can be transported from either side of the UCP1 in vesicles with similar K_m values.

The work presented here indicates that UCP1 must be able to transport the anion of a fatty acid if that fatty acid can induce UCP1-mediated uncoupling. The anion transport is essential. UCP1 is a member of the anion carrier family; there is neither a physiological basis known for the transport of Cl^- nor does UCP1 transport nucleotides; it is likely that the fatty-acid anions are the true substrate for UCP1. Taken together, these data are inconsistent with the buffering model but are consistent with the fatty-acid protonophore model.

Chapter Five

Investigation into the molecular mechanism of haUCP1 function using undecanesulfonate

5.1 Introduction

A characteristic property of UCP1 is its ability to transport Cl^- (Nicholls and Lindberg, 1973). The Cl^- activity was also found to be inhibited by GDP but not by albumin, indicating that fatty acids are not required for Cl^- transport. Further work using reconstituted UCP1 found a number of competitive inhibitors of Cl^- transport, namely alkylsulfonates, alkylsulfates, benzenesulfonate, oxohalogenides, hypophosphate, hexafluorophosphate and pyruvate (Ježek and Garlid, 1990). There is a large spectrum but strong structural requirements; monovalency, no polar groups attached to the alkyl or aryl chain and transport increases dramatically with anion hydrophobicity (Ježek and Garlid, 1990).

Alkylsulfonates have been the focus of attention, particularly by Garlid's group and the alkylsulfonate that has received the most attention is undecanesulfonate. Undecanesulfonate is identical to laurate except that, instead of an α-COO^- group, it has an α-SO_3^- group. It has a very low pK_a value (2), which means that at physiological pH, it is a permanent anion. Consequently, undecanesulfonate alone cannot catalyse electroneutral H^+ transport in the bilayer (Jabůrek *et al.,* 2001). Undecanesulfonate has not only been found to be a competitive inhibitor of laurate-induced H^+ transport, but it is also transported by UCP with a K_m value (12 μM) that is similar to that observed for laurate (8 μM) as it activated H^+ transport (Garlid *et al.,* 1996).

In the reconstituted system, transport of the anion undecanesulfonate is measured by the co-movement of K^+. The fluorescent probe PBFI increases in fluorescence on binding K^+. K^+ flux, in the presence of valinomycin, was used as a measure of anionic or protonic charge flux. As undecanesulfonate cannot catalyse H^+ flux (Figure 4.2.4; Ježek and Garlid, 1990) it follows that it is transported as the anion by UCP. The protonophore model of UCP-mediated uncoupling proposed by Skulachev (1988) involves UCP transporting the fatty-acid anion to the outer leaflet of the mitochondrial inner membrane. The fatty acid is then protonated, flips back across the

membrane (independent of UCP) to achieve uncoupling. Undecanesulfonate, as a permanent anion, allows for the observation of the anion part of this cycle separate from the H^+ activity.

Jabůrek *et al.* (2001) used propranolol to make a pseudo-fatty-acid out of undecanesulfonate. Propranolol forms permeant ion pairs with alkylsulfonates whereby H^+ is transported with the alkylsulfonate as a neutral ion pair – similar to the electroneutral flip-flop of the protonated fatty acid. In this case, undecanesulfonate can act exactly like laurate.

The aim of this work was to use undecanesulfonate to probe UCP1's mechanism of action. Transport by UCP1 can happen in both directions, with the electric gradient modulating the protein's activity (Klingenberg and Winkler, 1985). In this chapter whether undecanesulfonate can be transported by UCP1 across the vesicle membrane in either direction and whether there is a preferred transport in either direction are addressed.

5.2.1 Immunoblotting of BAT mitochondria.

Samples of BAT mitochondria to be used for the reconstitution of UCP1 were used for Immunoblotting. Figure 5.2.1 shows the presence of UCP1 at a molecular mass of 32 kDa. Liver mitochondria were used as a negative control as they do not contain any UCPs.

5.2.2 Reconstitution of UCP1 from BAT mitochondria.

The purification of UCP1 from BAT mitochondria using hydroxyapatite was based on the method of Lin and Klingenberg (1982). The proteoliposomes typically had an internal volume of 0.5 μl/ml of lipid and 0.3 μl/ml of lipid when GDP was incorporated into the vesicle. The protein concentration for each assay was typically 12 μg/mg of lipid. Figure 5.2.2 shows a typical trace of the change in concentration of K^+ (as measured by an increase in the PBFI fluorescence inside the vesicle) as a function of time. Undecanesulfonate is capable of supporting the movement of K^+. This transport is also inhibitable by GDP and requires GDP on both sides of the membrane for full inhibition.

5.2.3 Undecanesulfonate induces electrophoretic flux in liposomes reconstituted with UCP1.

Undecanesulfonate induces a strong K^+ flux (Figure 3.6) demonstrating that UCP1 transports the sulfonate anion. This flux is inhibitable by GDP, which is another property of these uncoupling proteins. No flux occurs in the absence of undecanesulfonate. However, some basal flux does occur through the membrane independent of the uncoupling protein as observed when GDP was present on both sides of the membrane. Assuming that the protein can have two orientations in the

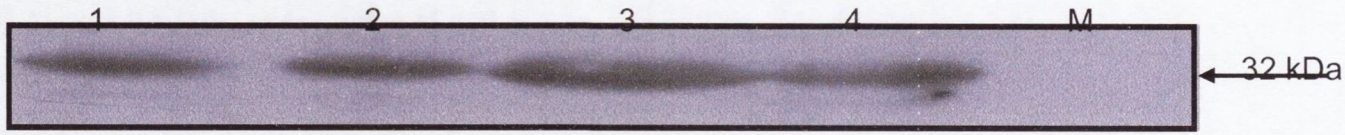


Figure 5.2.1 Immunoblot of Hamster BAT Mitochondria

Mitochondria isolated from BAT of cold-adapted hamsters were separated on a 12.5% polyacrylamide gel and then transferred to PVDF. UCP1 in these mitochondria was detected using the anti-UCP1 peptide antibody. Lanes 1 – 4 contain 20 µg of BAT mitochondrial protein. Position of molecular mass standard is indicated (Lane M).

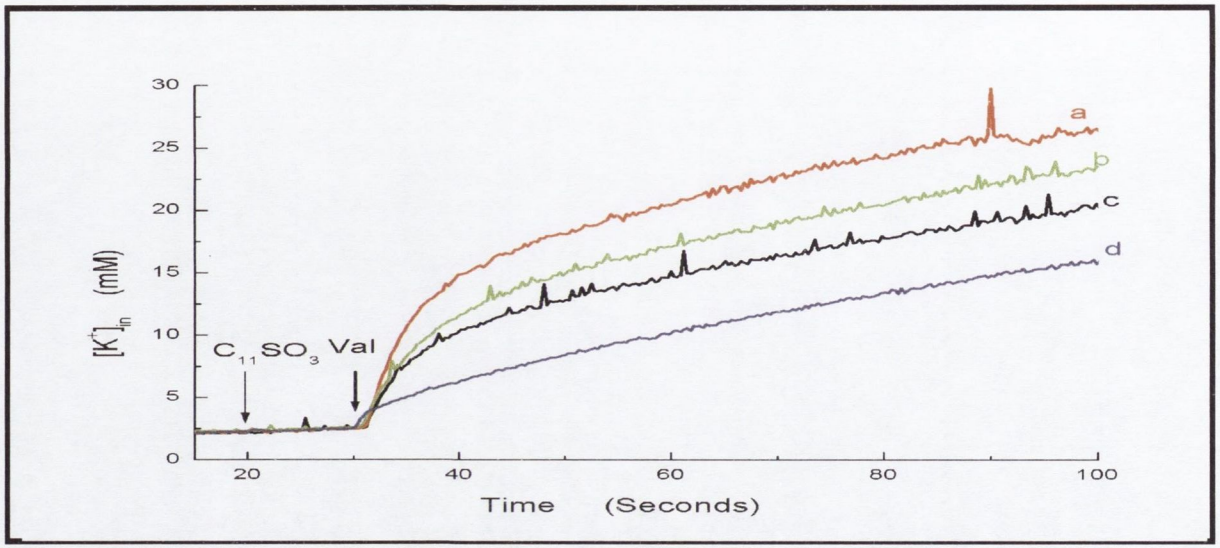


Figure 5.2.2 K^+ flux across vesicle membrane in response to haUCP1 interaction with undecanesulfonate

K^+ flux in proteoliposomes is determined by measuring changes in PBFI fluorescence on contact with K^+. This flux then corresponds to the flux of anions through haUCP1. Transport is initiated by the addition of 50 nM val.

Trace a: 40 µM undecanesulfonate

Trace b: 40 µM undecanesulfonate with 0.5 mM GDP outside the vesicles

Trace c: 40 µM undecanesulfonate with 0.5 mM GDP inside the vesicles

Trace d: 40 µM undecanesulfonate with 0.5 mM GDP present on both sides of the vesicle

K^+ flux was measured as the initial rate of flux.

membrane, with the GDP binding-site facing in or out of the vesicle, Figure 5.2.3 shows a 50:50 distribution of these orientations.

5.2.4 Calculation of the K_M value for undecanesulfonate with both orientations of UCP1.

Figure 5.2.4 shows no significant difference between the K_M values for both orientations of UCP1. The K_M value for UCP1 with the GDP binding-site facing inward (when GDP is on the outside of the vesicle) was 9.3 μM and when the GDP binding-site was facing outwards (when GDP was on the inside of the vesicle only) was 12.4 μM. V_{max} rates for each orientation were 30.2 μmol/min.mg^{-1} for GDP on the outside and 30.4 μmol/min.mg^{-1} with GDP on the inside.

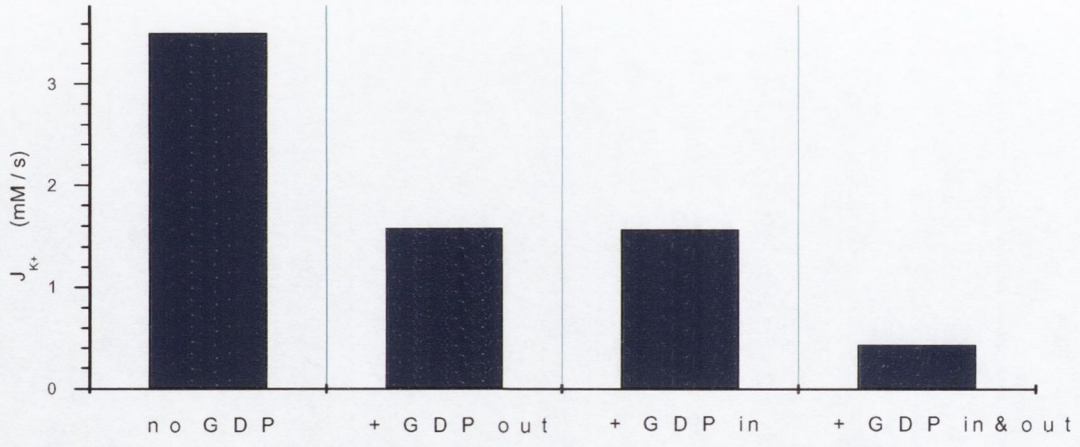


Figure 5.2.3 Examination of the Orientation of UCP1 in Proteoliposomes

K^+ flux in the presence of undecanesulfonate. PBFI fluorescence indicated K^+ movement and was converted to intraliposomal [K^+]. The experiment was carried out on two separate preparations, one containing no internal GDP and the other containing 1 mM internal GDP. Any external GDP added was at a concentration of 0.5 mM. Flux in the absence of GDP indicates maximum K^+ flux where as with GDP on both sides of the membrane, non-UCP1-mediated flux is measured.

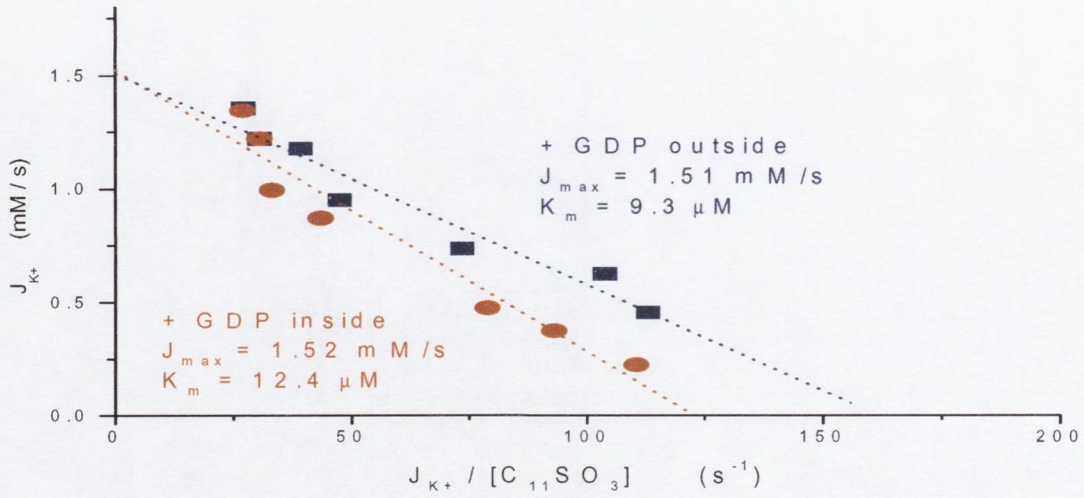


Figure 5.2.4 Kinetics of undecanesulfonate influx into proteoliposomes reconstituted with UCP1

J_{K^+} refers to the K^+ influx, which is an indirect measure of undecanesulfonate influx. Eadie-Hofstee plots constructed for the fluxes *J*, corrected for leak. Values estimated with 1 mM GDP inside and 0.5 mM GDP outside the vesicle. Linear regressions (dotted lines) of the data yield a K_M of 9.3 µM and a V_{max} of 30,200 nmol/min.mg^{-1} when GDP is outside and a K_M of 12.4 µM and a V_{max} of 30,400 nmol/min.mg^{-1} when GDP is inside

5.3 Discussion

Reconstitution of native haUCP1 has been used as UCP1 is in plentiful supply from hamster BAT. The system used was that of Ježek *et al.* (1990). Figure 5.2.1 shows that hamster BAT contains UCP1. Liver has been used as a control as it does not contain UCP1. The immunoreactive protein is exclusive to BAT in this case. Undecanesulfonate can catalyse the net movement of K^+ (Figure 5.2.2). This transport activity is inhibitable by GDP. The presence on GDP on one side of the membrane is incapable of inhibiting the protein fully.

Figure 5.2.3 shows the orientation of the protein. The 50:50 orientation of protein concurs with previous results using this technique (Garlid *et al.,* 1996). However, Klingenberg and Winkler (1985) have claimed that about 90% of the GDP binding sites are on the outside, as with the native form in mitochondria. The system of reconstitution used for the work herein differed to that of Klingenberg and Winkler (1985) in that detergent was removed quickly when forming the vesicles and the ionic composition of the media was completely different. Slower removal of detergent may give the protein and phospholipids time to form proteoliposomes that are similar to the mitochondrial inner membrane, where UCP1's binding site is on the outside. One point of note is that cardiolipin is used in these liposomes whereas phosphatidylcholine alone is used in the construction of liposomes in Klingenberg's laboratory. Cardiolipin has been found to inhibit GDP-binding with reconstituted UCP1 (Klingenberg, personal communication) so its presence in the proteoliposomes may have an influence on the orientation of the protein.

In the fatty-acid protonophore mechanism of uncoupling by UCP1, proton transport occurs independently of the protein via flip-flop of the protonated fatty acid. Fatty-acid anion transport is mediated by UCP1 and anion transport has been studied using undecanesulfonate (Garlid *et al.,* 1996). Undecanesulfonate is an analogue of laurate; however, it has a low pK_a value, which makes it a strong acid and therefore a permanent anion at

physiological pH. The low pK_a value of undecanesulfonate means that undecanesulfonate, unlike laurate, cannot support proton movement (Garlid *et al.,* 1996). K^+ flux across the liposomal membrane (indicated by the change in fluorescence of PBFI) cannot occur without an anion/cation balance; in this case, the undecanesulfonate transport balances the movement of K^+. The transport of undecanesulfonate was found to be inhibitable by GDP, thereby satisfying the proviso for UCP1 involvement (Figures 5.2.2 and 5.2.3). Proton transport across proteoliposomes with undecanesulfonate has been shown by making a pseudo fatty acid from the undecanesulfonate (Jabůrek *et al.,* 2001). This was achieved by making an ion-pair movement with undecanesulfonate and a proton using propranalol. The ion-pair movement allows the undecanesulfonate to act as a protonated fatty acid. Use of the ion-pair allows undecanesulfonate to support uncoupling of BAT mitochondria in a similar fashion to laurate whereas undecanesulfonate alone cannot uncouple BAT mitochondria (Jaburek *et al.,* 2001).

Figure 5.2.4 shows the kinetics of undecanesulfonate influx. As shown, the K_M and V_{max} values for undecanesulfonate with GDP outside are 9.3 μM and 30.2 $\mu mol/min.mg^{-1}$, respectively and, with GDP inside, are 12.4 μM and 30.4 $\mu mol/min.mg^{-1}$, respectively. These values agree with those previously published for undecanesulfonate (Garlid *et al.,* 1996). There are very small and insignificant differences in the kinetics of undecanesulfonate flux between the orientations. The affinity for undecanesulfonate from either side of the protein is very similar, and there was no significant difference between the K_M values (Figure 5.2.4). The binding site for undecanesulfonate is therefore accessible from either side of the protein. Either orientation can support transport of undecanesulfonate or, in other words, the protein can transport undecanesulfonate in either direction. The ability of the uncoupling protein to transport undecanesulfonate in either direction has been recorded before; GDP is required on both sides of the proteoliposomes to fully inhibit undecanesulfonate transport by UCP1 (Ježek *et al.,* 1990; Garlid *et al.,* 1994). The V_{max} values for each orientation

are practically identical. No matter how UCP1 is oriented in the membrane, undecanesulfonate transport can take place. Neither orientation hinders the transport in any way.

Ježek and Garlid (1990) found that increasing the hydrophobicity of the anion increased its transport by UCP1. Interestingly, Winkler and Klingenberg (1994) found that increasing the chain length of fatty acid caused greater activation of proton transport in UCP1 proteoliposomes. It appears that, in either system, the hydrophobicity of the anion or fatty acid increases transport. Only the water-soluble molecules are activating, as undispersed fatty acid will not participate in the partition between the aqueous and the vesicle-bilayer phase (Winkler and Klingenberg, 1994). Thus, the reduced-availability of long-chain fatty acids, such as oleic acid, can limit its activation efficiency, although the intrinsic efficiency of long-chain fatty acids may be high. Hydrophilic substitutions of long-chain fatty acids increase their solubility and indeed activation efficiency (Winkler and Klingenberg, 1994). The solubility of a fatty acid and, therefore, its ability to partition in the bilayer seems to limit its ability to activate UCP1. Sulfonates, being water-soluble, do not have this limit upon their activation ability. Increased hydrophobicity and availability of molecule in solution argues for a need of the fatty acid to partition into the phospholipid phase. Once partitioned into the phospholipid phase, the fatty acid can reach the binding site in the membrane. The results here indicate that the binding site for undecanesulfonate (or fatty acid) is deep within the membrane and at an equivalent position for either orientation of the protein. Due to the driving force set up using the potassium diffusion potential, the protein is forced to transport the undecanesulfonate. It would only be possible for each orientation to transport undecanesulfonate if the binding site was equally accessible from either side.

As displayed in the fatty-acid protonophore model (Figure 1.2), the hydrophobic chain interacts with the protein. Anion transport in UCP1 is not selective for the type of anion but does increase in accordance with the hydrophobicity of the anion (Ježek and Garlid, 1990). The hydrophobic

chain is important for transport, as highlighted by the fact that undecanesulfonate and laurate are transported with similar kinetics (Garlid *et al.,* 1996). Only the hydrophobic chains are similar between the laurate and undecanesulfonate molecules. The knowledge that UCP1 transports undecanesulfonate with similar kinetics in either direction gives an insight into the structure of the protein in the membrane and its accessibility to substrate. These elements are essential to UCP1 function and add another piece of the puzzle into how uncoupling happens via this protein and perhaps also for the homologues UCP2 and UCP3.

Chapter Six

Functional reconstitution of bacterially expressed hUCP1

6.1 Introduction

In this chapter, the kinetics of reconstituted expressed hUCP1 are investigated and the competence of the reconstituted protein is assessed. Successful reconstitution of native UCP1 from BAT mitochondria is aided by the high level of expression in this tissue (Bouillaud *et al.*, 1983; Strieleman *et al.*, 1985; Winkler and Klingenberg, 1985; Jezek *et al.,* 1990). This is not the case for UCP2 and UCP3 as the levels of UCP2 and UCP3 per mg of mitochondrial protein are estimated to be between 100 and 1000-fold less than that of UCP1. Hence, there is no record of their purification in their native form from mitochondria.

The history of providing functionally competent expressed UCP is interesting. In order to study the effect of mutations on the UCP1 protein, yeast expression was used. As yeast contain mitochondria this was a useful expression system for expressing UCP1 in its native form. UCP1 could then be purified by the method outlined for BAT mitochondria (Lin and Klingenberg, 1980) and reconstituted (Modriansky *et al.*, 1997; Echtay *et al.,* 1997). However, flaws were found in the yeast-expression system. Heidekaemper *et al.* (2000) found that hUCP3 and hUCP3s expressed in yeast was incapable of nucleotide-regulated H^+ activity, which was considered to be the measure of UCP activity. Furthermore, hUCP3 was found to be expressed in a deranged form. The evidence for a deranged form of yeast-expressed hUCP3 was supported by evidence of hUCP being expressed in extramitchondrial particles (Winkler *et al.*, 2001) – a "yeast inclusion body". Harper *et al.* (2002) then went on to show that matching UCP3 levels in yeast to those of mouse and rat skeletal muscle gave uncoupling that was not stimulated by fatty acids or inhibited by GDP – a proviso for UCP function. Stuart *et al.* (2001a) demonstrated that over-expression of mUCP1 in yeast cells led to an uncoupling that is not a physiological property of the native protein and is therefore artefactual. Similarly, it was found that when yeast expression levels of UCP2 matched those of mammalian expression levels, uncoupling of the mitochondria did

not occur (Stuart *et al.,* 2001b). It would appear that the yeast system was not suitable for studying the function of UCP2 and UCP3.

Expression in *E. coli* was an option as the proteins could be expressed to high level and were easy to purify in inclusion bodies. However, inclusion bodies give aggregated and non-functional protein so denaturation and refolding were necessary. The function of the protein was surely compromised. Initially yeast-expressed rUCP1 was compared to *E. coli*-expressed hUCP2 and hUCP3 (Jabůrek *et al.,* 1999) although such a comparison is not strict, as yeast-expressed rUCP1 did not need to be denatured and refolded like UCP2 and UCP3. Indeed, when examined, UCP2 and UCP3 were only responsive to very high concentrations of GDP; full activity was displayed in the presence of 100 μM GDP.

Sensitivity of *E. coli* expressed UCPs at a more physiological purine-nucleotide concentration was necessary before confidence in the reconstitution of a competent protein could be concluded. Surprisingly, Echtay *et al.* (2000) also suggested the necessity for addition of coenzyme Q_{10} to reconstituted bacterially-expressed haUCP1 for functional competence. UCP1 function in the presence of coenzyme Q_{10} was shown to be comparable to that of native UCP1 in BAT mitochondria and was highly responsive to purine nucleotides. It was also shown that coenzyme Q_{10} was necessary for fully competent hUCP2 and hUCP3 expressed in *E. coli* (Echtay *et al.* 2001). A system for assaying fully competent hUCPs now appeared to be in place. However, Jabůrek and Garlid (2003) then showed that, by applying a more careful refolding protocol to bacterially expressed UCPs, full activity of UCPs could be achieved without the addition of coenzyme Q_{10}. The effect of coenzyme Q_{10} was shown to be an artefact of solvent addition.

Having established a system for using bacterially-expressed UCPs, there was still the problem that only haUCP1 or rUCP1 could be compared to hUCP2 or hUCP3. If UCP1 was to be used as a paradigm for hUCP2 and hUCP3 function and mechanism of action, then, like must be compared with

like. Having expressed hUCP1 in *E. coli* (Chapter 3), a study of its kinetic parameters in the reconstituted system was desirable.

6.2.1 Reconstitution of recombinant hUCP1 into liposomes.

Once hUCP1 was reconstituted into liposomes, the protein content was determined using the Amido Black protein assay (Section 2.2.19). Typically, the protein content of hUCP1-containing vesicles was between 1 and 2 μg of protein per mg of lipid. The internal volume of the vesicles was typically 0.5 μl/mg of lipid.

It was shown that hUCP1 catalyses a fatty-acid-dependent, electrophoretic H^+ flux in proteoliposomes. Figure 6.2.1 shows the changes in intraliposomal [H^+] as a function of time. As the [H^+] changes so too does the [TES^-] and the fluorescent probe SPQ is quenched by the anion of TES. Fluxes were measured as the initial rate of change of [H^+] following the addition of valinomycin. Trace (a) shows the laurate-induced H^+ flux in the presence of 100 μM laurate and trace (c) shows the H^+ in the presence of 50 μM laurate. Trace (b) shows that the H^+ in the presence of 100 μM laurate is not inhibitable to any extent by the presence of external 1 mM GDP.

6.2.2 The effects of purine nucleotides on H^+-transport by hUCP1.

Purine nucleotides are known to inhibit native reconstituted UCP1 from hamster (Chapter 5) and rat (Chapter 4). However, purine nucleotides did not seem to inhibit the recombinant hUCP1 in these experiments. Figure 6.2.2 shows that concentrations of GDP ranging from 1 to 5 mM did not inhibit laurate-induced H^+-transport by hUCP1. Whether ATP could inhibit H^+ flux in hUCP1 containing liposomes was also examined. Figure 6.2.3 shows that, at ATP concentrations ranging from 1 to 5 mM, there was no inhibition of laurate-induced H^+-transport by hUCP1.

One possible explanation for the lack of purine nucleotide inhibition of H^+ flux through hUCP1 could be the fact that orientation of the protein may

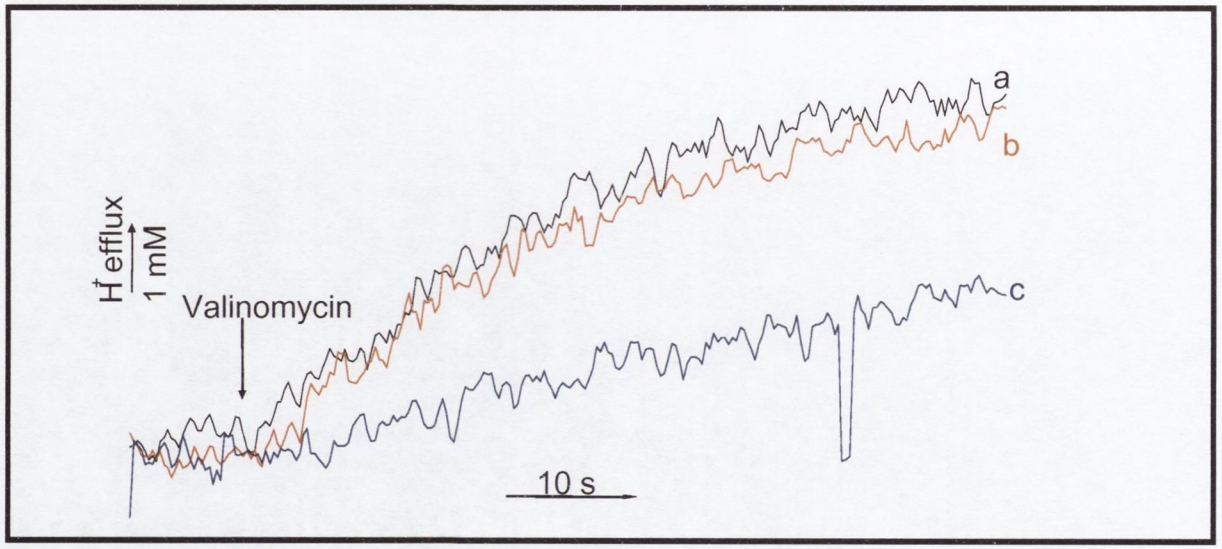


Figure 6.2.1 Laurate induced H^+ efflux from vesicles containing purified recombinant hUCP1.

H^+ flux in proteoliposomes containing hUCP1 was determined by measuring changes in SPQ fluorescence, which is quenched by the TES anion.
Trace a: 100 µM laurate
Trace b: 100 µM laurate plus 1 mM GDP outside
Trace c: 50 µM laurate
H^+ flux was measured as the initial rate of change in $[H^+]$ following the addition of 100 nM val. The data are representative of three independent experiments performed in triplicate.

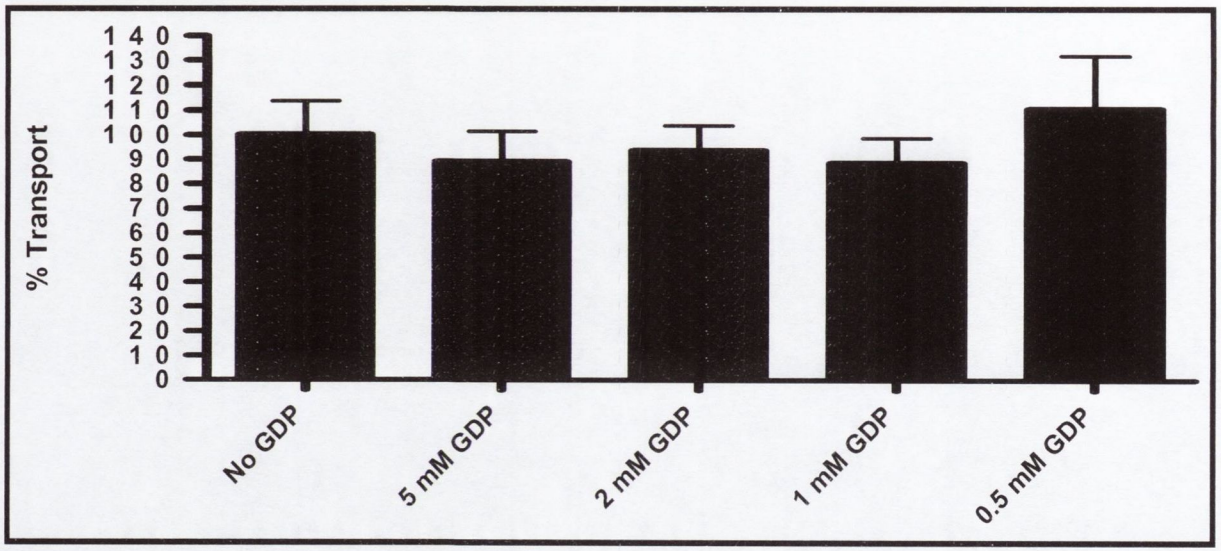


Figure 6.2.2 Effects of GDP concentrations on laurate-induced H^+ transport in proteoliposomes containing hUCP1

Recombinant hUCP1 was expressed in *E. coli* and reconstituted into liposomes. Transport was initiated by the addition of 100 nM val. H^+ flux was measured as the initial rate of change in fluorescence. Laurate was used at 150 μM and GDP was used as indicated. Transport in the absence of GDP was set to 100%. Data are expressed as the mean ± S.E.M. of at least three experiments performed in triplicate.

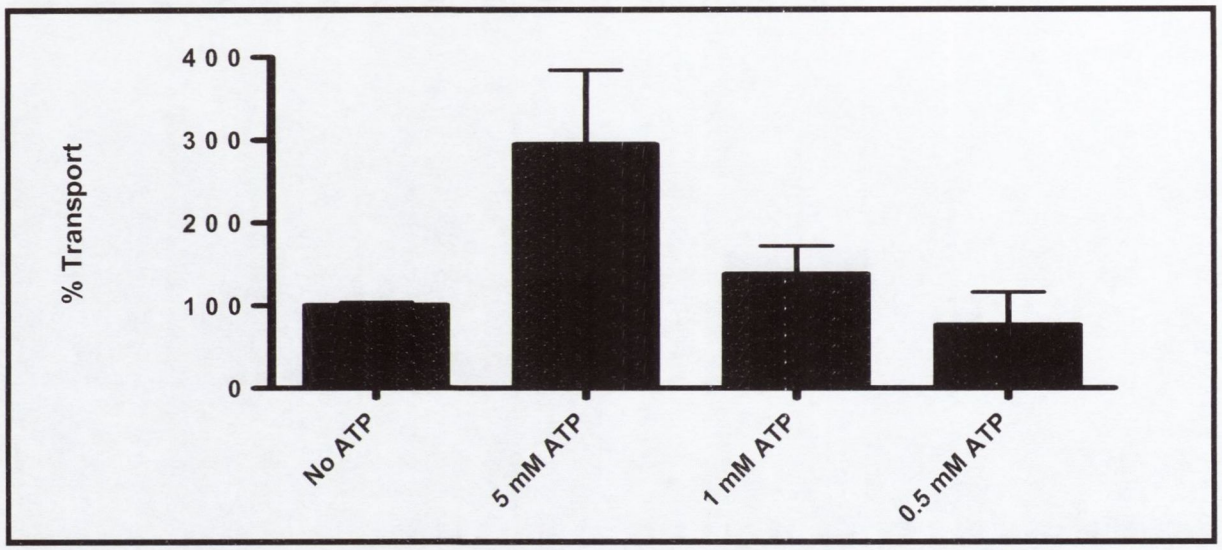


Figure 6.2.3 Effects of ATP concentrations on laurate-induced H^+ transport in proteoliposomes containing hUCP1

Recombinant hUCP1 was expressed in *E. coli* and reconstituted into liposomes. Transport was initiated by the addition of 100 nM val. H^+ flux was measured as the initial rate of change in $[H^+]$. Laurate was used at 150 μM and GDP was used as indicated. Transport in the absence of ATP was set to 100%. Data are expressed as the mean ± S.E.M. of at least three experiments performed in triplicate.

have been such that all nucleotide-binding sites were facing inside the vesicles. In order to cover this eventuality, vesicles were prepared with 5 mM ATP in the lumen and 5 mM ATP added outside the vesicles. Figure 6.2.7 shows that there was no difference in H^+ flux in the total absence or presence of ATP on both sides of the membrane.

6.2.3 The kinetics of the fatty acid-dependent H^+ transport mediated by expressed, reconstituted hUCP1.

As hUCP1 has never been reconstituted before, it was necessary to establish kinetic parameters for hUCP1 H^+-transport. Initially, the kinetics with respect to laurate were assessed. Figure 6.2.4 shows the dependence of H^+ on laurate concentration. At saturating concentrations of laurate, it was obvious that there was a diffusion component. This diffusion was not measurable directly as hUCP1 did not appear to be inhibited by GDP. However, diffusion could be estimated by extrapolation of a straight line from the kinetic curve (laurate) when substrate was saturating, and then replotting that line through the origin (Figure 6.2.4). The equation of this line was then determined by linear regression analysis. Using the equation of the line of diffusion, the kinetics of H^+-transport could be corrected for the rate of diffusion. Figure 6.2.5 shows the corrected kinetics of H^+ flux, i.e., the kinetics of H^+ flux due to hUCP1. The points on this curve were fitted to a rectangular hyperbola and the kinetic parameters of the hUCP1 transporter could be calculated. The Michelis-Menten estimated V_{max} value was 2.7 μmoles H^+/min.mg^{-1} and the K_m value was 82 μM for hUCP1 in liposomes.

The kinetics of H^+ flux for expressed reconstituted hUCP1 using palmitate as substrate were also estimated. Figure 6.2.6 shows the dependence of H^+ transport on palmitate concentration. At saturating concentrations of palmitate, there did not appear to be any diffusion component. Thus, by fitting a rectangular hyperbola to the data in Figure 6.2.6, a V_{max} value of 2.9 μmoles H^+/min.mg^{-1} and a K_m of 27.6 μM were estimated.

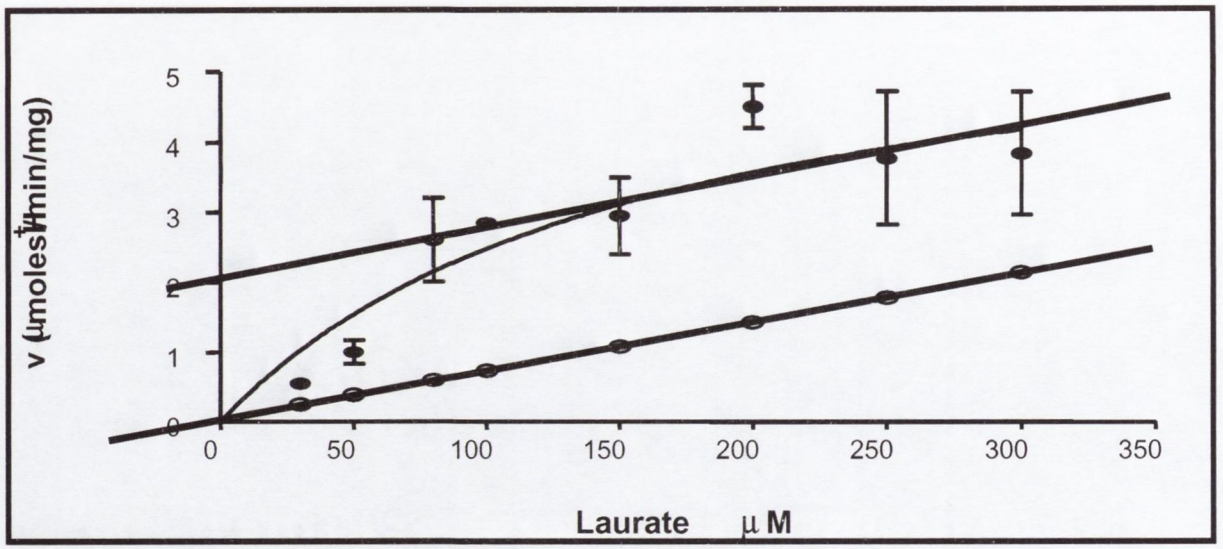


Figure 6.2.4 Laurate-dependent H^+ flux through hUCP1 proteoliposomes

Recombinant hUCP1 was reconstituted into liposomes and H^+ transport was initiated by the addition of 100 nM val. H^+ flux was measured as the initial rate of change in $[H^+]$. The rate of diffusion was estimated by extrapolating a line from the curve when substrate was saturating, followed by replotting of the line through the origin. The equation for the line through the origin was determined by linear regression analysis ($y = 0.00888x$) and was used to correct the kinetics of H^+ transport for diffusion (see Figure 6.2.3)

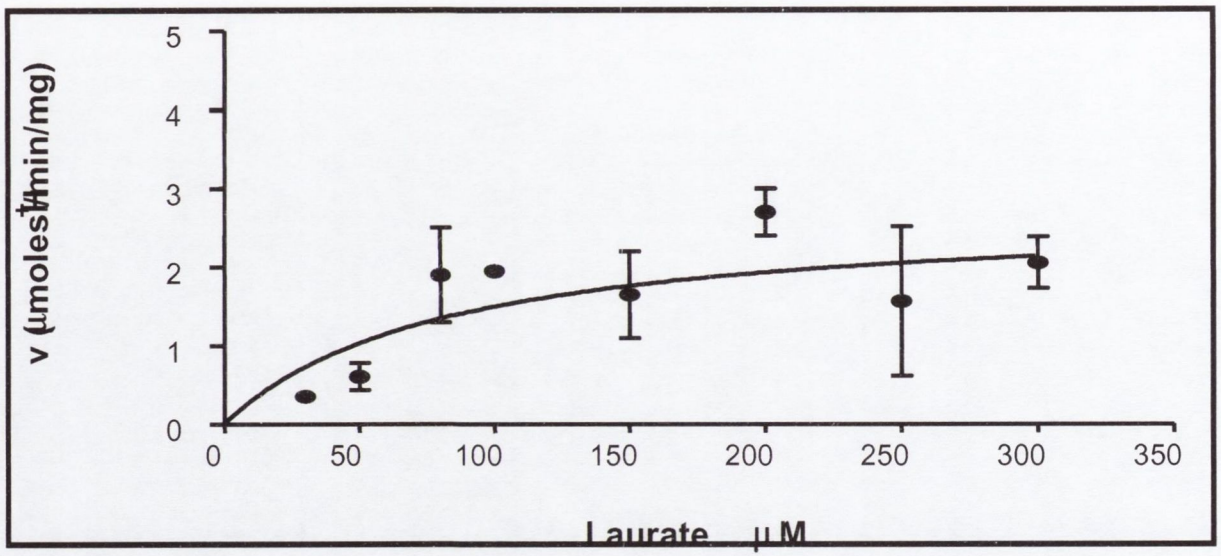


Figure 6.2.5 Saturable kinetics of reconstituted hUCP1 with laurate as substrate

Recombinant hUCP1 was reconstituted into liposomes. The graph shows the saturation kinetics of H^+ flux as a function of laurate concentration. The rate of diffusion of laurate was estimated in Figure 6.2.2 and subtracted from the original kinetic data. A rectangular hyperbola was fitted to the data. The V_{max} value was estimated to be 2.7 μmoles H^+/min/mg and the K_m value was estimated to be 82 μM.

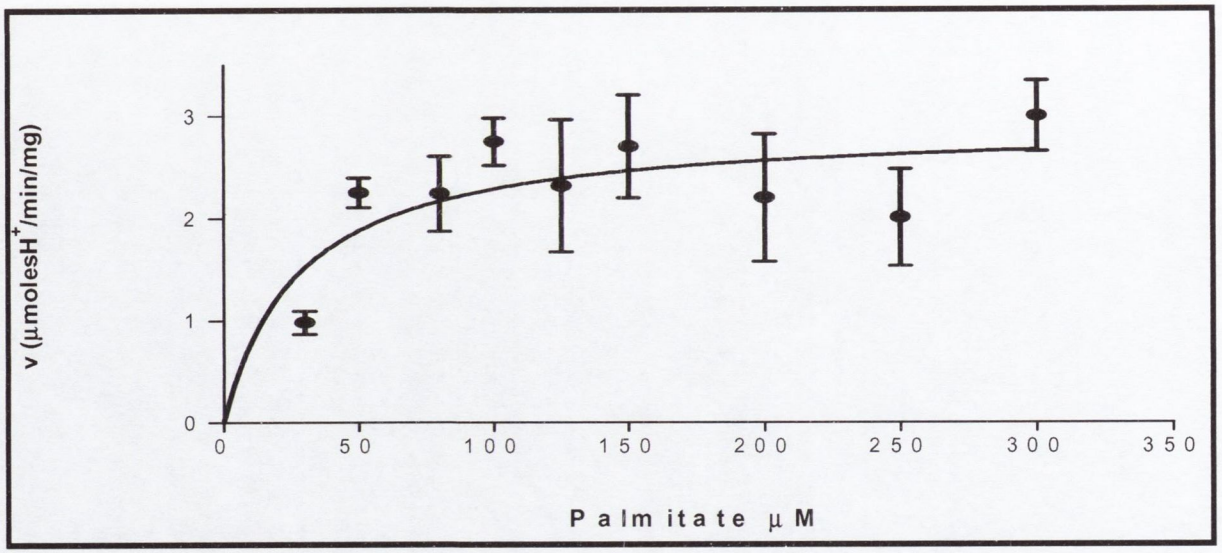


Figure 6.2.6 Saturable kinetics of reconstituted hUCP1 with palmitate as substrate

Recombinant hUCP1 was reconstituted into liposomes. The graph shows the saturation kinetics of H^+ flux as a function of palmitate concentration. A rectangular hyperbola was fitted to the data. The V_{max} value was estimated to be 2.9 µmolesH^+ /min/mg and the K_m value was estimated to be 27.6 µM.

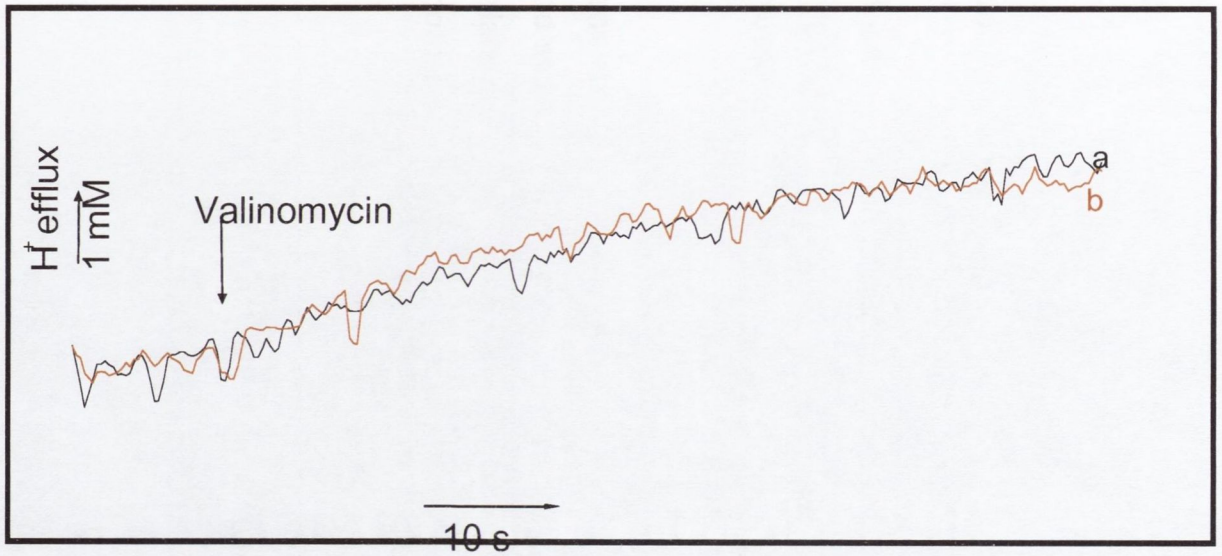


Figure 6.2.7 Laurate-induced H^+ efflux from vesicles containing purified recombinant hUCP1 in the absence and presence of ATP.

H^+ flux in proteoliposomes was determined by measuring changes in SPQ fluorescence, which is quenched by the anion of TES. Transport was initiated by the addition of 100 nM val.
Trace a: 150 µM laurate
Trace b: 150 µM laurate plus 5 mM ATP on both sides of the vesicle
H^+ flux was measured as the initial rate of $[H^+]$. The data are representative of three independent experiments performed in triplicate.

6.2.4 The effects of coenzyme Q_{10} on transport by hUCP1

In order to determine if coenzyme Q_{10} was necessary for H^+ flux in expressed reconstituted hUCP1 liposomes, coenzyme Q_{10} was also added during reconstitution. Figure 6.2.8 shows that there was an increase in the H^+ flux when coenzyme Q_{10} was added. However, this increase in H^+ flux was also found when the coenzyme Q_{10} solvent (dichloromethane) was added on its own.

6.2.5 Alignment of amino acid sequence of rUCP1 and hUCP1, highlighting those amino-acid motifs thought to be involved in purine-nucleotide binding

Using the ClustalW program, the amino-acid sequences for hUCP1 and rUCP1 were compared. The putative amino acids and motifs thought to be involved in purine-nucleotide binding were compared. Only a threonine to alanine change was found at position 265 and is scored with ":" as a conservative substitution.

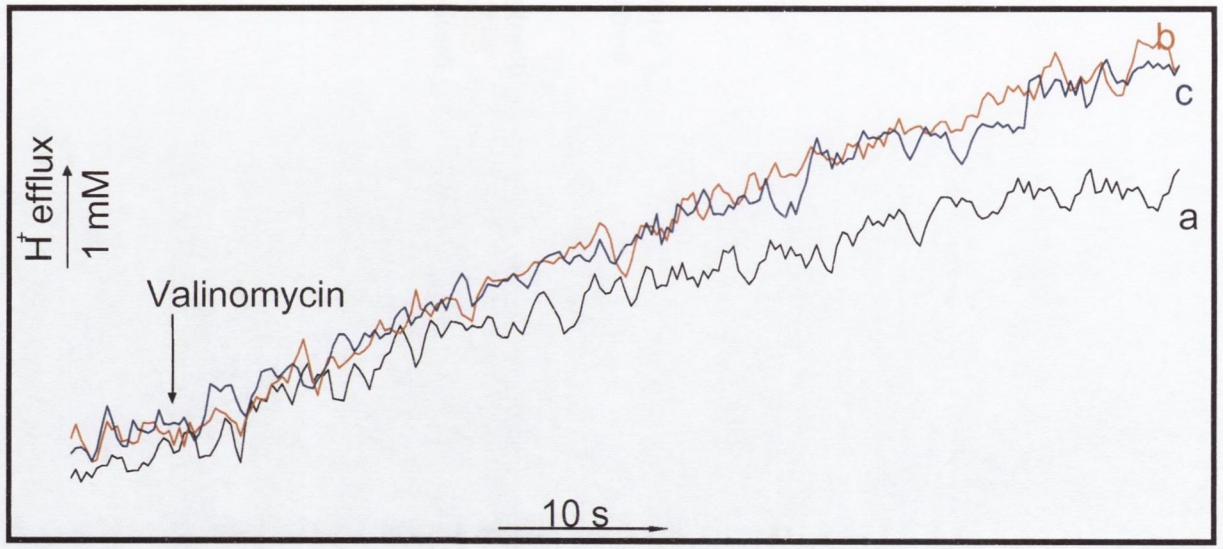


Figure 6.2.8 The effect of coenzyme Q_{10} and dichloromethane on laurate-induced H^+ transport in recombinant hUCP1-containing vesicles.

H^+ flux in proteoliposomes was determined by measuring changes in SPQ fluorescence, which is quenched by the anion of TES. Transport was initiated by the addition of 100 nM val.
Trace a: 150 µM laurate
Trace b: 150 µM laurate plus 10 nmoles of coenzyme Q_{10} in 4 µl of dichloromethane.
Trace c: 150 µM laurate plus 4 µl dichloromethane
H^+ flux was measured as the initial rate of $[H^+]$. The data are representative of two independent experiments performed in duplicate.

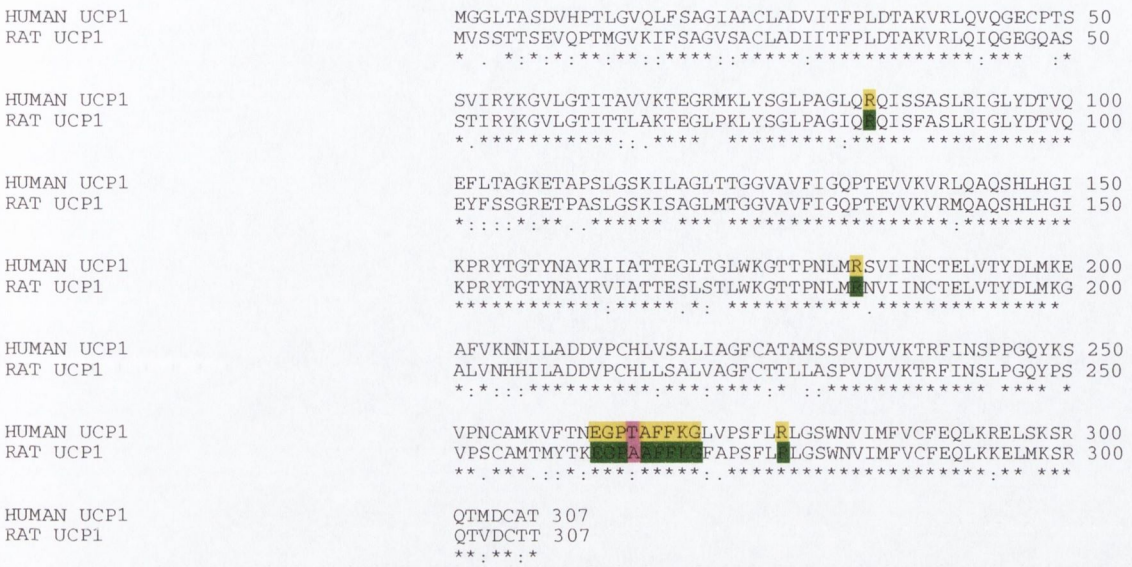


Figure 6.2.9 Multiple Sequence Alignment of hCP1 and rUCP1(ClustalW, Chenna *et al.*, 2003)

The peptide sequences of hUCP1 and rUCP1 were aligned using the ClustalW program on the http://www.ebi.ac.uk website. Highlighted residues for hUCP1 and rUCP1 are those believed to be essential for GDP binding. Any residues that differ between the sequences are also highlighted.

6.3 Discussion

The recombinant expression of hUCP1 has not been recorded before. Successful expression depended on the introduction of under-represented human tRNAs into *E. coli* (Rosetta strain by Novagen). Having expressed hUCP1, there was an onus to determine if the reconstituted protein was functional and, by default, in the correct conformation in the membrane. Although little work has been done on hUCP1, hUCP1 should be used as the paradigm for hUCP2 and hUCP3. Up until now, it has been work on haUCP1 and rUCP1 that has been used as the paradigm. Until recently, UCP1 was only found in BAT of mammals (including human infants, Himms-Hagen, 1990) but UCP1 has since been detected in rat and mouse thymus (Carroll *et al.,* 2005). By contrast UCP2 (intestine, macrophages, heart, WAT, kidney, spleen; Ricquier and Bouillaud, 2000) and UCP3 (skeletal muscle, BAT and spleen; Gong *et al.,* 1997; Carroll and Porter, 2004) have been found in many tissues. So, clearly an understanding of hUCP1 has implications for the function of hUCP2 and hUCP3.

The method of purification and reconstitution of hUCP1 was that of Jabůrek and Garlid (2003), which was used for rUCP1, hUCP2 and hUCP3. Initially, H^+ flux was shown to be dependent upon the addition of laurate (Figure 6.2.1). The requirements for UCP1 function have been well established (Strieleman *et al.,* 1985; Winkler and Klingenberg, 1994; Ježek *et al.*, 1994). Figure 6.2.1 also shows that H^+ flux is dependent upon the concentration of laurate. However, no inhibition of transport by the purine nucleotide, GDP was found. This will be discussed later.

A criterion for a properly folded hUCP1 protein would be GDP-sensitive H^+ flux. As a result the sensitivity of expressed reconstituted hUCP1-containing liposomes to purine nucleotides (GDP, 1 – 5 mM and ATP 1 - 5 mM) was studied. However, the results showed no purine-nucleotide-sensitive H^+ flux, suggesting a degree of improper folding of the protein or a problem with orientation. Reconstitution can result in two

orientations for UCP1. The purine-nucleotide binding site thus may have faced the lumen of the vesicle or may have faced the outside of the vesicle. Using this method of reconstitution, Jabůrek and Garlid (2003) recorded a 50:50 orientation of UCPs. Echtay *et al.* (2000) have shown that 80% of reconstituted-UCP was facing outwards [with a 100% phosphatidylcholine environment and slower detergent removal]. Therefore, the possibility was considered that all hUCP1 molecules reconstituted in this work had the purine-nucleotide binding site facing the lumen and no inhibition was possible by addition of nucleotides outside. No inhibition was found when hUCP1 was reconstituted with 5 mM ATP in the lumen of the vesicles, or when 5 mM ATP was present on both sides of the vesicles (Figure 6.2.7), suggesting that orientation was not the issue.

Despite the lack of purine-nucleotide inhibition, the kinetics of hUCP1 transport were established. Firstly, laurate-induced H^+ flux in hUCP1-containing liposomes was investigated. Figure 6.2.4 shows the laurate-dependent H^+ flux through hUCP1 proteoliposomes. The points were fitted to a rectangular hyperbola to establish Michelis-Menten kinetics. Analysis of the kinetic data suggested that there were two components to H^+ flux with laurate in hUCP1 containing liposomes. Due to the fact that hUCP1 could not be inhibited by GDP, this diffusion component could not be measured directly. Extrapolation of the diffusion line allowed the values for the laurate concentrations used to be corrected. Using the corrected values (Figure 6.2.3), the V_{max} was established as 2.7 μmolesH^+/min.mg^{-1} and the K_m value was 82 μM. The V_{max} values for hUCP1 derived in this study compared well to the values of 10-12 μmoles H^+/min.mg^{-1} for expressed reconstituted rUCP1 and 9 μmolesH^+/min/mg for native rUCP1 (Jabůrek and Garlid, 2003). Furthermore, the K_m value for expressed reconstituted rUCP1 (Jabůrek and Garlid, 2003) was found to be 37 μM laurate compared to 82 μM laurate for hUCP1 in this study. However, Echtay *et al.* (2000) found a K_m value for expressed reconstituted haUCP1 of 80 μM, which was similar to the one found here for expressed reconstituted hUCP1.

The lower V_{max} value estimated here for hUCP1 with laurate compared to the reported value for rUCP1 probably reflects the fact that we have corrected for diffusion. However, the lack of GDP-sensitive H^+ flux through hUCP1 probably reflects an improperly folded protein. The phospholipid environment in which hUCP1 has been reconstituted may also have a bearing. Soyabean phospholipids have been used successfully for reconstitution of functional hUCP2 and hUCP3. Egg-yolk phosphatidylcholine has been successfully used for the functional reconstitution of rUCP1 (Jabůrek *et al.,* 1999). hUCP1 may require a different phospholipid environment than that for rUCP1 and/or hUCP2 and hUCP3

H^+ flux was also measured using palmitate as substrate. In this instance, no diffusion component was evident and a rectangular hyperbola could be fitted to the kinetic data. Kinetic values for palmitate have not been recorded for any bacterially-expressed UCP1. It was estimated that the V_{max} value for hUCP1 in the presence of palmitate was 2.9 μmoles H^+/min.mg^{-1}, a value that compares with values of between 10-30 μmolesH^+/min/mg for hUCP2 and hUCP3 (Jabůrek *et al.*, 1999). The V_{max} value for hUCP1 may reflect a protein that was not fully active. The K_m value for hUCP1 of 27.6 μM and those of hUCP2 and hUCP3 of between 10 and 20 nmol palmitate/mg of lipid, or 5 and 10 μM, a similar order of magnitude, suggest that at least part of the protein is properly folded.

The possibility that hUCP1, unlike rUCP1 or haUCP1 many not have the full complement of amino acids required for purine nucleotide binding was also considered. Figure 6.2.9 shows a sequence alignment of hUCP1 and rUCP1, as well as the individual amino acids and the putative amino-acid motif required for GDP-binding (highlighted). The amino acids seem to be conserved except for an alanine-to-threonine substitution. This is considered a conservative substitution, so loss of purine-nucleotide binding capacity due to this substitution is unlikely. Thus, the overall conclusion is that conditions of reconstitution need to be investigated further to optimize the refolding conditions.

Another intriguing development in the literature was the observation that coenzyme Q_{10} was required for functionally active expressed reconstituted hUCP2 and hUCP3 (Echtay *et al.* 2001). In this study, the addition of coenzyme Q_{10} did appear to effect hUCP1 activity (Figure 6.2.8) but this effect was also seen when the equivalent amount of solvent (dichloromethane) in which coenzyme Q_{10} was dissolved, was added. Echtay *et al.* (2000 and 2001) did not show this solvent control experiment. Due to the hydrophobic nature of dichloromethane and its insolubility in H_2O, it would partition into the membrane and produce H^+ flux. The effect of dichloromethane on liposomes and its ability to induce H^+ flux was indeed recorded by Jabůrek and Garlid (2003). The lack of necessity for addition of coenzyme Q_{10} for hUCP1 function in proteoliposomes concurs with the results shown by Jabůrek and Garlid (2003).

hUCP1 has been expressed and reconstituted. While it was found to increase the H^+ conductance of proteoliposomes in a fatty-acid concentration-dependent manner, it did not show sensitivity to purine nucleotides. It suggests that the protein was partially, correctly folded but clearly the conditions of refolding and reconstitution of hUCP1 may need to be re-established. Consideration would also need to be given to the phospholipid requirement of this protein, which may be different to those of its homologues UCP2 and UCP3. Indeed, when bacterially expressed hUCP2 and hUCP3 were first reconstituted, they only responded to very high concentrations of ATP (Jabůrek *et al.*, 1999). Later reconstitutions using a refined refolding technique (the one described in this thesis) improved their responsiveness to ATP (Jabůrek and Garlid, 2003). Refolding problems with hUCP1 may be the case here. As UCP1 has been used as a paradigm of UCP function, it is necessary to establish the mechanism of action of hUCP1 if we are to apply this knowledge to hUCP2 and hUCP3.

Chapter Seven
General Discussion

7.1 General Discussion

UCP1 has been the paradigm for UCP function. However, work has never been recorded for any studies on hUCP1. Initially, work done by Nicholls (1976) elucidated the transport qualities of UCP1 in terms of H^+ and Cl^- transport in hamster BAT mitochondria and cells. Transport studies of haUCP1 moved on to the reconstituted system in the 1980s, confirming H^+ and Cl^- activity (Strieleman *et al.*, 1985a).

In this study, expression of hUCP1 in *E. coli* was achieved using Rosetta pLysS, a strain of bacteria that contains all under-represented human tRNA codons. If we are to gain knowledge about hUCP2 or hUCP3, it would seem intuitive to compare them to hUCP1 as opposed to haUCP1 or rUCP1. While work on other species does give clues regarding the function of proteins, it would be better to compare like with like. Until recently, it was believed that UCP1 was exclusive to BAT; however, a recent publication from our laboratory has described the detection of UCP1 in thymus of rat and mouse (Carroll *et al.*, 2005). Research on hUCP1 in the context of BAT may have little bearing on adults, but, if hUCP1 is detected in human thymus, then studies of hUCP1 will have an exciting new context in which to be studied. Suffice if to say that the role of UCP1 in rat and mouse is in itself a fascinating endeavour and the ability to express and reconstitute hUCP1 will aid that endeavour. No purification for native UCP2 or UCP3 from mitochondria has been recorded. It would appear that low levels of these proteins prevents their purification using current techniques. Expression of UCP3 in mitochondria of yeast has proven fruitless as all of the UCP3 expressed was shown to be deranged and to occur in extra-mitochondrial particles (Heidekaemper *et al.,* 2000). In terms of over-expression *E. coli* seem to be the best option. With the possibility of expressing hUCP1 in *E. coli,* all human UCPs can now be compared fairly. As shown in Chapter 3, all UCPs are expressed in inclusion bodies so require the same level of processing in order to study their kinetics in liposomes.

Detection of protein-expression patterns is another useful tool in research. The characterization of a specific anti-UCP1 antibody is described in Chapter 3. It is specific for UCP1 over UCP2 and UCP3 and other mitochondrial carriers (Cunningham *et al.,* 2003). In the case of thymus mitochondria, Nègre-Salvayre *et al.* (1997) showed expression of UCP2 mRNA and attributed the GDP-sensitive H_2O_2 production to UCP2 protein. We have used this antibody to confirm expression of UCP1 in thymus of rat and mouse (Carroll *et al.,* 2005). It would appear now that the effects found by Nègre-Salvayre *et al.* (1997) could be due to UCP1 and UCP2. The ability to specifically detect protein would be of much greater help than mRNA levels, which are only an indication of protein expression. A specific antibody for UCP3 has also been defined and it is selective for UCP3 over UCP2 and UCP1. Already this antibody has been instrumental in the discovery of UCP3 in spleen mitochondria of rat and thymus (Carroll and Porter, 2004).

The mechanism of action of UCP1 has long been contentious. Does UCP1 transport long-chain fatty-acid anions or catalyse the downward movement of H^+ through the mitochondrial inner membrane with assistance by long-chain fatty acids? The most convincing argument for the fatty-acid buffering model was the unsubstantiated report that glucose-*O*-ω-palmitate could activate UCP1 in proteoliposomes (Klingenberg and Huang, 1999). It has to be emphasized that neither the original data, nor the synthesis, purity or stability of the glycolipid have ever been presented . Gouin *et al.* (2005), in collaboration with our group, synthesized glucose-*O*-ω-palmitate and published the synthesis, and confirmed its purity and stability under ionic conditions. Results presented here unambiguously demonstrate that glucose-*O*-ω-palmitate cannot facilitate the uncoupling activity of UCP1 in either proteoliposomes or BAT mitochondria. Klingenberg himself claims that the glucose-substitution anchors the ω-end of palmitate to the membrane and the hydrophilic and bulky nature of glucose excludes this glycolipid from flipping across the membrane (Klingenberg *et al.*, 1999). The data presented in this thesis should resolve the issues surrounding UCP's

mechanism of action. The corollary of our observation suggests that the protonophore model proposed by Skulachev (1988) is correct. The anion of glucose-*O*-ω-palmitate could not be transported by UCP1, which may indicate that it is truly an un-flippable entity.

However, further work needs to be done to completely rule out the buffering model. Acyl chain length could be extended as the α-carboxy group may not be able to penetrate the protein enough in the case of glucose-*O*-ω-palmitate to activate by the buffering model. A longer chain length, such as C_{18} or C_{20} may solve this issue. Also, if the protonophore model is correct, it may be possible to facilitate H^+ flux by substituting the OH^- groups on the glucose of glucose-*O*-ω-palmitate with OCH_3 groups or benzoylate groups, to increase the hydrophobic character of the molecule. That is to say, by increasing the hydrophobicity of the glucose molecule in glucose-*O*-ω-palmitate, it may be possible for the glycolipid to be flipped across the membrane and it could be an activator of UCP1. It would also be an interesting control to see if the glycosidic bond between the glucose and the palmitate chain could be broken by glycosidase, to free up palmitate or hydroxypalmitate, which may facilitate H^+ flux.

Evidence that undecanesulfonate is active from either side of UCP1 is interesting in that it gives an insight as to where fatty-acid binding occurs in UCP1. Undecanesulfonate, as a permanent anion, allows for the observation of only one half of the cycle proposed by the protonophore model. Ježek *et al.* (1994) have shown that the laurate anion inhibits Cl^- transport by UCP1, which led them to believe that the laurate anion and Cl^- shared the same transport pathway. Garlid *et al.* (1996) then showed that undecanesulfonate inhibited laurate transport and that undecanesulfonate is transported with the same kinetics as laurate. With this evidence, it is a simple conclusion that the anion pathway is the true transport mechanism of UCP1. By learning that the site for anion transport is accessible from either side of the protein, some idea of the protein's structure within the membrane is gained. Indeed, Ježek and Garlid (1990) found that UCP1 had a preference for the hydrophobicity of the substrate. This need for

hydrophobicity shows that the binding site is deep within the hydrophobic core of the protein and therefore accessible from either side as long as the substrate is sufficiently hydrophobic.

Apart from expressing hUCP1, for the first time hUCP1 has been reconstituted into proteoliposomes. It has been shown that the transport kinetics are saturable for laurate and palmitate but transport also appears to be purine nucleotide insensitive. The fact that transport is purine-nucleotide-insensitive suggests that the protein is not folded properly. Results with reconstituted bacterially expressed UCPs have always been problematic. Initially, Echtay *et al.* (1999) reconstituted haUCP1 but could not find H^+ activity whereas Jabůrek *et al.* (1999) found that bacterially expressed hUCP2 and hUCP3 were poorly responsive to purine nucleotides. There is a possibility that hUCP1 is not inhibitable by purine nucleotides but sequence alignments with rUCP1 have shown that the putative amino acids involved in purine nucleotide binding are present in hUCP1. hUCP1 function was not improved by the presence of coenzyme Q as suggested by the work of Echtay *et al.* (2000) for bacterially expressed haUCP1. The observation that coenzyme Q does not effect expressed reconstituted UCP function agrees with Jabůrek and Garlid (2003). The effect of coenzyme Q observed by Echtay *et al.* is probably due to a solvent effect. Clearly, conditions for the expression and reconstitution of hUCP1 need to be refined further.

One limiting factor with regard to transport in reconstitution experiments is that the membrane potential is created by a K^+-diffusion potential that is lower than that achievable in mitochondria and wanes as it is used. Mitochondria have a sustainable higher membrane potential and this may have an effect on the UCP function. One way to improve the UCP transporter in proteoliposomes in the future would be to have sustainable membrane potentials. For instance, artificial photosynthetic reaction centres have been reconstituted into liposomes and shown to create H^+ gradients across the membrane (Steinberg-Yfrach *et al.,* 1997). The reaction centres could be co-reconstituted with UCP1 to provide a more "mitochondria-like" environment in the proteoliposomes.

New substrates are emerging for UCPs. Echtay *et al.* (2002) identified superoxide as an activator of UCP uncoupling. Superoxide is a reactive oxygen species (ROS) and is produced constantly by mitochondria. Components of the initial and middle parts of the respiratory chain are the main O_2 reductants involved in "parasitic" one-electron reduction of O_2 to superoxide. Among them, semiquinone (partially reduced CoQ) is employed quite often (Skulachev, 1998). By uncoupling mitochondria, the electron-transport chain becomes more efficient as electrons are not lost so easily. Echtay *et al.* (2002) found that fatty acids were necessary for uncoupling via UCPs with superoxide. Echtay *et al.* (2003) then went on to explain that superoxide was acting through lipid peroxidation. The formation of compounds such as 4-hydroxy-2-nonenal seemed to activate UCP. These lipid-peroxidation products would be interesting new substrates for study at the reconstitution level. Jabůrek *et al.* (2004) have already shown that linoleic acid hydroperoxides are more potent activators of UCP2 uncoupling than linoleic acid alone and concur with the protonophore model. It would be interesting to see if these peroxides interact with hUCP1 as this would have an implication for hUCP1 function in the thymus.

Chapter Eight
Bibliography

8.1 Bibliography

Abrahams, J.P., Leslie, A.G., Lutter, R. and Walker, J.E., 1994
"Structure at 2.8 A resolution of F1-ATPase from bovine heart mitochondria"
Nature **370,** 621-628

Andreyev, A.Yu., Bondareva, T.O., Dedukhova, V.I., Mokhova, E.N., Skulachev, V. and Volkov, N.I., 1988
"Carboxyatractylate inhibits the uncoupling effect of free fatty acids"
FEBS Letts, **226,** 265-269

Andreyev, A. Yu., Bondareva, T.O., Dedukhova, V.I., Mokhova, E.N., Skulachev, V.P., Tsofina, L.M., Volkov, N.I. and Vygodina, T.V., 1989
"The ATP/ADP-antiporter is involved in the uncoupling effect of fatty acids on mitochondria"
Eur. J. Biochem. **182,** 585-592.

Aquila, H., Link, T.A. and Klingenberg, M., 1985
"The uncoupling protein form brown fat mitochondria is related to the mitochondrial ADP/ATP carrier. Analysis of sequence homologies and folding of the protein in the membrane"
Embo. J., **4,** (9), 2369-2376

Bejma, J. and Ji, L.L. 1999
"Aging and acute exercise enhance free radical generation in rat skeletal muscle."
Journal of Applied Physiology **87,** 465 – 470.

Bielawski, J., Thompsom, T.E. and Lehninger, A., 1966
"The effect of 2,4-dinitrophenol on the electrical resistance of phospholipid bilayer membranes"
Biophys. Res. Commun. **24**, 948-954

Bisaccia, F., Tommasino, M and Palmieri, F., 1983
"Structure and function of membrane proteins"
Elsevier, Amsterdam

Bisaccia, F. and Palmieri, F., 1984
"Specific elution from hydroxylapatite of the mitochondrial phosphate carrier by cardiolipin"
Biochim Biophys Acta, **766(2)**:386-94

Boss, O., Samec, S., Paoloni-Giacobino, A., Rossier, C., Dulloo, A., Seydoux, J., Muzzin, P. and Giacobino, J.P., 1997
"Uncoupling protein-3: a new member of the mitochondrial carrier family with tissue-specific expression"
FEBS Letts., **408,** 39-42

Boss, O., Samec, S., Dulloo, A., Seydoux, J., Muzzin, P. and Giacobino, J.P., 1997b
"Tissue dependent regulation of rat UCP2 expression in response to fasting or cold"
FEBS Letters, **412**, 111 - 114.

Boss, O., Hagan, T. and Lowell, B.B. 2000
"Uncoupling proteins 2 and 3: potential regulators of mitochondrial energy metabolism"
Diabetes **49**, 143 - 156.

Bouillaud, F., Ricquier, D., Gulik-Krzywicki, T and Gary-Bobo, C.M., 1983
"The possible proton translocating activity of the mitochondrial uncoupling protein of brown adipose tissue"
FEBS Letts, **164,** (2), 272-276

Brand, M.D., Pakay, J.L., Ocloo, A., Kokoszka, J., Wallace, D.C., Brookes, P.S. and Cornwall, E.J. 2005
"The basal proton conductance of mitochondria depends on adenine nucleotide translocase content"
Biochem. J. Aug 2

Cadenas, S., Buckingham, J.A., Samec, S., Seydoux, J., Din, N., Dulloo, A.G. and Brand, M.D. 1999
"UCP2 and UCP3 rise in starved rat skeletal muscle but mitochondrial conductance remains unchanged"
FEBS Letters, **462**, 257 - 260.

Cadenas, S., Echtay, K.S., Harper, J.A., Jekabsons, M.B., Buckingham, J.A., Grau, E., Abiun, A., Chapman, H., Clapham, J.C. and Brand, M.D. 2002
"The basal proton conductance of skeletal muscle mitochondria from transgenic mice overexpressing or lacking uncoupling protein 3"
J. Biol. Chem., **277**, 2773 - 2778

Cannon, B., Hedin, A. and Nedergaard, J., 1982
"Exclusive occurrence of thermogenin in Brown Adipose Tissue"
FEBS Letts, **150,** 129-132

Cannon, B. and Vogel, G., 1977
"The mitochondrial ATPase of BAT. Purification and comparison with the mitochondria ATPase from beef heart"
FEBS Lett **76,** 284-289

Carroll, A.M., and Porter, R.K., 2004
"Starvation sensitive UCP3 expression in rat thymus and spleen"
Biochimica et Biophysica Acta, **1700**, 145 – 150.

Carroll, A.M., Haines, L.R., Pearson, T.W., Fallon, P., Walsh, C., Brennan, C.M., Breen, E.P. and Porter, R.K. 2005
"Detection of a functioning UCP1 in thymus"
J. Biol. Chem., **280**, 15534 – 15543.

Collins, S., Daniel, K., Rolf, E.M., Ramkumar, V., Taylor, I.L. and Gettys, T.W.1994
"Impaired expression and functional activity of the beta3 and beta 1-adrenergic receptors in adipose tissue of congenitally obese (C57BL/6J ob/ob) mice.
Molecular Endocrinology, 8, 518 - 527.

Crescenzo, R., Mainieri, D., Solinas, G., Montani, J.P., Seydoux, J., Liverini, S., Iossa, S. and Dulloo, A.G. 2003
"Skeletal muscle mitochondrial oxidative capacity and uncoupling protein 3 are differently influenced by semi-starvation and refeeding"
FEBS Letters **544**, 138 - 142.

Cunningham, O., McElligott, A.M., Carroll, A.M., Breen, E., Reguenga, C., Oliveira, M.E.M., Azevedo, J.E. and Porter, R.K., 2003
"Selective detection of UCP3 expression in skeletal muscle: effect of thyroid status and temperature acclimation"
Biochimica et Biophysica Acta, **1604**, 170 - 179.

Darszon, A., Vandenberg, C.A., Ellisman, M.H. and Montal, M., (1979)
"Incorporation of membrane proteins into large single bilayer vesicles. Application to rhodopsin".
J. Cell. Biol., **81,** 446-452

Desautels, M. and Himms-Hagen, J. 1981
"Brown adipose tissue mitochondria of cold-acclimated rats: changes in characteristics of purine nucleotide control of the proton electrochemical gradient"
Canadian Journal of Biochemistry **59**, 619 – 625.

Du, G., Mouithys-Mickalad, A. and Sluse, F.E. 1998
"Generation of superoxide anion by mitochondria and impairment of their functions during anoxia and reoxygenation in vitro"
Free Radical Biology and Medicine **25,** 1066 – 1074.

Echtay, K.S., Bienengraeber, M. and Klingenberg, M., 1997
"Mutagenesis of the uncoupling protein of brown adipose tissue. Neutralization of E190 largely abolishes pH control of nucleotide binding"
Biochemistry, **36,** 8253-8260

Echtay, K.S., Liu, Q., Caskey, T., Winkler, E., Frischmuth, K., Bienengraber, M. and Klingenberg, M., (1999)
"Regulation of UCP3 by nucleotides is different from regulation of UCP1,"
FEBS Letters, **450**, 8-12

Echtay, K.S., Winkler, E. and Klingenberg, M., 2000
"Coenzyme Q is an obligatory cofactor for uncoupling protein function"
Nature, **408,** 609-613

Echtay, K.S., Winkler, E., Frischmuth, K. and Klingenberg, M., 2001
"Uncoupling protein 2 and 3 are highly active H+ transporters and highly nucleotide sensitive when activated by coenzyme Q (ubiquinone)".
Proc. Natl Acad. Sci., **98**, 1416 – 1421.

Echtay, K.S. and Brand, M.D. 2001
"Coenzyme Q induces GDP-sensitive proton conductance in kidney mitochondria"
Biochem. Soc. Trans., **29**, 763-768

Echtay, K.S., Roussel, D., St-Pierre, J., Jekabsons, M.B., Cadenas, S., Stuart, J.A., Harper, J.A., Roebuck, S.J., Morrison, a., Pickering, S., Clapham, J.C. and Brand, M. 2002
"Superoxide activates mitochondrial uncoupling proteins"
Nature **415**, 96 – 99.

Echtay, K.S., Murphy, M.P., Smith, R.A.J., Talbot, D.A. and Brand, M.D. 2002b
"Superoxide activates mitochondrial uncoupling protein 2 from the matrix side: Studies using targeted antioxidants"
J. Biol. Chem., **277**, 47129 - 47135.

Echtay, K.S., Esteves, T.C., Pakay, J.L., Jekabsons, M.B., Lambert, A.J., Portero-Otín, M., Pamplona, R., Vidal-Puig, A.J., Wang, S., Roebuck, S.J. and Brand, M.D. 2003
"A signalling role for 4-hydroxy-2-nonenal in regulation of mitochondrial uncoupling"
The EMBO Journal **22**, 4103 – 4110.

Eytan, G.D. and Broza, 1978
"Role of charge and fluidity in the incorporation of cytochrome oxidase into liposomes"
J Biol Chem. **253(9)**:3196-202

Fiermonte, G., Walker, J.E. and Palmieri, F., 1993
"Abundant bacterial expression and reconstitution of an intrinsic membrane transport protein from bovine mitochondria"
Biochem. J., **294,** 293-299

Fleury, C., Neverova, M., Collins, S., Raimbault, S., Chaimpigny, O., Levi-Meyreuis, C., Bouillaud, F., Seldin, M.F., Sarwit, R.S., Ricquier, D. and Warden, C.H., 1997
"Uncoupling protein 2: a novel gene linked to obesity and hyperinsulinemia"
Nat. Genet., **15,** (3) 269-272

Garlid, K.D., Beavis, A.D. and Ratkje, S.K., 1989
"On the nature of ion leaks in energy-transducing membranes"
Biochim. et Biophys. Acta, **976,** 109 – 120

Garlid, K.D., Orosz, D.E., Modriansky, M., Vassanelli, S. and Ježek, P (1996) "On the mechanism of fatty acid induced proton transport by mitochondrial uncoupling protein"
J. Biol. Chem. **271**, 2615 - 2620.

Garlid, K.D., Jabůrek, M., Ježek , P., and Varecha, M., 2000
"How do uncoupling proteins uncouple?"
Biochem. Biophys. Acta., **1459 (2-3):** 383-389

Garlid, K.D., Jabůrek, M. and Ježek, P. (2001)
"Mechanism of uncoupling protein action".
Biochem. Soc. Trans. **29**, 803 - 806.

Gesner, C., (1551)
Medici Tigurini Historiae Animalium. Liber II, qui est de Quadrupedibus Ouiparis (de Mure Alpino), 840-843.

Gimeno, R., Dembski, M., Weng, X., Deng, N., Shyjan, A., Gimeno, A., Iris, F., Ellis, S.,Woolfe, E. and Tartaglia, L., 1997
"Cloning and characterisation of an uncoupling protein homolog. A potential modulator of human thermogenesis"
Diabetes **46**, 900 - 906.

Gong, D., He, Y., Karas, M. Karas, M. and Reitman, M. 1997
"Uncoupling protein 3 is a mediator of thermogenesis regulated by thyroid hormone, β3 adrenergic agonists and leptin"
The Journal of Biological Chemistry, **272**, 39 – 42.

Gong, D-W., Monemdjou, S., Gavrilova, O., Leon, L.R., Marcus-Samuels, B., Chou, C.J., Everett, C., Kozak, L.P., Li, C., Deng, C., Harper, M-E. and Reitman, M.L. 2000
"Lack of obesity and normal response to fasting and thyroid hormone in mice lacking uncoupling protein-3"
J. Biol. Chem., **275**, 16251 - 16257.

Grisshammer, R. and Tate, C.G., 1995
"Overexpression of intergral membrane proteins for structural studies"
Q. Rev. Biophys., **28,** 315-422

Gunn, F.J., Tate, C.G. and Henderson, P.J. 1994
"Identification of a novel sugar-H^+symport protein, FucP, for transport of L-fucose into *Escherichia coli"*
Mol. Microbiol, **12 (5):** 799-809

Hardy, H.A. and Pressman, B.C. 1956
"Effect of surface active agents on the latent ATPase of mitochondria"
Biochim Biophys Acta. **21(3)**:458-66

Harper, J.A., Stuart, J.A., Jekabsons, M.B., Roussel, D., Brindle, K.M., Dickins, K., Jones, R.B. and Brand, M.D. 2002
"Artifactual uncoupling by uncoupling protein 3 in yeast mitochondria at the concentrations found in mouse and rat skeletal-muscle mitochondria" Biochem. J., **361**, 49-56.

Heaton, G.M., Wagenwood, R.J., Kemp Jnr, A. and Nicholls, D.G., 1978
"Brown-Adipose-Tissue Mitochondria: Photoaffinity Labelling of the regulatory site of energy dissipation."
Eur. J. Biochem. **82,** 515-521

Hesselink, M.K.C., Greenhaff, P.L., Constantin-Toedosiu, D., Hultman, E., Saris, W.H.M., Nieuwlaat, R., Schaart, G., Kornips, E. and Schrauwen, P. 2003
"Increased uncoupling protein 3 content does not affect mitochondrial function in human skeletal muscle in vivo"
J. Clin. I., **111 (4)**, 479 - 486.

Himms-Hagen, J., 1990
"Brown adipose tissue thermogenesis: Inter-disciplinary studies"
FASEB Journal, **4**, 2890 - 2898.

Hittelman, H.K., Lindberg, O. and Cannon, B., 1969
"Oxidative phosphorylation and compartmentation of fatty acid metabolism in brown fat mitochondria"
Eur. J. Biochem. **11,** 183-192

Hodnỳ, Z., Kolřová, P., Rossmeisl, M., Horáková, M., Nibbelink, M., Penicaud, L., Casteilla, L. and Kopeckỳ, J., 1998
"High expression of uncoupling protein 2 in foetal liver".
FEBS Letters, **425,** 185 - 190.

Horvath, T.L., Miyamoto, D.S., Barry, S., Gatti, S., Alberati, D., Livaki, A., Lombardi, A., Moreno, M., Goglia, F., Mor, G., Hamilton, J., Kachinskas, D., Horqitz, B. and Warden, C.H. 2003
"Uncoupling proteins-2 and 3 influence obesity and inflammation in transgenic mice"
International Journal of Obesity Related Metabolic Disorders, **27**, 433 - 442.

Hwang, C.S. and Lane, M.D. 1999
"Up-regulation of uncoupling protein-3 by fatty acid in C_2C_{12} myotubes".
Biochem. Biophys. Res. Comm. **258**, 464 – 469.

Jabůrek, M., Varecha, M., Gimeno, R.E., Dembski, M., Jezek, P., Zhang, M., Burn, P., Tartaglia, L.A. and Garlid, K.D., 1999
"Transport function and regulation of mitochondrial uncoupling proteins 2 and 3"
J. Biol. Chem. **274,** (37), 26003-26007.

Jabůrek, M., Varecha, M., Jezek, P. and Garlid, K.D., 2001
"Alkylsulfonates as probes of uncoupling protein transport mechanism"
J. Biol. Chem., **276,** (34), 31897-31905

Jabůrek, M and Garlid, K.D. 2003
"Reconstitution of recombinant uncoupling proteins: UCP 1, -2, -3 have similar affinities for ATP and are unaffected by coenzyme Q_{10}"
J. Biol. Chem., **278**, 25825 – 25831

Jabůrek, M., Miyamoto, S., Di Mascio, P, Garlid, K.D. and Ježek , P, 2004
"Hydroperoxy fatty acid cycling mediated by mitochondrial uncoupling protein UCP2"
J. Biol. Chem., **279 (51),** 53097 - 53102

Jarmuszkiewicz, W., Sluse-Goffart, C.M., Hryniewiecka, L. and Sluse, F.E. 1999
"Identification and characterization of a protozoan uncoupling protein in Acanthamoeba castellanii"
J. Biol.Chem., **274**, 23198 - 23202.

Jarmuszkiewicz, W., Milani, G., Fortes, F., Schreiber, A.Z., Sluse, F.E. and Vercesi, A.E. 2000
"First evidence and characterisation of an uncoupling protein in fungi kingdom: CpUCP of Candida parapsilosis"
FEBS Letters **467**, 145 - 149.

Ježek , P. and Garlid, K.D. 1990
"New substrates and competitive inhibitors of the Cl^- translocating pathway of the uncoupling protein of brown adipose tissue mitochondria"
J. Biol. Chem., **265,** (31) 19303-19311

Ježek , P., Orosz, D.E. and Garlid, K.D., 1990
"Reconstitution of the uncoupling protein of brown adipose tissue mitochondria"
J. Biol. Chem., **265,** (31) 19296-19302

Ježek , P., Orosz, D.E., Modriansky, M and Garlid, K.D., 1994
"Transport of anions and protons by the mitochondrial uncoupling protein and its regulation by nucleotides and fatty acids"
J. Biol. Chem., **269,** 26184-26190.

Ježek, P., Žáčková, M., Řeháková, Z., Růžička, M., Borecký, J., Škobisová, E., Brucknerová, J., Garlid, K., Gimeno, R.E. and Tartaglia, L.A. 1999
"Existence of uncoupling protein-2 antigen in isolated mitochondria from various tissues"
FEBS Letts. **455**, 79 - 82.

Kamp, F. and Hamilton, J.A., 1992
"pH gradients across phospholipids membranes caused by fast flip-flop of unionized fatty acids"
Proc. Natl. Acad. Sci. USA, **89**, 11367-11370.

Kaplan, R.S. and Pedersen, P.L., 1985
"Determination of Microgram Quantities of Protein in the Presence of Milligram levels of lipid with Amido Black 10B"
Anal. Biochem., **150**, 97-104

Kasahara, M. And Hinkle, P.C., 1977
"Reconstitution and purification of the D-glucose transporter from human erythrocytes"
J. Biol. Chem. **252**, 7384 – 7390

Kaushik, S. and Kaur, J. 2003
"Chronic cold exposure affects the antioxidant defense system in various rat tissues"
Clin. Chim. Acta. **333**, 69 – 77.

Klingenberg, M. and Echtay, K.S., 2001
"Uncoupling proteins: the issues from a biochemist point of view"
Biochem. et Biophys. Acta., **1504,** 128-143

Klingenberg, M., Echtay, K.S., Bienengraeber, M., Winkler, E. and Huang, S.G., 1999
"Structure-function relationship in UCP1"
Int. J. Ob., **23,** S24-S29

Klingenberg, M. and Winkler, E., 1985
"The reconstituted isolated uncoupling protein is a membrane potential driven H^+ translocator"
Embo. J., **4,** 3087-3092

Krämer, R and Palmieri, F., 1989
"Molecular aspects of isolated and reconstituted carrier proteins from animal mitochondria"
Biochim. Biophys. Acta, **974**, 1-23

Krauss, S., Zhang, C.Y. and Lowell, B.B. 2002
"A significant portion of mitochondrial proton leak in intact thymocytes depends on expression of UCP2"
Proc. Natl. Acad. Sci., **99**, 118 - 122.

Laloi, M., Klein, M., Riesmeier, J.W., Muller-Rober, B., Fleury, F., Bouillaud, F. and Ricquier, D. 1997
"A plant cold-induced uncoupling protein".
Nature **389**, 135 - 136.

Lanni, A., Moreno, M., Lombardi, A. and Goglia, F. 2003
"Thyroid hormone and uncoupling proteins".
FEBS Letters, **543**, 5 – 10.

Lardy, H.A. and Pressman, B.C., 1956
"Effect of surface active agents on the latent ATPase of mitochondria"
Biochim Biophys Acta. **3** :458-66.

Larrouy, D., Laharrague, P., Carrera, G., Viguerie-Bascands, N., Levi-Meyrueis, C., Fleury, C., Pecqueur, C., Nibbelink, M., André, M., Casteilla, L. and Ricquier, D., 1997

"Kupffer cells are a dominant site of uncoupling protein 2 expression in rat liver"
Biochemica Biophyica Research Communications, **235**, 760 - 764.

Lasic, D.D., 1988
"The mechanism of vesicle formation"
Biochem J., **256(1)**:1-11.

Lepovsky, S., Wang, W., Koike, T., and Dimick, M.K. 1959
"The oxygen uptake by particulate suspensions (mitochondrial) form liver, brown and white fatty tissues"
Fed. Proc. **18,** 272

Li, B., Nolte, L.A., Ju, J-S., Han, D.H., Coleman, T., Holloszy, J.O. and Semenkovich, C.F. 2000
"Skeletal muscle respiratory uncoupling prevents diet-induced obesity and insulin resistance in mice"
Nature Medicine, **6**, 1115 - 1120.

Lin, C.S. and Klingenberg, M., 1980
"Isolation of the UCP from Brown Adipose Tissue mitochondria"
FEBS Letts, **113,** 299-303

Maia, I.G., Benedetti, L.E., Leite A., Turcinelli, S.R., Vercesi, A.E. and Arruda, P. 1998
"AtUCP: an Arabidopsis gene encoding a plant uncoupling protein"
FEBS Letters, **429**, 403 - 406.

Mao, W., Xian Yu, X., Zhong, A., Li, W., Brush, J., Sherwood, S.W., Adams, S.H. and Pan, G., 1999
"UCP4, a novel brain-specific mitochondrial protein that reduces membrane potential in mammalian cells"
FEBS Letts., **443,** 326-330

Markwell, M., Hass, S.M., Brecker, L. and Tolbert, N., (1978)
"A Modification of the Lowry procedure to simplify protein determination in membrane and lipoprotein samples,"
Anal. Biochem. **87**(1), 206-210.

Medvedev, A., Robidoux, J., Bai, X., Cao, W., Floering, L., Daniel, K., Collins, S. 2002
"Regulation of the uncoupling protein-2 gene in INS-1 beta-cells by oleic acid". J.. Biol. Chem., **277**, 42639 – 42644.

Mitchell, P., (1961)
"Coupling of phosphorylation to electron and hydrogen transfer by a chemiosmotic type of mechanism"
Nature 191**, 144-148**

Monemdjou, S., Kozak, L.P. and Harper, M.E., 1999
Mitochondrial proton leak in brown adipose tissue mitochondria of UCP1-deficient mice is GDP-insensitive"
Am. J. Physiol, **276,** E1073 - 1082

Moreno, M., Lombardi, A., Del Lange, P., Silvestri, E., Ragni, M., Lanni, A. and Goglia, F. 2003
"Fasting, lipid metabolism, and triiodothyonine in rat gastrocnemius muscle: interrelated roles of uncoupling protein 3, mitochondrial thioesterase and coenzyme Q"
FASEB Journal **17**, 1112 – 1114.

Nagase, I., Yoshida, T. and Saito, M. 2001
"Up-regulation of uncoupling proteins by beta-adrenergic stimulation in L6 myotubes"
FEBS Letters, **494**, 175 – 180.

Néchad, M. (1986)
"Structure and development of brown adipose tissue"
Brown Adipose Tissue (Edited by Trayhurn, P. and Nicholls, D.), pp. 1 - 30. Arnold, London

Nedergaard, J and Cannon B, 1985
"[^{3}H] GDP binding and thermogenin amount in brown adipose tissue mitochondria from cold-adapted rats"
Am. J. Physiol., **248,** C365 – C371

Nègre-Salvayre, A., Hirtz, C., Carrera, G., Cazenave, R., Troly, M., Salvayre, R., Pénicaud, L. and Casteilla, L. (1997)
"A role for uncoupling-protein 2 as a regulator of mitochondrial hydrogen peroxide generation".
FASEB Journal, **11**, 809 - 815.

Nicholls, D.G., 1974
"Hamster BAT mitochondria: the chloride permeability of the inner membrane under respiring conditions, the influence of purine nucleotides"
Eur.J. Biochem, **49,** 585-593

Nicholls, D.G., 1976
"Hamster Brown-Adipose-Tissue Mitochondria. Purine Nucleotide Control of the Ion Conductance of the Inner Membrane, the Nature of the Nucleotide Binding Site."
Eur. J. Biochem. **62,** 223-228.

Nicholls, D.G. and Ferguson, S.J., 1992
"Bioenergetics 2"
London Academic Press

Nicholls, D.G. and Linberg, O., 1973
"The influence of Albumin and Nucleotides on Passive Ion Permeabilities"
Eur. J. Biochem. **37,** 523-530

Nicholls, D.G, 1976
The bioenergetics of brown adipose tissue mitochondria"
FEBS Lett., **61:** 103-110

Nicholls, D.G. and Locke, R.M., 1984
"Thermogenic Mechanisms in Brown Fat"
Physiol. Rev., **64,** 1-40.

Parascandola, J., 1974
"Dinitrophenol and Bioenergetics: An Historical Perspective"
Molecular and Cellular Biochemistry, **5,** 69 – 77.

Pecqueur, C., Alves-Guerra, M.C., Gelly, C., Levi-Meyrueis, C., Couplan, E., Collins, S., Ricquier, D., Bouillaud, F. and Miroux, B. 2001
"Uncoupling protein 2, *in vivo* distribution, induction upon oxidative stress, and evidence for translational regulation"
The Journal of Biological Chemistry, **276**, 8705 - 8712.

Pedraza, N., Solanes, G., Iglesias, R., Vázqeuz, M., Giralt, M. and Villarroya, F. 2001
"Differential regulation of expression of genes encoding uncoupling proteins 1 and 3 in brown adipose tissue during lactation in mice"
Biochemical Journal, **355,** 105 - 111.

Queiroz, M.S., Shao, Y. and Ismail-Beigi, F. 2004
"Effect of thyroid hormone on uncoupling protein 3 mRNA expression in rat heart and skeletal muscle"
Thyroid **14,** 177 – 185.

Rafael, J., Ludolph, H-J. and Hohorst, H-J., 1969
"Mitochondria from brown adipose tissue: uncoupling of oxidative phosphorylation by long chain fatty acids and recoupling by guanosine-triphosphate"
Hoppe-Seyler's Z. Physiol. Chem. **350,** 1121-1131

Ragan, C.I. and Hinkle, P.C., 1975
"Ion transport and respiratory control in vesicles formed from reduced Nicotinamide Adenine Dinucleotide, Coenzyme Q reductase and phospholipids"
J. Biol.Chem., **250,** (12), 8472-8476

Raimbult, S., Dridi, S., Denjean, F., Lacheur, J., Couplan, E., Bouillaud, F., Bordas, A., Duchamp, C., Taouis, M. and Ricquier, D. 2001
"An uncoupling protein homologue putatively involved in facultative muscle thermogenesis"
Biochem. J.,I **353**, 441 -444.

Ricquier, D. and Kader, J-C., 1976
"Mitochondrial protein alteration in active brown fat: a sodium dodecyl sulphate polyacrylamide electrophoretic study."
Biochem. Biophys. Res. Commum. **73,** 577-583.

Ricquier, D. and Bouillaud, F., 2000
"The uncoupling protein homologues: UCP1, UCP2, UCP 3, StUCP and AtUCP"
Biochemical Journal, **345**, 161 - 179.

Rigaud, J.L., Bluzat, A. and Büschlen, S. (1983)
"Incorporation of bacteriorhodopsin into large unilamellar liposomes by reverse phase evaporation"
Biochem. Biophys. Res. Commun. **111,** 373 – 382

Rigaud, J.L., Pitard, B. and Levy, D., 1995
"Reconstitution of membrane proteins into liposomes: application to energy-transducing membrane proteins"
Biochim. et Biophys. Acta **1231,** 223-246

Rousset, S., Alves-Guerra, M.C., Ouadghiri-Bencherif, S., Kozak, L.P., Miro, B.,Richard, D., Bouillaud, F., Ricquier, D. and Cassard-Doulcier, A.M. 2003
"Uncoupling protein 2, but not uncoupling protein 1, is expressed in the female mouse reproductive tract"
J. Biol. Chem., **278**, 45843 - 45847.

Sambrook, J., Fritsch, E.F. and Maniatis, T., (1989)
Molecular Cloning: A Laboratory Manual, 2nd Edition.
Cold Spring Harbour Press, Cold Spring Harbour, NY, USA

Sanchis, D., Fleury, C., Chomiki, N., Goubern, M., Huang, Q., Neverova, M., Grégoire, F., Easlick, J., Raimbault, S., Lévi-Meyrueis, C., Miroux, B., Collins, S., Seldin, M., Richard, D., Warden, C., Bouillaud, F. and Ricquier, D., 1998
"BMCP1, a novel mitochondrial carrier with high expression in the central nervous system of humans and rodents, and respiration uncoupling activity in recombinant yeast"
J. Biol. Chem., **273,** (51), 34611-34615

Schrauwen, P. and Hesselink, M. 2003
"Uncoupling protein 3 and physical activity: the role of uncoupling protein 3 in energy metabolism revisited"
Proc. Nut. Soc., **2,** 635 – 643.

Sheldon,J.G., Williams, S.P., Fulton, A.M. and Brindle,K.M. 1996
"31P NMR magnetization transfer study of the control of ATP turnover in *Saccromyces cerevisia*"
Proc. Natl. Acad. Sci., USA, **93**,6399 - 6404

Silvestri, E., Moreno, M., Lombardi, A., Ragni, M., de Lange, P., Alexson, S., Lanni, A. and Goglia, F. 2005
"Thyroid hormone effects on putative biochemical pathways involved in UCP3 activation in rat skeletal muscle mitochondria"
FEBS Letters, **579**, 1639 – 1645.

Sivitz, W.I., Fink, B.D. and Donohue, P.A. 1999
"Fasting and leptin modulate adipose and muscle uncoupling protein: divergent effects between messenger ribonucleic acid and protein expression"
Endocrinology, **140**, 1511-1519.

Skulachev, V.P. 1988
Membrane Bioenergetics,
Springer, Berlin

Skulachev, V.P., 1991
"Fatty acid circuit as a physiological mechanism of uncoupling of oxidative phosphorylation"
FEBS Letts., **294,** (3), 158-162

Skulachev, V.P., 1996
"Why are mitochondria involved in apoptosis? Permeability transition pores and apoptosis as selective mechanisms to eliminate superoxide-producing mitochondria and cell".
FEBS Letters **397,** 7 – 10.

Skulachev, V.P., 1998
"Uncoupling: new approached to an old problem of bioenergetics"
Biochimica et Biophysica Acta **1363**, 100 - 124

Smith, R.E. and Horwitz, B.A., (1969)
"Brown fat and thermogenesis"
Physiol. Rev., **49** 330.

Steinberg-Yfrach, G., Liddel, P.A., Hung, S., Moore, A.L., Devens, G. And Moore, T.A., 1997
"Conversion of light energy to proton potential in liposomes by artificial photosynthetic reaction centres"
Nature, **385**, 239 – 241.

Strieleman, P.J., Schalinske, K.L. and Shrago, E., 1985a
"Partial purification and functional reconstitution of GDP sensitive brown adipose tissue mitochondrial UCP using octyl glucoside"
Biochem. Biophys. Res. Commun., **127,** 509-516

Strieleman, P.J., Schlinske, K.L. and Shrago, E., 1985b
"Fatty acid activation of the reconstituted brown adipose tissue mitochondria uncoupling protein"
J. Biol. Chem., **260,** 13402-13405

Venditti, P., De Rosa, R. and Di Meo, S. 2004
"Effect of cold induced hyperthyroidism on H_2O_2 production and susceptibility to stress conditions of rat liver mitochondria".
Free Radical Biology and Medicine. **36**, 348 – 358

Vercesi, A.E., Martins, I.S., Silva, M.A.P., Leite, H.M.F., Cuccovia, I.A. and Chaimovich, H. 1995
PUMPing Plants
Nature **375,** 24.

Vidal-Puig, A., Solanes, G., Grujic, D., Flier, J.S. and Lowell, B.B. 1997
"UCP3: An uncoupling protein homologue expressed preferentially and abundantly in skeletal muscle and brown adipose tissue".
Biochem. Biophys.Res. Comm. **235**, 79 – 82.

Vidal-Puig, A., Grujic, D., Zhang, C-Y., Hagen, T., Boss, O., Ido, Y., Szszepanik, A., Wade, J., Mootha, V., Cortright, R., Muoio, D.M. and Lowell, B.B. 2000
"Energy metabolism in uncoupling protein 3 gene knockout mice"
J. Biol. Chem., **275**, 16258 - 16266.

Weigle, D.S., Selfridge, L.E., Schwartz, M.W., Seeley, R.J., Cummings, D.E., Havel, P.J., Kuijper, J.L. and Baltrandelrio, H. 1998
"Elevated free fatty acids induce uncoupling protein 3 expression in muscle: a potential explanation for the effect of fasting".
Diabetes **47**, 298-302.

Winkler, E. and Klingenberg, M., 1994
"Effect of fatty acids on H^+ transport activity of the reconstituted uncoupling protein"
J. Biol. Chem., **269,** 2508-2515

Available online at www.sciencedirect.com
SCIENCE DIRECT®
Biochimica et Biophysica Acta 1604 (2003) 170–179
BIOCHIMICA ET BIOPHYSICA ACTA
BBA
www.bba-direct.com

Selective detection of UCP 3 expression in skeletal muscle: effect of thyroid status and temperature acclimation

O. Cunningham[a], A.M. McElligott[a], A.M. Carroll[a], E. Breen[a], C. Reguenga[b], M.E.M. Oliveira[b], J.E. Azevedo[b], R.K. Porter[a,*]

[a] *Department of Biochemistry, Trinity College Dublin, Biotechnology Building, Room 0.16, Dublin 2, Ireland*
[b] *Instituto de Biologia Molecular e Celular and Instituto de Ciências Biomédicas de Abel Salazar, Universidade do Porto, Oporto, Portugal*

Received 27 January 2003; received in revised form 12 May 2003; accepted 13 May 2003

Abstract

A novel peptide antibody to UCP 3 is characterized which is sensitive and discriminatory for UCP 3 over UCP 2, UCP 1 and other mitochondrial transporters. The peptide antibody detects UCP 3 expression in *E. coli*, COS cells and yeast expression systems. The peptide antibody detects a single ~ 33 kDa protein band in mitochondria from isolated rat skeletal muscle, mouse and rat brown adipose tissue, and in whole muscle groups (soleus and extensor digitorum longus) from mice. No 33 kDa band is detectable in isolated mitochondria from liver, heart, brain, kidney and lungs of rats, or gastrocnemius mitochondria from UCP 3 knock-out mice. From our data, we conclude that the peptide antibody is detecting UCP 3 in skeletal muscle, skeletal muscle mitochondria and brown adipose tissue mitochondria. It is also noteworthy that the peptide antibody can detect human, mouse and rat forms of UCP 3. Using the UCP 3 peptide antibody, we confirm and quantify the increased (2.8-fold) UCP 3 expression observed in skeletal muscle mitochondria isolated from 48-h-starved rats. We show that UCP 3 expression is increased (1.6-fold) in skeletal muscle of rats acclimated over 8 weeks to 8 °C and that UCP 3 expression is decreased (1.4-fold) in rats acclimated to 30 °C. Furthermore, UCP 3 expression is increased (2.3-fold) in skeletal muscle from hyperthyroid rats compared to euthyroid controls. In addition, we show that UCP 3 expression is only coincident with the mitochondrial fraction of skeletal muscle homogenates and not peroxisomal, nuclear or cytosolic and microsomal fractions.
© 2003 Elsevier Science B.V. All rights reserved.

Keywords: Uncoupling protein; UCP 3; Peroxisome; Mitochondria; Antibody; Thyroid; Skeletal muscle

1. Introduction

The function of the novel uncoupling proteins UCP 2 and UCP 3 is still a matter of contention. It has been reported that UCP 2 and UCP 3 act as uncoupling proteins, in the same manner as UCP 1, being conduits for proton translocation across the mitochondrial inner membrane [1]. Other data suggest that UCP 2 and UCP 3, like UCP 1, flip fatty acid anions across the mitochondrial inner membrane thus completing a cycle of protonated fatty acid diffusion and unprotonated fatty acid flipping leading to uncoupling [2]. In contrast, other data from isolated mitochondrial studies show no correlation between increased expression of UCP 2 and UCP 3 and increases in mitochondrial proton leak [3]. Dulloo et al. [4] have demonstrated a correlation between levels of UCP 3 transcript and fatty acid oxidation. Other evidence suggests that UCP 1, UCP 2 and UCP 3 facilitate superoxide translocation across the mitochondrial inner membrane [5]. UCP 2 knock-out mice have no obvious whole body metabolic phenotype to distinguish them from wild-type mice. However, UCP 2 knock-out mice do have an increased resistance to infection by *Toxoplasma gondii*. This resistance to infection has been attributed to increased reactive oxygen species (ROS) production by mitochondria in their macrophages [6]. Similarly, UCP 3 knock-out mice have no obvious phenotype to distinguish them from wild-

Abbreviations: ATCC, American Tissue Culture Center; BSA, bovine serum albumin; COIII, cytochrome oxidase subunit 3; cyt c, cytochrome *c*; ECL, enhanced chemiluminescence; EDL, extensor digitorum longus; EDTA, ethylenediaminetetraacetic acid; EGTA, ethylene glycol-bis(β-aminoethyl ether) *N,N,N,N*-tetraacetic acid; HRP, horseradish peroxidase; IPTG, isopropyl β-D-thiogalactopyranoside; OD, optical density; PBS, phosphate-buffered saline; PMSF, phenylmethylsulfonyl fluoride; ROS, reactive oxygen species; SDS, sodium dodecylsulfate; STE, sucrose Tris EGTA buffer; UCP, uncoupling protein

* Corresponding author. Tel.: +353-1-6081617; fax: +353-1-6772400.
E-mail address: rkporter@tcd.ie (R.K. Porter).

0005-2728/03/$ - see front matter © 2003 Elsevier Science B.V. All rights reserved.
doi:10.1016/S0005-2728(03)00057-4

type mice [7,8]. However, decreased proton leak has been observed in isolated skeletal muscle mitochondria from UCP 3 knock-out mice [8]. By contrast, overexpression of UCP 3 protein in skeletal muscle of mice causes hyperphagia and increases whole body metabolic rate and proton leak of mitochondria in skeletal muscle [9]. However, it is not clear whether the increased leak is attributable to an increased amount of protein in the inner membrane or whether it is a specific function of the UCP 3 protein.

Functional analysis aside, it is possible to get clues to the function of UCPs, and the context in which that function operates, by observing their pattern of expression under various physiological and pathological conditions. Detection of UCP transcript is useful but is not necessarily representative of expression of the functional entity, i.e. the protein. This has clearly been the case for UCP 2 where transcript studies suggested ubiquitous expression in many mammalian tissues [10], whereas protein detection studies suggest UCP 2 is confined to specific tissues, namely lung, spleen, kidney, stomach and white adipose tissue [11]. Few studies have focused on UCP 3 protein expression despite the fact that commercial peptide antibodies to UCP 3 are available from Calbiochem, Chemicon International and Lilly. Peptide antibodies to UCP 3 have also been developed in-house by a number of groups [7,12]. However, in most cases, the sensitivity and discriminatory nature of those antibodies to other UCPs, and mitochondrial transporters in general, have not been satisfactorily demonstrated [12].

Northern blot analysis and Western blot analysis using peptide antibodies to UCP 3, have shown that UCP 3 is found predominantly in skeletal muscle of mammals [10,13,14]. Furthermore, starvation has been shown to increase UCP 3 mRNA levels in mouse skeletal muscle [13] and UCP 3 protein expression in mitochondria from skeletal muscle of rats [3]. Short-term cold exposure also increases UCP 3 protein expression in skeletal muscle mitochondria [15]. UCP 3 mRNA has also been detected in brown adipose tissue [10].

In this study, a novel peptide antibody to UCP 3 is described that is sensitive and discriminatory for UCP 3 over UCP 2, UCP 1 and other mitochondrial transporters. The antibody detects UCP 3 in skeletal muscle and brown adipose tissue as predicted from UCP 3 transcript studies. Using the UCP 3 peptide antibody, we confirm and quantify the increased UCP 3 expression in skeletal muscle mitochondria isolated from starved rats. We show that this specific antibody is sensitive enough for use on whole muscle homogenates. We show that UCP 3 expression is increased in skeletal muscle of rats after long-term cold exposure and that UCP 3 expression is decreased in rats acclimated to 30 °C. We demonstrate that UCP 3 expression is increased in skeletal muscle mitochondria of hyperthyroid rats. Our data also show that UCP 3 expression is coincident with the mitochondrial fraction of skeletal muscle homogenates.

2. Materials and methods

2.1. Isolation of mitochondria from liver, kidney, lungs, brain, brown adipose tissue

Mitochondria were prepared essentially by the method of Chappell and Hansford [16]. Tissues were removed, weighed and placed in ice-cold sucrose Tris EGTA buffer (STE) buffer (250 mM Sucrose, 5 mM Tris–HCl, 2 mM ethylene glycol-bis(β-aminoethyl ether) *N,N,N′,N′*-tetraacetic acid (EGTA), pH 7.4). Tissues were chopped finely using scissors and washed several times with STE buffer. The tissue was homogenised by hand using a Dounce homogeniser as follows: four passes with a pestle of 0.26 inch clearance followed by six passes with a pestle of 0.12 inch clearance. The homogenate was centrifuged at 800 × *g* for 3 min at 4 °C, pelleting blood and debris. The pellet was discarded and the supernatant was centrifuged at 12,000 × *g* for 10 min at 4 °C yielding a "mitochondrial" pellet. The mitochondrial pellet was resuspended in STE buffer and recentrifuged as described above. The resulting mitochondrial pellet was resuspended in STE buffer to the desired concentration.

2.2. Isolation of heart and skeletal muscle mitochondria

Skeletal muscle mitochondria from rat hind leg muscle and rat heart mitochondria were isolated by the method of Bhattacharya et al. [17]. Hindquarter muscle (all leg and a small amount of back muscle) and hearts were removed, weighed and placed in ice-cold isolation medium (100 mM sucrose, 9 mM ethylenediaminetetraacetic acid (EDTA), 100 mM Tris–HCl, 46 mM KCl, pH 7.4). Muscle and heart were finely chopped on a pre-cooled glass tile with a razor blade, added to isolation medium (200 ml) containing 0.5% (w/v) bovine serum albumin (BSA) and 0.02% (w/v) nagarse (Sigma, Protease VII) and incubated on ice, with stirring, for 5 min. The tissue was further disrupted using a Waring commercial blender at half-maximum speed for 15 min. The homogenate was centrifuged at 1500 × *g* for 3 min at 4 °C. The whitish lipid layer on top of the supernatant was removed using a spatula and the supernatant was centrifuged at 12,000 × *g* for 10 min at 4 °C. The mitochondrial pellet was resuspended in ice-cold isolation medium and centrifuged as above. The final mitochondrial pellet was resuspended in ice-cold isolation medium to the desired concentration.

2.3. Preparation of muscle groups for analysis

The hind limb muscles soleus and extensor digitorum longus (EDL) were removed, ensuring complete removal of associated tendons and connective tissue and placed in ice-cold muscle isolation medium (100 mM sucrose, 9 mM EDTA, 1 mM EGTA, 46 mM KCl, 100 mM Tris–HCl, pH 7.5). Muscles were finely chopped on a pre-cooled glass tile

and frozen in approximately 10 ml of liquid nitrogen in a porcelain mortar. A porcelain pestle was used to grind the frozen muscle to a fine powder. Once ground, EDL and muscles from each animal were individually resuspended in 500 μl of cold muscle isolation medium. Samples were aliquoted in 100 μl volumes and stored at −20 °C.

2.4. Subcellular fractionation of muscle and liver tissue

Fractionation of skeletal muscle was performed essentially as described for fractionation of liver by Hartl et al. [18] with minor modifications from Gouveia et al. [19] using minced muscle or liver from 48-h-starved Wistar rats.

2.5. Expression of protein and isolation of inclusion bodies from E. coli

A colony of *E. coli* cells, BL21 pLysS, which had been transfected with the appropriate plasmid (pET 3a-haUCP 1, pET 21d-hUCP 2 or pET 21d-hUCP 3) containing cDNA for the UCP required was inoculated into 5 ml of LB medium (10 g tryptone, 5 g yeast extract, 5 g NaCl, 100 mg ampicillin in 1 l). The colony was amplified overnight and the following day, the culture was diluted to 500 ml and grown until OD_{600} had reached 0.4. Induction of expression of the UCP was carried out with 1 mM isopropyl β-D-thiogalactopyranoside (IPTG). Two hours following the addition of IPTG, the cells were harvested at $10,000 \times g$ and the bacterial pellets frozen at −20 °C for at least an hour. Pellets were then thawed and inclusion bodies were isolated as described in Echtay et al. [20].

2.6. Expression of UCP 3 in yeast

The human UCP 3 yeast expression vector pYU3HSL was a gift from Dr. Daniel Ricquier (Centre de Recherche sur l'Endocrinologie Moleculaire et le Developpement, Meudon, France). The UCP 3 transcript was excised from pYU3HSL and subcloned into the yeast expression vector pYES2 (Invitrogen). The *Saccharomyces cerevisiae* strain INVSC1 (Invitrogen) was transformed with either the UCP 3 containing pYES2 expression vector or pYU3HSL using the *S.c.* EasyComp™ Kit (Invitrogen). Empty pYES was also transformed as a negative control. UCP 3 was expressed in yeast as described by Zhang et al. [21] with modifications. In brief, transformants were selected on SC-ura plates and single colonies were grown to an OD_{600}>2 in a preculture of SC-ura medium (0.67% yeast nitrogen base, 0.1% KH_2PO_4, 0.12% $(NH_4)_2SO_4$, 0.1% glucose, 2% lactate, 0.1% casamino acids, 20 mg/l tryptophan, 40 mg/l adenine). The yeast were diluted in 100 ml of YPL medium (1% yeast extract, 2% bactopeptone, 3% lactate, pH 4.5 with 10 M NaOH), to OD_{600} of 0.04. The yeast were grown at 30 °C with vigourous shaking to an OD_{600} ~ 1.5, at which time 1% galactose was added and the cells were harvested after a further 8 h. Following harvesting, the yeast were incubated with zymolyase (Sigma) until >90% spheroplast formation. The spheroplasts were resuspended in homogenisation buffer (0.6 M mannitol, 10 mM Tris–malate, pH 7.4, 0.1% BSA, 1 mM EGTA, 1 mM EDTA, 1 mM PMSF) and homogenised using a Dounce homogeniser.

2.7. COS cell expression of UCP 3

The UCP 3 transcript was excised from pYU3HSL and subcloned into the mammalian expression vector pcDNA3.1 (Invitrogen). COS-1 cells were obtained from the American Tissue Culture Center (ATCC). All cell culture reagents were supplied by GIBCO (Invitrogen). COS-1 cells were seeded in six-well plates at ~ 2×10^5 cells per well and grown overnight at 37 °C in Dulbecco's modified Eagle medium (DMEM) supplemented with 10 U/ml penicillin, 100 mg/ml streptomycin sulfate and 10% foetal calf serum under 95% air/5% CO_2, then transiently transfected with pcDNA3.1 containing the UCP 3 transcript and pcDNA3.1 alone using Fugene (Roche) according to the manufacturers instructions. Twenty-four hours following transfection 100 μl of sodium dodecylsulfate (SDS) sample buffer (0.0625 M Tris–HCl, pH 6.8, 10% (w/v) glycerol, 4% (w/v) SDS, 5% (w/v) β-mercaptoethanol and 0.005% (w/v) bromophenol blue) was added to the wells and the cells were homogenised by being drawn up repeatedly through a narrow bore needle. The cell homogenates were stored at −20 °C until analysis.

COS-1 cells were also transfected with pcDNA3.1 containing the UCP 3 transcript and stable clones were isolated using neomycin selection. Colonies were isolated when they had grown to ~ 2 mm in diameter and expanded in selection media. Stable clones were harvested in SDS sample buffer as described above. Stable clones with the pcDNA3.1 vector alone were also isolated for use as a negative control.

2.8. Protein determination

Tissue and mitochondrial protein concentration was determined according to the procedure described by Markwell et al. [22].

2.9. Preparation of samples for polyacrylamide gel electrophoresis

Samples (10–100 μg protein) were solubilised in sample buffer; 0.0625 M Tris–HCl, pH 6.8, 10% glycerol, 2% SDS, 1.66% β-mercaptoethanol (added directly prior to use) and 0.001% bromophenol blue. Prior to loading on gel, samples were vortexed and pulsed in a minifuge before boiling at 100 °C for 5 min.

2.10. Polyacrylamide gel electrophoresis

Gels were run using the Laemmli [23] system for denaturing gels. Slight modifications were used as de-

scribed: 0.375 M Tris–HCl, pH 8.7 and 0.1% SDS were used in all solutions, except for the gels for the subcellular fractionation and peroxisome samples, which had 0.75 M Tris. Linear 12% polyacrylamide gels were prepared from a stock solution containing 30% (w/v) acrylamide; 0.4% (w/v) bis-acrylamide. Samples were prepared using Laemmli sample buffer containing either 5% (w/v) β-mercaptoethanol or 20–100 mM dithiothreitol, and subsequently incubated for 5 min at 100 °C or 20 min at 70 °C. The gel dimensions, for the subcellular fractionation and peroxisome samples, were 14 cm × 10 cm × 1 mm. Gels for whole muscle samples were 9 cm × 7 cm × 1.5 mm. All other gels were 9 cm × 7 cm × 0.75 mm. All gels were run on a Protean II or Protean III (Bio-Rad) gel system.

2.11. Western blotting analysis

Following polyacrylamide gel electrophoresis, proteins were transferred to nitrocellulose or polyvinylidene difluoride (PVDF) (Millipore). Transfer was achieved using a semi-dry apparatus for 2 h at 110 mA or a Bio-Rad Trans-Blot Transfer Cell for 1–4 h at 20 V/cm. After transfer was complete, blots were blocked for 1 h in phosphate-buffered saline (PBS)-Tween (0.14 M NaCl, 2.7 mM KCl, 11.5 mM Na_2PO_4, 1.8 mM KH_2PO_4, pH 7.4 with 0.1% Tween-20) containing 5% non-fat dried milk (Marvel). This was followed by three 10-min washes with PBS-Tween.

Blots were probed with primary antibody overnight at 4 °C in the same solution containing 1:5000 dilution of an affinity-purified anti-UCP 3 peptide antibody, a 1:5000 dilution of an affinity-purified anti-UCP 2 peptide antibody, a 1:5000 dilution of an affinity-purified anti-UCP 1 peptide antibody, a 1:1000 dilution of rabbit antiserum directed to human Pex14p [24], a 1:5000 dilution of a monoclonal antibody directed to the α-subunit of the mitochondrial ATP synthase (clone 7H10-BD4, Molecular Probes), a 1:500 dilution of purified mouse anti-cytochrome *c* monoclonal antibody (BD PharMingen), a 1:1000 dilution of peptide antibody to subunit III of cytochrome oxidase or a 1:10,000 dilution of the full-length UCP 1 antibody. These steps were followed by three 10-min washes in PBS-Tween.

Blots were then probed with secondary antibody incubated in 1:10,000 dilution of a goat anti-mouse IgG horseradish peroxidase (HRP) conjugate (for cytochrome *c*), a donkey anti-sheep IgG HRP conjugate (for full-length UCP 1 antibody) or a goat/donkey anti-rabbit IgG HRP conjugate (for all others) secondary antibody in PBS-Tween containing 5% non-fat dried milk for 1 h. After a further three 10-min washes in PBS-Tween, the blots were developed using an enhanced chemiluminescence (ECL) detection system (Amersham-Biosciences) and visualized by exposure to X-ray film. The ATP synthase ($F_1\alpha$) and Pex14p blots were developed using chloronaphthol (Sigma) and hydrogen peroxide as substrates for the HRP-linked secondary antibody. The antibody to the $F_1\beta$ was raised by the β-subunit of the ATP-synthase from *Neurospora crassa*.

2.12. Densitometry

Following Western blot development, the relative abundance of UCP 3 was determined by using densitometry. The band intensities of the exposed film were analysed using Scion Imaging Software (Scion Corporation, Maryland, USA).

2.13. UCP antibodies

Peptide synthesis, conjugation of peptides to BSA and injection of rabbits was undertaken by Eurogentec (Parc Scientifique du Sart Tilman, 4102 Seraing, Belgium). Polyclonal antibodies in the resulting rabbit anti-sera were affinity-purified on a protein A column. The peptides to which polyclonal antibodies were raised are as follows: UCP 1, 145...CHLHGIKPRYTGYNA...158; UCP 2, 147...QARAGGGRRYQSTVEA...162; UCP 3, 141...TGGERKYRGTMDAYRC...156. The full-length antibody to UCP 1 was a gift from Daniel Ricquier (Centre de Recherche sur l'Endocrinologie Moleculaire et la Developpement).

3. Results

In a bid to distinguish between the uncoupling proteins UCP 1, UCP 2 and UCP 3, antibodies were raised to peptide sequences unique to each uncoupling protein based on similarities with the rat sequences. The resulting affinity-purified polyclonal antibodies were tested for their ability to detect UCP 1, 2 and 3 protein expressed by *E. coli* (Fig. 1). Blot A shows that anti-UCP 3 peptide antibodies detected only UCP 3 (lane 1) and not UCP 2 (lane 2) or UCP 1 (lane 3). Blot B demonstrates that UCP 2 antibodies could not discriminate between the UCPs and detected UCP 3 (lane 1), UCP 2 (lane 2) and UCP 1 (lane 3). Blot C shows that the UCP 1 antibodies only detected UCP 1 (lane 3) and not UCP 2 (lane 2) or UCP 3 (lane 1). One general observation is that all expressed uncoupling proteins had apparent

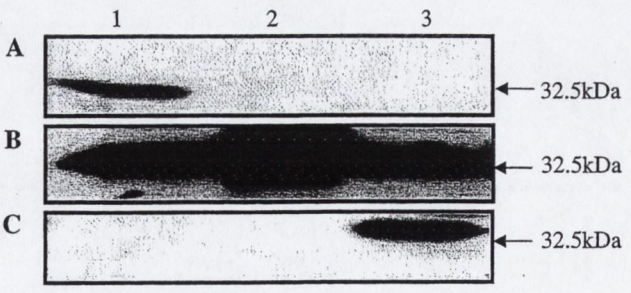


Fig. 1. Anti-UCP 3 peptide antibody is specific for *E. coli* expressed UCP 3. Lane 1, 5 μg of hUCP 3; lane 2, 20 μg hUCP 2; lane 3, 20 μg haUCP 1. Polyclonal peptide antibodies to rUCP 3 (Blot A), rUCP 2 (Blot B) and rUCP 1 (Blot C) were used at a dilution of 1:5000. Exposure time was the same for all samples (30 s).

molecular masses circa 32–34 kDa. All blots were exposed for equal time periods (30 s).

For the purpose of estimating increases in UCP 3 protein expression, we were able to show that there is a linear relationship between the amount of *E. coli* expressed UCP 3 and the resultant intensity of the bands on the exposed film of a given immunoblot (Fig. 2).

In addition to detection of UCP 3 expressed in *E. coli*, the polyclonal peptide antibodies to UCP 3 were able to detect UCP 3 transiently expressed in mammalian COS cells (Fig. 3A) using 10^6 (lane 1) and 10^5 (lane 2) cells. No protein was detected in COS cells transfected with an empty vector (lane 3). As might be expected, the polyclonal peptide antibodies to UCP 1 could not detect anything in mammalian COS cells transiently expressing UCP 3 at either cell concentration (results not shown). Fig. 3B shows that the polyclonal peptide antibodies to UCP 3 were able to detect UCP 3 expressed in a stably transfected clone of mammalian COS cells without having to isolate mitochondria (lane 1). Anti-UCP 2 or anti-UCP 1 peptide antibodies did not detect this band (results not shown). No protein was detected in control cells (lane 2).

UCP 3 was also expressed in yeast cells (Fig. 3C). The polyclonal peptide antibodies to UCP 3, detected a ~ 33 kDa band in cell homogenate containing plasmid expressing UCP 3 (lane 1) but detected nothing in yeast control cell homogenate (lane 2).

Fig. 4A shows that our anti-UCP 3 antibody detected a 33 kDa band in yeast cells expressing UCP 3 (lane 1), in mitochondria isolated from skeletal muscle of non-starved rats (lane 4) (no particular muscle group selected), in mitochondria isolated from skeletal muscle of starved rats (lane 5) and in mitochondria from brown adipose tissue of cold-adapted rats (lane 7). No UCP 3 was detected in rat liver mitochondria (lane 2), rat heart mitochondria (lane 3), mitochondria from rat brain (lane 6), mitochondria from rat kidney (lane 8) or mitochondria from rat lung (lane 9). Although 100 μg of mitochondria were used in the blots in Fig. 4, the anti-UCP 3 peptide antibody will detect UCP 3 at total skeletal muscle mitochondrial protein concentrations of

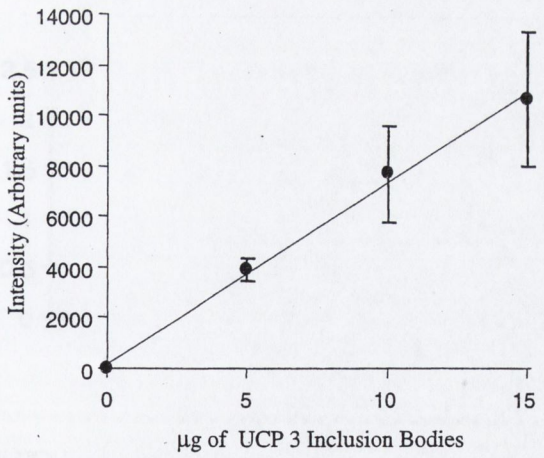


Fig. 2. UCP 3 immunoblot detection intensity as a function of amount of expressed UCP 3. Antibody to UCP 3, at a dilution of 1:5000, was used for *E. coli*-expressed inclusion bodies over a range of concentrations detected (0, 5, 10, and 15 μg). The relative abundance of UCP 3 was determined using densitometry. The band intensities of the exposed film were analysed using Scion Imaging. Intensity is measured in arbitrary units. The graph represents data for duplicate samples at each concentration (mean ± range). The line was fitted using regression analysis ($R = 0.999$).

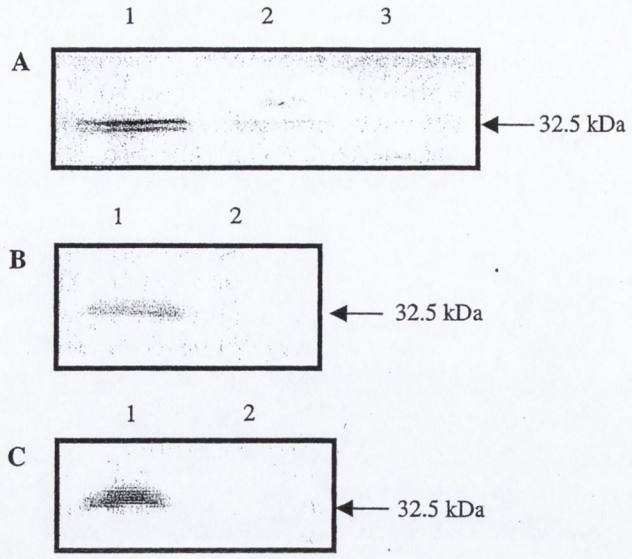


Fig. 3. Anti-UCP 3 peptide antibody detects UCP 3 expressed in mammalian and yeast cells. Blot A: lane 1, COS cells (~ 10^6 cells) transiently expressing UCP 3; lane 2, COS cells (~ 10^5 cells) transiently expressing UCP 3; lane 3, COS cells (~ 10^6 cells) containing empty vector. Blot B: lane 1, stable transfects of COS cells (~ 10^6 cells); lane 2, non-transfected COS cells (~ 10^6 cells). Blot C: lane 1, yeast cells (50 μg) transfected with pYES vector expressing UCP 3; lane 2, yeast cells (50 μg) transfected with pYES vector without UCP 3. Anti-UCP 3 peptide antibodies were used at a dilution of 1:5000. Only a single band was detected using the anti-UCP 3 antibody.

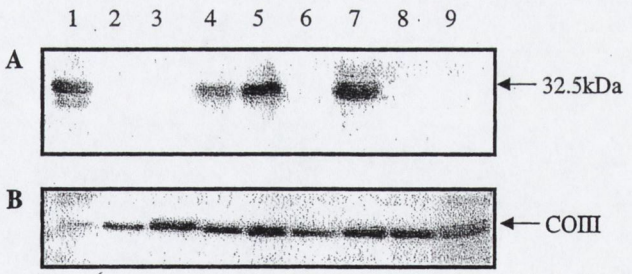


Fig. 4. Anti-UCP 3 peptide antibody detects UCP 3 in rat skeletal muscle mitochondria and brown adipose tissue. (A) UCP 3 peptide antibody and (B) antibody to cytochrome oxidase subunit III to: lane 1, yeast (~ 50 μg) expressing UCP 3; lane 2, liver mitochondria (100 μg) from non-starved rats; lane 3, heart mitochondria from non-starved rats (100 μg); lane 4, skeletal muscle mitochondria (100 μg) from non-starved rats; lane 5, skeletal muscle mitochondria (100 μg) from 48-h-starved rats; lane 6, rat mitochondria from whole brain (100 μg); lane 7, brown adipose tissue mitochondria from rats acclimated to the cold (8 ± 2 °C) for 8 weeks (100 μg); lane 8, rat kidney mitochondria (100 μg); lane 9, rat lung mitochondria (100 μg).

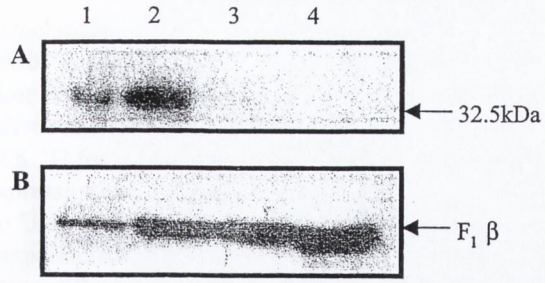


Fig. 5. Anti-UCP 3 peptide antibody detects UCP 3 in gastrocnemius mitochondria from wild-type but not UCP 3 knock-out mice. Immunoblots of UCP 3 peptide antibody (Blot A) and antibody to the β-subunit of the F_1-ATP synthase (Blot B): lane 1, yeast (~ 50 μg) expressing UCP 3; lane 2, gastrocnemius muscle mitochondria from C57BL/6J wild-type (WT) 6-week-old female mice; lane 3, gastrocnemius muscle mitochondria from C57BL/6J UCP 3 knock-out 6-week-old female mice; lane 4, rat liver mitochondria (100 μg).

50 μg from non-starved rats (results not shown). Fig. 4B gives a relative measure of the amount of mitochondrial protein loaded in each lane.

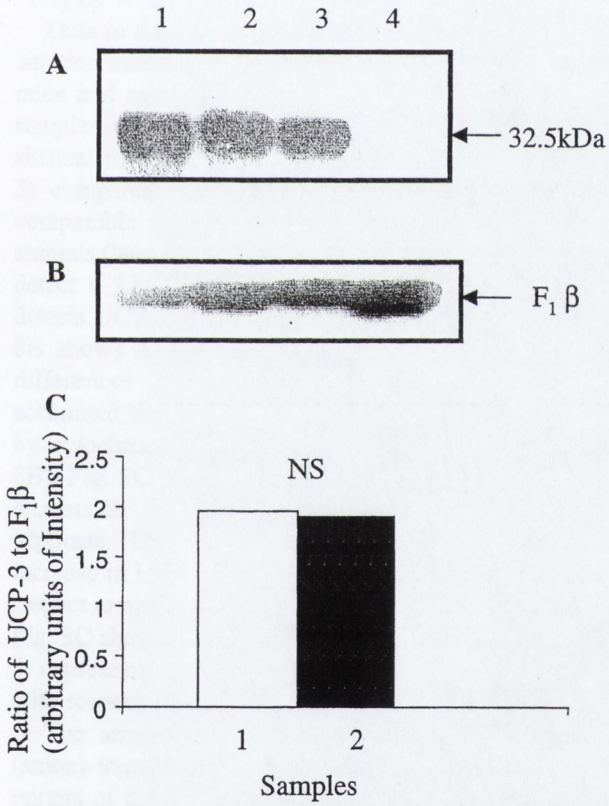


Fig. 6. Anti-UCP 3 peptide antibody detects equivalent amounts of UCP 3 in brown adipose tissue mitochondria from wild-type and UCP 1 knock-out mice. Immunoblots of UCP 3 peptide antibody (Blot A) and antibody to the β-subunit of the F_1-ATP synthase (Blot B): lane 1, yeast (~ 50 μg) expressing UCP 3; lane 2, brown adipose tissue mitochondria from C57BL/6J wild-type (WT) mice (100 μg); lane 3, brown adipose tissue mitochondria from C57BL/6J UCP 1 knock-out mice (100 μg); lane 4, mouse liver mitochondria (100 μg). The relative abundance of UCP 3 in brown adipose tissue mitochondria from UCP 1 wild-type (sample 1) and UCP 1 knock-out mice (sample 2) is given in panel C (mean ± S.E.M.). (NS, not significant).

The primary in vivo site of UCP 3 mRNA and protein expression is skeletal muscle. In Fig. 5, the peptide antibody to UCP 3 detects a 33 kDa protein in the yeast expressing UCP 3 (lane 1) and in mitochondria isolated from the gastrocnemius of wild-type mice (lane 2). However, no 33 kDa protein is detected in mitochondria isolated from the gastrocnemius of UCP 3 knock-out mice (lane 3) or in rat liver mitochondria (lane 4).

The most abundant UCP in brown adipose tissue would be UCP 1 [10]. Therefore, we wished to reassure ourselves that our UCP 3 antibody was not detecting native UCP 1. Fig. 6A and B demonstrate that the intensity of UCP 3 detection is not different when comparing brown adipose mitochondria from wild-type (lane 2) and UCP 1 knock-out mice (lane 3) and this is demonstrated graphically (Fig. 6C). As expected, UCP 3 was detected in yeast expressing UCP 3 (lane 1) but not in mouse liver mitochondria (lane 4).

The immunoblot in Fig. 7A shows that expression of UCP 3 protein in rat skeletal muscle is sensitive to temperature acclimation of the animal. As previously demonstrated, UCP 3 is detectable using the polyclonal anti-UCP 3 peptide antibody in yeast cells expressing UCP 3 (lane 1) and in mitochondria from non-starved rats housed at a constant 20 °C room temperature (lane 2). Skeletal muscle

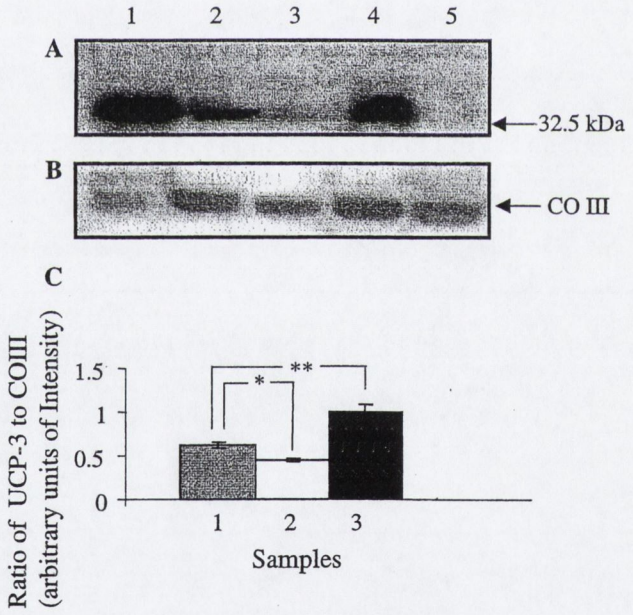


Fig. 7. The effect of temperature acclimation of rats on UCP 3 expression in skeletal muscle mitochondria. (A) UCP 3 peptide antibody and (B) antibody to cytochrome oxidase subunit III to: lane 1, yeast expressing UCP 3 (~ 50 μg); lane 2, skeletal muscle mitochondria from rats kept at 20 °C (100 μg); lane 3, skeletal muscle mitochondria (100 μg) from rats exposed to 30 ± 2 °C for 8 weeks; lane 4, skeletal muscle mitochondria from rats exposed to the cold (8 ± 2 °C) for 8 weeks (100 μg); lane 5, liver mitochondria (100 μg) from rats at 20 ± 2 °C for 8 weeks. (C) The ratio of UCP 3 protein expression to that of cytochrome oxidase, subunit 3 (COIII), for (sample 1) skeletal muscle mitochondria from rats acclimated to 20 °C, (sample 2) skeletal muscle mitochondria from rats acclimated to 30 °C and (sample 3) skeletal muscle mitochondria from rats acclimated to 8 °C. Data are from three separate preparations. $*P < 0.0047$ $**P < 0.0113$.

mitochondria isolated from rats acclimated to a temperature of 30 °C demonstrates a 3-fold decreased UCP 3 expression (lane 3) compared to those at 20 °C, while skeletal muscle mitochondria isolated from rats acclimated to a temperature of 8 °C for 8 weeks (lane 4) demonstrate increased UCP 3 expression compared to those at 20 °C (lane 2). As expected, no UCP 3 was detected in liver mitochondria (lane 5). The temperature acclimation experiments were repeated several times with similar results. Fig. 7B gives a relative measure of the amount of mitochondrial protein loaded in each lane and demonstrates that the amount of mitochondrial protein loaded in each lane cannot account for the differences observed in the amount of UCP 3 protein in lanes 1–4. In addition, there is a significant ($P<0.0047$; $n=3$) 1.4-fold decrease in UCP 3 expression observed in mitochondria isolated from skeletal muscle of rats acclimated to 30 °C when compared to mitochondria from rats acclimated to 20 °C and there is a significant ($P<0.0113$; $n=3$) 1.6-fold increase in UCP 3 expression observed in mitochondria isolated from skeletal muscle of rats acclimated to 8 °C when compared to mitochondria from rats acclimated to 20 °C (Fig. 7C).

Data in the literature show that thyroid hormone administration increases transcripts of UCP 3 in skeletal muscle of mice and rats [10]. Fig. 8A shows a representative set of samples where UCP 3 protein expression is increased in skeletal muscle mitochondria from hyperthyroid rats (lane 5) compared to euthyroid controls (lane 3), an increase comparable with that found in mitochondria from starved animals (lane 4). The peptide antibody to rat UCP 3 does not detect a 33 kDa band in liver mitochondria (lane 2) but detects UCP 3 expressed in yeast (lane 1) as expected. Fig. 8B shows a representative set of samples indicating that differences in UCP 3 expression (Fig. 8A) cannot be accounted for by differences in lane loading as indicated by cytochrome oxidase subunit 3 (COIII) detection (Fig. 8B). Fig. 8C gives the ratio of UCP 3 expression to COIII expression for four separate preparations determined in triplicate. The results show a 2.3-fold ($P<0.002$, $n=4$) increase in UCP 3 expression in the hyperthyroid state with respect to mitochondria from euthyroid animals. In addition, Fig. 8C shows a 2.8-fold ($P<0.001$, $n=4$) increase in UCP 3 expression in mitochondria from 48-h-starved animals with respect to mitochondria from euthyroid control rats.

The amino acid motif used to define mitochondrial (anion) transporters has also been found to occur in transporters of the peroxisomal membrane [25]. Thus it seemed possible that UCP 3 might also exist in peroxisomes. A subcellular fractionation of skeletal muscle from 48-h-starved rats was performed in order to separate peroxisomes (identified using anti-Pex14p) from mitochondria (identified using antibody to the anti-$F_1\alpha$ subunit of the ATP synthase) (Fig. 9). Pure rat liver peroxisomes (lanes 1 and 14) were also identified using the anti-Pex14p antibody (blot B) and despite a small amount of mitochondrial contamination (blot C), it can be seen that the UCP 3 antibody does not react

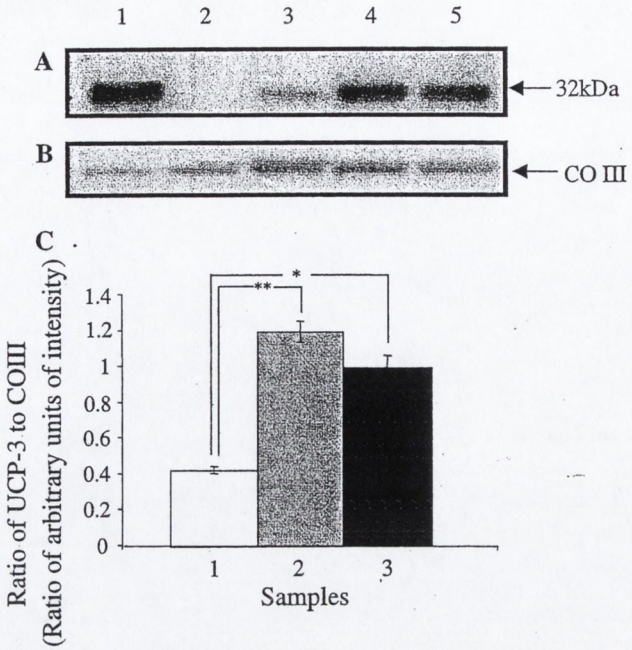


Fig. 8. The effect of thyroid status on UCP 3 expression levels in isolated mitochondria from rat skeletal muscle. Lane 1, 50 μg of mitochondria from yeast expressing UCP 3; lane 2, 100 mg of liver mitochondria from euthyroid rats; lane 3, 100 μg skeletal muscle from euthyroid rats; lane 4, 100 μg of skeletal muscle mitochondria from 48-h-starved rats; lane 5, 100 μg of skeletal muscle mitochondria from rats made hyperthyroid. Panel (A) is an immunoblot probed with a 1:5000 dilution of anti-UCP 3 peptide antibody. Panel (B) is an immunoblot probed with 1:1000 dilution of anti-COIII peptide antibody. Panel (C) shows the ratio of expression of UCP 3 to COIII for skeletal muscle mitochondria from euthyroid rats (sample 1), skeletal muscle mitochondria from 48-h-starved rats (sample 2) and skeletal muscle mitochondria from rats made hyperthyroid (sample 3). The graph represents data from four separate mitochondrial preparations each determined in triplicate. *$P<0.002$, **$P<0.001$.

with pure peroxisomes from rat liver (blot A). The UCP 3 antibody (blot A) detects protein in the supernatant from the $600\times g$ centrifugation of rat skeletal muscle homogenate (lanes 2 and 13), which is coincident with mitochondrial protein detection (blot C). However, peroxisomes are not detected in the $600\times g$ supernatant fraction from rat skeletal muscle homogenate (blot B). The pellet from the $600\times g$ centrifugation (cells and nuclei) (lanes 3 and 12) contains small amounts of UCP 3 (blot A), no peroxisomes (blot B) and some mitochondria (blot C). The resulting centrifugation of the $600\times g$ supernatant at $2350\times g$ resulted in a pellet termed heavy mitochondria (lanes 4 and 11) which contained a strong band for UCP 3 (blot A), a strong band for mitochondria (blot C) but no detection of peroxisomes (blot B). The supernatant from the centrifugation at $2350\times g$ was then centrifuged at $12{,}300\times g$ yielding a supernatant termed cytosolic and microsomal protein (lanes 5 and 10). A small amount of UCP 3 (blot A) and mitochondria (blot C) but no peroxisomes (blot B) were found in this fraction. The pellet from the $12{,}300\times g$ centrifugation contains a fraction termed light mitochondria (lanes 6 and 9). This fraction contains a lot of UCP 3 (blot

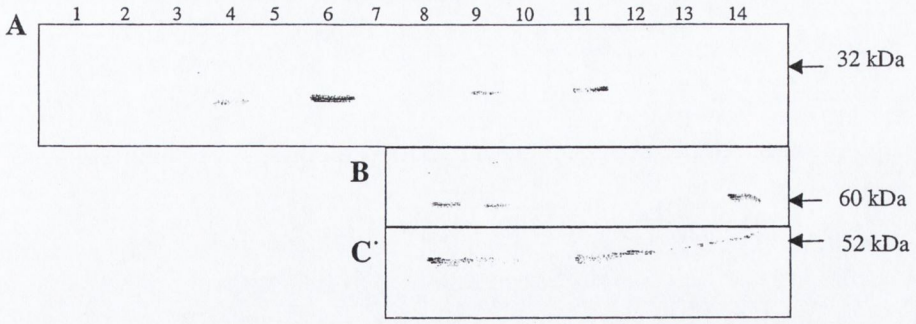


Fig. 9. Immunoblot of skeletal muscle tissue fractionation from 48-h-starved rats using anti-UCP 3 peptide antibody. Lanes 1 and 14, pure peroxisomes from rat liver. Lanes 5 and 10 cytosolic and microsomal proteins. Lanes 2 and 13, supernatant from a 600 × *g* centrifugation. Lanes 6 and 9, light mitochondria. Lanes 3 and 12, cells and nuclei. Lanes 7 and 8, pure peroxisomes. Lanes 4 and 11, heavy mitochondria. Blot A shows the distribution of UCP 3 using a 1:5000 dilution of anti-UCP 3 peptide antibody. Blot B shows the distribution of peroxisomes throughout the subcellular fractionation using a 1:1000 dilution of an antiserum directed to human Pex14p, a peroxisomal marker protein. Blot C shows the distribution of mitochondria throughout the subcellular fractionation using a 1:5000 dilution of a monoclonal antibody raised against the α-subunit of the mitochondrial F_1-ATPase.

A), a lot of peroxisomes (blot B) and a lot of mitochondria (blot C). Attempts to purify peroxisomes from this fraction using discontinuous Nycodenz density gradient centrifugation were not very successful. As shown in Fig. 9, no major enrichment of Pex14p can be observed in the organelles obtained after this procedure (compare lanes 8 and 9, panel B). However, a significant depletion (ca. 50%) of both $F_1\alpha$ and UCP 3 in these organelles can be easily observed (compare lanes 8 and 9 of panels A and C). Taken together, these data suggest (indicate) that UCP 3 (like $F_1\alpha$) is a mitochondrial protein (or is not a peroxisomal protein). An equivalent tissue fractionation was performed on rat liver from non-starved rats but no UCP 3 was detectable in any fractionation (results not shown).

Fig. 10A demonstrates that the anti-UCP 3 antibody can detect UCP 3 in whole muscle homogenates without the need to isolate mitochondria. Lane 1 demonstrates the anti-UCP 3 antibody detecting UCP 3 in yeast cells expressing UCP 3. UCP 3 could be detected in mouse EDL muscle (lanes 2 and 3) a predominantly glycolytic muscle and in mouse soleus muscle (lanes 4 and 5) a predominantly oxidative muscle. In Fig. 8B, antibodies to cytochrome *c* were used to give a relative measure of mitochondria density in the muscle groups (lanes 2–5). This particular antibody to cytochrome *c* works well on mammalian tissue but is known not to detect cytochrome *c* in yeast, as exemplified in lane 1.

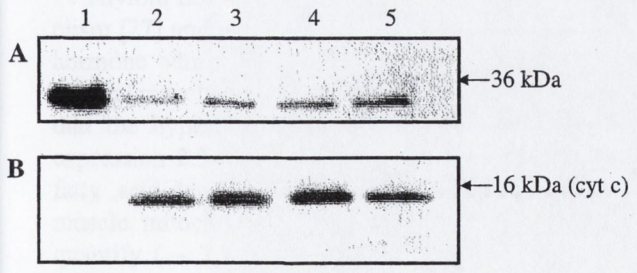


Fig. 10. UCP 3 detected in individual muscle groups (total muscle homogenates) from mouse. (A) 1:5000 dilution of UCP 3 antibody. (B) 1:5000 dilution of cytochrome *c* antibody. Lane 1, yeast expressing UCP 3. Lanes 2 and 3, extensor digitorum longus muscle (100 μg). Lanes 4 and 5, soleus muscle (75 μg). The cytochrome *c* antibody is known not to detect yeast cytochrome *c* (lane 1), but can detect mammalian cytochrome *c* (lanes 2–5).

Interestingly, the antibody to full-length UCP 1 detected a 33 kDa protein in cells transiently transfected with plasmid containing hUCP 3 and rat skeletal muscle mitochondria (results not shown).

4. Discussion

Although the function of UCP 3 is still contentious, clues to its physiological function can be obtained from observing their pattern of expression. As the protein is the functional entity, sensitive and discriminatory UCP detection antibodies are desirable. Northern blot analysis has shown that UCP 3 is expressed predominantly in skeletal muscle but also in brown adipose tissue [13]. However, limited immunodetection data exists for UCP 3. In this study, we demonstrate the selectivity and sensitivity of a peptide antibody to UCP 3.

Using uncoupling proteins purified from inclusion bodies expressed in *E. coli*, we showed that the anti-UCP 3 peptide antibody is selective for UCP 3 over UCP 2 and UCP 1 (Fig. 1) and that intensity of the UCP 3 bands correlates with abundance of UCP 3 protein (Fig. 2). In addition, the anti-UCP 1 antibody would also appear to be selective, detecting only *E. coli* expressed UCP 1 over UCP 2 and UCP 3 (Fig. 1).

The anti-UCP 3 peptide antibodies were also capable of detecting UCP 3 expressed in COS and yeast cells (Fig. 3). The same peptide antibody detected nothing in COS cells or yeast cells transfected with empty vector although both cell types contain mitochondria which themselves express transporters of an equivalent size. As might be

predicted, antibodies to the UCP 1 peptide antibody were unable to detect UCP 3 in these cells. But interestingly, antibodies to full-length UCP 1 were able to detect UCP 3 expressed in COS cells and in rat skeletal muscle mitochondria.

The pattern of the UCP 3 protein detection data (Fig. 4) are consistent with the UCP 3 mRNA detection data [10]. The antibody detected UCP 3 protein in skeletal muscle mitochondria and brown adipose tissue of rats. No UCP 3 was detected in mitochondria from tissues known to contain UCP 2 protein (kidney, brain and lungs) [11,26], nor was UCP 3 protein detected in heart or liver. The conclusion from these data is that the anti-UCP 3 antibody was detecting UCP 3 and not another member of the mitochondrial anion transporter family.

Our polyclonal UCP 3 peptide antibody can detect UCP 3 in mitochondria isolated from gastrocnemius of wild-type but not UCP 3 knock-out mice. Furthermore, in Fig. 6, it can be seen that the UCP 3 antibody detects UCP 3 to the same extent in brown adipose tissue of wild-type and UCP 1 knock-out mice. Taken together, it can be concluded that the anti-UCP 3 peptide antibody is selective for UCP 3 and is not detecting another member of the mitochondrial anion transport family.

Having established the discriminatory nature of the anti-UCP 3 peptide antibodies, we looked at the effect of long-term temperature acclimation on expression of native UCP 3. It was shown that cold-acclimated rats had increased (1.6-fold) UCP 3 expression compared to controls kept at room temperature (Fig. 7), whereas rats acclimated to 30 °C had decreased (1.4-fold) UCP 3. The suggestion is that UCP 3 protein expression is temperature-sensitive. These results again show our antibody to be sensitive to changes in the amount of UCP 3 expression per milligram of mitochondria. These results possibly contrast with those of Boss et al. [13] who showed that UCP 3 mRNA levels in mouse skeletal muscle do not increase with 48 h (short-term) cold exposure yet possibly compliment those of Simonyan et al. [15] who show that UCP 3 protein levels increase after 24 h (short-term) cold exposure.

Thyroid hormone is a major determinant of basal metabolism [27] and there are reports in the literature that thyroid hormone administration increases transcripts of UCP 3 in skeletal muscle of mice and rats [10]. In this study, we found that the hyperthyroid condition increases UCP 3 protein expression 2.3-fold (Fig. 8). The data are consistent with a fatty acid-dependent increase in proton leak in skeletal muscle mitochondria [28]. In addition, we were able to quantify (~ 2.8-fold) and confirm a previously observed [3] increase in UCP 3 protein expression in skeletal muscle mitochondria from starved rats. No increase in proton leak was observed in that instance [3]. In this context, as previously pointed out by others, one would expect to see an increase in UCP 3 levels upon starvation, as opposed to the observed decrease [3,13]. However, if UCP 3 has a role in fatty acid oxidation as suggested by Dulloo et al. [4], then increased UCP 3 expression on starvation would be consistent with that role.

Recent evidence demonstrated that transporters across the peroxisomal membrane also contain the 'mitochondrial' transporter motif [25]. However, subcellular fractionation of skeletal muscle from starved rats demonstrated that UCP 3 was exclusive to mitochondrial fractions (Fig. 9).

The sensitivity of the anti-UCP 3 antibody in detecting UCP 3 is further emphasized by the fact that there is no need to isolate mitochondria from muscle for UCP 3 to be detected. Our anti-UCP 3 antibody was able to detect UCP 3 associated with mitochondria in homogenates of mouse EDL muscle, a predominantly glycolytic muscle and mouse soleus muscle, a predominantly oxidative muscle. Although these particular results aren't novel, they confirm those of Giacobino [14] and compliment studies on glycolytic and oxidative muscle from humans [12].

In conclusion, our data shows that we have a peptide antibody raised to a rat UCP 3 sequence that is sensitive and discriminatory for UCP 3 over UCP 2, UCP 1 and other mitochondrial transporters. The UCP 3 peptide antibody also detects UCP 3 in isolated mitochondria from skeletal muscle and brown adipose tissue of rats and mice but not mitochondria isolated from UCP 3 knock-out mice. UCP 3 is also detectable using this antibody in whole mouse muscle homogenates without the need for isolation of mitochondria. We confirm and quantify the results of Cadenas et al. [3] that UCP 3 expression is increased in mitochondria isolated from starved animals. We show that UCP 3 expression is increased in cold-acclimated rats and decreased in rats acclimated to 30 °C, suggesting temperature-sensitive expression. In addition, we show that UCP 3 expression is thyroid-sensitive.

Acknowledgements

The Human Frontiers Science Programme Organisation Grant (RG307/98), Bioresearch Ireland. The clones for human UCP 1, 2 and 3 were a gift from Dr. Daniel Ricquier (Centre de Recherche sur l'Endocrinologie Moleculaire et le Developpement, Meudon, France). The clone for hamster (haUCP 1) was a gift from Prof. Martin Klingenberg, Institut für Physiologische Chemie der Universität München, Germany. The mitochondria isolated from gastrocnemius of wild-type and UCP 3 knock-out mice were a gift from Prof. Jean-Paul Giacobino, Département de Biochimie Médicale, Université of Genève, Switzerland. The mitochondria isolated from brown adipose tissue of wild-type and UCP 1 knock-out mice were a gift from Dr. Jan Nedergaard, the Wenner-Gren Institute, Stockholm University, Sweden. The antibodies to the β-subunit of the F_1 ATP synthase were a gift from Dr. Matt Harmey, Department of Botany, University College Dublin, Ireland.

References

[1] K.S. Echtay, E. Winkler, K. Frischmuth, M. Klingenberg, Uncoupling proteins 2 and 3 are highly active H(+) transporters and highly nucleotide sensitive when activated by coenzyme Q (ubiquinone), Proc. Natl. Acad. Sci. 98 (2001) 1416–1421.

[2] M. Jabůrek, M. Vařecha, R.E. Gimeno, M. Dembski, P. Ježek, M. Zhang, P. Burn, L.A. Tartaglia, K.D. Garlid, Transport function and regulation of mitochondrial uncoupling proteins 2 and 3, J. Biol. Chem. 274 (1999) 26003–26007.

[3] S. Cadenas, J.A. Buckingham, S. Samec, J. Seydoux, N. Din, A.G. Dulloo, M.D. Brand, UCP 2 and UCP 3 rise in starved rat skeletal muscle but mitochondrial proton conductance is unchanged, FEBS Lett. 462 (1999) 257–260.

[4] A.G. Dulloo, S. Samec, J. Seydoux, Uncoupling protein 3 and fatty acid metabolism, Biochem. Soc. Trans. 29 (2001) 785–790.

[5] K.S. Echtay, D. Roussel, J. St-Pierre, M.B. Jekabsons, S. Cadenas, J.A. Stuart, J.A. Harper, S.J. Roebuck, A. Morrison, S. Pickering, J.C. Clapham, M.D. Brand, Superoxide activates mitochondrial uncoupling proteins, Nature 415 (2002) 96–99.

[6] D. Arsenijevic, H. Onuma, C. Pecqueur, S. Raimbault, B.S. Manning, B. Miroux, E. Couplan, M.-C. Alves-Guerra, R. Surwit, F. Bouillaud, D. Richard, S. Collins, D. Ricquier, Disruption of the uncoupling protein-2 gene in mice reveals a role in immunity and reactive oxygen species production, Nat. Genet. 26 (2000) 435–439.

[7] A.J. Vidal-Puig, D. Grujic, C.-Y. Zhang, T. Hagen, O. Boss, Y. Ido, A. Szczepanik, J. Wade, V. Mootha, R. Cortright, D.M. Muoio, B.B. Lowell, Energy metabolism in uncoupling protein 3 gene knockout mice, J. Biol. Chem. 275 (2000) 16258–16266.

[8] D.-W. Gong, S. Monemdjou, O. Gavrilova, L.R. Leon, B. Marcus-Samuels, C.J. Chou, C. Everett, L.P. Kozak, C. Li, C. Deng, M.E. Harper, M.L. Reitman, Lack of obesity and normal response to fasting and thyroid hormone in mice lacking uncoupling protein-3, J. Biol. Chem. 275 (2000) 16251–16257.

[9] J.C. Clapham, J.R. Arch, H. Chapman, A. Haynes, C. Lister, G.B. Moore, V. Piercy, S.A. Carter, I. Lehner, S.A. Smith, L.J. Beeley, R.J. Godden, N. Herrity, M. Skehel, K.K. Changani, P.D. Hockings, D.G. Reid, S.M. Squires, J. Hatcher, B. Trail, J. Latcham, S. Rastan, A.J. Harper, S. Cadenas, J.A. Buckingham, M.D. Brand, A. Abuin, Mice overexpressing human uncoupling protein-3 in skeletal muscle are hyperphagic and lean, Nature 406 (2000) 415–418.

[10] D. Ricquier, F. Bouillaud, The uncoupling protein homologues: UCP1, UCP2, UCP 3, StUCP and AtUCP, Biochem. J. 345 (2000) 161–179.

[11] C. Pecqueur, M.-C. Alves-Guerra, C. Gelly, C. Levi-Meyrueis, E. Couplan, S. Collins, D. Ricquier, F. Bouillaud, B. Miroux, Uncoupling protein 2, in vivo distribution, induction upon oxidative stress, and evidence for translational regulation, J. Biol. Chem. 276 (2001) 8705–8712.

[12] M.K.C. Hesselink, H.A. Keizer, L.B. Borghouts, G. Schaart, C.F.P. Kornips, L.J. Slieker, K.W. Sloop, W.H.M. Saris, P. Schrauwen, Protein expression of UCP 3 differs between human type 1, type 2a, and type 2b fibers, FASEB J. 15 (2001) 1071–1073.

[13] O. Boss, S. Samec, F. Kühne, P. Bijlenga, F. Assimacopoulos-Jeannet, J. Seydoux, J.-P. Giacobino, P. Muzzin, Uncoupling protein-3 expression in rodent skeletal muscle is modulated by food intake but not by changes in environmental temperature, J. Biol. Chem. 273 (1998) 5–8.

[14] J.-P. Giacobino, Uncoupling protein 3 biological activity, Biochem. Soc. Trans. 29 (2001) 774–777.

[15] R.A. Simonyan, M. Jimenez, R.B. Ceddia, J.-P. Giacobino, P. Muzzin, V.P. Skulachev, Cold-induced changes in the energy coupling and the UCP 3 level in rodent skeletal muscles, Biochim. Biophys. Acta 1505 (2001) 271–279.

[16] J.B. Chappell, R.G. Hansford, in: G.D. Birnie (Ed.), Subcellular Components: Preparation and Fractionation, Butterworths, London, 1972, pp. 77–91.

[17] S.K. Bhattacharya, J.H. Thakar, P.L. Johnson, D.R. Shanklin, Isolation of skeletal muscle mitochondria from hamsters using an ionic medium containing ethylenediaminetetraacetic acid and nagarse, Anal. Biochem. 192 (1991) 344–349.

[18] F.U. Hartl, W.W. Just, A. Koster, H. Schimassek, Improved isolation and purification of rat liver peroxisomes by combined rate zonal and equilibrium density centrifugation, Arch. Biochem. Biophys. 237 (1985) 124–134.

[19] A.M.M. Gouveia, C. Reguenga, M.E.M. Oliveira, C. Eckerskorn, C. Sá-Miranda, J.E. Azevedo, Alkaline density gradient floatation of membranes: polypeptide composition of the mammalian peroxisomal membrane, Anal. Biochem. 724 (1999) 270–277.

[20] K.S. Echtay, Q. Liu, T. Caskey, E. Winkler, K. Frischmuth, M. Bienengraber, M. Klingenberg, Regulation of UCP 3 by nucleotides is different from regulation of UCP1, FEBS Lett. 450 (1999) 8–12.

[21] C.-Y. Zhang, T. Hagen, V.K. Mootha, L.J. Slieker, B.B. Lowell, Assessment of uncoupling activity of the human uncoupling protein 3 short form and three mutants of the uncoupling protein gene using a yeast heterologous expression system, FEBS Lett. 449 (1999) 129–134.

[22] M.A. Markwell, S.M. Haas, L.L. Bieber, N.E. Tolbert, A modification of the Lowry procedure to simplify protein determination in membrane and lipoprotein samples, Anal. Biochem. 87 (1978) 206–210.

[23] U.K. Laemmli, Cleavage of structural proteins during the assembly of the head of bacteriophage T4, Nature 227 (1970) 680–685.

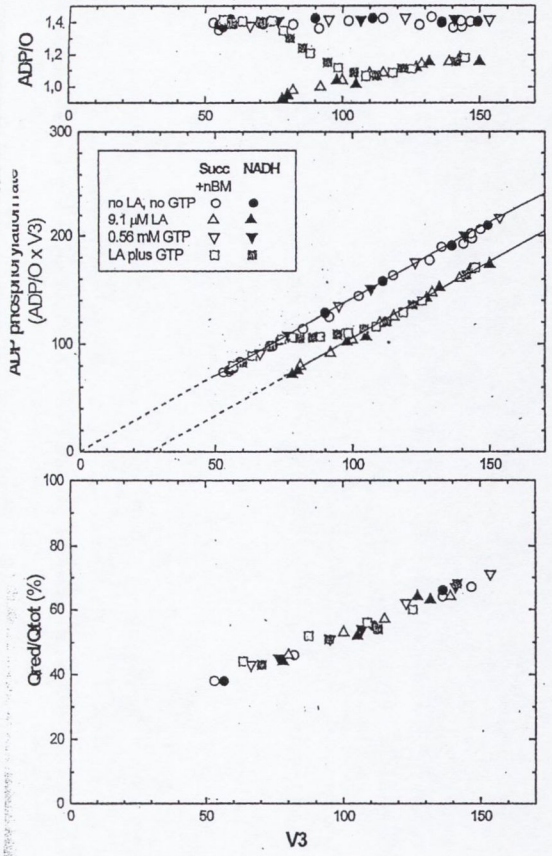
[24] C. Reguenga, M.E. Oliveira, A.M. Gouveia, C. Sá-Miranda, J.E. Azevedo, Characterization of the mammalian peroxisomal import machinery: Pex2p, Pex5p, Pex12p, and Pex14p are subunits of the same protein assembly, J. Biol. Chem. 276 (2001) 29935–29942.

[25] F.E. Weber, G. Minestrini, J.H. Dyer, M. Werder, D. Boffelli, S. Compassi, E. Wehrli, R.M. Thomas, G. Schulthes, H. Hauser, Molecular cloning of a peroxisomal Ca^{2+}-dependent member of the mitochondrial carrier superfamily, Proc. Natl. Acad. Sci. 94 (1997) 8509–8514.

[26] K.S. Echtay, M.D. Brand, Coenzyme Q induces GDP-sensitive proton conductance in kidney mitochondria, Biochem. Soc. Trans. 29 (2001) 763–768.

[27] M.D. Brand, L.-F. Chien, E.K. Ainscow, D.F.S. Rolfe, R.K. Porter, The causes and functions of mitochondrial proton leak, Biochim. Biophys. Acta 1187 (1994) 132–139.

[28] A. Lanni, L. Beneduce, A. Lombardi, M. Moreno, O. Boss, P. Muzzin, J.P. Giacobino, F. Goglia, Expression of uncoupling protein-3 and mitochondrial activity in the transition from hypothyroid to hyperthyroid state in rat skeletal muscle, FEBS Lett. 444 (1999) 250–254.



inhibitors, i.e., when the rate of quinol (QH_2)-oxidizing pathway is decreased. On the contrary, the progressive decrease of state 3 respiration by declining respiratory substrate availability (by succinate uptake limitation or by decreasing external NADH concentration), i.e., when the rate of Q-reducing pathways is decreased, progressively leads to a full inhibitory effect of GTP (Fig. 1). Moreover, in *A. castellanii* mitochondria isolated from cold-treated cells, where a higher uncoupling protein activity is observed, the inhibition of the LA- induced proton leak by GTP is revealed for the same low value of the Q reduction level. These results are in agreement with those obtained for rat skeletal muscle [2] and potato tuber [3] mitochondria.

Supported by the State Committee of Scientific Research (KBN, Poland) grant No. 0290/P04/2003/25.

1. Jarmuszkiewicz W, Swida A, Czarna M, Antos N, Sluse-Goffart CM, Sluse FE (2005) In phosphorylating Acanthamoeba castellanii mitochondria the sensitivity of uncoupling protein activity to GTP depends on the redox state of quinone. *J. Bioenerg. Biomembr.* 37: 97-107.
2. Jarmuszkiewicz W, Navet R, Alberici LC, Douette P, Sluse-Goffart C, Sluse FE, Vercesi AE (2004) Redox state of endogenous conenzyme Q modulates the inhibition of linoleic acid-induced uncoupling by guanosine triphosphate in isolated skeletal muscle mitochondria. *J. Bioenerg. Biomembr.* 36: 493-502.
3. Navet R, Douette P, Puttine-Marique F, Sluse-Goffart CM, Jarmuszkiewicz W, Sluse FE (2005) Regulation of uncoupling protein activity in phosphorylating potato tuber mitochondria. *FEBS Letters* 579: 4437-4442.

6-03. Elucidation of the mechanism of mitochondrial uncoupling protein function using a synthetic glycolipid (glucose-*O*-ω-palmitate).

SG Gouin[1], EP Breen[2], W Pilgrim[1], PV Murphy[1], Richard K Porter[2]

[1]*Centre Synthesis Chemical Biology, Dept. Chemistry, Conway Inst. Biomolecular Biomedical Research, Univ. College Dublin, Dublin 4;* [2]*Dept. Biochemistry, Trinity College Dublin, Dublin 2, Ireland. - rkporter@tcd.ie*

Mitochondrial uncoupling protein 1 (UCP1) is a 32kDa protein situated in the inner membrane of mitochondria from brown adipose tissue (BAT) of mammals and human infants. The protein uncouples ATP synthesis from oxygen consumption by catalysing the dissipation of the proton electrochemical gradient across the mitochondrial inner membrane. UCP1 function is the basis of non-shivering thermogenesis generated by BAT under conditions of cold exposure [1]. Long chain fatty acids, such as palmitate are known to increase proton leak through UCP1, however the mechanism is unclear. Two main models for the mechanism of action of UCP1 have been proposed: (i) that UCP1 acts as a proton conduit across the mitochondrial inner membrane and importantly that fatty acids act as cofactors/activators providing an additional carboxyl group at a key intra-membrane site [2] and (ii) that protonated fatty acids freely flip across the mitochondrial inner membrane and uncouple the mitochondria, and that UCP1 act as a 'flippase', translocating the fatty acid anions back across the bilayer leaflets of the inner membrane [3]. In order to distinguish between the two models, we synthesised glucose-*O*-ω-palmitate [4], which theoretically cannot flip across the inner membrane but can provide the carboxyl group for catalysis of proton translocation. Glucose-*O*-ω-palmitate was shown to be 93 % pure, by ^{1}H-NMR, and stable even under acidic conditions. We show that glucose-*O*-ω-palmitate cannot facilitate UCP1 function, either in liposomes containing reconstituted native UCP1 or in BAT mitochondria. Our data do not support the activation model but lend weight to the 'flippase' model of UCP function.

1. Cannon B, Nedergaard J (2004) Brown adipose tissue: function and physiological significance. *Physiol. Rev.* 84: 277-359.
2. Garlid KD, Jabůrek M, Ježek P, Vařecha P (2000) How do uncoupling proteins uncouple? *Biochim. Biophys. Acta* 1459: 383-389.
3. Klingenberg M, Huang S-G (1999) Structure and function of the uncoupling protein from brown adipose tissue. *Biochim. Biophys. Acta* 1415: 271-296.
4. Gouin SG, Pilgrim W, Porter RK, Murphy PV (2005) Synthesis of a glycolipid for studying mechanisms of mitochondrila uncoupling proteins. *Carb. Res.* 340: 1547-1552.

6-04. Functional and proteomic impacts of variations of the expression of uncoupling proteins in living cells.

P Douette, R Navet, Francis E Sluse

Lab. Bioenergetics, Dept. Life Sciences, Univ. Liège, Belgium. – f.sluse@ulg.ac.be

Uncoupling proteins (UCPs) are consumers of the proton electrochemical gradient built up by the respiratory chain and in this way they compete with the processes of oxidative phosphorylation, including ADP and inorganic phosphate import and ATP synthesis. In some way, their (over)expression in a cell can be considered as a stress at the energetic level. Indeed, in front of a decrease in the oxidative phosphorylation yield (uncoupling due to the presence and the activity of UCPs), cells do not remain neutral and react by promoting their general metabolic capacity. This concept will be illustrated at the functional and proteomic levels, by recombinant UCP1 from BAT expressed in a UCP-free cell i.e. the yeast *Saccharomyces cerevisiae.* UCP1 activity is stimulated by free fatty acids and inhibited by purine nucleotides. Here we investigated how active and regulated recombinant UCP1 expressed in yeast at ~1 and ~10 µg/mg of total mitochondrial proteins induced changes in the mitochondrial proteome and in oxygen free radicals production. Using two-dimensional differential in-gel electrophoresis (2D-DIGE), we found that most of the proteins involved in the response to ectopically expressed UCP1 are related namely to energy metabolism. We also quantified the cellular H_2O_2 release in the absence or in the presence of UCP1. Our results suggest that UCP1 has a dual influence on free radicals generation. On one side, FFA-activated UCP1 was able to decrease the superoxide anion production, demonstrating that a decrease in the generation of reactive oxygen species is an obligatory outcome of UCP1 activity even in a heterologous context. On the other side, an increase in UCP1 content was concomitant with an increase in the basal release of superoxide anion by mitochondria as a side-consequence of the overall increase in oxidative metabolism. Some pathologies and exogenous stresses that are accompanied by an increase in the expression of tissue-specific UCPs will also be analysed at the level of the mitochondrial proteome.

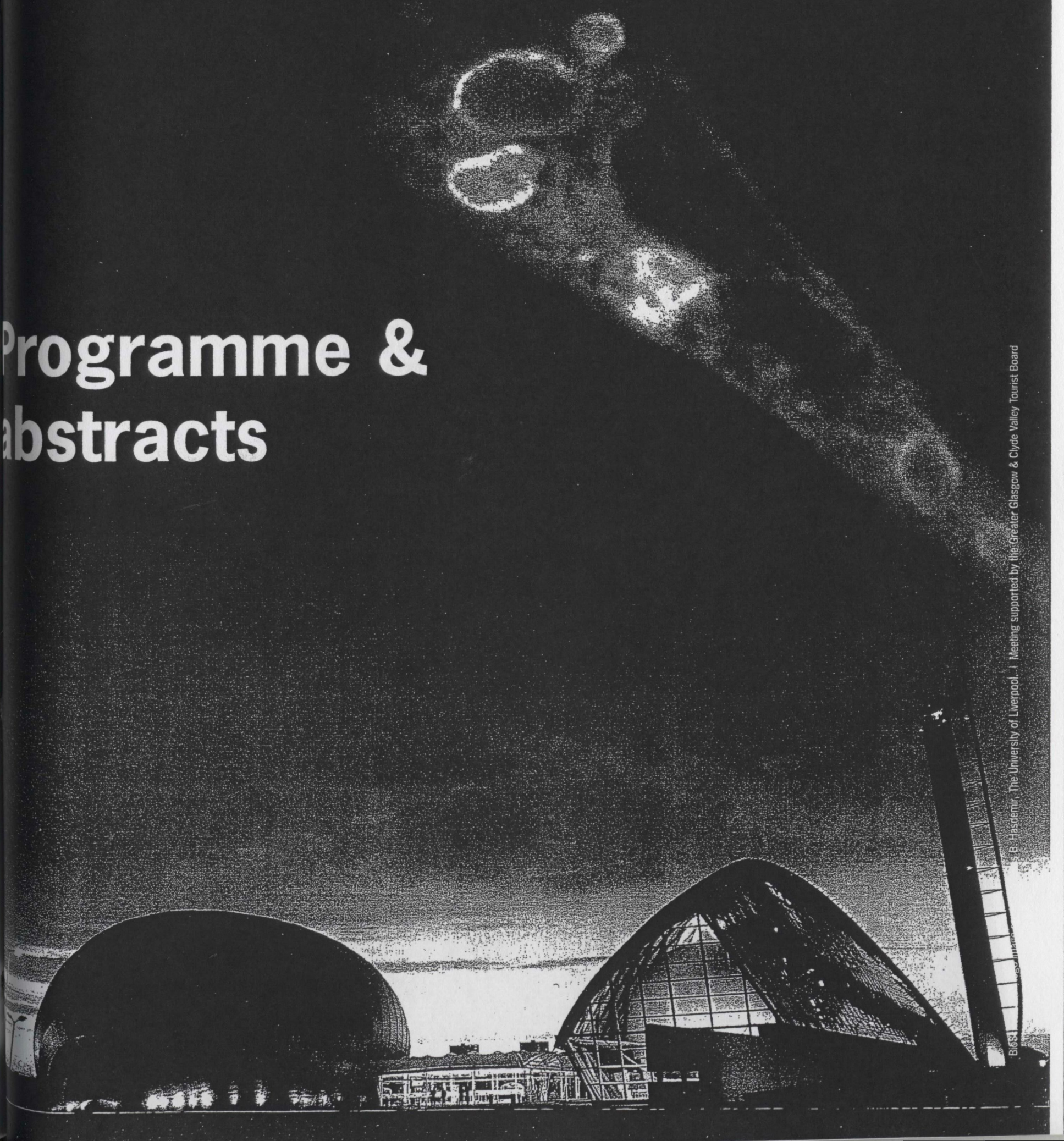
Supported by the *Biochemical Journal* – promoting international scientific communication

BioScience 2005

from genes to systems

17–21 July 2005 | SECC Glasgow, UK

Programme & abstracts



B.B. Hasdemir, The University of Liverpool... | Meeting supported by the Greater Glasgow & Clyde Valley Tourist Board

Bi6S

0588 *Elucidation* of the mechanism of mitochondrial uncoupling protein function using a synthetic glycolipid (Glucose-*O*-ω-palmitate).

[#]Sebastien G. Gouin, [¶]Eamon P. Breen, [#]Wayne Pilgrim, [#]Paul V. Murphy, [¶]Richard K. Porter

[#]*Centre for Synthesis and Chemical Biology, Department of Chemistry, Conway Institute of Biomolecular and Biomedical Research, University College Dublin and* [¶] *Department of Biochemistry, Trinity College Dublin.*

Mitochondrial uncoupling protein 1 (UCP 1) is a 32kDa protein situated in the inner membrane of mitochondria from brown adipose tissue (BAT) and is the basis of non-shivering thermogenesis. Two models for the mechanism of action of UCP 1 have been proposed: (i) UCP 1 acts as a proton conduit across the mitochondrial inner membrane and importantly that fatty acids act as cofactors/activators providing an additional carboxyl group at a key intra-membrane site and (ii) protonated fatty acids freely flip across the mitochondrial inner membrane and uncouple the mitochondria, and UCP 1 acts as a 'flippase', translocating the fatty acid anions back across the bilayer leaflets of the inner membrane. In order to distinguish between the two models, we synthesised glucose-*O*-ω-palmitate, which theoretically cannot flip across the inner membrane but can provide the carboxyl group for catalysis of proton translocation. We show that glucose-*O*-ω-palmitate cannot facilitate UCP 1 function, either in liposomes containing reconstituted native UCP 1 or in BAT mitochondria. Our data do not support the activation model of UCP function.

ELSEVIER

BIOCHIMICA ET BIOPHYSICA ACTA

BBA

BIOENERGETICS

Abstract book:
13th European Bioenergetics Conference

21 August – 26 August 2004
Pisa, Italy

p-3. Improved insulin sensitivity and reduced adipose tissue mass in relation to mitochondrial function, energy and PPAR activation

Berge[¤], K.J. Tronstad[¤], O.A. Gudbrandsen[¤], K. Berge[¤], H. Wergedahl[¤], H.J. Grav[‡]
berge@med.uib.no
titute of Medicine, Lipid Research Group, Haukeland University Hospital, N-5021 Bergen
titute for Nutrition Research, University of Oslo, N-0316 Oslo, Norway

Much data indicates that lowering of plasma triglyceride levels by hypolipidemic agents is caused by a shift in the liver ular metabolism, resulting in increased peroxisome proliferator activated receptor (PPAR) alpha regulated fatty acid abolism in mitochondria. Feeding rats with tetradecylthioacetic acid (TTA) leads to hypolipidemia, and our results suggest a TTA-induced increase in hepatic fatty acid oxidation and ketogenesis drains fatty acids from blood and extrahepatic ues and that this contributes significantly to the beneficial effects of TTA on fat mass accumulation and peripheral insulin sitivity (Berge, R.K., Skorve, J., Tronstad, K.J., et.al. (2002). Curr Opin Lipidol 13, 295–304.). These effects are associated h altered energy state parameters of the liver at the tissue-, cellular, and mitochondrial level (Grav, H.J., Tronstad, K.J., dbrandsen, O.A., et.al. (2003). J Biol Chem 278, 30525–30533). The hepatic phosphate potential, energy charge, and spiratory control coefficients were lowered, while rates of oxygen uptake and oxidation of pyridine nucleotide redox pairs re elevated. This is compatible with the mild uncoupling observed in liver mitochondria after TTA administration, nfirming increased proton conductance of the inner membrane. TTA treatment induced expression of hepatic uncoupling otein 2 (UCP-2) in rat as well as in wild type and PPAR alpha-deficient mice. However, it might be that TTA-mediated tivation of other PPARs (e.g., PPAR delta)can compensate for deficiency of PPAR alpha.

D p-4. Identification of a functioning mitochondrial uncoupling protein 1 in rat thymus

M. Carroll[#], L.R. Haines, T.W. Pearson, C. Brennan[#], E. Breen[#], R.K. Porter[#]
Department of Biochemistry, Trinity College Dublin, Dublin 2, Ireland and Department of Biochemistry and Microbiology, niversity of Victoria, Victoria, British Columbia, Canada
rrespondence to
-mail: rkporter@tcd.ie

We present evidence that rat thymus contains a functioning mitochondrial uncoupling protein (UCP 1). Using reverse nscriptase-polymerase chain reaction we showed that rat thymus contains RNA transcripts for UCP 1. Antipeptide ntibodies specific for UCP 1 detected UCP 1 protein in mitochondria isolated from thymus. No significant difference was ound in the amount of UCP 1 protein expressed in thymus tissue taken from fed or fasted animals. Evidence for functional CP 1 in rat thymus mitochondria was obtained by a comparative analysis with the kinetics of GDP binding in mitochondria om brown adipose tissue. Both tissues showed equivalent BMAX and KD values. In addition, a large component of the onphosphorylating oxygen consumption by thymus mitochondria was inhibited by GDP and subsequently stimulated by ddition of nanomolar concentrations of palmitate. We purified UCP 1 from thymus mitochondria by hydroxyapatite hromatography and identified the isolated protein by peptide mass mapping and tandem mass spectrometry using MALDI-TOF and LC-MS/MS, respectively. We conclude that rat thymus contains a functioning UCP 1 that has the capacity o regulate metabolic flux and production of reactive oxygen-containing molecules in the thymus.

Submitted to The Journal of Biological Chemistry

On the Mechanism of Mitochondrial Uncoupling Protein 1 Function

[#]Eamon P. Breen, [¶]Sebastien G. Gouin, [#]Andrew F. Murphy, [§]Lee R. Haines, [§]Angela M. Jackson, [§]Terry W. Pearson, [¶]Paul V. Murphy & [#]Richard K. Porter

From the [#]Department of Biochemistry, Trinity College Dublin, Dublin 2, Ireland, [¶]The Conway Institute, University College Dublin, Belfield, Dublin 4, Ireland and the [§]Department of Biochemistry and Microbiology, University of Victoria, Victoria, British Columbia, Canada.

Running Title: UCP 1 mechanism

Address correspondence to: Dr. Richard K. Porter, Tel. +353-1-608-1617 Fax +353-1-677-2400
email: rkporter@tcd.ie

Native uncoupling protein 1 (UCP 1) was purified from rat mitochondria by hydroxyapatite chromatography and identified by peptide mass mapping and tandem mass spectrometry. Native and expressed UCP 1 were reconstituted into liposomes and proton flux through UCP 1 was shown to be fatty acid dependent and GDP-sensitive. In order to investigate the mechanism of action of UCP 1, we determined whether hydrophilic modification of the ω-carbon of palmitate effected its transport function. We show that proton flux was greater through native UCP 1-containing proteoliposomes when facilitated by less hydrophilically modified palmitate (palmitate>ω-methoxypalmitate> ω-hydroxypalmitate with little or no proton flux due to glucose-*O*-ω-palmitate or undecanesulfonate). We show that non-proton dependent charge transfer was greater when facilitated by less hydrophilically modified palmitate (palmitate/undecanesulfonate>ω-methoxypalmitate> ω-hydroxypalmitate, with no non-proton dependent charge transfer flux due to glucose-*O*-ω-palmitate). We show that the GDP-inhibitable oxygen consumption rate in brown adipose tissue mitochondria was reversed by palmitate (as expected), but not by glucose-*O*-ω-palmitate. Our data are consistent with the model that UCP 1 flips long chain fatty acid anions and contradict the "cofactor" model of UCP 1 function.

In brown adipose tissue (BAT[1]), dissipation of the proton electrochemical gradient (Δp) across the mitochondrial inner membrane by uncoupling protein 1 (UCP 1; also known as UCP and thermogenin) is the molecular basis of non-shivering thermogenesis in mammals, including human infants (1-5). Consequently, UCP 1 acts as a major regulator of metabolic flux in BAT and as a heat regulator in the whole animal. UCP 1 has also recently been found in thymus tissue of rats and mice (6) where it's physiological function is still a matter of investigation.

Despite our knowledge about the physiological function of UCP 1 in BAT, the mechanism of its uncoupling action is

still unclear (7-9). What is clear is that there is a long chain fatty acid requirement for uncoupling activity and that this activity is purine nucleotide sensitive. Two models have been proposed for the fatty acid dependent mechanism of UCP 1 function. The first proposes that UCP 1 acts as a proton conduit across the mitochondrial inner membrane and, importantly, that fatty acids act as cofactors/activators providing an additional carboxyl moiety at a key intra-membrane site, thus enhancing the rate of proton movement (8,10,11). The second model, proposes a two step event, whereby the protonated fatty acids freely flip across the mitochondrial inner membrane, independently of UCP 1; protons dissociate from the fatty acids into the matrix and the resulting fatty acid anions are flipped back across (non-proton dependent charge transfer) the inner membrane by UCP 1 (7,9,12). The strongest evidence for this "flippase" model comes from the observations that undecanesulfonate, which has a pK ~2, and is thus predominantly an anion at neutral pH, can be flipped by UCP 1 (13-15). The key piece of evidence for the cofactor/activation model comes from an unsubstantiated report, cited in two reviews, that the "unflippable" glycolipid, glucose-*O*-ω-palmitate, activates native reconstituted UCP 1 (8,10). However, no original data were ever presented to substantiate this report nor has the synthesis, purity or stability of the resulting glycolipid ever been reported.

In this study we set out to re-investigate the cofactor/activation model, by using a long chain fatty acid (palmitate) with hydrophilic additions to the ω-carbon. Two of the glycolipids were synthesis *de novo*, namely the aforementioned glucose-*O*-ω-palmitate (16), and methoxy-*O*-ω-palmitate, the synthesis of which is described in a supplemental figure to this manuscript. If the "cofactor/activator" model is correct, modification to the ω-carbon of palmitate should not impair access of the α-carbon carboxyl to the intra-membrane site of UCP 1. The "flippase"model would predict that such modifications should hinder or at least not facilitate proton flux (and charge transfer flux) in UCP 1 containing liposomes, nor should they affect uncoupling activity in UCP 1 containing mitochondria, as such fatty acids are less likely to flip or be flipped across the mitochondrial inner membrane.

EXPERIMENTAL PROCEDURES

Tissue sources and isolation of mitochondria

Wistar rats (*Rattus norvegicus*; 180-200 g) were provided by the BioResources Unit at Trinity College, Dublin. All rats were housed at room temperature and fed *ad libitum*. Mitochondria from brown adipose issue and whole thymus, were isolated by homogenisation followed by differential centrifugation according to the procedure of Chappell & Hansford (17). Mitochondrial protein concentrations were determined by the reduction of Folins-Ciocalteau phosphomolybdic-phosphotungstic reagent according to the method of Markwell *et al.* (18).

Polyacrylamide gel electrophoresis

One-dimensional sodium dodecyl sulfate-polyacrylamide gel electrophoresis (SDS-PAGE) under reducing conditions was used to examine UCP 1 after purification by hydroxyapatite chromatography (6,19). Proteins were detected by staining gels with colloidal Coomassie Brilliant Blue G-250 (20). This stain is very sensitive (can detect 8-10 ng of protein in a single gel band or spot) and is compatible with the post-staining processing required for mass spectrometry (see below).

Oxygen consumption by non-phosphorylating brown adipose tissue mitochondria

Oxygen consumption rates were measured using an Oxygraph Respirometer (Oroboros™, Innsbrück, Austria) as previously described (6,21). Mitochondria (1 mg/ml) were incubated at 37 °C in medium containing 120 mM KCl, 5 mM HEPES- KOH, pH 7.4, 1 mM EGTA, 16 μM fatty-acid free BSA, 5 μM atractyloside, 5 μM rotenone and 1 μg/ml oligomycin. Non-phosphorylating (state 4) oxygen consumption rates were measured as the steady-state rates achieved on addition of 7.5 mM succinate (succinate-KOH, pH, 7.4). The sensitivity of this state 4 oxygen consumption rate to GDP (500 μM) was then determined. The sensitivity of the resulting oxygen consumption rate to palmitate or glucose-*O*-ω-palmitate (in ethanol) (64 μM)(~40 nM free) was then determined. Finally, the mitochondrial uncoupler 2,4-dinitrophenol (DNP; 4 μM) was added to the chamber to determine the maximum oxygen consumption rate attainable due to uncoupling. The Oxygraph Respirometer was calibrated according to the procedure of Reynafarje *et al.* (22) assuming that 406 nmoles of oxygen atoms were dissolved in 1 ml of ionic incubation medium at 37 °C.

Purification of UCP 1 from rat mitochondria

Purification of UCP 1 was performed using an hydroxyapatite (HTP) column chromatography procedure as described by Lin & Klingenberg (23) with slight modification. Intact thymus or BAT mitochondria (8-10 mg) suspended in STE buffer, (250 mM sucrose, 5 mM Trizma-base, 2 mM EGTA, pH 7.4) were centrifuged at 22,600 x g for 10 min at 4 °C. The mitochondrial pellet was solubilised in 13% (v/v) pentaethylene glycol monooctyl ether (C_8E_5) in STE (total volume ~500 μl) and incubated on ice for 10 min prior to loading the solubilised mitochondrial proteins onto a HTP column. The column was prepared by soaking 0.34 g of HTP in 10 ml of STE buffer, pH 7.4, at 4 °C, for 6 hours prior to pouring it into a 1 ml column (BioRad; diameter 1cm, length 6 cm). The soaking solution was removed from the column by centrifugation at 800 x g for 2 min at room temperature immediately prior to loading of the mitochondrial proteins. The HTP column, containing the solubilised mitochondrial proteins, was incubated at room temperature for 10 min (to denature the adenine nucleotide carrier) followed by 25 min incubation at 4 °C. The column was then centrifuged at 800 x g for 2 min to remove the HTP eluate (UCP 1-enriched fraction), leaving behind the unwanted bound proteins. The protein concentration of the HTP eluate was determined (18) and the C_8E_5 detergent was removed using a Biobead (BioRad) column. The Biobead column was prepared by placing 2 ml of Biobeads (suspended in distilled/deionised H_2O) into a 2 ml syringe barrel and allowing them to settle. The H_2O was removed from the Biobeads by centrifugation at 800 x g for 2 min. The Biobeads were equilibrated in ~2 ml of STE buffer (pH 7.4) for 30 min prior to use and were further centrifuged at 800 x g for 2 minutes to remove excess STE buffer. The HTP eluate was loaded onto the Biobeads with gentle mixing and incubated for two-hours at 4 °C with periodic slight agitation using a vortex-type mixer. The Biobead column was centrifuged at 800 x g for 2 min and the protein eluate was collected. The protein concentration of this elute was determined and approximately 5-10 μg of protein were analyzed by SDS-PAGE and colloidal Coomassie Brilliant Blue G-250 staining.

Expression of human UCP 1 in E. coli

Human UCP 1 open reading frames were amplified by PCR and inserted into the pET 21d vector (Novagen). Plasmids were transformed into *E. coli* strain Rosetta pLysS (Novagen). Transformation

and expression were undertaken as described in Cunningham et al. (2003). The transformed colony was amplified overnight at 37 ^{0}C and diluted to an OD_{600} = 0.4-0.8. Expression was induced with isopropyl-β-D-thiogalactopyranoside at 30 ^{0}C for 2h. Cells were harvested at 10,000 x g and bacterial pellets frozen at –80 ^{0}C.

Extraction of huUCP 1 from inclusion bodies

Extraction of huUCP 1 from *E. coli* inclusion bodies was performed essentially as described by Jabůrek and Garlid (24). The pelleted inclusion bodies (about 2 mg of protein) were washed two times in sodium salts of 0.15 M phosphate, 25 mM EDTA, 10 mM dithithretiol, 0.2% sodium laurylsarcosinate (sarcosyl), pH 7.8, and centrifuged at 14,000 x g for 10 min. The resulting pellet was resuspended in 4 ml of 50 mM CAPS, 25 mM dithiothretiol, 2 mM phenylmethylsulfonyl fluoride, 10% glycerol, 2% sarcosyl, pH 10.0 adjusted by the addition of Tris base. After 30 min incubation at room temperature, the extract was centrifuged at 14,000 x g for 10 min to remove unsolubilized particles. The supernatant was diluted rapidly in 6 ml of 10% glycerol, 1% Triton X-114, and 1mM ATP. This mixture was incubated for 2 h at 4 ^{0}C with mixing. To remove sarcosyl, the extract was either dialyzed or passed through a 2.5 ml Dowex 11A8 column (flow rate 0.5 ml/min). The collected protein was supplemented with 5 mg/ml phosphatidylcholine and 1 mM ATP. After 2h incubation at 4 ^{0}C, the extract was concentrated two-fold in a Millipore Ultrafree-15 centrifuge filter device. 1ml aliquots were stored at –20 ^{0}C.

Reconstitution of UCP 1

Reconstitution of native and expressed protein was performed essentially as described in Jabůrek and Garlid (24). Essentially, phospholipids (asolecithin supplemented with 5% cardiolipin, or 100% phophatidycholine) were dried under nitrogen and stored under vacuum overnight. The dried phospholipids were solubilized with detergent, pentaethylene glycol monooctyl ether (C_8E_5), to which protein and fluorescent probe were added. The protein/lipid mixture was incubated with Bio-Beads SM-2 (Bio-Rad) to remove detergent and form vesicles. The vesicles were passed through a Sephadex G-50-300 column to remove external probe.

Fluorescent measurements of ion fluxes

Ion flux in proteoliposomes was measured using a Perkin-Elmer LS 55 spectrofluorimeter essentially as described by Jabůrek et al. (14). Measurements of H^+ fluxes were obtained from changes in 6-methoxy-N-(3-sulfopropyl)quinolinium (SPQ) fluorescence due to quenching by the anion of TES. Measurement of K^+ fluxes, reflecting the movement of ion charge across the liposome membrane, were obtained from changes in K^+-binding benzofuran isophthalate (PBFI) fluorescence. Internal and external media contained K^+ or TEA^+ salts of TES buffer (30 mM), SO_4 (80 mM) and EDTA (1mM), pH 7.2. Each proteoliposome preparation was individually calibrated from fluorescent probe response and the internal volume was estimated from the volume of distribution of the fluorescent probe.

Sample preparation for mass spectrometry

A 30-33 kDa colloidal Coomassie Brilliant Blue G-250 stained protein band was excised from a 1-D SDS-PAGE gel (Figure 1A) and was transferred to a 1.5 ml Eppendorf microcentrifuge tube (previously autoclaved and rinsed with 50% HPLC grade methanol to remove any contaminants) containing 100 µl of 20% (w/v) ammonium sulphate. The excised band was de-stained for two days in

several washes of 50% (v/v) methanol/5% (v/v) acetic acid), dehydrated with acetonitrile, reduced for 30 min with 10 mM dithiothreitol at 56 °C and alkylated for 30 min with 100 mM iodoacetamide at 45 °C as described previously (32). The carboxyamidomethylated protein band was digested overnight at 37 °C with 40 µl of 20 ng/µl sequencing grade, modified porcine trypsin according to the manufacturer's directions (Promega, Madison, WI). Peptides were extracted from the gel using a series of elutions with 10% (v/v) formic acid. The resulting eluate pool was reduced to a final volume of 20 µl in a Speed Vac Concentrator (Savant, Hicksville, NY) and processed for mass spectrometry.

Peptide mass mapping and sequencing

Peptide mass mapping and sequence determination was performed using matrix-assisted laser desorption ionization time of flight, time of flight (MALDI TOF/TOF) mass spectrometry. A 5 µL amount of the trypsin-digested sample was desalted and concentrated using a ZipTip C18 (C18 resin; P10, Millipore Corporation, Bedford, MA). The peptide mixture was eluted from the ZipTip with 1 µL of 50% acetonitrile, 0.1% TFA and spotted onto a stainless steel Opti-TOF sample plate (Applied Biosystems, Foster City, CA). The sample was dried and overlaid with 1 µL alpha-cyano-4-hydroxycinnamic acid based MALDI TOF/TOF matrix (Sigma Chemical Co. St. Louis, MO). An Applied Biosystems/MDS SCIEX 4800 mass spectrometer (Applied Biosystems/MDS SCIEX, Foster City, CA) running in delayed extraction, positive reflector mode was used to acquire both MS and MS/MS spectra. Selected peptide masses were submitted to two online search algorithms that use peptide masses to identify proteins from primary sequence databases: Mascot (Matrix Science, London, UK: http://www.matrixscience.com/) and Aldente (ExPASY: Swiss Institute of Bioinformatics, Basel, Switzerland: http://www.expasy.org/tools/aldente/). The three most intense peptides present in the peptide mass fingerprint spectrum were fragmented to produce product ion spectra for *de novo* sequencing. The *de novo* peptide sequences were submitted to Mascot (Matrix Science, London, UK: http://www.matrixscience.com/) for assignment of protein identities.

Synthesis of glucose -O-ω-palmitate and ω–methoxy-palmitate.

The detail experimental procedures for the synthesis of glucose-*O*-ω-palmitate are reported in Gouin et al. (16). Glucose-*O*-ω-palmitate is stable under ionic conditions and at neutral pH and was shown by NMR quantitation to be >93% pure. The pathway for the synthesis of methoxy-ω-palmitate is shown in supplementary figure 1 (Scheme 1).

RESULTS

Hydoxyapatite chromatography procedures previously used for purification of UCP 1 from hamster BAT (23) were adapted for rat BAT and identification of the purified protein was determined using mass spectrometry. After 1-D SDS-PAGE and staining with colloidal Coomassie Blue G-250, a distinct broad band of approximately 30-33 kDa (the expected mass of UCP 1) was observed (Figure 1A). The stained band was excised using a scalpel and tryptic peptides prepared for analysis. Seven peptides were identified using MALDI-TOF/TOF MS by peptide mass mapping by comparison with previous UCP 1 MS data (6) or by TOF/TOF analysis of the three most intense peptides in the peptide mass fingerprint spectrum.(Fig. 1B). With the latter, BLAST searching of nonredundant

databases with the peptide sequences unequivocally identified mitochondrial brown fat uncoupling protein 1 (UCP 1) from *Rattus norvegicus*.

Native UCP 1 from rat and recombinant, expressed huUCP 1 were reconstituted in liposomes and shown to be functional. This is illustrated in Figure 2 which shows the change in proton concentration (as a result of changes in SPQ fluorescence inside the proteoliposomes) as a function of time. Each trace represents a different experiment. Proton flux was measured as the initial rate of change of proton concentration following addition of valinomycin. Figure 2 shows a sample trace of proton flux data for liposomes containing native BAT UCP 1, native thymus UCP 1 and expressed human UCP 1, in the presence of laurate.

In order to re-investigate the cofactor/activation model of UCP 1 activity, we first used proteoliposomes containing native UCP 1 from rat brown adipose tissue and looked at the effect of modifying the ω-carbon of palmitate on UCP 1 activation. Theoretically, modifications to palmitate at the ω-carbon should make no difference to proton flux measurements in UCP 1 containing proteoliposomes when compared to palmitate alone, as these modification should not hinder access of the α-carbon carboxyl to the intra-membrane site. The structures of fatty acids used in this study (undecanesulfonate, palmitate, ω-hydroxylpalmitate, ω-methoxypalmitate and glucose-*O*-ω-palmitate) are presented in Figure 3.

Figure 4A shows sample traces of proton flux data for palmitate, glucose-*O*-ω-palmitate and undecanesulfonate in the presence and absence of GDP, for liposomes containing native rat BAT UCP 1. Figure 4B shows sample traces of proton flux data for palmitate, ω-hydroxylpalmitate and ω-methoxypalmitate in the presence and absence of GDP, for liposomes containing native rat UCP 1. Figure 4C summarises proton flux data (μmoles H^+/min/mg), in bar-chart format, for vesicles containing reconstituted native rat UCP 1 in the presence of the fatty acid (analogues). The rates for palmitate (9.9 ± 0.7) were greater than those for ω-methoxypalmitate (7.6 ± 1.3), ω-hyroxypalmitate (3.5 ± 1.0), glucose-*O*-ω-palmitate (0.7 ± 0.1) and undecanesulfonate (0.03 ± 0.03). There was a significant difference in the rate of proton flux in the presence of palmitate compared with glucose-*O*-ω-palmitate ($p = 0.0001$). The rates in the presence of GDP are also shown. As expected, there was a significant difference ($p = 0.001$) in the rate of proton flux when comparing palmitate in the presence and absence of GDP. There was no significant difference in the rate of proton flux when comparing glucose-*O*-ω-palmitate in the presence and absence of GDP.

Non-proton dependent charge transfer assay is used as a measure of "flippase" activity and was also investigated. Figure 5A shows a typical trace showing the change in concentration of K^+ (as measured by a change in PBFI fluorescence inside the proteoliposomes) as a function of time for palmitate, undecanesulfonate and glucose-*O*-ω-palmitate. Each trace represents a different experiment and flux was measured as the initial rate of change of K^+ concentration, in the presence of fatty acid (analogues), following addition of valinomycin. Figure 5B shows collated data for non-proton dependent charge transfer flux (μmoles K^+/min/mg) for vesicles containing reconstituted native rat BAT UCP 1 in the presence of fatty acid analogues. The rates for palmitate (34.8 ±

3.9) were greater than those for undecanesulfonate (30.7 ± 1.4), ω-methoxypalmitate (27 ± 10), ω-hyroxypalmitate (14.4 ± 1.8) and glucose-*O*-ω-palmitate (3.0 ± 1.8). There was a significant difference in the rate of non-proton dependent charge transfer flux in the presence of palmitate compared with glucose-*O*-ω-palmitate ($p = 0.0012$). The rates in the presence of GDP are also shown. As expected, there was a significant difference in the rate of charge transfer flux for palmitate in the presence and absence of GDP ($p = 0.0012$) and undecanesulfonate in the presence and absence of GDP ($p = 0.0001$). There was no significant difference in the rate of charge transfer flux for glucose-*O*-ω-palmitate in the presence and absence of GDP.

The dependency of UCP 1 function on long chain fatty acids can also be observed in BAT mitochondria. Figure 6A shows that the non-phosphorylating oxygen consumption rates (state 4; expressed as picomoles of dioxygen atoms per minute per mg mitochondrial protein) of BAT mitochondria is inhibited by addition of 500 μM GDP (from 1512 ± 48 to 1078 ± 52). The oxygen consumption rate was subsequently and significantly stimulated by nanomolar amounts of palmitate (~40 nM free fatty acid) to 1535 ± 92 ($p = 0.0003$). These rates are close to the maximal uncoupled rate of 1553 ± 92 induced by the addition of 2,4-dinitrophenol (DNP). In contrast, figure 6B shows that non-phosphorylating oxygen consumption rate (1486 ± 63), inhibited by GDP (1057 ± 63) is not stimulated (978 ± 47, $p = 0.332$) by addition of glucose–*O*-ω-palmitate. The lack of activation by glucose–*O*-ω-is not a result of mitochondrial dysfunction as a maximal uncoupled rate of (1339 ± 73) can be induced by the addition of DNP.

DISCUSSION

We have purified native UCP 1 from rat BAT mitochondria and have confirmed the identity of the protein by mass spectrometry. Gel electrophoresis of the isolated material followed by staining with colloidal Coomassie Brilliant Blue, revealed a single broad 30-33 kDa band, in correspondence with the predicted molecular mass of UCP 1 (33,458 Daltons). MALDI-TOF mass spectrometry results revealed uncoupling protein 1 from rat to be present in the purified fraction. The mass spectrometry results for UCP 1 from rat brown adipose are consistent with those presented by us for UCP 1 purified from rat thymus mitochondria (6). UCP 2 or UCP 3 protein, both of which are known to be expressed in brown adipose tissue, (6,19,25,26) were not detected.

Although hamster BAT is the usual source of native UCP 1 for reconstitution studies (8,10,13-15), .we showed here, that native BAT UCP 1, native thymus UCP 1 and expressed recombinant human UCP 1 can be reconstituted to give a functionally competent transporter. Our success in expressing human UCP 1 is probably due to the selection of a strain of *E. coli* (Rosetta), which preferentially uses human codons.

In order to re-investigate the evidence for the cofactor/activation model of UCP 1 function, we used liposomes containing native rat BAT UCP 1, the principle behind the experiments being that the hydrophilic modifications at the ω-carbon of palmitate should have no effect on the ability of the palmitate α-carboxyl to "activate" UCP 1 if the cofactor model is correct. On the other hand, such modifications should impede or at least should not facilitate proton and/or charge transfer in the "flippase" model. Of the fatty acids used, undecanesulfonate has a low pK (~2) and thus exists predominantly

in the ionized state at neutral pH. It has been shown previously to facilitate charge transfer but not proton leak in reconstituted systems (27). Palmitate is known to facilitate UCP 1 function in mitochondria and in artificially reconstituted systems (6,10,27). In addition, ω-hydroxypalmitate been used previously in reconstituted systems and has been shown to partially facilitate proton flux and charge transfer (10,27). We also synthesized two compounds: glucose-*O*-ω-palmitate (16) and ω-methoxypalmitate, the former having a large hydrophilic moiety at the ω-end of the fatty acid, the latter more hydrophobic than that of the hydroxyl group.

Our results clearly showed that the initial rate of change in proton concentration with time, in proteoliposomes containing native UCP 1, was greatest for palmitate, less for ω-methoxypalmitate and less again for ω-hydroxypalmitate, glucose-*O*-ω-palmitate and undecanesulfonate. The collated data showed that the increased proton flux was coincident with the hydrophobic nature of the modification to the ω-carbon of palmitate. tThis was also supported by the complete absence of transport as predicted for undecanesulfonate. That is to say, no modification of the ω-carbon of palmitate yielded faster rates than the methoxy group modification, which was faster than the hydroxyl group modification, which in turn was faster than that obtained with glucose-*O*-ω-palmitate modification. Glucose-*O*-ω-palmitate gave a rate approximately one fourteenth that of palmitate and there was no significant difference in the rate due to glucose-*O*-ω-palmitate in the presence or absence of GDP. Thus we conclude that glucose-*O*-ω-palmitate cannot facilitate proton conductance through UCP 1 in proteoliposomes.

The GDP-sensitive, fatty-acid dependent, non-proton dependent, charge transfer assay using reconstituted UCP 1 has been used as a measure of the 'flippase' activity of UCP 1 (9). We showed that undecanesulfonate is 'flippable' on UCP 1, as has been shown by others (27), and at a similar rate to palmitate, as expected. The increased charge transfer rate or 'flippase' rate was coincident with the hydrophobic nature of the modification to the ω-carbon of palmitate, ie. the absence of modification of the ω-carbon of palmitate, yeilded faster rates than the methoxy group modification, which was faster than the hydroxyl group modification, which in turn was faster than glucose-*O*-ω-palmitate modification. In fact, glucose-*O*-ω-palmitate gave a rate approximately one fourtieth that of palmitate and there was no significant difference in the charge transfer rate due to glucose-*O*-ω-palmitate in the presence or absence of GDP (Figure 5). We conclude that glucose-*O*-ω-palmitate cannot facilitate fatty acid–dependent charge transfer through UCP 1 in proteoliposomes.

Our data in proteoliposomes are also consistent with our data for isolated mitochondria from rat BAT. We showed that glucose-*O*-ω-palmitate, unlike palmitate, could not reverse GDP-inhibited UCP 1 function in isolated BAT mitochondria. Thus we conclude that glucose-*O*-ω-palmitate cannot facilitate uncoupling through UCP 1 in mitochondria from BAT.

Taken together, our data show that hydrophilic modification of the ω-carbon of palmitate reduced or abolished the ability of palmitate to facilitate UCP function. Glucose-*O*-ω-palmitate cannot substitute for palmitate in facilitating proton flux through UCP1 in liposomes, charge transfer through UCP 1 in

liposomes or uncoupling in mitochondria, as would be predicted from the cofactor model and as was reported in the reviews by Klingenberg et al. (8) and Klingenberg & Huang (10). We presume that the inability of glucose-*O*-ω-palmitate to facilitate proton flux in liposomes and mitochondria is due to its inability to flip or be flipped across the membrane, due to the nature of the large hydrophilic moiety attached to the ω-carbon of palmitate. We also presume that the inability of glucose-*O*-ω-palmitate to facilitate charge transfer in UCP 1 containing proteoliposomes is due to the fact that glucose-*O*-ω-palmitate is not a substrate for UCP 1. Although our data are not consistent with the cofactor/activation model, they are consistent with the buffering model of UCP 1 function (7-9).

Acknowledgements: RKP thanks Prof. Keith D. Garlid and Prof. Martin Klingenberg for teaching the reconstitution techniques to EPB. Funding was provided by Enterprise Ireland (ref. PC/2003/028 to RKP) and by a Discovery Grant to TWP from the Natural Sciences and Engineering Research Council of Canada (NSERC).

[1]Abbreviations: BAT, brown adipose tissue; BSA, bovine serum albumin; Δp, proton electrochemical gradient; 1-D SDS-PAGE, one-dimensional sodium dodecylsulphate polyacrylamide gel electrophoresis; C_8E_5, pentaethylene glycol monooctyl ether; CAPS, 3-(cyclohexylamino)-1-propanesulfonic acid; EDTA, ethylenediaminetetraacetic acid; EGTA, ethylene glycol-bis(β-aminoethyl ether) N,N,N',N'-tetraacetic acid; HEPES, (N-(2-hydroxyethyl)piperazine-N'-(2-ethanesulfonic acid)); FBS, foetal bovine serum; HTP, hydroxyapatite; MALDI-TOF MS, matrix-assisted laser desorption ionization time of flight mass spectrometry; NCBI, national centre for Biotechnology Information; PBFI, benzofuran isophthalate; SDS-PAGE, sodium dodecyl sulfate-polyacrylamide gel electrophoresis; S.E.M., standard error of the mean; SPQ, 6-methoxy-N-(3-sulfopropyl)quinolinium; STE, sucrose trizma EGTA medium; TEA, tetraethylammonium; TES, N-[tris(hydroxymethyl)methyl]-2-aminoethane-sulfonic acid; TFA, trifluoroacetic acid; UCP, uncoupling protein;

REFERENCES

1. Nicholls, D.G. (1976) *Eur. J. Biochem.* **62**, 223-228

2. Nicholls, D.G. and Locke, R.M. (1984) *Physiol Rev.* **64**, 1-64

3. Ricquier, D. and Bouillaud, F. (1986) *Brown Adipose Tissue*, pp86-104, (Paul Trayhurn and David G. Nicholls eds.) Edward Arnold Publishers, London. UK.

4. Cannon, B and Nedergaard, J. (2004) *Physiol. Rev.* **84**, 277-359

5. Nicholls, D.G. (2004) *Biochem. Soc. Trans.* **29**, 751-755

6. Carroll, A.M., Haines, L.R., Pearson, T.W., Fallon, P., Walsh, C., Brennan, C., Breen, E.P. & Porter, R.K. (2005) *J. Biol. Chem.* **280**, 15534-15543

7. Skulachev, V.P. (1991) *FEBS Lett.* **294**, 158-162

8. Klingenberg, M., Echtay, K.S., Bienengraeber, M., Winkler, E. and Huang, S.G. (1999) *Int. J. Obes. Relat. Metab. Disord. Suppl* **6**, S24-S29

9. Garlid, K.D., Jabůrek, M., Ježek, P. and Vařecha, M. (2000) *Biochim. Biophys. Acta.* **1459**, 383-389

10. Klingenberg, M. & Huang, S-G. (1999) *Biochim. Biophys. Acta* **1415**, 271-296

11. Nicholls, D.G. and Rial, E. (1999) *J. Bioenerg. Biomembr.* **31**, 399-406.

12. Garlid, K.D., Jabůrek, M. and Ježek, P. (2001) *Biochem. Soc. Trans.* **29,** 803-806

13. Garlid, K.D., Orosz, D.E., Modrianský, M, Vassanelli, S. and Ježek, P. (1996) *J. Biol. Chem.* **271,** 2615-2620

14. Jabůrek, M., Vařecha, M. Gimeno, R.E., Demdski, M., Ježek, P., Zhang, M., Burn, P., Tartaglia, L.A. and Garlid, K.D., (1999) *J. Biol. Chem.* **274,** 26003-26007

15. Ježek, P. (1999) *J. Bioenerg. Biomembr.* **31,** 457-466.

16. Gouin, S., Pilgrim, W., Porter, R.K. and Murphy, P.V. (2005) *Carb. Res.***340**, 1547-1552

17. Chappell, J.B. and Hansford, R.G. (1972) *Subcellular Components: Preparation and Fractionation* (Birnie, G.D., Ed.), pp. 77-91, Butterworths, London. UK.

18. Markwell, M.A., Haas, S.M., Bieber, L.L. and Tolbert, N.E. (1978) *Anal. Biochem.* **87**, 206-210

19. Cunningham, O., McElligott, A.M., Carroll, A.M., Breen, E., Reguenga, C., Oliveira, M.E.M., Azevedo, J.E. and Porter, R.K. (2003) *Biochim. Biophys. Acta* **1604,** 170-179

20. Neuhoff, V., Arold, N., Taube, D. and Ehrhardt, W. (1998). *Electrophoresis.* **9**, 255-262

21. González-Barroso, M., Fleury, C., Bouillaud, F., Nicholls, D.G. and Rial, E. (1998) *J. Biol. Chem.* **273**, 15528-15532

22. Reynafarje, B., Costa, L.E. and Lehninger, A.L. (1985) *Anal. Biochem.* **145,** 406-418

23. Lin, C.S. and Klingenberg, M. (1980) *FEBS Lett.* **113,** 299-303

24. Jabůrek, M. and Garlid, K.D. (2003) *J. Biol. Chem.* **278,** 25825-25831.

25. Ricquier, D. and Bouillaud, F. (2000) *Biochem. J.* **345,** 161-179

26. Pecqueur, C., Alves-Guerra, M-C., Gelly, C., Levi-Meyrueis, C., Couplan, E., Collins, S., Ricquier, D., Bouillaud, F. and Miroux, B. (2001) *J. Biol. Chem.* **276**, 8705-8712

27. Ježek, P., Modrianský, M and Garlid. K.D. (1997) *FEBS Lett.* **408,** 166-170

Figure 1. Identification of isolated rat brown adipose tissue UCP 1 proteins by mass spectrometry.

A. One-dimensional gel electrophoresis analysis of purified UCP 1 from rat brown adipose tissue mitochondria. The gel was stained with colloidal Coomassie Blue G-250. The broad band at 30-33 kDa was excised and in-gel digestion with trypsin was performed prior to mass spectrometric analysis of tryptic cleavage products. Molecular mass markers are shown in the right-hand lane. **B.** UCP 1 peptides identified by peptide mass fingerprinting. Bold: previously identified peptide sequences. Underlined: peptide sequences identified by TOF/TOF.

Figure 2. Proton flux data for reconstituted UCP1 from different sources

Proton flux in liposomes containing was measured using changes in luminal 6-methoxy-N-(3-sulfopropyl)quinolinium (SPQ) fluorescence due to quenching by the anion of TES. Liposomes contained (a) native rat UCP 1 from BAT (plus 100μM laurate acid) in the absence, (b) native rat UCP 1 from thymus (plus 400μM laurate acid) (c) expressed human UCP 1 (plus 100μM laurate acid). Each proteoliposome preparation was individually calibrated for fluorescent probe response, and the internal volume was estimated from the volume of distribution of the fluorescent probe. Each trace represents a different experiment. Proton flux was measured as the initial rate of change of proton concentration, in the presence of fatty acid following addition of valinomycin.

Figure 3. Structures of palmitate analogues used in the study.

Figure 4. Proton flux data for reconstituted BAT UCP1 in the presence of palmitate analogues

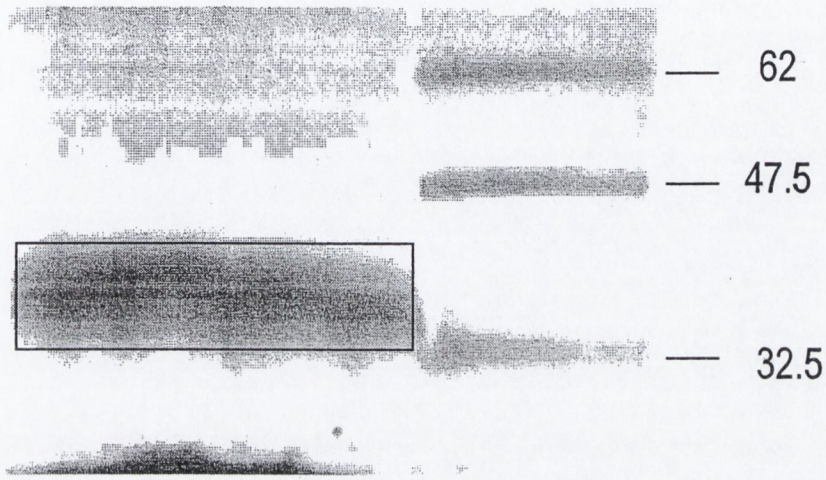
Proton flux in liposomes was measured using changes in luminal 6-methoxy-N-(3-sulfopropyl)quinolinium (SPQ) fluorescence due to quenching by the anion of TES. Liposomes contained native rat UCP 1 from BAT (A) plus (i) 100μM palmitate in the absence (a) and presence (d) 500μM GDP, (ii) 100μM glucose-*O*-ω-palmitate in the absence (b) and presence (e) 500μM GDP and (iii) 100μM undecanesulfonate in the absence (c) and presence (f) of 500μM GDP. (B) plus (i) 100μM palmitate in the absence (a) and presence (d) 500μM GDP, (ii) 100μM ω-methoxypalmitate in the absence (b) and presence (e) of 500μM GDP and (iii) 100μM ω-hyoxypalmitate in the absence (c) and presence (f) of 500μM GDP. (C) Collated proton flux data for liposomes containing rat UCP 1 from BAT in the presence of palmitate, glucose-*O*-ω-palmitate, ω-hydroxypalmitate, ω-methoxypalmitate and undecanesulfonate in the absence (□) and presence (■) of 500μM GDP. Each trace represents a different experiment. Proton flux was measured as the initial rate of change of proton concentration, in the presence of fatty acid following addition of valinomycin. Bar charts represent data from at least 3 separate experiments performed in triplicate.

Figure 5. Sample traces of charge transfer flux from the fluorescent spectrometer. Charge transfer flux in liposomes was measured using changes in luminal K^+ fluxes, reflecting the movement of ion charge across the liposome membrane as a result of changes in K^+ fluxes in liposomes was measured using changes in luminal 6-methoxy-N-(3-sulfopropyl)quinolinium (SPQ) fluorescence due to quenching by the anion of TES. Liposomes contained native rat UCP 1 from BAT (A) plus (i) 100mM palmitate (a) 100μM undecanesulfonate (b) and 100μM glucose-*O*-ω-palmitate (c) in the absence GDP. (B)

Collated charge flux data for liposomes containing rat UCP 1 from BAT in the presence of palmitate, glucose-*O*-ω-palmitate, ω-hyoxypalmitate, ω-methoxypalmitate and undecanesulfonate, in the absence (□) and presence (■) of 500μM GDP. Each trace represents a different experiment. Charge transfer flux was measured as the initial rate of change of proton concentration, in the presence of fatty acid following addition of valinomycin. Bar charts represent data from at least 3 separate experiments performed in triplicate.

Figure 6. Measurement of oxygen consumption rates in BAT mitochondria from rat. Mitochondria (0.5 mg/ml) from rat BAT were incubated in the presence of 120 mM KCl, 5 mM HEPES-KOH, pH 7.0, 1 mM EGTA, 7.5 mM succinate (K^+-salt), 16 μM de-fatted BSA, 5 μM rotenone, 1 μg/ml oligomycin and 5 μM atractyloside. Steady-state oxygen consumption rates were then measured, following addition of 1 mM GDP, and either (A) 64 μM palmitate (~40 nM free) or (B). 64 μM glucose-*O*-ω-palmitate followed by addition of 40 μM DNP in both instances. Data are shown as the mean ± S.E.M from at least 3 independent experiments each performed in triplicate.

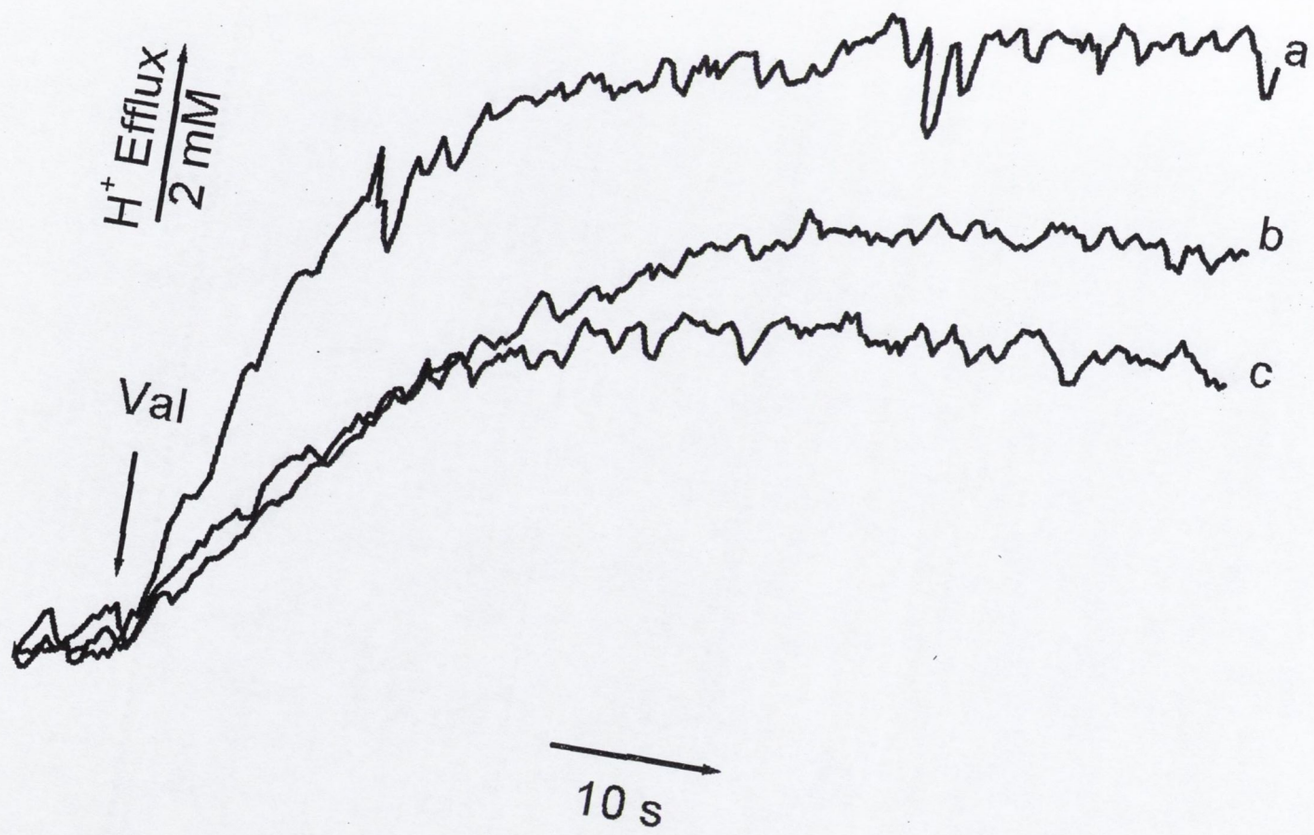
A

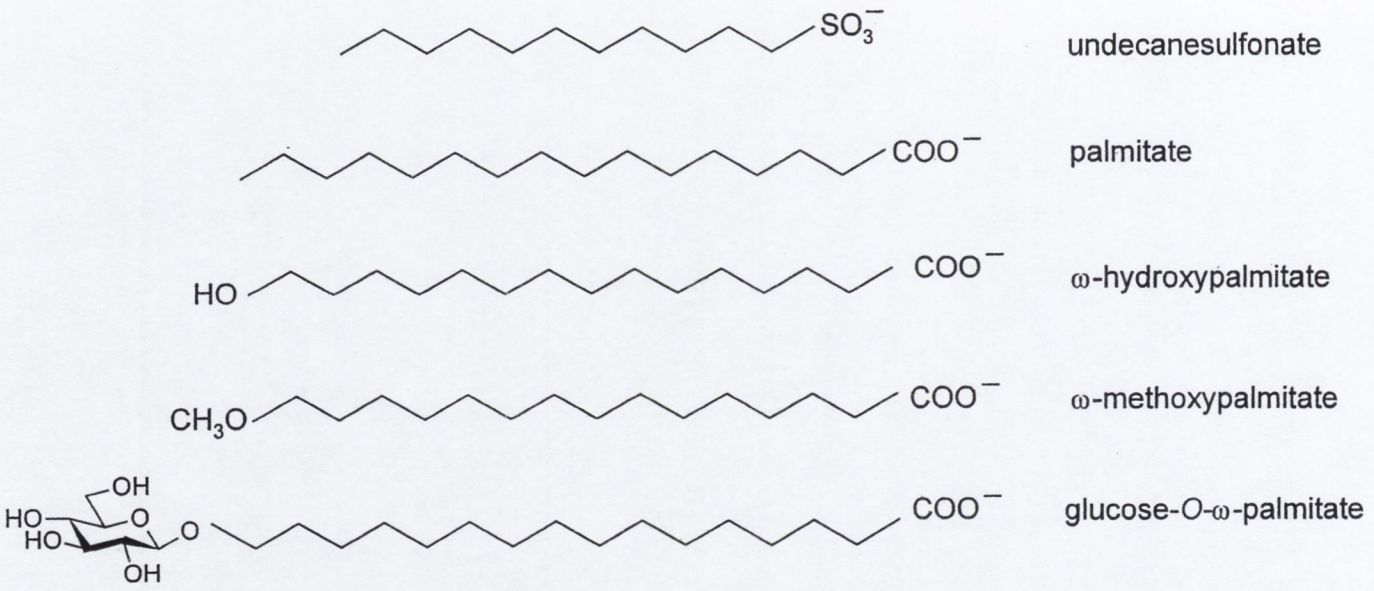


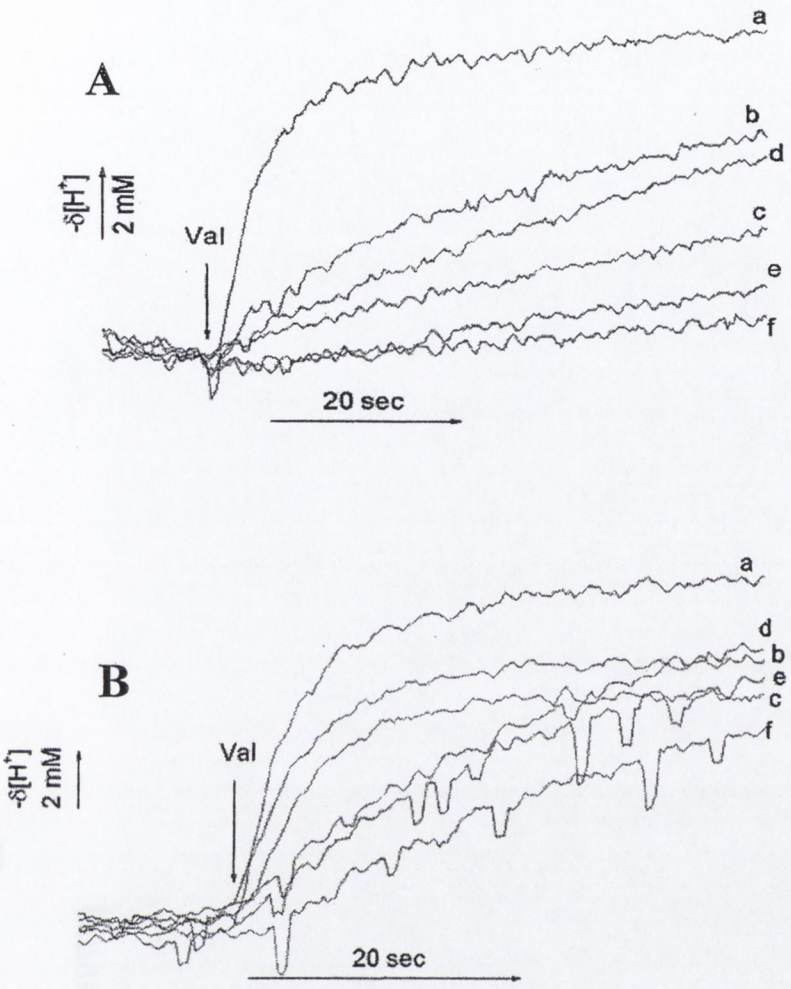
B

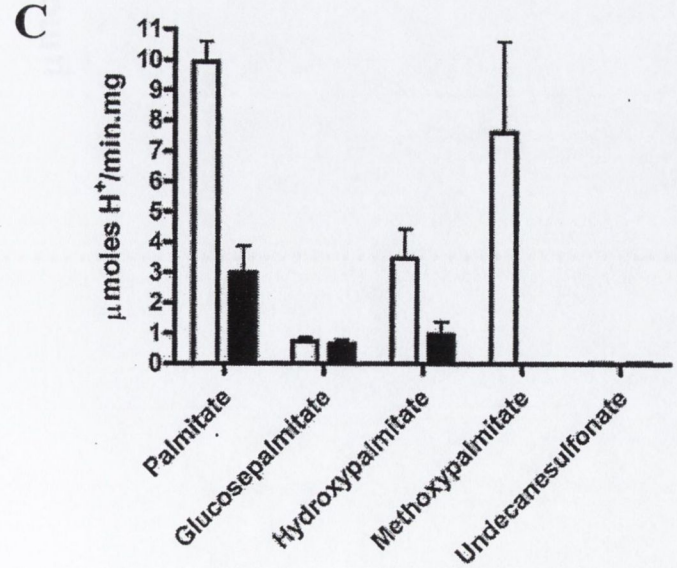
MVSSTTSEVQPTMGVKIFSAGVSACLADIITFPLDTAKVR**LQIQG**
EGQASSTIRYKGVLGTITTLAKTEGLPK**LYSGLPAGIQRQISFAS**
LRIGLYDTVQEYFSSGRETPASLGSKISAGLMTGGVAVFIGQPTE
VVKVR**MQAQSHLHGIKPRYTGTYNAYR**VIATTESLSTLWKGTTPN
LMRNVIINCTELVTYDLMKGALVNHHILADDVPCHLLSALVAGFC
TTLLASPVDVVKTRFINSLPGQYPSVPSCAMTMYTK**EGPAAFFKG**
FAPSFLRLGSWNVIMFVCFEQLKKELMKSRQTVDCTT

28% protein coverage with 8 peptide masses
Rattus norvegicus gi|56789456

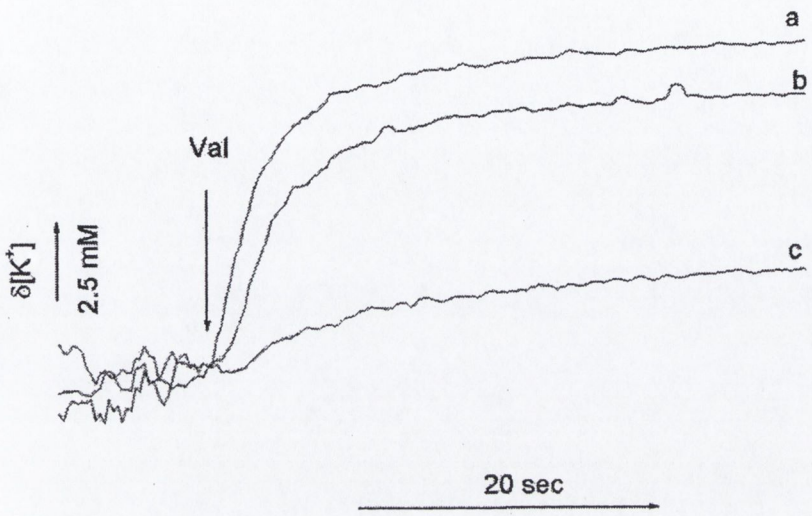

H+ Efflux
2 mM
Val
a
b
c
10 s


SO3−
undecanesulfonate
COO−
palmitate
HO
COO−
ω-hydroxypalmitate
CH3O
COO−
ω-methoxypalmitate
OH
HO
O
HO
O
OH
COO−
glucose-O-ω-palmitate

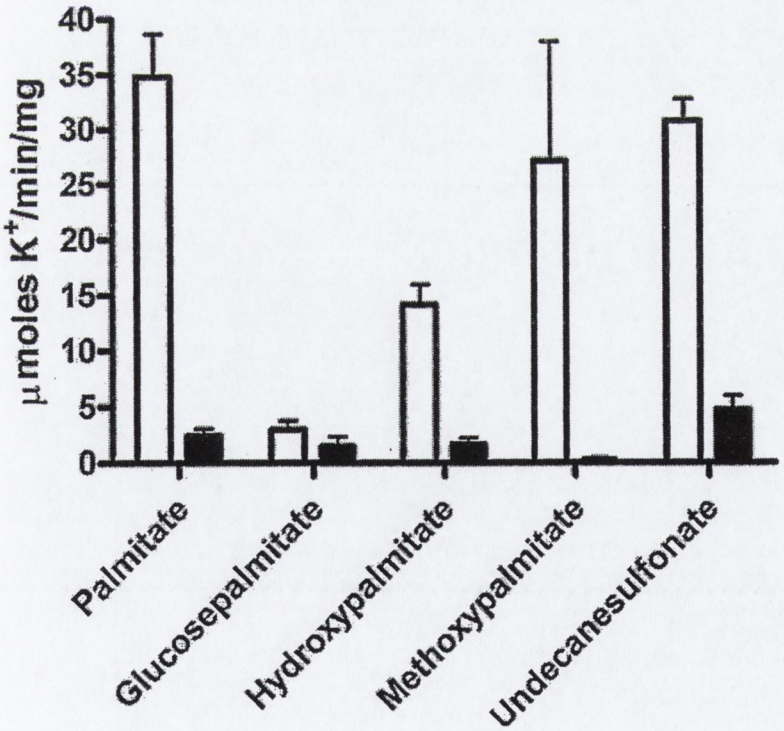

A
-δ[H+]
2 mM
Val
20 sec
a
b
d
c
e
f
B
-δ[H+]
2 mM
Val
20 sec
a
d
b
e
c
f


C
µmoles H+/min.mg
0
1
2
3
4
5
6
7
8
9
10
11
Palmitate
Glucosepalmitate
Hydroxypalmitate
Methoxypalmitate
Undecanesulfonate

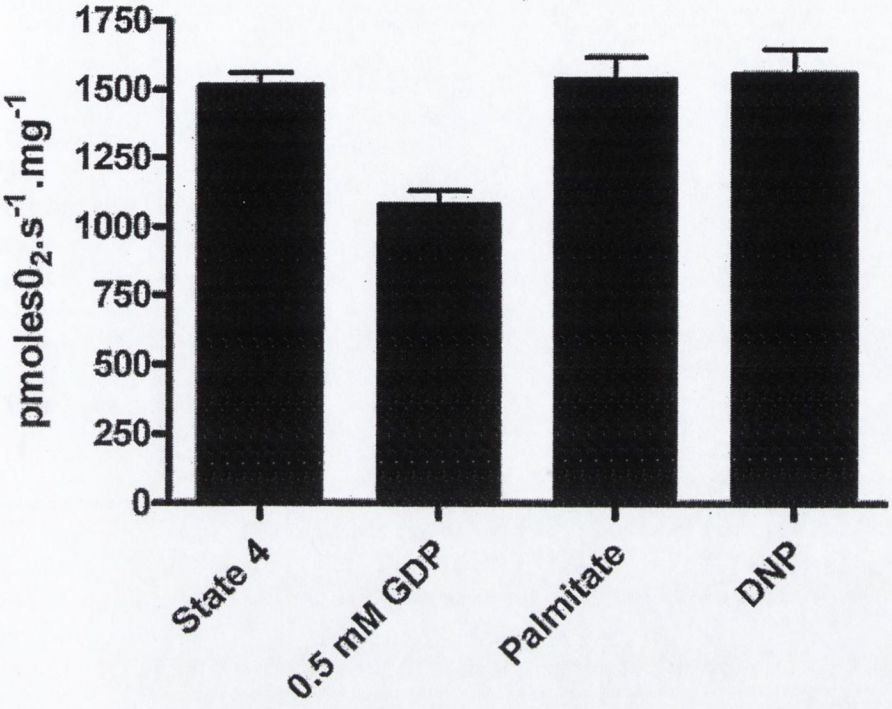
A


a
b
c
Val
δ[K+]
2.5 mM
20 sec

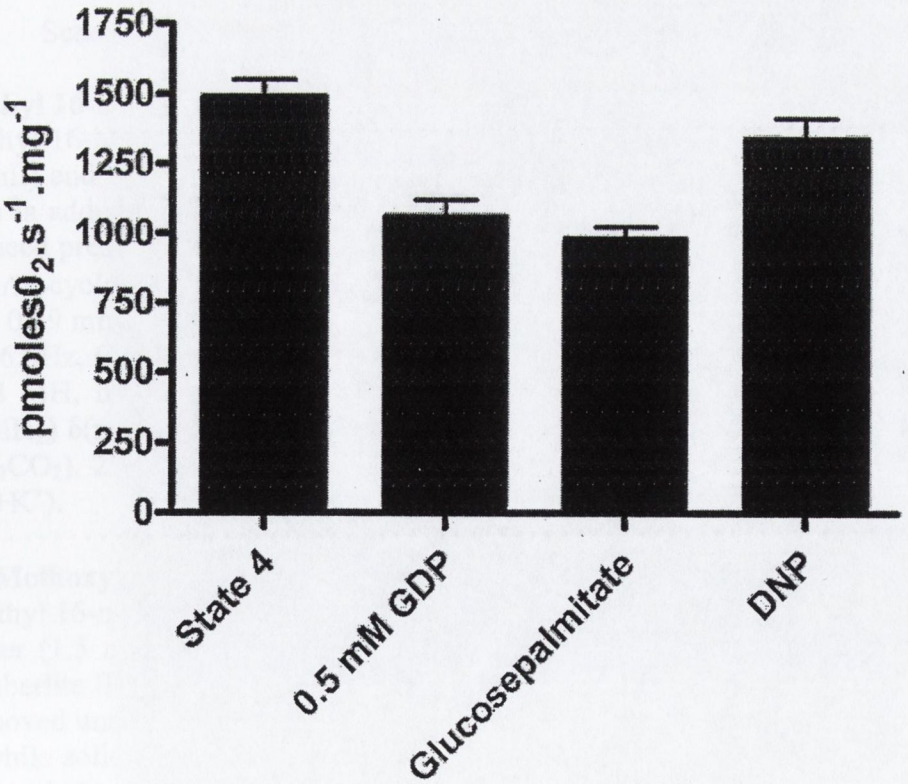
B


μmoles K+/min/mg
40
35
30
25
20
15
10
5
0
Palmitate
Glucosepalmitate
Hydroxypalmitate
Methoxypalmitate
Undecanesulfonate

A


1750
1500
1250
1000
750
500
250
0
pmoles0_2.s^{-1}.mg^{-1}
State 4
0.5 mM GDP
Palmitate
DNP

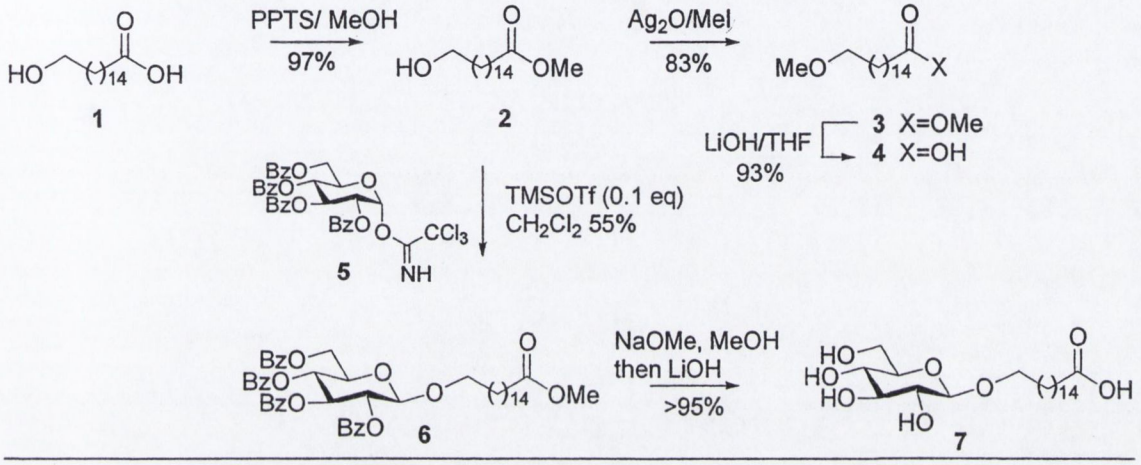
B


1750
1500
1250
1000
750
500
250
0
pmoles0_2.s^{-1}.mg^{-1}
State 4
0.5 mM GDP
Glucosepalmitate
DNP

Supplementary Figure 1.

Synthesis of glucose -O-ω-palmitate and ω–methoxy-palmitate.

The detail experimental procedure for the synthesis of glucose- O-ω-palmitate is reported by us in Gouin et al. (2005) as shown in scheme 1. Glucose-*O*-ω-palmitate is stable under ionic conditions and at neutral pH and was shown by NMR quantitation to be >93% pure (Gouin et al., 2005). The synthesis of methoxy-ω-palmitate **4** was achieved as shown in Scheme 1. This involved alkylation of ester **2,** prepared from 16-hydroxypalmitic acid, using silver oxide and methyl iodide and subsequent saponification of the ester to give **4**.



Scheme 1

Methyl 16-methoxyhexadecanoate 3

Methyl 16-hydroxyhexadecanoate (100 mgs, 0.35 mmol) **2** was dissolved in dry CH_2Cl_2 (2 mL) and MeI (213μL, 3.4 mmol) added. After stirring at r.t. for 10 days, CH_2Cl_2 (20 mL) is added and the mixture is filtrated under celite. The solvent was removed under reduced pressure. and the residue purified by silica gel chromatography (gradient elution, EtOAc-cyclohexane 1:9 to 1:0). ω–Methoxypalmitate was isolated as a white solid (87 mg, 0.29 mmol). ^{1}**H**-NMR ($CDCl_3$, 300MHz) δ (ppm): 3.66 (3H, s, CH_3OCO), 3.36 (2H, t, J 6.6Hz, CH_3OCH_2), 3.33 (3H, s, CH_3O), 2.30 (2H, t, J 7.5Hz, $CH_2CH_2CO_2Me$), 1.64-1.54 (4H, m, CH_2CH_2CO+CH_2CH_2OMe), 1.25 (22H, se, $11CH_2$). ^{13}C-NMR ($CDCl_3$, 75MHz) δ(ppm): 174.2 (s, *C*O), 72.9 (t, CH_2O), 58.5 (q, OCH_3), 51.4 (q, OCH_3), 34.1 (t, CH_2CO_2), 29.6, 29.5, 29.4, 29.2, 29.1, 26.1, 25.9, 24.9 (each t, $13CH_2$). **ESMS:** 339.2 ($M+K^+$).

ω–Methoxypalmitate 4

Methyl 16-methoxyhexadecanoate (54 mg, 0.18 mmol) was dissolved in THF (2 mL) and water (1.5 mL) is added with LiOH (20 mg, 0.83 mmol). After stirring at rt for 8 h, Amberlite IR-120+ is added until pH 5 is reached. The mixture is filtered and the solvent removed under reduced.pressure. The title compound (48 mgs, 0.17 mmol) is obtained as a while solid after flash chromatography on silica gel (gradient elution, CH_2Cl_2-MeOH, 1:0 to 1:9); ^{1}H-NMR ($CDCl_3$, 300MHz) δ (ppm): 3.37 (2H, t, J 6.6Hz, CH_3OCH_2), 3.33

(3H, s, C*H*$_3$O), 2.34 (2H, t, J 7.5Hz, $CH_2CH_2CO_2Me$), 1.67-1.52 (4H, m, CH_2CH_2CO+CH_2CH_2OMe), 1.25 (22H, se, 11C*H*$_2$). ^{13}C-NMR ($CDCl_3$, 75MHz) δ (ppm): 179.8 (s, *C*O), 73.1 (t, *C*H$_2$O), 58.6 (q, O*C*H$_3$), 34.2 (t, CH_2CO_2), 29.7, 29.6, 29.5, 29.4, 29.2, 26.1, 25.9, 24.9 (each t, 13*C*H$_2$). **ESMS:** 309.2 ($M+Na^+$). Anal. Calcd for $C_{17}H_{34}O_3$: C, 71.28; H, 11.96. Found: C, 70.78; H, 11.74.

THE JOURNAL OF BIOLOGICAL CHEMISTRY
Vol. 280, No. 15, Issue of April 22, pp. 15534–15543, 2005
Printed in U.S.A.
© 2005 by The American Society for Biochemistry and Molecular Biology, Inc.

Identification of a Functioning Mitochondrial Uncoupling Protein 1 in Thymus*[S]

Received for publication, November 26, 2004, and in revised form, January 18, 2005
Published, JBC Papers in Press, January 28, 2005, DOI 10.1074/jbc.M413315200

Audrey M. Carroll‡, Lee R. Haines§, Terry W. Pearson§, Padraic G. Fallon‡, Caitríona M. Walsh‡, Clare M. Brennan‡, Eamon P. Breen‡, and Richard K. Porter‡¶

From the ‡Department of Biochemistry, Trinity College Dublin, Dublin 2, Ireland and the §Department of Biochemistry and Microbiology, University of Victoria, Victoria, British Columbia V8W 3P6, Canada

We present evidence that rat and mouse thymi contain mitochondrial uncoupling protein (UCP 1). Reverse transcriptase-PCR detected RNA transcripts for UCP 1 in whole thymus and in thymocytes. Furthermore, using antibodies to UCP 1 the protein was also detected in mitochondria isolated from whole thymus and thymocytes but not in thymus mitochondria from UCP 1 knock-out mice. Evidence for functional UCP 1 in thymus mitochondria was obtained by a comparative analysis with the kinetics of GDP binding in mitochondria from brown adipose tissue. Both tissues showed equivalent B_{max} and K_D values. In addition, a large component of the nonphosphorylating oxygen consumption by thymus mitochondria was inhibited by GDP and subsequently stimulated by addition of nanomolar concentrations of palmitate. UCP 1 was purified from thymus mitochondria by hydroxyapatite chromatography. The isolated protein was identified by peptide mass mapping and tandem mass spectrometry by using MALDI-TOF and LC-MS/MS, respectively. We conclude that the thymus contains a functioning UCP 1 that has the capacity to regulate metabolic flux and production of reactive oxygen-containing molecules in the thymus.

UCP1 (uncoupling protein 1 also known as UCP and thermogenin) has been associated exclusively with brown adipose tissue (BAT)[1] (1, 2) and is a prerequisite for nonshivering thermogenesis in mammals. UCP 1 is known to transport protons and dissipates the proton electrochemical gradient (Δp) across the mitochondrial inner membrane. UCP 1 thus acts as a major regulator of metabolic flux in mitochondria and as a heat regulator in the whole animal (1–4). Recent evidence obtained *in vitro* also suggests that UCP 1 also plays a role in regulating superoxide production by mitochondria (5–8).

UCP 1 synthesis, mitochondrial biogenesis, and thermogenesis are controlled by sympathetic nerve activity and thyroid status. Isolated brown adipocytes from cold-acclimated animals have increased oxygen consumption compared with those from room temperature animals, and the mitochondria isolated from active BAT are uncoupled (1). Although the mechanism of the uncoupling phenomenon is still a matter of investigation (9–11), it is known that long chain fatty acids are required for uncoupling activity and that purine nucleotides inhibit uncoupling through UCP 1 in mitochondria and in the reconstituted systems. The purine nucleotide-binding site on UCP 1 in mitochondria faces the cytosolic side of the inner membrane, and in the presence of saturating amounts of purine nucleotides *in vitro*, oxygen consumption rates due to UCP 1 activity are inhibited. Subsequent addition of nanomolar concentrations of long chain free fatty acids *in vitro* restores the activity of UCP 1-containing mitochondria, and oxygen consumption rate increases (1, 4).

UCP 1 transcripts in BAT have been determined by using Northern blot analysis, and the UCP 1 protein has usually been detected by using polyclonal antibodies specific for the full-length protein. In addition, UCP 1 abundance in BAT (12–14) and the degree of masking (binding sites already occupied) of the purine nucleotide-binding sites (15) have been measured by binding of labeled GDP to mitochondria. To date, UCP 1 protein has not been found in any tissue other than BAT, although it has been sought in liver, heart, epididymal white adipose tissue, parametrial white adipose tissue, and thigh muscle (4, 16); and a previous study, using Northern blot analysis, failed to detect UCP 1 transcripts in thymus (17). However, in this study, we have detected UCP 1 transcripts in whole thymus and thymocytes by using RT-PCR. We have detected UCP 1 protein by using immunoblotting in mitochondria isolated from whole thymus and thymocytes. We have purified and identified UCP 1 from thymus mitochondria by using mass spectrometry. We have also shown that mitochondria isolated from thymus bind GDP with kinetics consistent with the presence of UCP 1 and have a GDP-sensitive and fatty acid-dependent proton leak indicative of the presence of UCP 1.

MATERIALS AND METHODS

Tissue Sources and Isolation of Mitochondria—Wild-type C57BL/6J mice, female CD-1 mice (20–25 g), and female Wistar rats (*Rattus norvegicus*; 180–200 g) were provided by the BioResources Unit, Trinity College Dublin. UCP 1 knock-out mice on a C57BL/6J background (18), originally provided by Dr. Leslie Kozak, were bred in-house. All mice and rats were housed in a specific pathogen-free facility and were fed *ad libitum* unless otherwise stated. Some samples of brown adipose tissue mitochondria from UCP 1 knock-out and wild-type mice, both on a C57BL/6J background, were gifts from Dr. Jan Nedergaard (Werner-

* This work was supported by The Human Frontiers Science Programme Organization Grant RG307/98, Bioresearch Ireland, Science Foundation Ireland, IRCSET, and by a Discovery grant (to T. W. P.) from the Natural Sciences and Engineering Research Council of Canada. The costs of publication of this article were defrayed in part by the payment of page charges. This article must therefore be hereby marked "*advertisement*" in accordance with 18 U.S.C. Section 1734 solely to indicate this fact.

[S] The on-line version of this article (available at http://www.jbc.org) contains a figure.

¶ To whom correspondence should be addressed: Dept. of Biochemistry, Trinity College Dublin, Dublin 2, Ireland. Tel.: 353-1-608-1617; Fax: 353-1-677-2400; E-mail: rkporter@tcd.ie.

[1] The abbreviations used are: BAT, brown adipose tissue; BSA, bovine serum albumin; FCCP, carbonyl cyanide *p*-trifluoromethoxyphenylhydrazone; HTP, hydroxyapatite; LC-MS/MS, liquid chromatography/tandem mass spectrometry; MALDI-TOF MS, matrix-assisted laser desorption ionization time of flight mass spectrometry; octyl-POE, octylpentaoctylethylene; RT, reverse transcription; UCP, uncoupling protein; VDAC, voltage-dependent anion channel.

This paper is available on line at http://www.jbc.org

Gren Institute, Stockholm, Sweden). Skeletal muscle mitochondrial samples from UCP 3 knock-out (19) and wild-type mice, both on a C57BL/6J background, were gifts from Dr. Jean-Paul Giacobino (University of Geneva, Switzerland).

Thymocytes were isolated from Wistar rats (180–200 g) essentially as described by Buttgereit *et al.* (20). The thymus was removed from the rat, trimmed clean of connective tissue and brown fat (if present), and transferred into RPMI 1640 (Invitrogen) supplemented with 100 units/ml penicillin and 100 μg/ml streptomycin (Sigma). A single cell suspension was prepared by passage through 70-μm nylon sieves (Falcon). The thymocyte suspension was washed extensively. The viability of cells was >99% by trypan dye exclusion. Cells were incubated with fluorescein isothiocyanate-conjugated mouse anti-rat Thy-1 (CD90; MRC OX-7; Serotec) or a fluorescein isothiocyanate-conjugated mouse IgG1 isotype control (Pharmingen). Data were collected on a FACScan flow cytometer (BD Biosciences) and analyzed using Cellquest software.

Oxygen consumption rates by thymocytes isolated from rats were measured in the aforementioned medium using an Oxygraph Respirometer (Oroboros™, Innsbruck, Austria). Mitochondria isolated from whole mouse thymus, whole rat thymus, rat thymocytes, rat kidney, and rat and mouse liver were isolated by homogenization followed by differential centrifugation according to the procedure of Chappell and Hansford (21). Mitochondria were isolated from rat skeletal muscle by mincing the muscle and treating the tissue with nagarse (protease VII, Sigma). Mitochondria were separated from the homogenate by differential centrifugation according to the procedure of Bhattacharya *et al.* (22). Mitochondrial protein concentrations were determined by the reduction of Folins-Ciocalteau phosphomolybdic-phosphotungstic reagent according to the method of Markwell *et al.* (23).

PCR and Analysis of the Products—Total RNA was purified from rat BAT, whole rat thymus, rat Thy-1-positive thymocytes, and liver using Tri Reagent™ (Sigma) containing guanidine thiocyanate. Total RNA (1 μg) was reverse-transcribed to cDNA by using avian myeloblastosis virus-reverse transcriptase and random primers (Promega, Southampton, UK). Primers used to amplify UCP 1 were as described by Carroll and Porter (24). Primers for application of the glyceraldehyde-3-phosphate dehydrogenase sequence were used as a housekeeping gene control. Glyceraldehyde-3-phosphate dehydrogenase (GenBank™ accession number M32599) primers were designed according to Tokunga *et al.* (25). PCR amplification conditions were as follows: initial denaturation of 5 min at 95 °C followed by 35 cycles of 45 s at 95 °C, 45 s at 55 °C, and 2 min at 72 °C with a final extension for 10 min at 72 °C. The PCR mixtures were electrophoresed on a 1% (w/v) agarose gel incorporating ethidium bromide and visualized under ultraviolet light.

Polyacrylamide Gels and Immunoblot Analysis—One-dimensional SDS-PAGE under reducing conditions was used to examine UCP 1 purity after hydroxyapatite chromatography. Proteins were detected by staining gels with colloidal Coomassie Brilliant Blue G-250 (26). This stain is very sensitive (can detect 8–10 ng of protein in a single gel band or spot) and is compatible with the post-staining processing required for mass spectrometry (see below).

SDS-PAGE (reducing conditions) was also used to separate proteins prior to immunoblot analysis. UCP 2 purified from inclusion bodies expressed in *Escherichia coli* and UCP 3 protein from yeast, as described by Cunningham *et al.* (27), were used as positive controls in immunoblot experiments. Following SDS-PAGE, resolved proteins were transferred onto polyvinylidene difluoride membranes (Immobilon-P^{SQ}; Millipore), as described by Cunningham *et al.* (27). Polyclonal antibodies to UCP 1 and UCP 3 peptides were raised in rabbits by Eurogentec (Herstal, Belgium) as detailed by Cunningham *et al.* (27). Commercial anti-UCP 1 (amino acids 145–159) and anti-UCP 2 (amino acids 144–157) rabbit antisera were purchased from Calbiochem. A goat antiserum to full-length rabbit UCP 1 protein was a gift from Dr. Daniel Ricquier, CNRS, Meudon, France. A rabbit antiserum specific for the β-subunit of F_1-ATP synthase from *Neurospora crassa* was a gift from Dr. Matt Harmey, Department of Botany, University College Dublin, Ireland. The antisera were all used at 1:1000 dilution. Following blocking and a 1-h primary antibody incubation, the blots were incubated with a horseradish peroxidase-conjugated goat anti-rabbit secondary antibody (1:10,000 dilution) in phosphate-buffered saline, 0.5% (v/v) Tween 20, 5% (w/v) milk powder for 1 h at room temperature. Blots were developed using an ECL detection system (Amersham Biosciences), and immunoreactions were visualized by exposure to Kodak X-Omat LS film.

GDP Binding Assay—Endogenous residual bound nucleotides were removed from isolated mitochondria using an anion exchanger (Dowex 21K) by the procedure described by Huang and Klingenberg (15). Isolated mitochondria at a concentration of 2 mg/ml in a buffer containing 250 mM sucrose, 20 mM HEPES, 1 mM EDTA, pH 8.0, were shaken with Dowex (120 mg/mg protein) at room temperature for 1 h. Measurement of binding of tritiated GDP was performed by a modification of the procedure described by Scarpace *et al.* (28). Mitochondria (50 μg) were incubated with [^{3}H]GDP (0.1–6.0 μM, 11.0 Ci/mmol) and [^{14}C]sucrose (250 μCi/ml) for 15 min at 37 °C in the absence (total binding) and presence (nonspecific binding) of unlabeled GDP (1.5 mM). Specific binding was calculated from the difference between total and nonspecific binding. The Michaelis dissociation constant (K_D) and the maximal binding capacity (B_{max}), describing the saturable binding of [^{3}H]GDP, were obtained by fitting mean values for specific binding sites on the y axis and free radioligand concentrations used on the x axis by using the program "Sigma Plot," version 5 (SPSS Inc. Chicago). The data were fitted to a rectangular hyperbola by nonweighted, nonlinear least squares regression.

Oxygen Consumption by Nonphosphorylating Mitochondria—Oxygen consumption rates were measured using a Clark-type oxygen electrode as described by González-Barroso *et al.* (29). Mitochondria (1 mg/ml) were incubated at 37 °C in medium containing 120 mM KCl, 5 mM HEPES-KOH, pH 7.4, 1 mM EGTA, 16 μM fatty-acid free BSA, 5 μM atractyloside, 5 μM rotenone, and 1 μg/ml oligomycin. Nonphosphorylating (state 4) oxygen consumption rates were measured as the steady-state rates achieved on addition of 7.5 mM succinate (succinate-KOH, pH 7.4). The sensitivity of this state 4 oxygen consumption rate to GDP (1 mM) was then determined. The sensitivity of the resulting oxygen consumption rate to palmitate (in ethanol) (64 μM) (~40 nM free) was then determined. Finally, the mitochondrial uncoupler cyanide-*p*-trifluoromethoxyphenylhydrazone (40 nM FCCP) was added to the chamber to determine the maximum oxygen consumption rate attainable due to uncoupling. The Clark-type oxygen electrode was calibrated according to the procedure of Reynafarje *et al.* (30) assuming that 406 nmol of oxygen atoms were dissolved in 1 ml of incubation medium at 37 °C.

Purification of UCP 1 from Rat Thymus Mitochondria—Purification of UCP 1 was performed using a hydroxyapatite (HTP) column chromatography procedure as described by Lin and Klingenberg (31) with slight modification. Intact thymus mitochondria (8–10 mg) suspended in STE buffer (250 mM sucrose, 5 mM Trizma (Tris base), 2 mM EGTA, pH 7.4) were centrifuged at 22,600 × *g* for 10 min at 4 °C. The mitochondrial pellet was solubilized in 13% (v/v) octylpentaoctylethylene (octyl-POE) ether in STE (total volume ~500 μl) and incubated on ice for 10 min prior to loading the solubilized mitochondrial proteins onto an HTP column. The column was prepared by soaking 0.34 g of HTP in 10 ml of STE buffer, pH 7.4, at 4 °C, for 6 h prior to pouring it into a 1-ml column (Bio-Rad) (diameter 1 cm, length 6 cm). The soaking solution was removed from the column by centrifugation at 800 × *g* for 2 min at room temperature immediately prior to loading of the mitochondrial proteins. The HTP column, containing the solubilized mitochondrial proteins, was incubated at room temperature for 10 min (to denature the adenine nucleotide carrier) followed by 25 min of incubation at 4 °C. The column was then centrifuged at 800 × *g* for 2 min to remove the HTP eluate (UCP 1-enriched fraction), leaving behind the unwanted bound proteins. The protein concentration of the HTP eluate was determined (23), and the octyl-POE detergent was removed using a Bio-Bead (Bio-Rad) column. The Bio-Bead column was prepared by placing 2 ml of Bio-Beads (suspended in distilled/deionized H_2O) into a 2-ml syringe barrel and allowing them to settle. The H_2O was removed from the Bio-Beads by centrifugation at 800 × *g* for 2 min. The Bio-Beads were equilibrated in ~2 ml of STE buffer, pH 7.4, for 30 min prior to use and were further centrifuged at 800 × *g* for 2 min to remove excess STE buffer. The HTP eluate was loaded onto the Bio-Beads with gentle mixing and incubated for 2 h at 4 °C with periodic slight agitation using a vortex-type mixer. The Bio-Bead column was centrifuged at 800 × *g* for 2 min, and the protein eluate was collected. The protein concentration of this elute was determined, and ~5–10 μg of protein were analyzed by SDS-PAGE and colloidal Coomassie Brilliant Blue G-250 staining.

Sample Preparation for Mass Spectrometry—A 30–33-kDa colloidal Coomassie Brilliant Blue G-250-stained protein band was excised from a one-dimensional SDS-polyacrylamide gel (Fig. 6*A*) and was transferred to a 1.5-ml Eppendorf microcentrifuge tube (previously autoclaved and rinsed with 50% high pressure liquid chromatography grade methanol to remove any contaminants) containing 100 μl of 20% (w/v) ammonium sulfate. The excised band was de-stained for 2 days in several washes of 50% (v/v) methanol, 5% (v/v) acetic acid, dehydrated with acetonitrile, reduced for 30 min with 10 mM dithiothreitol at 56 °C, and alkylated for 30 min with 100 mM iodoacetamide at 45 °C as described previously (32). The carboxyamidomethylated protein band was digested overnight at 37 °C with 40 μl of 20 ng/μl sequencing grade,

modified porcine trypsin according to the manufacturer's directions (Promega, Madison, WI). Peptides were extracted from the gel by using a series of elutions with 10% (v/v) formic acid. The resulting eluate pool was reduced to a final volume of 20 μl in a SpeedVac Concentrator (Savant, Hicksville, NY) and processed for mass spectrometry.

Peptide Mass Mapping—Peptide mass mapping was performed using matrix-assisted laser desorption ionization time of flight (MALDI-TOF) mass spectrometry. A 5-μl amount of the trypsin-digested sample was desalted and concentrated using a micro ZipTip μ-C_{18} (C18 resin; P10, Millipore Corp., Bedford, MA). The peptide mixture was eluted from the ZipTip with 1 μl of the MALDI-TOF matrix, α-cyano-4-hydroxycinnamic acid (10 mg/ml in 50% acetonitrile, 0.1% trifluoroacetic acid, Sigma), and spotted onto a Voyager stainless steel MALDI plate (Applied Biosystems, Foster City, CA). An Applied Biosystems Voyager DE-STR mass spectrometer (Applied Biosystems, Foster City, CA) running in delayed extraction and reflectron mode was used to acquire MALDI-TOF data. Selected peptide masses were submitted to four on-line search algorithms that use peptide masses to identify proteins from primary sequence data bases as follows: MS-Fit (Protein Prospector software package; San Francisco, CA, prospector.ucsf.edu/), Mascot (Matrix Science, London, UK, www.matrixscience.com/), ProFound (Prowl, Rockefeller University, prowl.rockefeller.edu), and PeptideSearch (EMBL Bioanalytical Research Group, Heidelberg, Germany, www.mann.embl-heidelberg.de/GroupPages/PageLink/peptidesearch/Services/PeptideSearch/FR_PeptideSearchFormG4.html).

Liquid Chromatography/Tandem Mass Spectrometry—The remaining peptide digest was analyzed using LC-MS/MS. The peptide samples were first desalted and concentrated on a PepMap C18 precolumn and then separated on a PepMap C18 column (LC Packings-Dionex, The Netherlands) followed by tandem mass spectrometry using a PE Sciex QStar Pulsar i Quadrupole time-of-flight mass spectrometer (Applied Biosystems).

The independent data acquisition parameters were as follows: after a 1-s survey scan from 400 to 1500 *m/z*, peaks with signal intensity over 10 counts with charge state +2 to +4 were selected for MS/MS fragmentation followed by a 2-s MS/MS from 65 to 1800 *m/z* for the four most intense ions in the survey scan. Once an ion was selected for MS/MS fragmentation, it was put on an exclude list for 180 s to prevent that ion from being gated again. A 4-atomic mass unit peak window was used to avoid gating of masses from the same isotopic cluster during the survey scan. Keratin and porcine trypsin peak masses were put on an exclude list to prevent these ions from being selected for MS/MS analysis. Independent acquisition data were submitted to ProID (proprietary Applied Biosystems software) for bioinformatics analysis of public protein data base (NCBInr) and subsequent protein identification.

RESULTS

By using RT-PCR, UCP 1 transcripts were detected in rat thymus and BAT (Fig. 1, *lane 4* in each case). As shown previously (24), rat liver was negative for UCP 1 transcripts. The specificity of our primers for detection of transcripts encoding uncoupling proteins 1–3 in rat brown adipose tissue, known to express all of these transcripts, has been demonstrated previously (24). Although it was clear that transcripts for UCP 1 were present in rat thymus, it was important to know whether UCP 1 protein was expressed.

To that end we used an anti-UCP 1 polyclonal antibody (from Calbiochem). The specificity of the antibody (Calbiochem) is demonstrated in the supplemental figure. We showed that UCP 1 protein was present in mitochondria isolated from rat brown adipose tissue (Fig. 2*A*, *lane 1*) and mitochondria isolated from whole rat thymus of fed (*lane 2*) and fasted (*lane 3*) animals (and in thymocytes from fed and fasted rats; results not shown). UCP 1 was clearly expressed at higher levels in mitochondria from brown adipose tissue (Fig. 2*A*, *lane 1*). As expected, no UCP 1 protein was detected in equivalent amounts of mitochondria isolated from rat liver (Fig. 2*A*, *lane 4*). As a control for assessing protein loading, an antibody to the F_1 β-subunit of ATP synthase was used in immunoblots on the same mitochondrial preparations (Fig. 2*B*). Collation of data for three separate preparations and experiments demonstrated that there was no statistically significant difference in expression of the UCP 1 protein in mitochondria isolated from rat

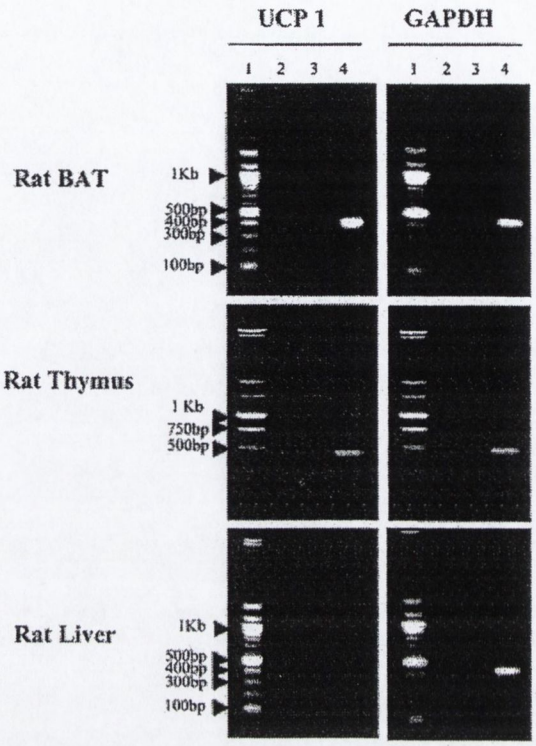
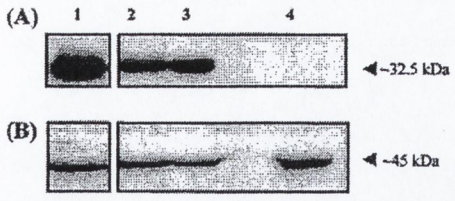


FIG. 1. **Detection of uncoupling protein 1 mRNA transcripts in various tissues.** *Lane 1*, DNA molecular markers (1 kb); *lane 2*, RT-PCR control reaction containing primers but no mRNA; *lane 3*, PCR control reaction containing primers but no cDNA; *lane 4*, RT-PCR product using primers to UCP 1 (399 bp) and glyceraldehyde-3-phosphate dehydrogenase (*GAPDH*) (444 bp) for rat BAT, rat thymus, and rat liver.

thymus when compared with the fed and fasted states (Fig. 2*C*; or rat thymocytes; results not shown). These results were confirmed using other anti-UCP 1 antibodies, namely a UCP 1-specific anti-peptide antibody characterized by Cunningham *et al.* (27) and also an antibody to the full-length UCP 1 (results not shown).

The anti-UCP 1 peptide antibody also detected UCP 1 in mitochondria isolated from the thymus of wild-type mice (Fig. 3, *lane 6*) but not in mitochondria from thymus of UCP 1 knock-out mice (Fig. 3, *lane 5*). The immunoblot also shows detection of UCP 1 in mitochondria isolated from BAT of wild-type mice (Fig. 3, *lane 8*) but not in mitochondria from BAT of UCP 1 knock-out mice (*lane 7*) as expected. No protein was detected using this antibody in mitochondria isolated from liver (Fig. 3, *lane 2*) or kidney (*lane 4*) of wild-type mice or liver (*lane 1*) or kidney (*lane 3*) of UCP 1 knock-out mice.

BAT can be present in the vicinity of the thymus. Therefore, a reasonable concern is that the detection of UCP 1 in mitochondria isolated from whole thymus could be due to BAT contamination of the thymus preparation. As BAT is visibly distinguishable from the translucent white thymus when present, it is easily removed (results not shown). However, to formally ensure there was no BAT contamination of the thymus, a single cell suspension of thymocytes was prepared from thymus from rats or mice. By using flow cytometry, it was confirmed that >99% of cells in the resulting thymocyte suspension from rats, and also mice, were positive for the thymocyte-specific marker, Thy-1 (Fig. 4*A*; data not shown). Consistent with the data from whole thymus (Figs. 1 and 3), both UCP-1 transcripts and UCP 1 protein were detected in this thymocyte preparation (Fig. 4, *B* and *C*).



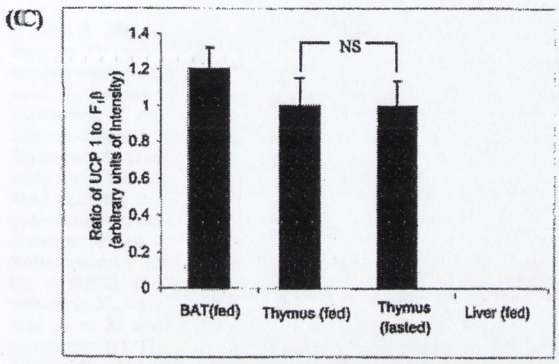


FIG. 2. **Detection of UCP 1 protein expression in mitochondria isolated from thymus of fed and fasted rats.** *A*, immunoblot using the anti-UCP 1 peptide antiserum (Calbiochem). *B*, immunoblot using the antibody to the β-subunit of the F_1-ATP synthase. *Lane 1*, BAT mitochondria isolated from fed rats. *Lane 2*, thymus mitochondria isolated from fed rats. *Lane 3*, thymus mitochondria isolated from fasted rats. *Lane 4*, liver mitochondria isolated from fed rats. *C*, the relative abundance of UCP 1 protein expression as a ratio to $F_1\beta$-subunit of the ATP synthase, as determined by densitometry, for three separate preparations. Data are expressed as mean ± S.E. No significant (*NS*) difference in UCP 1 expression was observed in thymus mitochondria in a comparison with the fed or fasted states ($p < 1.0$). In each lane 100 μg of protein was loaded.

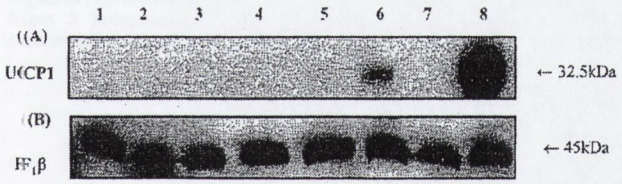


FIG. 3. **Detection of UCP 1 protein expression in mitochondria isolated from wild-type but not UCP 1 knock-out mice.** *A*, immunoblot using the anti-UCP 1 peptide antibody (Calbiochem) to mitochondria isolated from liver of UCP 1 knock-out (*lane 1*) and wild-type (*lane 2*) mice, kidney (*lane 3*) of UCP 1 knock-out and wild-type mice (*lane 4*) mice, mitochondria isolated from thymus of UCP 1 knock-out (*lane 5*) and wild-type mice (*lane 6*), mitochondria isolated from BAT of UCP 1 knock-out (*lane 7*) and wild-type mice (*lane 8*). *B*, an $F_1\beta$-subunit-specific antibody was used as a control for the presence of mitochondria. In *lanes 1–6*, 60 μg of protein was loaded, whereas in *lanes 7* and *8*, 20 μg was used.

UCP 1 is known to contain a purine nucleotide-binding site that is accessible from the cytoplasmic side of the mitochondrial inner membrane. Thus, in the presence of atractyloside/carboxyatractyloside (which inhibits function and prevents purine nucleotide binding to the adenine nucleotide carrier), purine nucleotide binding to brown adipose tissue mitochondria can be used as a measure of UCP 1 abundance. However, experience from working with brown adipose tissue mitochondria taken from animals held at room temperature has shown that some of the purine nucleotide-binding sites in UCP 1 may be masked, *i.e.* purine nucleotides already bound. Unmasking can be achieved by treating mitochondria with Dowex ion-exchange resin that removes bound purine nucleotides (15).

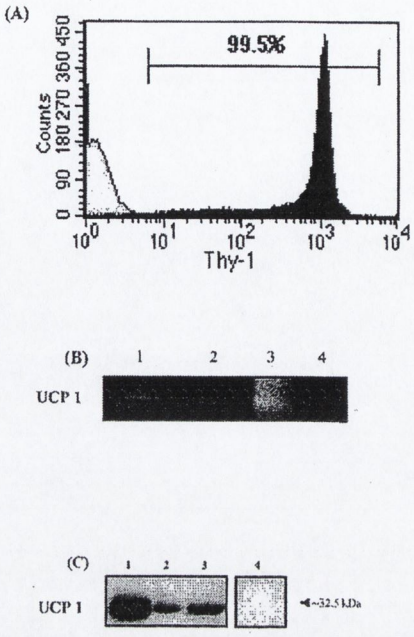


FIG. 4. **Detection of UCP 1 transcripts and protein in thymocytes.** *A*, flow cytometry analysis of the cell suspension prepared from the thymus of rats. Representative histogram image showing >99% of the thymocyte suspension are Thy-1-positive (*dark shading*) with gates set from isotype control IgG1 (*gray shading*). *B*, RT-PCR product using primers to UCP 1 (399 bp) in rat thymocytes (*lanes 1* and *2*). *Lane 3*, RT-PCR product using primers to UCP 1 (399 bp) in rat BAT; *lane 4*, PCR containing primers but no cDNA. *C*, immunoblot using the anti-UCP 1 peptide antiserum (Calbiochem) and immunoblot using the antibody to the β-subunit of the F_1-ATP synthase. *Lane 1*, brown adipose tissue (*BAT*) mitochondria isolated from fed rats; *lane 2*, thymocyte mitochondria isolated from fed rats; *lane 3*, thymocyte mitochondria isolated from fasted rats; *lane 4*, liver mitochondria isolated from fed rats. In each lane 100 μg of protein was loaded.

Unmasking manifests itself as an increase in the measured B_{max} of [^{3}H]GDP binding to brown adipose tissue mitochondria isolated from rats at room temperature (294 ± 29 pmol/mg (n = 3) to 394 ± 25 pmol/mg (n = 3), p = 0.048) as exemplified in Fig. 7*A*. The affinity of the binding site for GDP in brown adipose tissue mitochondria appeared not to be affected by Dowex treatment, as the K_D values are similar (0.6 ± 0.2 μM (n = 3) and 0.7 ± 0.2 μM (n = 3), respectively) (Fig. 5*A*). By using Dowex-treated mitochondria from various sources (to maximize the possibility of detecting binding), we showed that mitochondria containing UCP 1 from thymus could bind [^{3}H]GDP in a saturable manner with an equivalent K_D (0.7 ± 0.4 μM (n = 3)) and a B_{max} value (290 ± 46 pmol/mg (n = 3)) to mitochondria from BAT of rats that were kept at room temperature (394 ± 25 pmol/mg (n = 3) and 0.7 ± 0.2 μM (n = 3)) (Fig. 5*B*). Furthermore, in rat liver mitochondria, which contain no constitutively expressed UCPs (16, 27), rat skeletal muscle mitochondria (which contain UCP 3) (27), and rat spleen mitochondria, which contain UCP 2 (16), no saturable GDP binding was detected (Fig. 5*B*) (results not shown for spleen mitochondria). Thus the data show that the saturable GDP binding is because of the UCP 1 present in thymus mitochondria, as is the case for BAT mitochondria.

By having established that thymus mitochondria have a UCP 1-dependent GDP-binding site, it remained to be determined whether binding of the ligand could affect UCP 1 uncoupling function. Fig. 6*A* shows that the nonphosphorylating oxygen consumption rates (state 4; expressed as nanomoles of oxygen atoms/min/mg of mitochondrial protein) of non-Dowex-treated BAT mitochondria from rats kept at room temperature

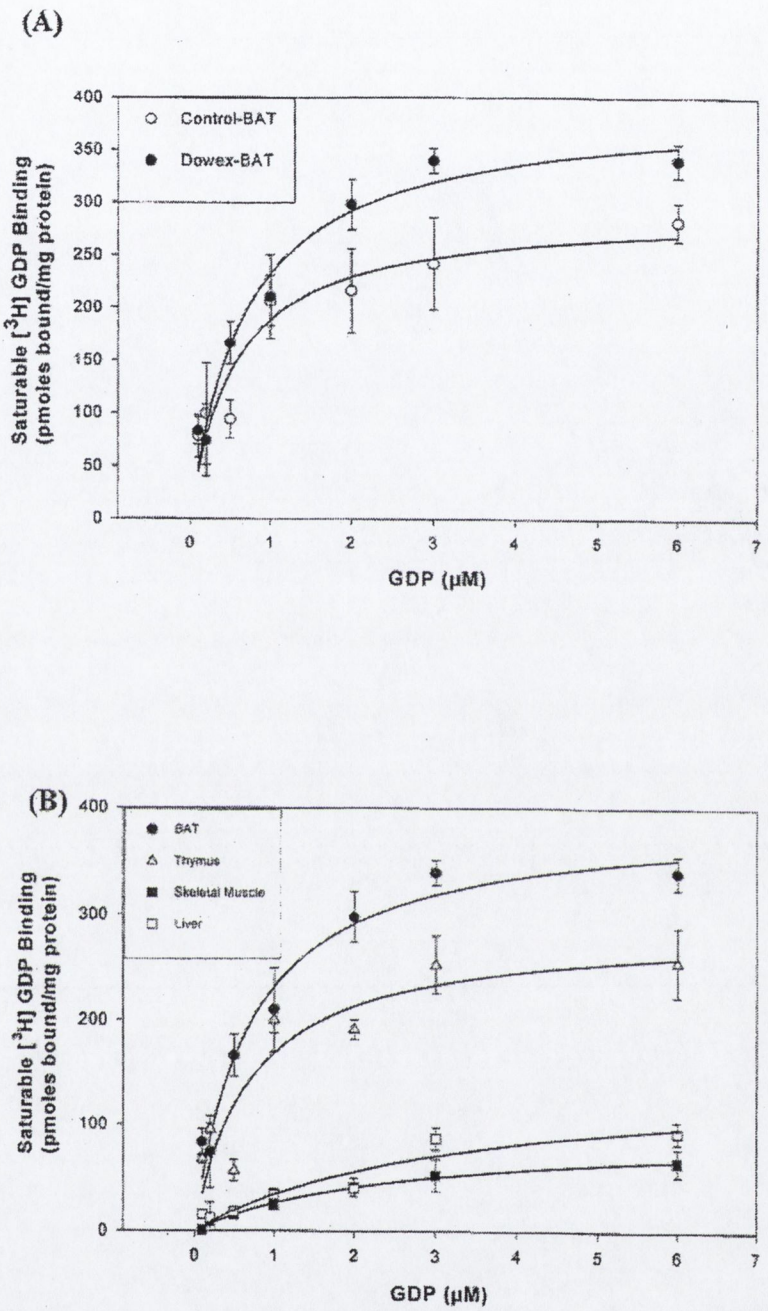


FIG. 5. **Measurement of GDP binding by thymus mitochondria.** Experiments were performed to determine B_{max} and K_D values for the GDP binding parameters. *A*, non-Dowex-treated (○) and Dowex-treated (●) BAT mitochondria from rat. *B*, Dowex-treated rat mitochondria from BAT (●), thymus (△), liver (□), and skeletal muscle (■). B_{max} values for non-Dowex-treated (294 ± 29 (n = 3)) and Dowex-treated (394 ± 25 (n = 3)) BAT mitochondria are significantly different (p = 0.048, unpaired Student's t test), whereas K_D values are similar (0.6 ± 0.2 μM (n = 3) and 0.7 ± 0.2 μM (n = 3) respectively). The B_{max} and K_D values for Dowex-treated thymus mitochondria are similar to those for Dowex-treated BAT mitochondria (290 ± 46 (n = 3) and 0.7 ± 0.4 (n = 3) respectively). The Michaelis dissociation constant (K_D) and the maximal binding capacity (B_{max}), describing the saturable binding of [^{3}H]GDP, were obtained by fitting mean values for specific binding sites on the y axis and the free radioligand concentrations used on the x axis by using the program Sigma Plot, version 5 (SPSS Inc. Chicago). The data were fitted to a rectangular hyperbola by nonweighted, nonlinear least squares regression. Data are mean ± S.E. from 3 independent experiments each performed in triplicate.

in the presence of inhibitors of the adenine nucleotide carrier and ATP synthase is inhibited by addition of 1 mM GDP (from 175 ± 6 to 128 ± 5; p = 0.0038). In turn, the oxygen consumption rate was significantly stimulated by nanomolar amounts of palmitate (~40 nM free fatty acid) to 190 ± 11 (p = 0.0088), close to the maximal uncoupled rate of 230.8 ± 14.2 induced by the addition of FCCP. In order to determine whether the UCP 1 in mitochondria (non-Dowex-treated) from thymus or thymocytes from rats kept at room temperature was functionally active, we measured the state 4 oxygen consumption rates under the same conditions, and we determined whether these rates were inhibited by GDP or activated by palmitate (buffered by defatted BSA). In addition, the maximal uncoupled oxygen consumption rate was determined. Fig. 6*B* shows that state 4 oxygen consumption rate by thymus/thymocyte mitochondria (64 ± 3) was significantly inhibited by GDP (34 ± 4) (p = 0.004) and was subsequently stimulated by the presence of a nanomolar concentration of palmitate (55 ± 6) (p = 0.04). The maximal uncoupled rate (+FCCP) is 107 ± 4 for thymus mitochondria. In contrast, state 4 oxygen consumption rates by (non-Dowex-treated) mitochondria from rat liver (39.4 ± 1.4; Fig. 6*C*), which contain no constitutively expressed UCPs, rat skeletal muscle mitochondria (101 ± 22), which only contain UCP 3 (Fig. 6*D*), and rat kidney mitochondria (65.5 ± 12.9) and rat spleen mitochondria (results not shown), both of which only contain UCP 2 (Fig. 6*E*), are GDP- and palmitate-insensitive. This insensitivity was not due to poor quality mitochondria preparations as the maximal oxygen consumption rates due to the uncoupler FCCP were 131 ± 12, 268.0 ± 16, 226 ± 19.0 for mitochondria from liver, skeletal muscle, and kidney, respec-

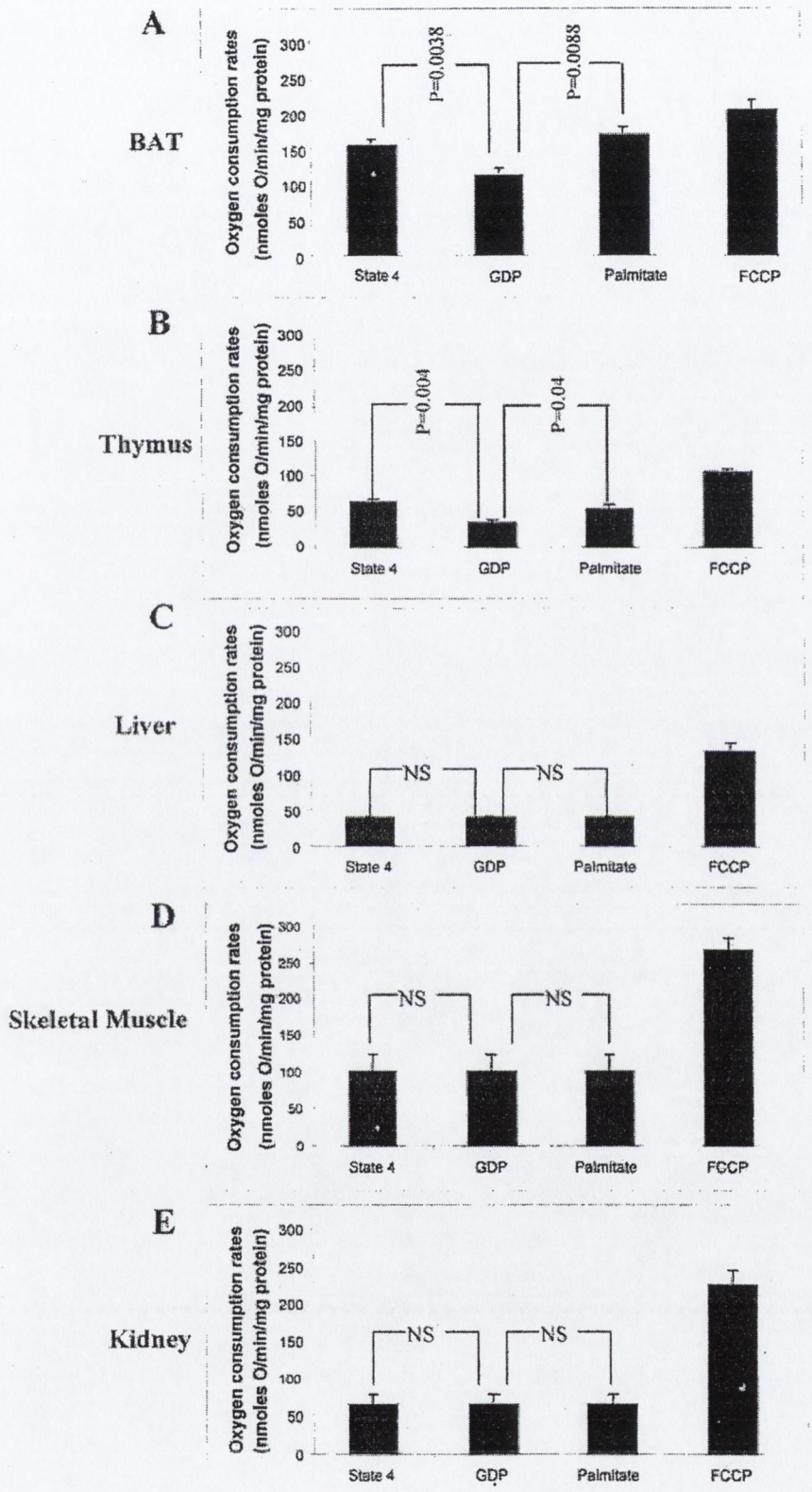


FIG. 6. **Measurement of state 4 oxygen consumption by thymus mitochondria in the presence of purine nucleotides and fatty acids.** Mitochondria (0.5 mg/ml; non-Dowex-treated) from BAT (*A*), thymus (*B*), liver (*C*), skeletal muscle (*D*), and kidney (*E*) of rats kept at room temperature were incubated in the presence of 120 mM KCl, 5 mM HEPES-KOH, pH 7.0, 1 mM EGTA, 7.5 mM succinate (K^+ salt), 16 μM de-fatted BSA, 5 μM rotenone, 1 μg/ml oligomycin, and 5 μM atractyloside. Steady-state oxygen consumption rates were then measured, following addition of 1 mM GDP, 64 μM palmitate (~40 nM free), and 40 nM FCCP. Data are shown as the mean ± S.E. from at least three independent experiments each performed in triplicate.

tively. We also observed that the state 4 oxygen consumption rate was GDP- and palmitate-insensitive when thymus/thymocyte mitochondria were respiring on complex I substrates (glutamate plus malate or pyruvate plus malate, instead of succinate plus rotenone) (results not shown). This most probably reflects limitations in the supply of reducing equivalents to the mitochondria, as we also observed that addition of uncoupler failed to increase oxygen consumption in thymus/thymocyte mitochondria with these substrates (results not shown).

The immunoblot analyses and GDP binding assays led us to believe that there would be enough of the UCP 1 protein expressed in mitochondria from rat thymus to allow its purification. Hydroxyapatite chromatography procedures previously used for purification of UCP 1 from BAT (31) were adapted for rat thymus. After one-dimensional SDS-PAGE and staining with colloidal Coomassie Blue G-250, a distinct broad band of ~30–33 kDa (the expected mass of UCP 1) was observed (Fig. 7*A*). The band was excised, and tryptic peptides were prepared for analysis by mass spectrometry. The mass spectrum obtained using MALDI-TOF MS is shown in Fig. 7*B*. After internal calibration, base-line correction, and peak selection, 33 peptides were submitted for peptide mass fingerprinting. Searching the nonredundant data bases with the peptide masses (using all four search algorithms) identified mitochondrial brown fat UCP 1 from *R. norvegicus* as having the top Mowse score (best data base "hit"). Nine tryptic peptides and 15 montryptic peptide matches (Table I) were identified, which provided 77% coverage of the UCP 1 protein (237 of 307 amino acids; Fig. 7*C*). This unequivocally identified rat UCP 1 as a major protein in the gel band. Most interestingly, when the error tolerance was relaxed to 0.5 Da, the data base search algorithms Profound and MS-FIT (but not the other two search algorithms) identified two presumably co-digested proteins (voltage-dependent anion-selective channel protein 1 and mitochondrial carnitine acylcarnitine translocase carrier protein). Peptides from these proteins were present in small amounts unlike those of UCP 1. These were also identified by LC-MS/MS (see next paragraph).

To refine the mass spectrometric identification of the isolated protein, tandem mass spectrometry (LC-MS/MS) was performed. Peptides were separated by liquid chromatography, gated, and fragmented, and the fragmentation data were used to search the data base. The results are shown in Table II. Four peptides (covering 15% of the protein) identified rat UCP. Other tryptic peptides were also sequenced, and data base searching identified three other mitochondrial proteins: voltage-dependent anion-selective channel protein 1 (VDAC 1), VDAC 2, and carnitine/acylcarnitine carrier protein. It is interesting that the masses of these proteins ranged from 32.4 to 33.5 kilodaltons, thus explaining why they were all present in the same protein band from the one-dimensional gel.

DISCUSSION

The aim of this study was to investigate the nature of the proton leak in thymus. As already mentioned, the specificity and selectivity of our primers for detection of transcripts encoding uncoupling proteins 1–3 have been demonstrated previously (24). In this study we clearly demonstrate that rat thymus contains UCP 1 transcripts. The results compliment our recent observations that rat thymus also contains transcripts for UCP 2 and UCP 3 (24). Our results, however, are in contrast to a previous study that failed to detect UCP 1 transcripts in rat thymus using Northern blot analysis (17). The inability to detect UCP 1 transcripts in that study may reflect a low abundance of UCP 1 mRNA in the thymus of rats kept at room temperature, which would only be detected by the more sensitive RT-PCR method used in this study. Previous studies on uncoupling proteins have emphasized the importance of determining whether mRNA levels reflect protein expression levels. For instance, by using Northern blot analysis, UCP 2 mRNAs were detected in many mammalian tissues (16), yet UCP 2 protein was only detected in a small subset of these tissues by immunoblot analysis (33). Discrepancies in UCP expression may also reflect difference in animal husbandry, *e.g.* basal room temperature, between different laboratories.

As with UCP 2, the detection of UCP 1 transcripts in thymus may not have necessarily reflected the presence of the UCP 1 protein. To that end, we characterized the UCP 1-peptide antibody (from Calbiochem) for it selectivity and sensitivity to UCP 1. Our data clearly demonstrate that the UCP 1-peptide antibody (Calbiochem) was selective for UCP 1 protein over UCP 2, UCP 3, and other mitochondrial transporters present in these mitochondria. Application of the UCP 1-peptide (Calbiochem) to mitochondria isolated from rat whole thymus detects UCP 1, a result that was reinforced by using a polyclonal anti-UCP 1 antibody produced for us by Eurogentec (27) and a polyclonal antibody to the full-length UCP 1 protein (a gift from Dr. Ricquier). Furthermore, we were able to detect UCP 1 in mitochondria isolated from mouse thymus but not in mitochondria isolate from UCP 1 knock-out mice. This observation further emphasizes the fact that we were detecting UCP 1 in the thymus and that the antibody was not cross-reacting with a mitochondrial protein present in thymus but not in other mitochondria.

We have ensured that the presence of UCP 1 in thymus is not because of BAT contamination of thymus. BAT can exist in the vicinity of the thymus, and when present it is easily discernible and excisable. Furthermore, in a highly processed cell suspension of thymocytes, which contained >99% Thy-1 (CD90)-positive lymphocytes, UCP 1 transcripts were detected by RT-PCR, and mitochondria isolated from these cells contain the UCP 1 protein. Future work will address why UCP 1 is present in thymocytes. In this respect, it is noteworthy that under conditions of acute starvation, which are known to diminish thymus function (34) and also reduce UCP 1 expression in BAT (35), we could detect no significant difference in the abundance of UCP 1 in mitochondria isolated from rat thymus. These data suggest that UCP 1 plays a different role in thymus than in BAT.

The presence of UCP 1 in rat thymus implied that mitochondria isolated from this organ might bind purine nucleotides. To improve the sensitivity of the purine nucleotide binding assay, we decided to treat the mitochondria to remove any endogenously bound purine nucleotide that might be present. Huang and Klingenberg (15) have shown that removal of any endogenously bound purine nucleotide can be achieved by treating the mitochondria with Dowex ion-exchange resin. We showed that Dowex-treated thymus mitochondria isolated from rats kept at room temperature could bind [^{3}H]GDP with similar affinity (K_D) and with a 75% B_{max} of that determined for BAT mitochondria. No saturable binding was detected in mitochondria from tissues such as spleen and kidney (which constitutively express UCP 2 protein), skeletal muscle (which constitutively expresses UCP 3), and liver (which does not express any UCPs) (16, 27, 36). We conclude that the [^{3}H]GDP binding observed in thymus mitochondria was due to UCP 1 protein.

The function of UCP 1 in BAT mitochondria is to generate heat by increasing metabolic flux in that tissue. BAT mitochondria have high oxygen consumption rates, *in vitro*, due to UCP 1 proton leak activity, an activity that is inhibited by purine nucleotides (*e.g.* GDP) and activated by long chain fatty acids (*e.g.* palmitate). Our evidence for the existence of UCP 1 protein in thymus mitochondria and the capability of those mitochon-

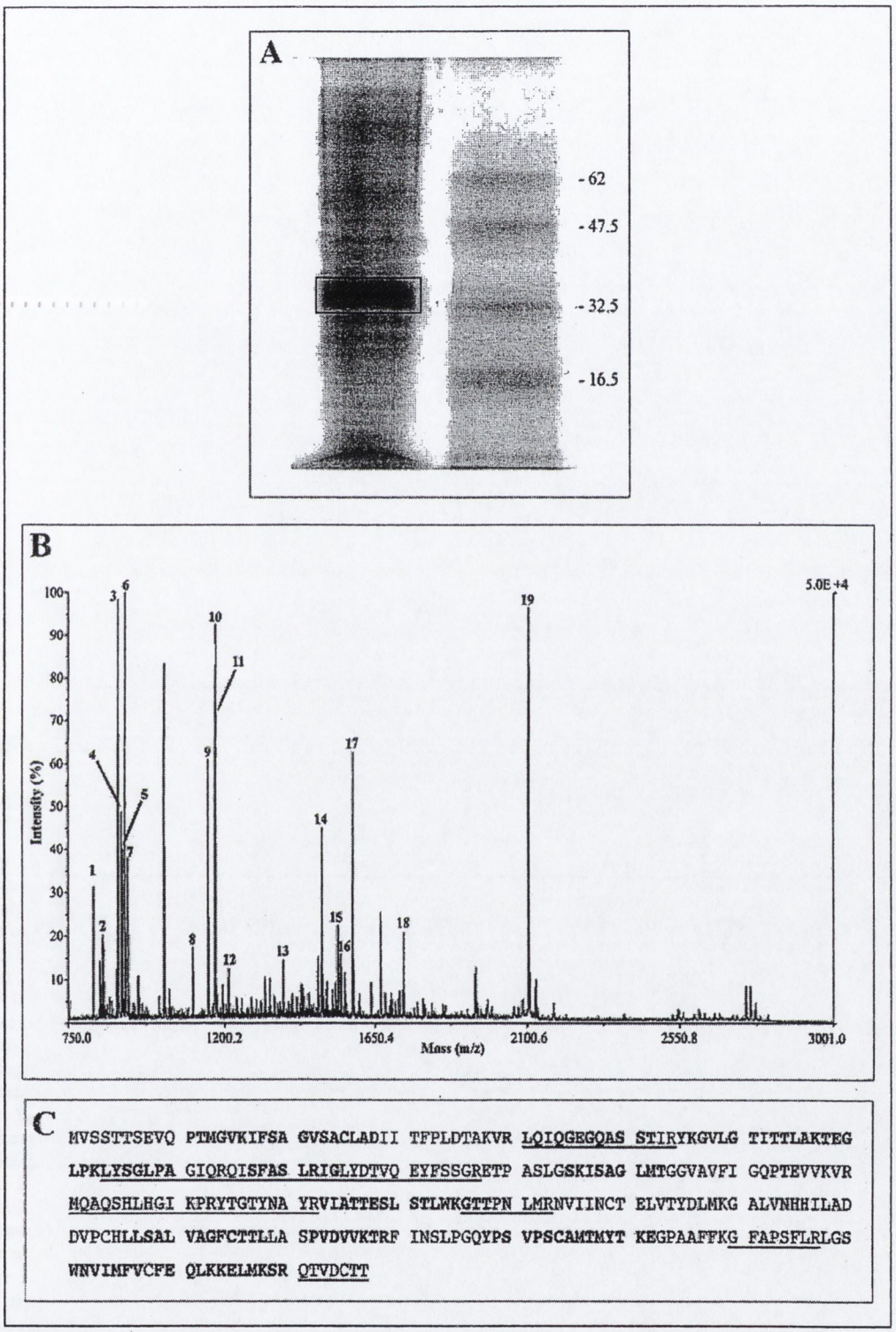


FIG. 7. **Identification of isolated rat thymus proteins by mass spectrometry.** *A*, one-dimensional gel electrophoresis analysis of purified UCP 1 from rat thymus mitochondria. The gel was stained with colloidal Coomassie Blue G-250. The broad band at 30–33 kDa was excised, and in-gel digestion with trypsin was performed prior to mass spectrometric analysis of tryptic cleavage products. Molecular mass markers are shown in the *right-hand lane*. *B*, the peptide mass spectrum obtained using MALDI-TOF MS. *C*, UCP 1 peptides identified by peptide mass fingerprinting. *Boldface*, tryptic peptide sequences. *Underlined*, nontryptic peptide sequences.

dria to bind GDP led us to determine whether thymus mitochondria had a UCP 1-catalyzed proton leak similar to that which had been observed for UCP 1 isolated from BAT. Although the state 4 oxygen consumption rates in thymus mitochondria were approximately a third that of BAT mitochondria, there was a UCP 1-catalyzed proton leak inhibited by GDP and

TABLE I
MALDI-TOF identification of UCP 1 from peptide mass fingerprinting

Spectrum no.[a]	Peptide mass	Start amino acid	End amino acid	Peptide sequence	Fragment type
1[b]	824.474912	301	307	QTVDCTT-	Tryptic
2	850.448461	87	94	SFASLRIG	Nonspecific
3	894.493114	270	277	GFAPSFLR	Tryptic
4	905.497616	176	183	GTTPNLMR	Tryptic
	907.490526	115	123	SKISAGLMT	Nonspecific
5	908.492171	281	287	WNVIMFV	Nonspecific
6	913.461099	232	239	PVDVVKTR	Nonspecific
7	921.522377	85	92	QISFASLR	Tryptic
8	1108.521850	154	162	YTGTYNAYR	Tryptic
9	1153.651495	17	28	IFSAGVSACLAD	Nonspecific
10	1173.635104	69	79	EGLPKLYSGLP	Tryptic
11	1174.673948	74	84	LYSGLPAGIQR	Tryptic
12	1195.612911	217	228	LSALVAGFCTTL	Nonspecific
	1320.589168	154	164	YTGTYNAYRVI	Nonspecific
13	1374.692431	40	52	RLQIQGEGQASST	Nonspecific
14	1487.803679	41	54	LQIQGEGQASSTIR	Tryptic
	1502.814700	141	153	MQAQSHLHGIKPR	Tryptic
15	1536.851824	289	300	FEQLKKELMKSR	Nonspecific
16	1544.834032	66	80	AKTEGLPKLYSGLPA	Nonspecific
	1556.835564	90	102	SLRIGLYDTVQEY	Nonspecific
17	1580.820221	11	26	PTMGVKIFSAGVSACL	Nonspecific
	1707.832029	163	178	VIATTESLSTLWKGTT	Nonspecific
18	1734.866656	93	107	IGLYDTVQEYFSSGR	Tryptic
19	2103.272073	55	74	YKGVLGTITTLAKTEGLPKL	Nonspecific

[a] Masses without numerical designation were not abundant enough to be seen on the spectra without amplification of the base line.
[b] C terminus of UCP 1

TABLE II
LC-MS/MS identification of R. norvegicus mitochondrial proteins using peptide fragmentation data

Protein identification	GenBank™ accession no.	pI	Mass	No. peptides matched	Coverage of identified protein
			Da		%
Mitochondrial brown fat UCP 1	P04633	9.21	33458	4	15
VDAC-2	O9JI32	7.44	32353	3	11
VDAC-1	Q9Z2L0	8.35	32540	4	11
Mitochondrial carnitine/acylcarnitine carrier protein	CAA66410	9.55	33474	3	7

activated by nanomolar palmitate. As expected, there was no GDP-sensitive proton leak in liver mitochondria (which contain no UCPs), skeletal muscle mitochondria (which contain UCP 3)), or spleen or kidney mitochondria (which contain UCP 2) (16, 36). We conclude that the GDP-inhibited and palmitate-activated proton leak measured in rat thymus mitochondria is not due to UCP 2 or UCP 3 but is due to the activity of UCP 1.

The detection of UCP 1 in rat thymus mitochondria using immunoblotting and the extent of the saturability of the GDP binding in thymus mitochondria suggested to us that sufficient UCP 1 protein exists in thymus mitochondria to attempt its purification. We used procedures for purification of UCP 1 from BAT mitochondria (31), and we found that rat thymus mitochondria yielded a single broad 30–33-kDa band on a one-dimensional SDS-polyacrylamide gel, in accordance with the predicted molecular mass of UCP 1 (33,458 daltons). MALDI-TOF mass spectrometry results revealed that the predominant protein was uncoupling protein 1 from rat (GenBank™ accession number P04633). The abundant peptide masses showed that UCP 1 protein was by far the predominant molecule in the excised band from the one-dimensional gel. LC-MS/MS analysis confirmed the presence of UCP 1 peptides. LC-MS/MS analysis also revealed peptides from three other proteins, VDAC-1, VDAC-2, and mitochondrial carnitine/acylcarnitine carrier protein. These proteins have masses of 32,540, 32,353, and 33,474 Da, respectively; thus, it is not surprising that they migrate with UCP 1 (33,458 Da) as a single broad band on a one-dimensional gel. However, the isoelectric points of the four proteins are all distinct and range from 7.44 to 9.55. This would allow their separation by two-dimensional gel electrophoresis, a procedure with much higher resolution than simple one-dimensional gel electrophoresis. Most interestingly, no native UCP 2 (or UCP 3) was detected in the purified 30–33-kDa band despite the fact that properly folded expressed UCP 2 (or UCP 3) passes through an hydroxyapatite column (38, 39). We can only assume that the abundance of UCP 1 protein in thymus is far greater than that for UCP 2 (or UCP 3).

The discovery of UCP 1 protein in rat thymus mitochondria has implications for understanding the bioenergetics, metabolism, and immune function of the thymus. Previous studies (20, 37) have described a proton leak (and a UCP 2-dependent proton leak) *in situ* in thymocytes, and therefore we might expect UCP 1 to play a major role in determining metabolic flux in the thymus. There is also evidence suggesting that UCP 1 plays a role in regulating superoxide production by mitochondria (5–8). The insensitivity of UCP 1 expression in thymus to starvation suggests a different role for UCP 1 in thymus than in BAT. The discovery of UCP 1 in rat thymus mitochondria has thus uncovered a new avenue for research into thymus bioenergetics, metabolism, development, and function.

Acknowledgments—We thank Dr. Daniel Ricquier (Centre de Recherche sur l'Endocrinologie Moleculaire et le Developpement, Meudon, France) for human UCP 2 and 3 clones; Prof. Jean-Paul Giacobino (Département de Biochimie Médicale, Université of Genève, Switzerland) for the mitochondria isolated from the skeletal muscle hind limb (gastrocnemius) of wild-type and UCP 3 knock-out mice; Dr. Jan Nedergaard (Wenner-Gren Institute, Stockholm University, Sweden) for the mitochondria isolated from brown adipose tissue of wild-type and UCP 1 knock-out mice; and Dr. Matt Harmey (Department of Botany, University College Dublin, Ireland) for the antibodies to the β-subunit of the F_1-ATP synthase.

REFERENCES

1. Nicholls, D. G., and Locke, R. M. (1984) *Physiol. Rev.* **64,** 1–64
2. Nicholls, D. G. (2004) *Biochem. Soc. Trans.* **29,** 751–755
3. Nicholls, D. G. (1976) *Eur. J. Biochem.* **62,** 223–228
4. Ricquier, D., and Bouillaud, F. (1986) in *Brown Adipose Tissue* (Trayhurn, P., and Nicholls, D. G., eds) pp. 86–104, Edward Arnold Publishers, London
5. Echtay, K. S., Murphy, M. P., Smith, R. A. J., Talbot, D. A., and Brand, M. D. (2002) *J. Biol. Chem.* **277,** 47129–47135
6. Echtay, K. S., Roussel, D., St-Pierre, J., Jekabsons, M. B., Cadenas, S., Stuart, J. A., Harper, J. A., Roebuck, S. J., Morrison, A., Pickering, S., Clapham, J. C., and Brand, M. D. (2002) *Nature* **415,** 96–99
7. Echtay, K. S., Esteves, T. E., Pakay, J. L., Jekabsons, M. B., Lambert, A. J., Portero-Otin, M., Pamplona, R., Vidal-Puig, A. J., Wang, S., Roebuck, S. J., and Brand, M. D. (2003) *EMBO J.* **22,** 4103–4110
8. Murphy, M. P., Echtay, K. S., Blaikie, F. H., Asin-Cayuela, J., Cochemé, H. M., Green, K., Buckingham, J., Taylor, E. R., Hurrell, F., Hughes, G., Miwa, S., Cooper, C. E., Svistunenko, D. A., Smith, R. A. J., and Brand, M. D. (2003) *J. Biol. Chem.* **278,** 48534–48545
9. Skulachev, V. P. (1991) *FEBS Lett.* **294,** 158–162
10. Klingenberg, M., Echtay, K. S., Bienengraeber, M., Winkler, E., and Huang, S. G. (1999) *Int. J. Obes. Relat. Metab. Disord.* **6,** S24–S29
11. Garlid, K. D., Jabůrek, M., Ježek, P., and Vařecha, M. (2000) *Biochim. Biophys. Acta* **1459,** 383–389
12. Sundin, U., and Cannon, B. (1980) *Comp. Biochem. Physiol. B Comp. Biochem.* **65,** 463–471
13. Huang, S.-G., and Klingenberg, M. (1996) *Biochemistry* **35,** 16806–16814
14. Porter, R. K. (2001) *Biochim. Biophys. Acta* **1504,** 120–127
15. Huang, S. G., and Klingenberg, M. (1995) *Eur. J. Biochem.* **229,** 718–725
16. Ricquier, D., and Bouillaud, F. (2000) *Biochem. J.* **345,** 161–179
17. Nègre-Salvayre, A., Hirtz, C., Carrera, G., Cazenave, R., Troly, M., Salvayre, R., Penicaud, L., and Casteilla, L. (1997) *FASEB J.* **10,** 809–815
18. Enërback, S., Jacobsson, A., Simpson, E. M., Harper, M.-E., and Kozak, L. P. (1997) *Nature* **387,** 90–94
19. Vidal-Puig, A. J., Grujic, D., Zhang, C. Y., Hagen, T., Boss, O., Ido, Y., Szczepanik, A., Wade, J., Mootha, V., Cortright, R., Muoio, D. M., and Lowell, B. B. (2000) *J. Biol. Chem.* **275,** 16258–16266
20. Buttgereit, F., Grant, A., Muller, M., and Brand, M. D. (1994) *Eur. J. Biochem.* **15,** 513–519
21. Chappell, J. B., and Hansford, R. G. (1972) in *Subcellular Components: Preparation and Fractionation* (Birnie, G. D., ed) pp. 77–91, Butterworth, London
22. Bhattacharya, S. K., Thakar, J. H., Johnson, P. L., and Shanklin, D. R. (1991) *Anal. Biochem.* **192,** 344–349
23. Markwell, M. A., Haas, S. M., Bieber, L. L., and Tolbert, N. E. (1978) *Anal. Biochem.* **87,** 206–210
24. Carroll, A. M., and Porter, R. K. (2004) *Biochim. Biophys. Acta* **1700,** 145–150
25. Tokunga, K., Nakamura, Y., Sakata, K., Fujimori, K., Ohkubo, M., Sawada, K., and Sakiyama, S. (1987) *Cancer Res.* **47,** 5616–5619
26. Neuhoff, V., Arold, N., Taube, D., and Ehrhardt, W. (1998) *Electrophoresis* **9,** 255–262
27. Cunningham, O., McElligott, A. M., Carroll, A. M., Breen, E., Reguenga, C., Oliveira, M. E. M., Azevedo, J. E., and Porter, R. K. (2003) *Biochim. Biophys. Acta* **1604,** 170–179
28. Scarpace, P. J., Bender, B. S., and Borst, S. E. (1991) *Can. J. Physiol. Pharmacol.* **69,** 761–766
29. González-Barroso, M., Fleury, C., Bouillaud, F., Nicholls, D. G., and Rial, E. (1998) *J. Biol. Chem.* **273,** 15528–15532
30. Reynafarje, B., Costa, L. E., and Lehninger, A. L. (1985) *Anal. Biochem.* **145,** 406–418
31. Lin, C. S., and Klingenberg, M. (1980) *FEBS Lett.* **113,** 299–303
32. Kinter, M., and Sherman, N. E. (2000) *Protein Sequencing and Identification Using Tandem Mass Spectrometry,* pp. 147–165, John Wiley & Sons, Inc., New York
33. Pecqueur, C., Alves-Guerra, M.-C., Gelly, C., Levi-Meyrueis, C., Couplan, E., Collins, S., Ricquier, D., Bouillaud, F., and Miroux, B. (2001) *J. Biol. Chem.* **276,** 8705–8712
34. Kendall, M. D., and al-Shawaf, A. A. (1991) *Brain Behav. Immun.* **5,** 9–28
35. Boss, O., Muzzin, P., and Giacobino, J.-P. (1998) *Eur. J. Endocrinol.* **139,** 1–9
36. Echtay, K. S., and Brand, M. D. (2001) *Biochem. Soc. Trans.* **29,** 763–768
37. Krauss, S., Zhang, C. Y., and Lowell, B. B. (2002) *Proc. Natl. Acad. Sci. U. S. A.* **99,** 118–122
38. Jekabsons, M. B., Echtay, K. S., and Brand, M. D. (2002) *Biochem. J.* **366,** 565–571
39. Jabůrek, M., and Garlid, K. D. (2003) *J. Biol. Chem.* **278,** 25825–25831

Immunodetection of UCP1 in rat thymocytes

A.M. Carroll*, L.R. Haines†, T.W. Pearson†, C. Brennan*, E.P. Breen* and R.K. Porter*[1]

*Department of Biochemistry, Trinity College Dublin, Dublin 2, Ireland, and †Department of Biochemistry and Microbiology, University of Victoria, Victoria, BC, Canada

Abstract

Thymi were dissected from rats and connective tissue was removed. Mitochondria were purified from isolated thymocytes and immunoblot analysis was performed using an antibody specific for uncoupling protein 1, which detected a 32.5 kDa protein associated with mitochondria from the thymocytes. This implies that rat thymocytes contain uncoupling protein 1.

Redacted

©2004 Biochemical Society



©2004 Biochemical Society